

## ABSTRACT

Title of Dissertation:                   EXPLORING ENDOGLYCOSIDASES FOR  
ANTIBODY GLYCOENGINEERING

Xin Tong, Doctor of Philosophy, 2019

Dissertation directed by:           Professor, Dr. Lai-Xi Wang, Department of  
Chemistry and Biochemistry

Monoclonal antibodies (mAbs) comprise a rapidly growing class of therapeutics with great potential in treating infections, inflammations, cancers, and autoimmunities. The glycosylation of an antibody determines its functional efficacy and structural integrity, but stringent control of the intrinsically heterogeneous N-glycans on an antibody remains a formidable challenge. Recent development of a chemoenzymatic glycosylation remodeling strategy using a family of carbohydrate-modifying enzymes called endoglycosidases is emerging as an attractive method for producing homogeneous antibody glycoforms. The success of this method depends on the discovery of efficient endoglycosidases and glycosynthase mutants.

Here, we describe mutagenesis studies on several endoglycosidases and their applications in expanding the current chemoenzymatic glycoengineering strategy to different antibodies. Five projects related to this effort are described here. First, glycosynthase variants of Endo-S were generated by mutagenesis to provide

enhanced transglycosylation activities and diminished tendency to hydrolyze the product. Second, mutational studies on another endoglycosidase, Endo-S2, identified novel glycosynthase variants with broader substrate specificity and higher catalytic efficiency than Endo-S mutants. This work also provided the first kinetic studies for Endo-S and Endo-S2 mutants, with important mechanistic implications. Third, the unique properties of Endo-S allowed us to develop an alternative glycan remodeling strategy to synthesize several antibody glycoforms that were not easily accessible using the conventional glycoengineering approaches. This new method can be applied in a facile, one-pot fashion to modify antibody glycosylation without the need for purifying intermediates or switching enzymes. Fourth, to further expand the toolbox for antibody glycoengineering, the substrate specificity of a newly discovered endoglycosidase Endo-CC was characterized. The highly flexible selectivity of this enzyme for protein framework substrates paved the way for glycoengineering of additional antibody isotypes, particularly IgE, as a single N-glycan was found to be indispensable for the biological functions. Finally, remodeling of IgE glycosylation with alternative glycan structures was achieved for the first time by endoglycosidases. These novel IgE glycoforms displayed distinct binding properties for IgE receptors and revealed important new aspects of the structure-function relationship of IgE antibody glycosylation. Together, these studies should facilitate the development of novel antibody-based therapeutics that are optimized in their glycosylation patterns.

EXPLORING ENDOGLYCOSIDASES FOR ANTIBODY GLYCOENGINEERING

by

Xin Tong

Dissertation submitted to the Faculty of the Graduate School of the  
University of Maryland, College Park, in partial fulfillment  
of the requirements for the degree of  
Doctor of Philosophy  
2019

Advisory Committee:  
Professor Lai-Xi Wang, Chair  
Professor Douglas Julin  
Professor Kwaku Dayie  
Professor Jason Kahn  
Professor Xiaoping Zhu

© Copyright by  
Xin Tong  
2019

## Acknowledgements

I would like to express my sincere gratitude to everyone who helped me with my study and research at graduate school. I received a lot of help and support from people around me, and I would not have completed my degree without them.

I would like to first thank my research advisor, Prof. Lai-Xi Wang, for his mentoring and guidance during all these years of research. Thank you for teaching me not only the knowledge and skills but also the scientific way of thinking and writing.

I want to thank my committee members, Dr. Julin, Dr. LaRonde, Dr. Dayie, Dr. Kahn, and Dr. Zhu for their constructive criticism. Thank you all for helping me learn how to communicate my research with the general scientific community.

I am extremely grateful to the current and past members of Wang group for their contribution to my research. I thank Dr. Tiezheng Li for being my mentor in the first few years of my graduate study. I also would like to thank Dr. Chao Li and Dr. Qiang Yang for their intellectual input in helping me face the challenges in several of my research projects. I enjoyed my time working as a graduate student in Wang lab.

I am very grateful to all my friends, especially Jingheng Wang, who shared his valuable experience as a graduate student with me on a regular basis and helped me go through the final and most difficult stage of my degree.

Finally, I would like to thank my parents for their long-standing support and encouragement. Without their understanding and financial help, I would never have the courage to travel so far to pursue education overseas. I love you very much!

# Table of Contents

Acknowledgements.....	ii
List of Tables .....	x
List of Figures.....	xi
List of Abbreviations .....	xvi
Chapter 1: Introduction.....	1
<b>A. Introduction to antibodies.....</b>	<b>1</b>
1. Monoclonal antibody-based therapeutics .....	1
2. Overview of antibody structure and function .....	4
<b>B. Antibody glycosylation and its importance in biological functions .....</b>	<b>9</b>
1. Structure and functional diversity of antibody glycosylation.....	10
2. Glycosylation modulates effector functions of IgG and IgE antibodies.....	11
3. Structural heterogeneity of antibody N-glycans .....	14
<b>C. Engineering antibody glycosylation by biosynthetic manipulation.....</b>	<b>16</b>
1. Biosynthetic pathways of N-glycans in eukaryotic expression systems.....	17
2. Antibody glycan remodeling by biosynthetic pathway perturbation.....	20
<b>D. Antibody glycosylation remodeling by chemoenzymatic modifications ..</b>	<b>23</b>
1. Introduction to endo- $\beta$ -N-acetylglucosaminidase (ENGase).....	25
2. Catalytic mechanism of ENGases and development of sugar oxazolines as activated glycan substrates for transglycosylation.....	27
3. Glycosynthase mutants of ENGases for antibody glycan remodeling.....	29
4. Examples of ENGase-mediated antibody glycoengineering .....	32

<b>E. Scope and limitations of current chemoenzymatic antibody remodeling strategy mediated by ENGases .....</b>	<b>37</b>
1. Efficiency of transglycosylation catalyzed by existing Endo-S glycosynthase mutants Endo-S D233Q and Endo-S D233A.....	37
2. Substrate specificity of current ENGases for different N-glycans.....	38
3. Glycosylation remodeling of antibodies beyond the IgG isotype.....	38
<b>F. Organization of the dissertation.....</b>	<b>40</b>
Chapter 2: Generation and comparative analysis of new glycosynthase mutants from endoglycosidase S (Endo-S) for antibody glycoengineering.....	43
<b>A. Introduction.....</b>	<b>43</b>
<b>B. Results .....</b>	<b>51</b>
1. Generation of additional glycosynthase mutants of Endo-S through site-directed saturation mutagenesis at the catalytic residue Asp-233. ....	51
2. Transglycosylation and hydrolysis activities of Endo-S mutants.....	52
3. Enzyme kinetic analysis of Endo-S mutants D233M and D233A.....	57
4. Chemical synthesis of complex glycan thiazoline inhibitor for Endo-S.....	59
5. Inhibitory activity assays for the synthetic thiazoline-based inhibitor .....	61
6. Investigation on non-enzymatic side reactions of glycan oxazoline .....	62
<b>C. Discussion.....</b>	<b>66</b>
<b>D. Conclusion .....</b>	<b>71</b>
<b>E. Materials and Methods.....</b>	<b>72</b>
1. Chemicals and biochemical materials.....	72
2. Mutagenesis, expression, and purification of Endo-S and mutants .....	73

3. Synthesis of deglycosylated antibody by wild-type Endo-S as acceptor substrate for transglycosylation .....	74
4. Synthesis of S <sub>2</sub> G <sub>2</sub> F rituximab by mutant Endo-S D233Q as starting material for hydrolysis assays.....	75
5. Liquid Chromatography-Mass Spectrometry (LC-ESI-MS) analysis of antibody glycoforms .....	75
6. Quantification of hydrolysis and transglycosylation reaction products using internal standard and a single-point normalization factor.....	76
7. Transglycosylation and hydrolysis activity assays for Endo-S mutants.....	76
8. Measurements of K <sub>M</sub> and V <sub>max</sub> of Endo-S mutants for SCT-oxa .....	77
9. Measurements of K <sub>M</sub> and V <sub>max</sub> of Endo-S mutants for antibody.....	78
10. Chemical synthesis of complex glycan-based thiazoline inhibitor.....	78
11. Inhibition assays of thiazoline glycan inhibitor against ENGases.....	79
12. Comparison of non-enzymatic glycosylations by enzyme treatment. ....	80
<b>F. Supporting Information.....</b>	<b>82</b>
Chapter 3: Development of alternative antibody glycoengineering methods with relaxed substrate specificity for different glycan structures .....	
	83
<b>A. Introduction.....</b>	<b>83</b>
<b>B. Results .....</b>	<b>87</b>
1. Cloning, expression, and characterization of Endo-S2.....	87
2. Generation of glycosynthase mutants of Endo-S2.....	87
3. Generation and comparative studies on the hydrolytic and transglycosylation activities of 19 glycosynthase mutants and wild-type enzyme of Endo-S2....	88

4. Enzyme kinetic parameters of Endo-S2 D184M and Endo-S2 D184A.....	92
5. Endo-S2 D184M showed relaxed glycan substrate specificity.....	94
6. Transglycosylation of different N-glycans by Endo-S2 D184M.....	97
7. Transglycosylation efficiencies of Endo-S2 and Endo-S mutants.....	98
8. Antibody transglycosylation using reduced amount of glycan oxazoline. ...	100
9. Endo-S hydrolysis of antibody glycoforms and N-glycan oxazolines.....	102
10. Endo-S transglycosylation of antibody with additional glycans.....	106
11. One-pot glycosylation remodeling of rituximab via wild-type Endo-S.....	109
12. One-pot glycosylation remodeling of commercial antibody with modified glycan oxazolines by wild-type Endo-S .....	112
<b>C. Conclusion .....</b>	<b>115</b>
<b>D. Materials and Methods.....</b>	<b>118</b>
1. Chemical and biochemical materials .....	118
2. Expression and purification of Endo-S WT and Endo-SD233Q .....	118
3. Mutagenesis, expression, and purification of Endo-S2 and mutants .....	119
4. Liquid Chromatography Mass Spectrometry (LC-ESI-MS) analysis.....	120
5. HPAEC-PAD analysis of glycans and oxazolines.....	121
6. Comparison of Endo-S hydrolysis against rituximab N-glycoforms.....	122
7. Comparison of Endo-S hydrolysis towards different oxazolines .....	122
8. Evaluation of Endo-S transglycosylation on deglycosylated rituximab using SCT-Oxa, HM-Oxa and Hyb-Oxa as glycosyl donors. ....	122

9. Evaluation of transglycosylation activities of Endo-S WT and Endo-S D233Q towards deglycosylated rituximab antibody using HM-Oxa 5 and Hyb-Oxa 6 as glycosyl donors.....	123
10. Transglycosylation of rituximab with Hyb-Oxa and HM-Oxa by Endo-S WT in a one-pot manner. ....	124
11. Transglycosylation of rituximab with Man <sub>3</sub> -Oxa and AzideMan <sub>3</sub> -Oxa by Endo-S WT in a one-pot fashion. ....	124
<b>E. Supporting Information.....</b>	<b>125</b>
Chapter 4: Revisiting the substrate specificity of endoglycosidase Endo-CC and its mutants in hydrolysis and transglycosylation.....	
	126
<b>A. Introduction.....</b>	<b>126</b>
<b>B. Results and Discussions .....</b>	<b>131</b>
1. Cloning, expression, and comparison of recombinant Endo-CC and Endo-CC fusion protein (CPD).....	131
2. Generation of glycosynthase mutants from recombinant Endo-CC .....	133
3. Substrate specificity of Endo-CC in hydrolysis of glycoproteins.....	135
4. Studies on the substrate specificity of Endo-CC in transglycosylation .....	140
<b>C. Conclusion .....</b>	<b>146</b>
<b>D. Materials and Methods.....</b>	<b>147</b>
1. Chemical and biochemical materials .....	147
2. Mutagenesis, expression, and purification of recombinant Endo-CC .....	148
3. Transglycosylation using wild-type Endo-CC and its mutants.....	149
4. Transglycosylation by Endo-CC N180H with different N-glycans.....	149

5. Enzymatic deglycosylation of ribonuclease B .....	150
6. Enzymatic deglycosylation of sialylglycopeptide (SGP) with and without the core fucose .....	150
7. Differential deglycosylation of erythropoietin (EPO) containing a mixture of core-fucosylated and non-fucosylated N-glycans .....	151
8. Differential deglycosylation of antibody glycoforms with core-fucosylated, non-fucosylated complex type, and high-mannose N-glycans. ....	151
9. Differential transglycosylation of deglycosylated antibody by wild-type Endo- CC and Endo-CC N180H.....	152
<b>E. Supporting Information.....</b>	<b>153</b>
Chapter 5: Glycosylation remodeling of IgE antibody and effects of Fc N-glycans on FcεR binding.....	
	154
<b>A. Introduction.....</b>	<b>154</b>
<b>B. Results and Discussion.....</b>	<b>158</b>
1. Selective glycosylation remodeling of commercial and recombinant full- length IgE antibodies and binding analyses on IgE N-glycoforms.....	158
2. Generation of the mutant IgE-Fc containing only one oligomannose N-glycan with comparable FcεRI-binding capacity to full-length IgE. ....	163
3. Generation of IgE-Fc oligomannose glycoforms using enzymatic modification and biosynthetic engineering and their binding properties to FcεRI. ....	164
4. Glycosylation remodeling of IgE-Fc-Asn394only showed limited impact on binding capacity to low-affinity IgE receptor, CD23 (FcεRII).....	174

5. Chemoenzymatic glycosylation remodeling of IgE-Fc with complex N-glycan using the active glycosyl oxazoline and glycosynthase mutants .....	179
<b>C. Conclusion .....</b>	<b>187</b>
<b>D. Materials and Methods.....</b>	<b>189</b>
1. Mammalian cell culture: cell lines, strains and expression conditions .....	189
2. Expression, purification and characterization of recombinant endoglycosidases Endo-CC, Endo-M, Endo-S and Endo-S2 and glycosynthase mutants .....	189
3. Site-specific glycan remodeling of full-length IgE antibodies .....	190
4. Deglycosylation of high-mannose IgE-Fc-Asn394only-HM to afford IgE-Fc-Asn394only-GlcNAc intermediate and IgE-Fc-Asp394.....	190
5. Generation of glycoforms IgE-Fc-Asn394only-Man <sub>5</sub> and IgE-Fc-Asn394only-Man <sub>4-7</sub> N-glycoforms by enzymatic modifications .....	191
6. MALDI-TOF mass spectrometry.....	191
7. Surface Plasmon Resonance (SPR) .....	192
8. Assay for hydrolytic activities of Endo-CC, Endo-S, Endo-S2 and Endo-M against recombinant IgE-Fc-Asn394only-HM .....	192
9. Glycan remodeling of deglycosylated IgE-Fc-Asn394only to a homogenous galactosylated complex type (G2-CT) N-glycoform .....	193
<b>E. Supporting Information.....</b>	<b>194</b>
Chapter 6: Summary and future directions .....	195
Bibliography .....	204

## List of Tables

Table 1. Comparison of specific transglycosylation efficiencies of Endo-S mutants measured by LC-ESI-MS using a commercial antibody rituximab as substrate .....	56
Table 2. Kinetic parameters of Endo-S mutants D233M and D233A for SCT-Oxa ..	58
Table 3. Kinetic parameters of Endo-S mutants D233M and D233A for rituximab ..	58
Table 4. Comparison of the specific hydrolytic activities of Endo-S2 D184 mutants using the synthetic complex type rituximab (S <sub>2</sub> G <sub>2</sub> -rituximab) as starting material....	90
Table 5. Comparison of specific transglycosylation activity of Endo-S2 D184 mutants using glycan oxazoline as donor and deglycosylated rituximab as acceptor .....	91
Table 6. Kinetic parameters of Endo-S2 D184M and D184A for SCT-Oxa.....	93
Table 7. Kinetic parameters of Endo-S2 D184M and D184A for rituximab.....	93
Table 8. Kinetic parameters and binding affinities of commercial and recombinant anti-OVA IgE antibodies binding to FcεRIα obtained from SPR analysis.....	162
Table 9. Kinetics and binding affinities of IgE-Fc N-glycoforms for FcεRI.....	173
Table 10. Kinetic parameters of IgE-Fc-Asn394only N-glycoforms with immobilized soluble domain of IgE-Fc low-affinity receptor CD23 measured by SPR. ....	178

## List of Figures

Figure 1. Market of monoclonal antibody therapeutics between 2002 and 2017.....	3
Figure 2. A schematic representation of genetic and structural elements for a typical immunoglobulin molecule.....	5
Figure 3. Overall structural arrangements of immunoglobulin classes and subclasses with glycosylation distributions highlighted.....	8
Figure 4. A simplified representation of the five major classes of glycosidic linkages found in protein glycosylation .....	9
Figure 5. A simplified 3D structure of a IgG antibody with N-glycans attached at a conserved glycosylation site Asn-297 in C <sub>H</sub> 2 domain of IgG-Fc region.....	12
Figure 6. Selected N-glycoforms detected at Asn297 site of IgG–Fc domain. ....	15
Figure 7. Biosynthetic pathway of (a) N-glycoproteins in eukaryotic cells and (b) GDP-l-fucose in mammalian cells.....	19
Figure 8. Glycoengineering methods to produce both low-fucose or nonfucosylated monoclonal antibodies <i>in vivo</i> . ....	22
Figure 9. General concepts of ENGase-mediated glycosylation remodeling strategy of (a) glycoproteins and (b) glycopeptides.....	25
Figure 10. Crystal structure of endoglycosidase Endo-A (PDB: 3FHA).....	26
Figure 11. Catalytic mechanisms of the ENGases showing key catalytic residues for some enzymes from: (a) family GH18 and (b) family GH85.....	29
Figure 12. Mechanism-based design of mutant glycosynthases of ENGases.....	31
Figure 13. Selected examples of antibody glycan remodeling using ENGases.....	33

Figure 14. Glycosylation remodeling of IgG antibody rituximab using Endo-S and Endo-S glycosynthase mutants .....	35
Figure 15. Glycoengineering of a core-fucosylated therapeutic antibody rituximab..	46
Figure 16. Chemoenzymatic remodeling of core fucosylated antibody rituximab to a non-fucosylated G2 glycoform using $\alpha$ -fucosidase and Endo-S mutants.....	47
Figure 17. The general procedure of site-directed saturation mutagenesis of Endo-S using degenerate primers. ....	51
Figure 18. Schematic presentation of hydrolysis and transglycosylation reactions by Endo-S and its mutants using antibody rituximab as starting material.....	53
Figure 19. Comparison of transglycosylation reactions catalyzed by Endo-S D233M and previously reported Endo-S D233Q and D233A mutants.....	55
Figure 20. Michaelis-Menten plots of Endo-S D233M and Endo-S D233A.....	59
Figure 21. The chemical structure of the complex type N-glycan oxazoline (1) and the corresponding complex type N-glycan thiazoline (2).....	60
Figure 22. Inhibition effects of Endo-S, Endo-S2, and Endo-M by CT-thiazoline ....	62
Figure 23. Mass spectrometry analysis of antibody N-glycoforms generated by glycan remodeling of a therapeutic antibody trastuzumab (Herceptin). ....	64
Figure 24. Non-enzymatic transfer of sialylated complex type glycan oxazoline to deglycosylated trastuzumab antibody in the absence of Endo-S enzymes.....	65
Figure 25. Molecular mechanism of Endo-S based on co-crystallized structure with the G2 glycan substrate.....	68
Figure 26. Sequence alignment of Endo-S2 and Endo-S.....	88

Figure 27. Schematic presentation of hydrolysis and transglycosylation by Endo-S2 and its mutants using rituximab as substrate.....	89
Figure 28. Michaelis-Menten curves of Endo-S2 D184M and D184A .....	93
Figure 29. Evaluation of substrate specificity of Endo-S2 D184M on different glycan structures (HM, CT, and Hyb type).....	96
Figure 30. Comparison of Endo-S2 D184M-catalyzed transglycosylation reactions with different N-glycans. ....	98
Figure 31. Comparison of transglycosylation reactions catalyzed by selected mutants Endo-S2 D184Q, Endo-S2 D184M, and Endo-S D233Q.....	100
Figure 32. Transglycosylation of antibody with reduced oxazoline substrate at different Endo-S D184M concentrations.....	101
Figure 33. Structures of rituximab N-glycoforms and N-glycan oxazolines used for the assessment of Endo-S activity.....	103
Figure 34. Hydrolytic activity of Endo-S WT on different antibody N-glycoforms and oxazolines. ....	105
Figure 35. Endo-S-catalyzed transglycosylation reactions with oxazolines SCT-Oxa, HM-Oxa, Hyb-Oxa of deglycosylated rituximab .....	108
Figure 36. One-pot glycosylation remodeling of commercial rituximab to give rise to hybrid and high-mannose rituximab N-glycoforms, Hyb-RTX and HM-RTX .....	110
Figure 37. Endo-S WT-catalyzed one-pot transglycosylation reactions with mannose (HM-Oxa <b>5</b> ) and hybrid (Hyb-Oxa <b>6</b> ).....	111
Figure 38. Endo-S WT-catalyzed one-pot transglycosylation reactions with the chemically modified glycan oxazoline. ....	114

Figure 39. Hydrolysis of glycoprotein RNase B by recombinant Endo-CC and Endo-CC fusion protein (CPD)..	132
Figure 40. Transglycosylation of deglycosylated RNase B by recombinant Endo-CC and Endo-CC (CPD)..	135
Figure 41. Comparison of Endo-CC-catalyzed hydrolysis against fucosylated and non-fucosylated sialoglycoprotein (SGP)	137
Figure 42. Selective deglycosylation of non-fucosylated N-glycans by Endo-CC from the heterogeneous N-glycoforms of erythropoietin (EPO).	138
Figure 43. Selective removal of non-fucosylated IgG N-glycans by Endo-CC.	139
Figure 44. Comparison of transglycosylation efficiency of Endo-CC N180H for three major types of N-glycan oxazolines.	141
Figure 45. Comparison of transglycosylation reactions catalyzed by selected Endo-CC mutants.	143
Figure 46. Transglycosylation reactions for deglycosylated antibody by Endo-CC and Endo-CC N180H enzymes at varied concentrations.	145
Figure 47. Site-selective N-glycosylation remodeling of the full-length human IgE antibodies using endoglycosidase Endo-H.	160
Figure 48. Surface plasmon resonance (SPR) representative sensorgrams of binding between full-length IgE antibodies and immobilized soluble domain of high-affinity IgE receptor FcεRI	161
Figure 49. Glycan remodeling of oligomannose IgE-Fc-Asn394only-HM (Man <sub>5-9</sub> ) using a combination of glycan remodeling strategies	164

Figure 50. MALDI-TOF mass spectrometry identification of released N-glycans from IgE-Fc-Asn394only N-glycoforms generated through glycan remodeling .....	166
Figure 51. Schematic representation of the substrate specificity of $\alpha$ 1-2 and $\alpha$ 1-2, 3, 6 mannosidase against differentially linked mannose residues of the high-mannose Asn-linked oligosaccharides in glycoproteins .....	169
Figure 52. Surface plasmon resonance (SPR) representative sensorgrams of binding events analyzed between remodeled IgE-Fc-Asn394only glycoforms and immobilized soluble domain of high-affinity IgE receptor Fc $\epsilon$ RI .....	172
Figure 53. Representative surface plasmon resonance (SPR) sensorgrams of binding between homogeneous IgE-Fc-Asn394only N-glycoforms and immobilized soluble domain of IgE-Fc low-affinity receptor CD23/ Fc $\epsilon$ R2 .....	177
Figure 54. Hydrolytic selectivities of ENGase Endo-S, Endo-S2, Endo-M and Endo-CC against high-mannose IgE-Fc-Asn394only-HM (Man <sub>5-9</sub> ) N-glycoforms.. .....	181
Figure 55. Comparison of enzymatic hydrolysis on native IgE-Fc-Asn394only-HM (Man <sub>5-9</sub> ) N-glycoforms by Endo-CC, Endo-M, Endo-S, and Endo-S2. ....	182
Figure 56. Transglycosylation of IgE-Fc-Asn394only-GlcNAc with galactosylated complex type glycan oxazoline (CT-Oxa) using Endo-CC N180H. ....	184
Figure 57. Synthesis of IgE-Fc-Asn394only-CT (G2) N-glycoform and its binding properties for high-affinity receptor Fc $\epsilon$ RI .....	186
Figure 58. Design for therapeutic intervention as IgE replacement therapy using a combination of anti-IgE antibodies and glycoengineered IgE-Fc. ....	203

## List of Abbreviations

3D	Three-dimension
ADC	Antibody-drug conjugates
ADCC	Antibody-dependent cellular cytotoxicity
CBP	Carbohydrate-binding proteins
CD	Cluster of differentiation
CDC	Complement-dependent cytotoxicity
CDG	Congenital disorders of glycosylation
CDR	Complementarity-determining regions
DiAcTridH	2,4,-diacetamido 2,4,6-trideoxyhexose
EMA	European Medicines Agency
ENGase	Endo- $\beta$ -N-acetylglucosaminidases
EPO	Erythropoietin
ESI	Electrospray Ionization
Fab	Antigen-binding fragment
Fc	Crystallizable fragment
Fc $\alpha$ R	Fc alpha receptor
Fc $\gamma$ R	Fc gamma receptor
FDA	Food and Drug Administration
Fmoc	Fluorenylmethyloxycarbonyl chloride

FUT	$\alpha$ 1,6-fucosyltransferase
GnT	Glycosyltransferase
GPI	Glycosylphosphatidylinositol
HM	High-mannose
HPAEC-PAD	High-Performance Anion-Exchange Chromatography Coupled with Pulsed Amperometric Detection
HPLC	High-performance liquid chromatography
Hyb	Hybrid
Ig	Immunoglobulin
MAb	Monoclonal antibody
MeCN	Acetonitrile
MS	Mass spectrometry
OST	Oligosaccharyltransferase
PBS	Phosphate Buffered Saline
RNase B	Ribonuclease B
RTX	Rituximab
SCT	Sialylated complex type
SGP	Sialylated glycoprotein
Tris	Tris(hydroxymethyl)aminomethane

## Chapter 1: Introduction

### **A. Introduction to antibodies**

#### 1. Monoclonal antibody-based therapeutics

The monoclonal antibodies (mAb) represent one of the most important classes of biopharmaceutical treatments for a variety of health conditions.<sup>1</sup> Since the licensing of the first therapeutic mAb muromonab-CD3 (under trade name Orthoclone OKT3) in 1986,<sup>2</sup> over seventy mAb and mAb-based proteins, including the antibody fragments, antibody-drug conjugates and crystallizable fragment (Fc) fusion proteins, have been approved for clinic use by either the Food and Drug Administration (FDA) in the United States (US) or the European Medicines Agency (EMA) in the European Union (EU).<sup>1</sup> The annual approval rate for mAb-related therapeutics has also significantly increased over the past decade (Figure 1A). Based on public reports released by the FDA and EMA, a total of 35 new mAbs were granted a first approval between 2012 and 2017 with an average of 5.8 approvals per year, whereas only an average of 1.6 mAb-based therapeutics were approved annually during 2002-2011.<sup>3</sup>

The first therapeutic mAb, called muromonab-CD3, was prescribed as an anti-rejection therapy to treat kidney failure caused by organ transplant rejection.<sup>2</sup> The therapeutic mAbs are now applied to treat a diverse range of disease targets, including various types of malignancies/cancers, inflammatory and cardiovascular disorders, and infectious diseases (Figure 1B). The manufacturing systems for monoclonal antibodies have also undergone significant changes since 1986 to improve the safety

and efficacy of antibody products, starting from the murine system to the chimeric and finally the fully humanized production.<sup>4</sup>

Despite their successes in the clinic, the cost-effectiveness issue of antibody therapeutics has limited their development and prevented new beneficial drugs from being readily accessible to the general population worldwide.<sup>5</sup> Recently, there has been a growing interest in the pharmaceutical industry in developing “biosimilar” antibodies as affordable alternatives to reduce the costs and potentially improve the clinical performance of many antibody-based therapeutics. Recent research progress in protein engineering and post-translation modifications has driven new designs of “biobetter” antibodies that demonstrated enhanced therapeutic outcomes and reduced side effects when compared with their parent antibody molecules.<sup>5</sup> Such efforts are represented by the ongoing development of antibody-drug conjugates (ADCs) and multi-specific antibodies against various cancers and viral infections.<sup>6</sup> Improvements in the manufacturing process of antibodies, such as expression system and purification protocol, and more stringent quality controls are urgently needed to facilitate the development of more efficient antibody products. For instance, research into the degradation and recycling mechanisms of antibody proteins are contributing to the development of mAbs with prolonged serum half-life.<sup>7</sup> In addition, recent studies on the site-specific modifications of antibodies by both chemical and enzymatic methods are currently being explored to improve the delivery and effector functions of several important classes of antibody-based therapeutics, which will be discussed in detail in the following sections.<sup>8</sup>

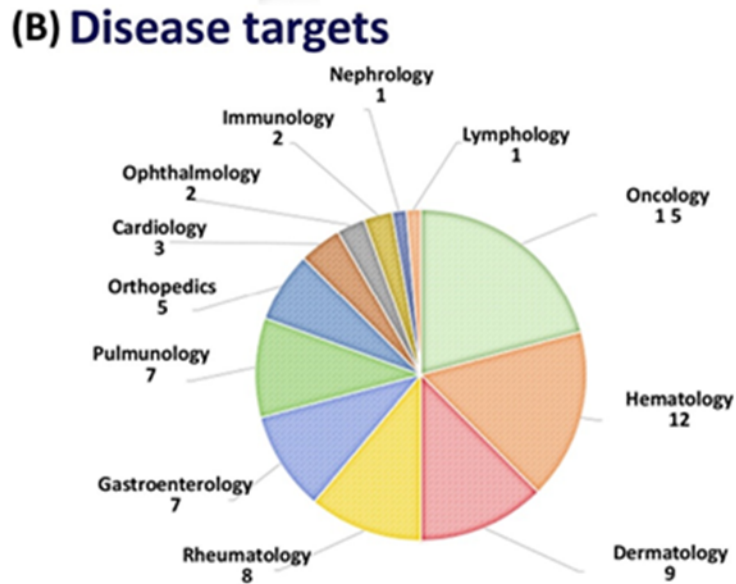
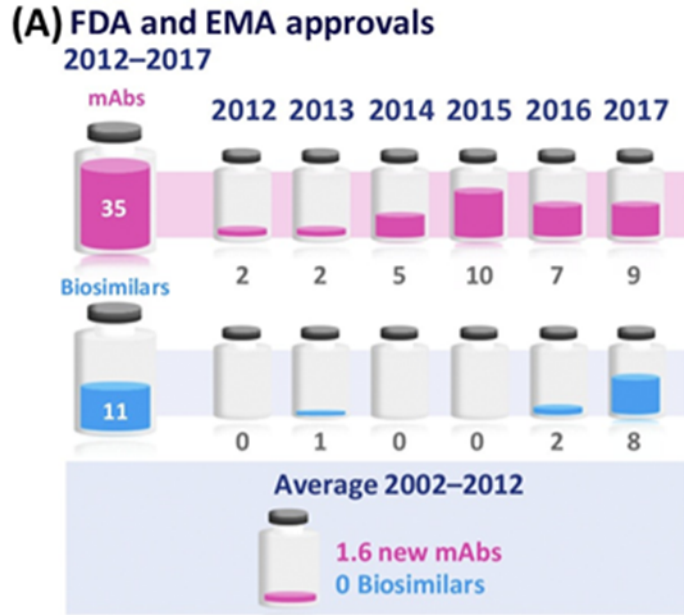


Figure 1. Market analysis of monoclonal antibody-related therapeutics between 2002 and 2017. (A) Trend of the number of mAb products approved annually by the FDA and EMA between 2002 and 2017. (B) Distribution of disease indications targeted by antibody therapeutics. Therapeutic mAbs are now prescribed for a variety of health conditions. Oncology and hematology remain the disease areas most targeted by mAbs according to the public reported data by the FDA and EMA.<sup>3</sup>

## 2. Overview of antibody structure and function

Antibodies, also known as immunoglobulins (Igs), are soluble biomolecules generated by the immune system to specifically recognize and neutralize foreign pathogens and toxins during activation of an immune response.<sup>9</sup> The immunoglobulin is typically a multi-subunit heterodimer that consists of four polypeptides, including two identical light (L) chains and two identical heavy (H) chains linked by multiple disulfide linkages (Figure 2). The structural components of each light (L) and heavy (H) chain are further functionally divided into the “variable” (V) and “constant” (C) domains located at the NH<sub>2</sub>- and COOH-terminus of the heavy chain, respectively. The V domains from both H and L chains of antibody are responsible for recognizing the pathogens through binding to foreign structures called antigens with high affinity and selectivity, whereas the constant (C) domains from H chains mediate the effector functions of immunoglobulins by interacting with the other components of the host immune system.<sup>10</sup>

### 2.1. Immunoglobulin fold: the basic building block of antibody structure

The overall structural arrangement of immunoglobulin is highly conserved across a large protein family called the immunoglobulin superfamily (IgSF), and the conserved Ig domain can be found in many proteins whose functions are related to the immune system.<sup>11</sup> These proteins typically adopt a common conformation known as the immunoglobulin fold, which is composed of a  $\beta$ -sandwich framework connected by disulfide bonds and multiple loop structures. A pair of pleated  $\beta$ -sheets consisting of antiparallel  $\beta$ -strands form the hydrophobic core of the  $\beta$ -sandwich. The unique

conformation of the immunoglobulin fold contains several structural features that are necessary for antibody molecules to efficiently regulate the immune response, which are discussed in detail below.<sup>12</sup>

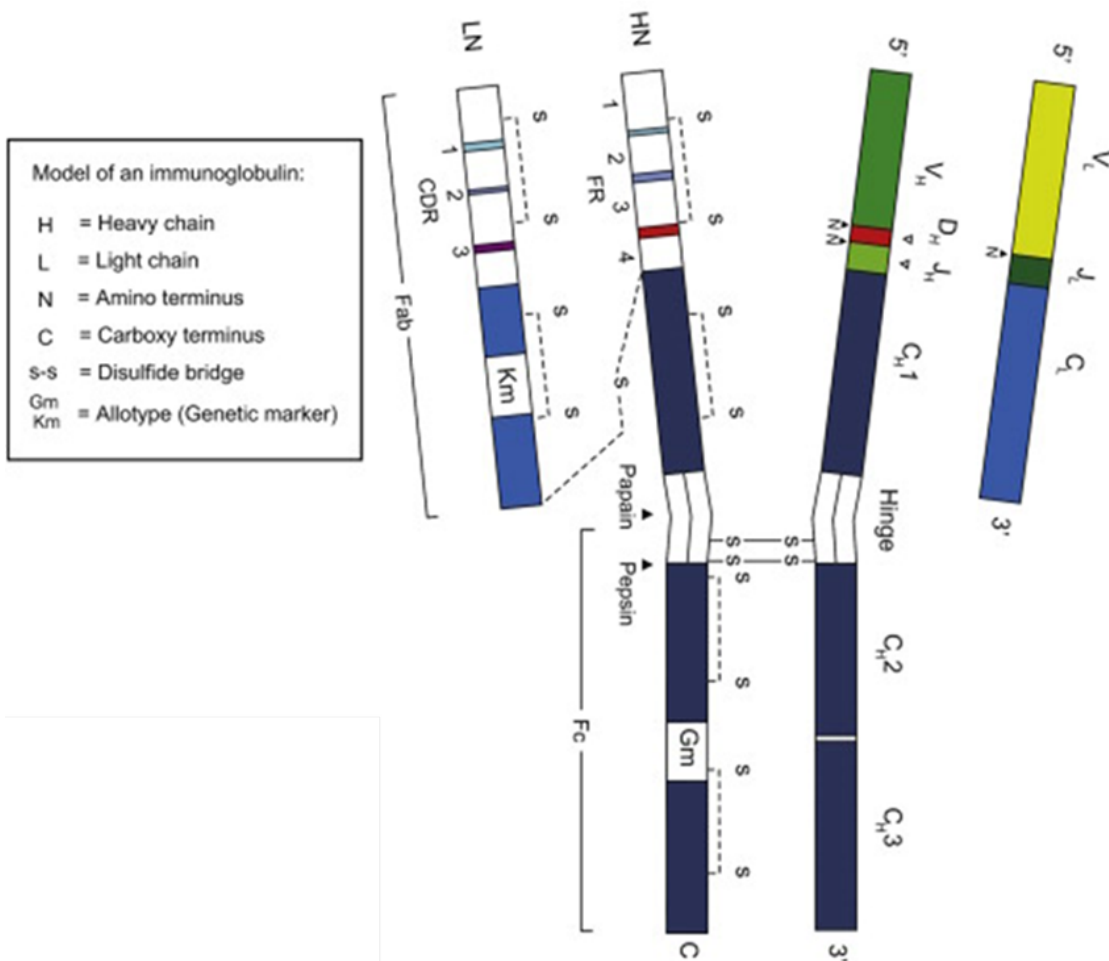


Figure 2. A schematic representation of genetic and structural elements for a typical immunoglobulin molecule. The genetic segments of H and L chains are illustrated at the right section of the structure. The amino acid information such as disulfide bonds and functional regions (such as CDR, FR and pepsin-digestion sites) are shown at the left section of the antibody scheme.<sup>9</sup>

## 2.2. Hypervariable (V) domain of antigen binding (Fab) fragment and antibody-antigen recognition

An antibody can be cleaved into three functional fragments by protease, which result in two antigen-binding fragments (Fab) that specifically recognize the non-self antigens and one crystallizable fragment (Fc) that modulate effector functions.<sup>13</sup> The Fab consists of a complete L chain and a portion of H chain, whereas the Fc contains the constant domains from both H chains of antibody tetramer. Specific amino acid residues located within the connecting loops at the N-terminus of the Fab variable (V) domain form the binding pocket for antigen recognition. These regions, also known as the complementarity-determining regions (CDRs), are intrinsically hypervariable. The variability of V domains is the result of a series of genetic regulatory events, including gene segment organization and rearrangement, somatic hypermutation, and affinity maturation.<sup>14</sup> This hypervariability provide the molecular basis for antibodies to recognize an extremely diverse range of antigens with high selectivity. The complementarity-determining regions of L and H chains together contribute to the antigen-binding site of each Fab domain of antibody.

## 2.3. Constant (C) domain of crystallizable fragment (Fc) and antibody Fc receptors

The isotypes and subclasses of an antibody are determined by constant domains of its heavy chains. Based on this classification, there are five antibody isotopes found in human circulation, including IgG, IgM, IgD, IgE, and IgA, each of which embodies unique structural properties and biological functions.<sup>15</sup> As illustrated in Figure 3, in IgA, IgD and IgG, a flexible “hinge region” with no defined secondary

structure connects their Fc and Fab fragments, whereas this region is replaced by a more rigid Ig domain in IgE and IgM.<sup>16, 17</sup> The Fc fragments of immunoglobulins modulate immune responses primarily through interactions with a variety of antibody Fc receptors found on the surface of cells associated with immune regulation.<sup>18</sup> These receptors serve as the mediators between the humoral adaptive immune response and the innate immune machinery.<sup>19</sup> The overall efficacy of an antibody-mediated immune response is largely dependent on the relative abundance of these Fc receptors on the immune cell surface, and an accurate regulation of the antibody/receptor interactions plays an important role in mounting an effective immune response against various types of infectious agents.<sup>20</sup> Therefore, alteration in the structural compositions of antibody Fc domains can have profound impact on the immunoregulatory activity of antibodies and, as a result, the neutralization of foreign pathogens and infected cells.

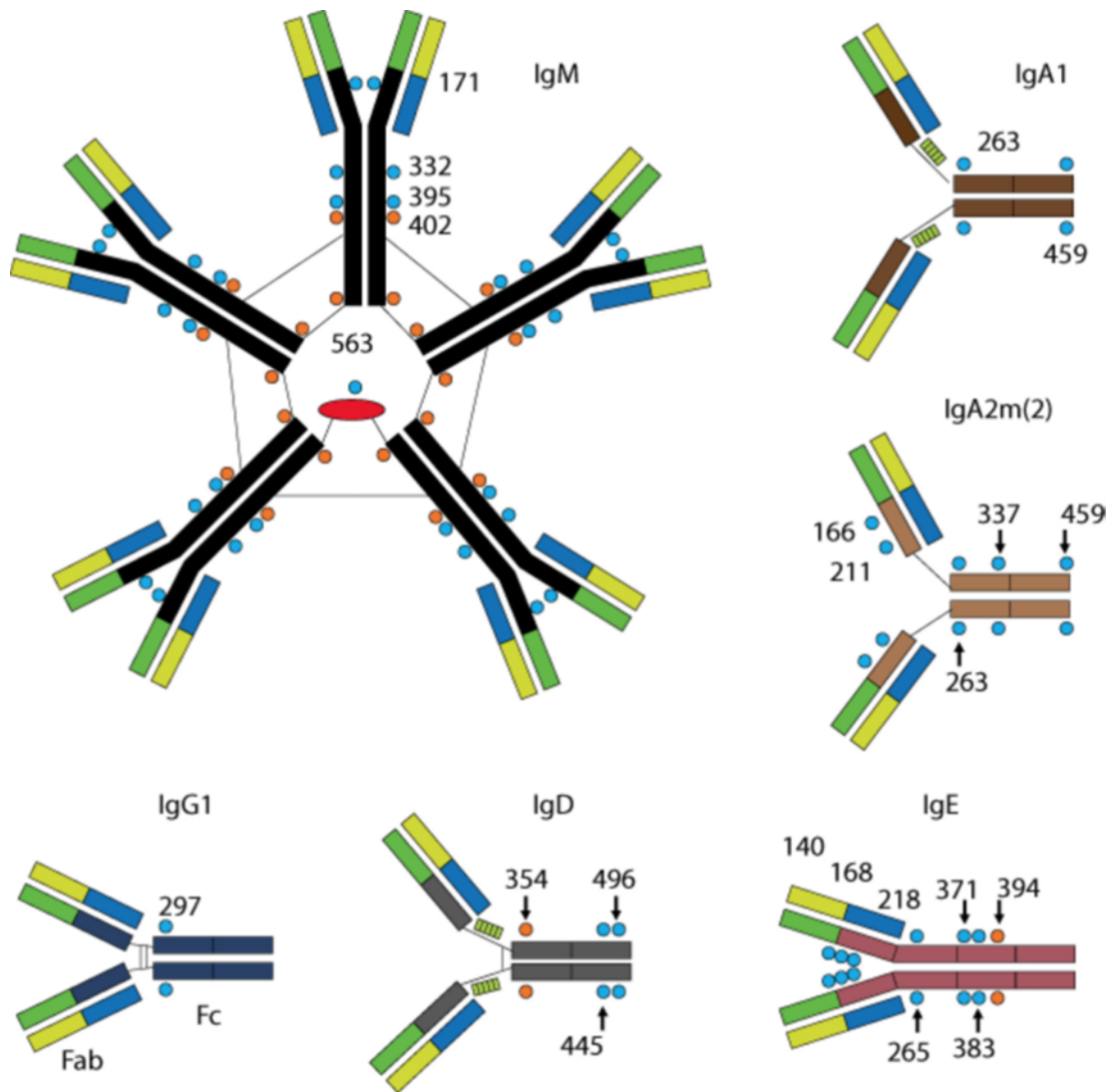


Figure 3. Overall structural arrangements of immunoglobulin classes and subclasses with glycosylation distributions highlighted. For IgM, a joint chain (J chain) protein is also marked in red. The J chain polypeptide is required for the IgM to be secreted into mucosa. The conserved glycosylation sites of each antibody isotype are marked at the amino acid residues where N-glycans are covalently attached.<sup>21</sup>

## B. Antibody glycosylation and its importance in biological functions

The covalent linkages between sugars and amino acid residues comprise one of the most ubiquitous post-translation modifications of proteins in nature. A series of enzymatic modifications on the protein-associated carbohydrate structures lead to the biosynthesis of a large collection of glycoproteins with diverse biological functions.<sup>22</sup> These processes can be found across the entire phylogenetic spectrum, from bacteria and Archaea to higher eukaryotes. Depending on the specific amino acid residues and monosaccharides involved in forming the glycosidic linkages, more than 40 types of glycosidic bond can be found in proteins with unique anomeric configurations, which can be divided into different types of glycosylation: the N (Asn)-, O (Ser/Thr)- and C (Trp)-linked glycans, glypiation, and phosphoglycosylation (Figure 4).<sup>23</sup>

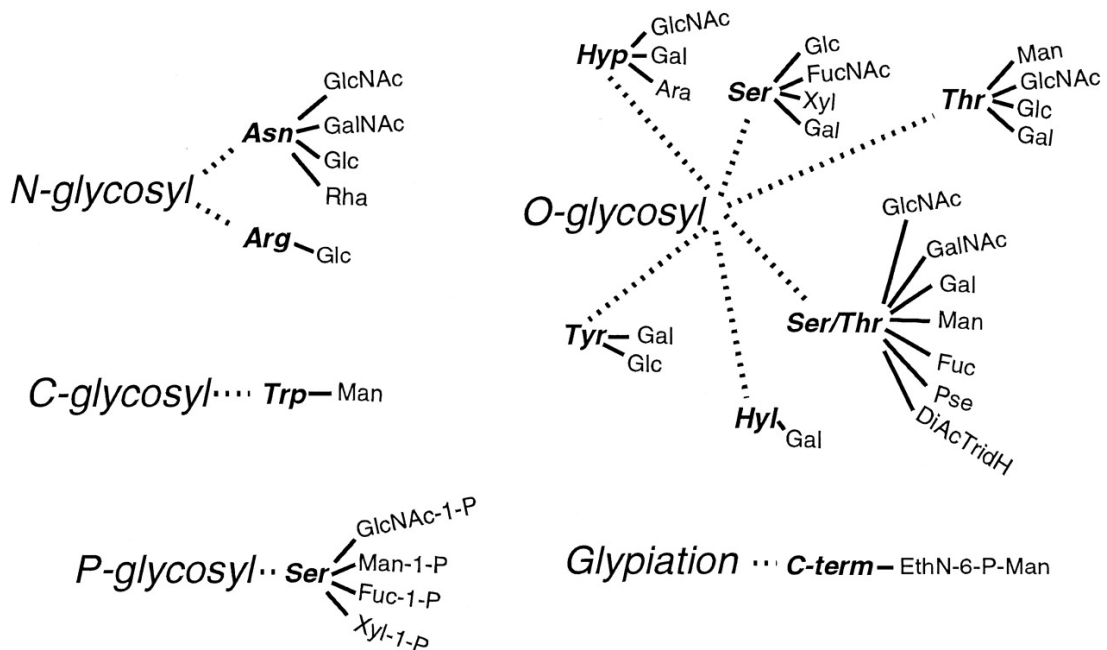


Figure 4. A simplified representation of the five major classes of glycosidic linkages found in protein glycosylation. The DiAcTridH refers to the 2,4,-diacetamido 2,4,6-trideoxyhexose, and the C-term refers to the carboxy-terminal group.<sup>24</sup>

## 1. Structure and functional diversity of antibody glycosylation

Antibodies are glycosylated proteins, and the location and relative abundance of oligosaccharides attached to the Fc and Fab regions of antibodies vary significantly among the immunoglobulin isotypes (Figure 3).<sup>25</sup> Both N- and O-linked glycans can be found on the Fc, Fab and hinge regions of antibodies. Up to 15% of the molecular weight of an antibody (~150 kDa) can be contributed by multiple N-glycans (~ 2 kDa) attached to each of the heavy chains, whereas no conserved glycosylation sites can be found on the light chains. These associated oligosaccharides, if not contacted by the surrounding amino acid residues, are typically not rigid and adopt a dynamic structure due to the flexible N-glycosidic linkages.<sup>26</sup>

The biological functions of antibody N-glycans are multifaceted, ranging from maintaining the structural integrity of antibody to participating in binding of antibody with other mediators such as lectins and immunoglobulin receptors.<sup>27-30</sup> Some of the most important functions of antibody N-glycans include: extending the serum half-life; facilitating the cellular transport, secretion and endocytosis; and regulating the effector functions by recruiting other immune components to the site of infections. In addition to the direct effects of N-glycosylation on antibody structure and function, the aberrant glycosylation pattern of certain serum immunoglobulins are associated with various underlying diseases, including rheumatoid arthritis, Berger's disease, and congenital disorders of glycosylation (CDGs).<sup>31</sup> Other aspects of antibody functions, including the Fab-mediated antigen recognition, can also be affected by antibody glycosylation. For instance, the neutralization activity of certain anti-HIV antibodies was found to be associated with their glycosylation profiles at the Fab region, and a

non-neutralizing anti-HIV antibody acquired potent antiviral activity when produced in an engineered expression system that optimized the glycosylation profile of the proteins produced. It was therefore suggested that the Fab-glycans of antibody could facilitate neutralization of HIV viruses by blocking their entry into the host cells.<sup>32</sup>

## 2. Glycosylation modulates effector functions of IgG and IgE antibodies

Currently, all approved antibody therapeutics are based on the IgG isotype, which accounts for approximately 70%-75% of the human antibodies secreted into the bloodstream daily.<sup>33</sup> Human IgG antibodies typically contain the biantennary complex-type N-linked oligosaccharides based on a heptasaccharide core structure composed of mannoses (Man) and N-acetylglucosamines (GlcNAc) at the conserved Asn-297 residue within the CH<sub>2</sub> domains of the Fc region (Figure 5).<sup>34</sup> Studies demonstrate that the N-glycans are crucial in maintaining the IgG conformation,<sup>35</sup> and the carbohydrates attached at this site could be recognized as molecular epitopes for carbohydrate-binding proteins (CBPs) such as lectins and other regulatory factors associated with immune system.<sup>36</sup>

Glycosylation patterns of IgG can have a profound impact on its interactions with receptors and factors involved in immune regulation. For instance, the binding affinity of IgG for the Fc gamma receptor FcγR was significantly reduced when the conserved glycosylation site is removed by mutagenesis, which confirmed that this N-glycan was necessary for the optimal binding between IgG and FcγRs.<sup>29</sup> However, this phenomenon was not observed between IgA and the Fc alpha receptors (FcαRs),

as recombinant IgA binds to Fc $\alpha$ Rs regardless of the presence of its conserved N-glycans.<sup>37</sup>

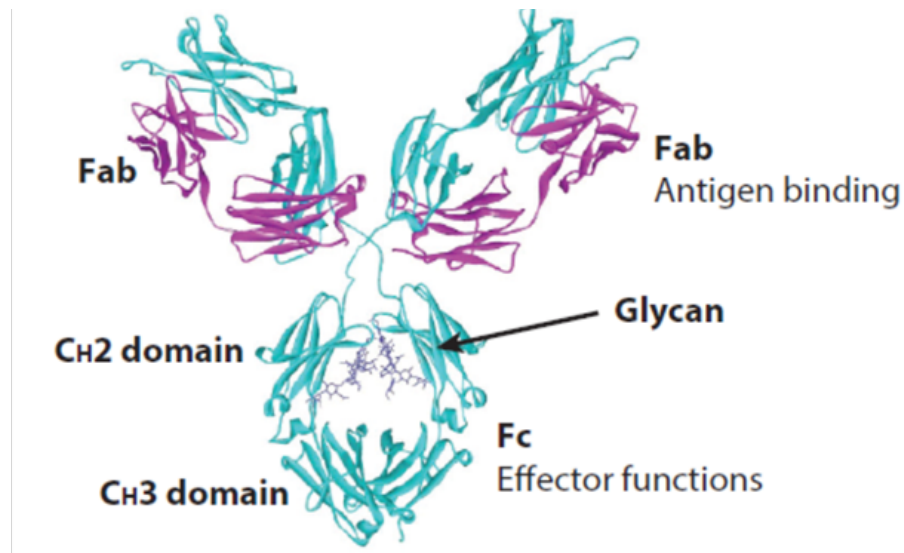


Figure 5. A simplified 3D structure of a typical IgG antibody with N-glycans attached at a conserved glycosylation site Asn-297 in the C<sub>H2</sub> domain of the IgG-Fc region. The diagram shown here is based on the structure of a human IgG (PDB: 1HZH). The alpha backbone of heavy chains and light chains of antibodies are shown in cyan and purple, respectively, and the Fc glycans are colored in navy blue.<sup>38</sup>

One of the major mechanisms by which antibodies control and neutralize pathogenic factors during the humoral immune response is antibody-dependent cellular cytotoxicity (ADCC). Through ADCC, the Fc fragments of IgG in complex with the antigen interact with the Fc $\gamma$ Rs on the surface of effector cells, such as natural killer (NK) cells and eosinophils, to promote the destruction of the antibody-coated targets.<sup>39</sup> Recent studies have further elaborated on the functional role of N-glycans in the Fc $\gamma$ R-receptor binding.<sup>28, 29, 40, 41</sup> For example, the removal of a core fucose monosaccharide from the conserved IgG-Fc N-glycans significantly enhanced

the ADCC activity of several IgG antibodies, which was due to increased binding affinities of the modified IgG-Fc for the Fc $\gamma$ IIIa receptor.<sup>28</sup> This important finding provided the molecular basis for the development of novel antibody therapeutics with a lower core-fucosylation level and better clinic performance in treating various types of malignancy.<sup>42</sup>

Complement-dependent cytotoxicity (CDC) is another critical mechanism of action for antibodies to mediate cellular killing. The common pathway of CDC is initiated by interactions between IgG-Fc and the complement component factor C1q. A complex-type N-glycan consisting of N-acetylglucosamines, galactoses and sialic acids is typically required for the optimal binding between the Fc fragment and C1q as well as the subsequent activation of the rest of the complement machinery.<sup>43, 44</sup>

The human intravenous immunoglobulin (IVIG), when administrated at high dosages, has been successfully applied to treat a number of inflammatory disorders.<sup>45</sup> In contrast to the proinflammatory activities of the IgG N-glycans mentioned above, the terminal  $\alpha$ 2,6-sialic acid found in a small percentage of human IVIG preparations was discovered to be responsible for the anti-inflammatory effects in animal models<sup>46</sup>. It was later proposed that the interactions between the sialylated IgG N-glycoforms and certain sialic acid-binding factors could reduce inflammation by up-regulating the expression of certain inhibitory receptors Fc $\gamma$ Rs.<sup>47-49</sup>

Unlike IgG antibodies, the functional relationship of N-glycosylation and IgE biology largely remains a question to be answered by future studies, even though IgE contains the highest level of N-glycosylation among all monomeric antibody isotypes, with seven conserved N-linked glycosylation sites located in the primary sequence of

its heavy chain.<sup>50-52</sup> However, a recent groundbreaking study on IgE N-glycosylation discovered a single oligomannose N-glycan attached at Asn-394 residue in Fc region of IgE antibody, which was found to be necessary for IgE to mediate the acute allergic response.<sup>53, 54</sup> According to this study, genetic mutations and functional studies all suggested that this unique N-glycan located at Asn-394, which is homologous to the Asn-297 site of IgG antibodies, plays an obligatory role in determining the secondary structure of IgE-Fc region and, as a result, the ability of IgE to interact with its cognate IgE-Fc epsilon receptors (FcεRs) to mediate anaphylaxis. A more comprehensive introduction of IgE N-glycosylation will be given in chapter 5.

### 3. Structural heterogeneity of antibody N-glycans

Analysis of the N-glycan structures of antibodies either extracted from human serum samples or expressed as recombinant proteins have shown extensive structural variations. For purified IgG antibodies, according to X-crystallographic structures, the N-glycans located at the two identical Asn-297 residues of the IgG-Fc homodimer can be significantly different.<sup>55</sup> As illustrated in Figure 6, each Asn-297 residue can be associated with a large collection of oligosaccharides that can be categorized into three major N-glycoforms, IgG-G2, -G1, and -G0. On the basis of the heptasaccharide core, the IgG-G0 contains an additional GlcNAc residue at the terminal position of each of the two branches of the complex N-glycan, which accounts for approximately 35% of total IgG glycoforms found in human serum.<sup>56</sup> Another relatively abundant IgG glycoform (~ 34% of the total serum IgG) is the IgG-G1 form, which has another terminal galactose (Gal) added to one of the two GlcNAc residues of the IgG-G0

glycoform.<sup>57</sup> Finally, the IgG-G2 glycoform contains two galactose residues located at the terminal ends of the IgG-G0 form, which also represents the least abundant IgG N-glycoform in the serum (~17%). The rest of the human serum IgG glycoforms (~14%) undergo further processing by having one or two terminal sialic acid residues linked to the galactose residues of the G1 or G2 forms. Additional variations also come from potential modifications such as core fucosylation (70% of the total IgG glycoforms) and the bisecting GlcNAc (30% of the total IgG glycoforms).<sup>58</sup>

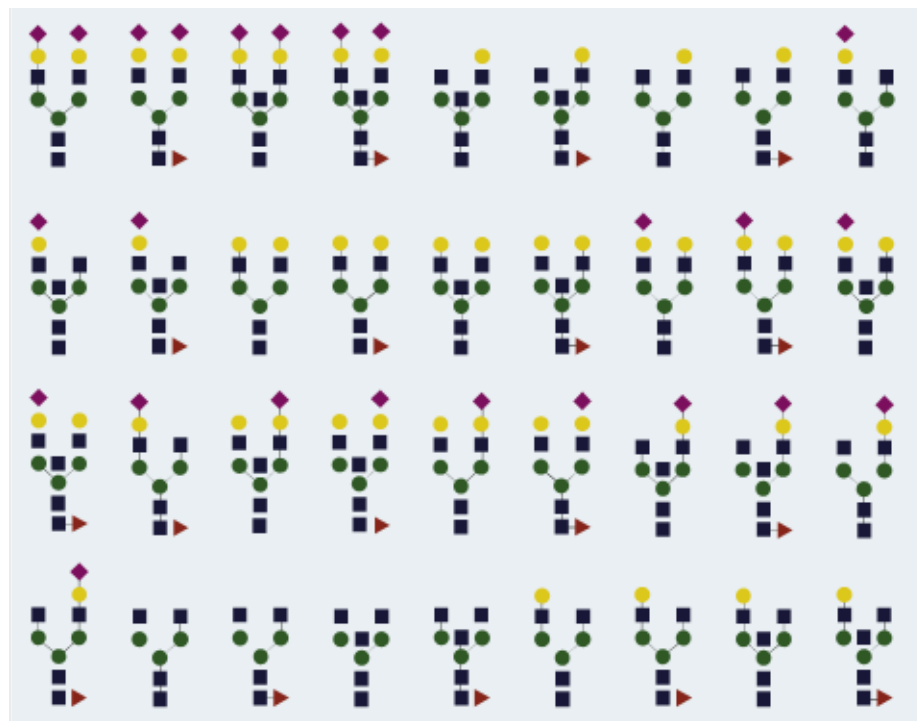


Figure 6. Selected N-glycoforms detected at the Asn297 site of IgG–Fc domain. All symbols of monosaccharide comply with the standard symbol nomenclature for the representing glycans: galactose (Gal) (yellow circle); mannose (Man) (green circle); N-acetylglucosamine (GlcNAc) (blue square); N-acetylneuraminic acid (NeuAc) (purple diamond); fucose (Fuc) (red triangle).<sup>20</sup>

### C. Engineering antibody glycosylation by biosynthetic pathway manipulation

Because the naturally existing and conventionally produced antibodies show a high level of heterogeneity in their N-glycosylation profiles, it has been extremely challenging to obtain the pure or enriched samples of antibody N-glycoforms under normal circumstances.<sup>59-61</sup> As a result, methods to generate homogeneous antibody N-glycoforms containing well-defined N-glycan structures are of high demand both in academia and biopharmaceutical industry.

Therefore, in order to optimize the glycosylation of recombinant antibodies, a number of promising strategies have been developed with success. One approach is to manipulate the biosynthetic pathways of certain N-glycans associated with antibodies *in vivo* by exploiting the enzymes involved in this process.<sup>62</sup> The success of this method has led to the development of monoclonal antibodies with improved clinic performance. However, limitations still exist in this method due to the extremely dynamic and complex cellular environment inherent in the expression systems<sup>62</sup>. Another promising concept for antibody glycoengineering is through *in vitro* chemoenzymatic modifications using various glycan-modifying enzymes combined with chemically modified substrates<sup>63</sup>. This section will highlight several recent examples of progress in antibody glycoengineering based on manipulation of the N-glycan biosynthetic pathways in mammalian cells and other host systems.

## 1. Biosynthetic pathways of N-glycans in eukaryotic expression systems

Production of recombinant antibodies in well-established systems such as the Chinese Hamster Ovary (CHO) and Human Embryonic Kidney (HEK) cells often results in mixtures of different antibody N-glycoforms, which makes it difficult to carry out subsequent functional studies or therapeutic applications.<sup>59</sup> Manipulation in the biosynthetic pathways of protein N-glycans provides an opportunity to control the structural variations of carbohydrate in some expression systems. Specifically, this strategy has been successfully applied to enhance the therapeutic efficacy of certain monoclonal antibody-based therapeutics by optimizing the N-glycosylation patterns.<sup>64</sup>

One of the most successful applications of *in vivo* antibody glycoengineering is the development of antibody variants with reduced or completely abolished core fucosylation. Such studies have attracted tremendous attention in the past decade because of the functional relationship between the core fucosylation and the ADCC effects of IgG antibodies. As mentioned in the previous section, the removal of the core fucose from IgG antibodies can significantly enhance its ADCC activity and the neutralization efficacy against target cells.<sup>28</sup> Perturbation to the biosynthesis of fucose *in vivo* by either genetic interference or manipulation in the expression medium can lead to glycoproteins with a lower core fucosylation level.<sup>65</sup>

To understand the molecular mechanism of this biosynthetic glycoengineering approach, a brief introduction to the general aspects of N-glycoprotein biosynthesis in the eukaryotic system is provided here (Figure 7).<sup>26</sup> The biosynthesis of all eukaryotic N-glycans initially takes place on the cytoplasmic side of the ER membrane, where fourteen monosaccharides are sequentially added to a lipid-phosphate (Dol-P) anchor

to form an oligosaccharide precursor, namely the Dol-P-Glc<sub>3</sub>Man<sub>9</sub>GlcNAc<sub>2</sub>. The complete oligosaccharide is then transferred to an Asn residue within a conserved N-glycosylation sequon (Asn-X-Ser/Thr) of a nascent polypeptide by the function of a crucial biosynthetic enzyme called the oligosaccharyltransferase (OST). The now-attached N-glycan then undergoes further processing in the ER lumen and Golgi apparatus by a series of membrane-associated glycosidases and glycosyltransferases (Figure 7a). Certain glycan intermediates, such as mono-glucosylated and non-glucosylated N-glycans, can be recognized by lectins to facilitate protein folding. In the case of fucosylation, an unique enzyme called the  $\alpha$ 1,6-fucosyltransferase (FUT8) is responsible for adding the core fucose to the nascent glycoproteins. The FUT8 recognizes the GlcNAcMan<sub>3</sub>GlcNAc<sub>2</sub> intermediate as the glycosyl acceptor substrate and transfers the fucose from a nucleotide GDP-l-fucose as the glycosyl donor. The *de novo* biosynthetic pathway of GDP-l-fucose donor is also illustrated in Figure 7b.

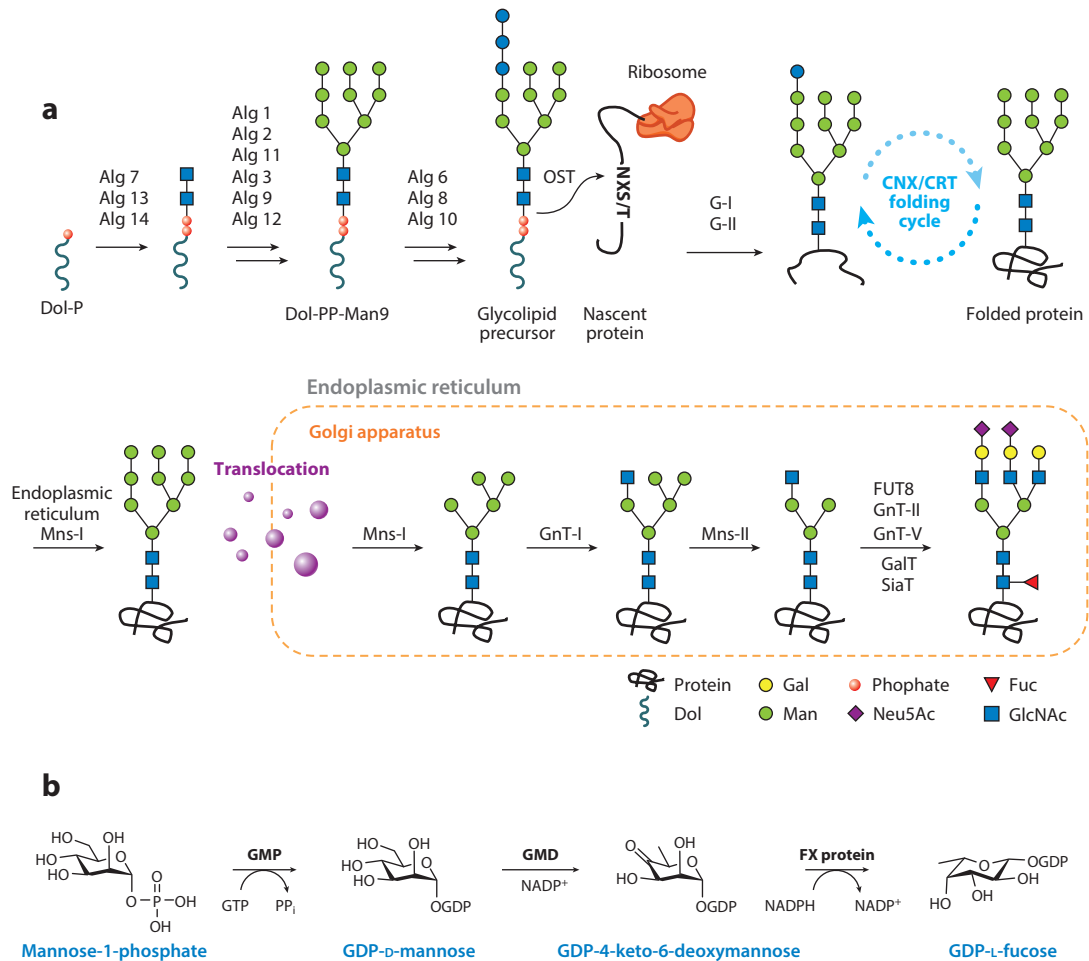


Figure 7. Biosynthetic pathway of (a) N-glycoproteins in eukaryotic cells and (b) GDP-L-fucose in mammalian cells.<sup>26</sup> Abbreviations are shown: Alg, asparagine-linked glycosylation enzyme; CNX/CRT, calnexin/calreticulin; Dol, dolichol; Fuc, fucose; FUT8,  $\alpha$ 1,6-fucosyltransferase; FX, GDP-4-keto-6-D-deoxymannose epimerase; G-I, II, III,  $\alpha$ -glucosidase I, II, III; Gal, galactose; GalT, galactosyltransferase; GDP, guanosine diphosphate; GlcNAc, N acetylglucosamine; GMD, GDP-mannose 4,6-dehydratase; GMP, guanosine monophosphate; GnT, acetylglucosaminyltransferase; Man, mannose; Mns,  $\alpha$ -mannosidase; NeuAc, N-acetylneuraminic acid; NXS/T, consensus amino acid sequence for N-glycosylation, where X is any amino acid except proline; OST, oligosaccharyltransferase; SiaT, sialyltransferase.

## 2. Antibody glycan remodeling by biosynthetic pathway perturbation

Based on the biosynthetic pathway of the core fucosylated N-glycans, several approaches to generate antibody N-glycoforms *in vivo* with reduced core fucose have been developed. The general concepts of these methods are summarized in Figure 8. The majority of these strategies take advantages of the key enzymes involved in the biosynthesis of core fucose and its precursors. For instance, down regulation of the genes expressing the GDP-mannose 4,6-dehydratase (GMD) and FUT8 has led to a lower presence of core fucose in the expressed antibodies in certain systems.<sup>65, 66</sup> Two fucose-reduced mAbs, roledumab<sup>67</sup> and ublituximab<sup>68</sup>, were produced in this fashion and are currently tested in phase II clinical trials. Other examples using the similar concept include the overexpression of GnTIII, a glycosyltransferase responsible for adding the bisecting GlcNAc to the N-glycans, which will block access of FUT8,<sup>69</sup> and complete knockout of FUT8, which prevents transfer of the GDP-l-fucose to the target glycoprotein. Using the GnTIII overexpression method, an anti-cancer antibody called obinutuzumab was developed and was approved by the FDA for treating non-Hodgkin's lymphoma and chronic lymphocytic leukemia.<sup>70</sup> Furthermore, a FUT8-knockout cell line was able to produce a non-fucosylated antibody with a 100-fold more potent ADCC activity than its unmodified counterpart. The resultant antibody glycovariant, mogamulizumab, was licensed in 2012 in Japan to combat the relapsed or refractory adult T cell leukemia/lymphoma.<sup>71</sup>

Since GDP-l-fucose is the essential substrate for FUT8, several attempts were made to reduce core fucosylation by depleting the intracellular level of GDP-fucose or its precursors. A successful example was the generation of a GDP-4-keto-6-D-

deoxymannose epimerase GDP-4-keto-6-L-galactose reductase (FX)-knockout cell using CRISPR/Cas9 gene editing technology.<sup>72</sup> Similar approaches also targeted the GDP-fucose transporter pathways by gene editing techniques to reduce the available GDP-fucose for FUT8.<sup>73</sup> Alternatively, various monosaccharide analogs, including 2-fluorofucose<sup>74</sup>, 5-alkynylfucose<sup>75</sup>, 6,6,6-trifluorofucose<sup>76</sup>, and arabinose<sup>77</sup>, were tested as potential biosynthetic inhibitors against the GDP-fucose. Finally, non-mammalian systems devoid of the endogenous FUT8 expression, such as insect<sup>78</sup>, plant<sup>79</sup>, fungi<sup>80</sup> and yeast<sup>81</sup>, were also exploited for glycoengineering of antibody core fucosylation.

Because terminal sialylation<sup>82</sup> and galactosylation<sup>43</sup> have been associated with complement-dependent cytotoxicity and anti-inflammatory activity of IgG antibodies, respectively, there have been efforts to enrich these specific glycoforms for functional analysis and therapeutic studies. These efforts often involve genetic regulation of the enzymes, such as galactosyltransferases and sialyltransferases, responsible for adding the terminal sialic acid and galactose during the final processing steps. In addition, mutations at some amino acid sequences surrounding the glycosylation sites may also alter the terminal glycosylation level of certain antibodies due to steric hindrance.<sup>83, 84</sup>

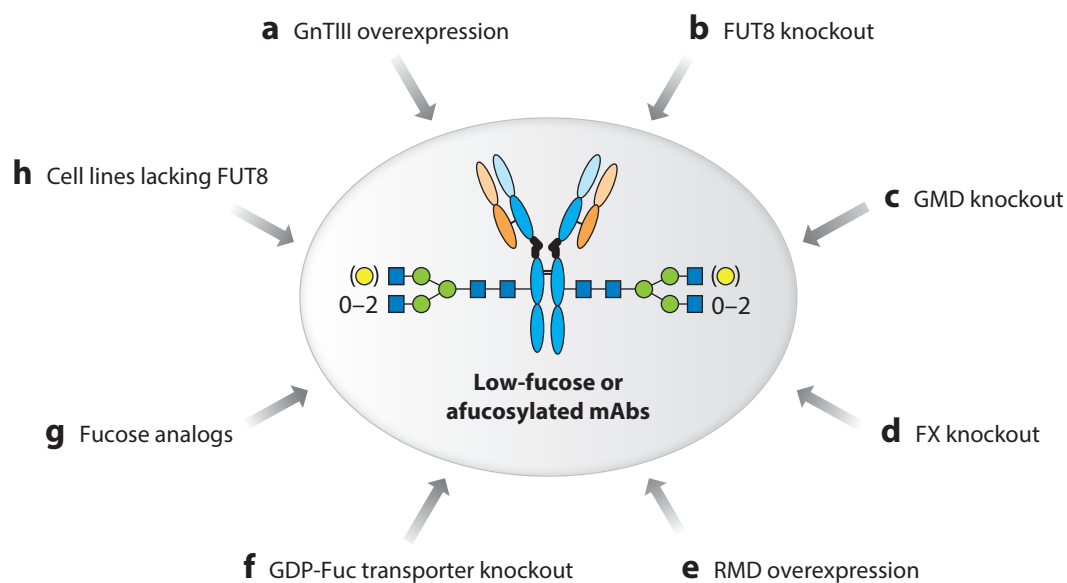


Figure 8. Glycoengineering methods to produce low-fucose or nonfucosylated mAbs *in vivo*. (a) Overexpression of GnTIII in CHO cells. (b) Knockout of FUT8 in CHO cells. (c) Knockout of GMD in CHO cells. (d) Knockout of FX in CHO cells. (e) Overexpression of RMD in CHO cells. (f) Knockout of GDP-fucose transporter in CHO cells. (g) Use of fucose analogs that block GDP-fucose production (inhibition of GMD). (h) Expression in cells that have low or no endogenous FUT8 expression. Additional abbreviations: FX, GDP-4-keto-6-D-deoxymannose epimerase, RMD, resistant maltodextrin.<sup>20</sup>

#### **D. Antibody glycosylation remodeling by chemoenzymatic modifications**

Although the biosynthetic glycan engineering strategy has been successful in producing some important antibody N-glycoforms, there are several clear limitations associated with this approach.<sup>25, 31, 59</sup> First, only a limited number of N-glycoforms can be efficiently generated using this method based on the existing biosynthetic pathways of N-glycans in conventional expression systems. Certain intermediate or aberrant glycoforms, such as the hybrid and triantennary N-glycans, might be difficult to obtain by manipulating the natural biosynthetic network.<sup>85</sup> In addition to the target diversity issue, accurate regulation of antibody glycosylation is still challenging, as the levels of key enzymes involved in the production of antibody glycoforms are highly sensitive to the biochemical and physiological state of the cells used for expression, which can be easily affected by many factors during manufacturing.<sup>86</sup>

An alternative strategy to optimize the N-glycosylation pattern of antibodies is to directly modify the native antibody N-glycans *in vitro* through the use of glycan processing enzymes and chemically modified sugar substrates. For example, partial enrichment for the terminal galactose and bisecting GlcNAc on an IgG antibody was achieved by treating the antibody with a recombinant GnTIII.<sup>87</sup> Functional studies on these enriched antibody glycoforms revealed that the terminal galactose could affect the CDC activity of IgG regardless of the bisecting GlcNAc. In 2014, another study from the Bosques group further demonstrated that glycoengineered IVIG preparation with increased levels of galactosylation and sialylation exhibits better anti-inflammatory activity than the primary IVIG.<sup>88</sup> However, a broad application of this glycoengineering strategy is hindered by the limited availability of suitable starting

antibody N-glycoforms. In addition, a large library of glycosidases and glycosyltransferases with different substrate specificities are needed for the construction of a full-length glycan chain by the step-wise addition or removal of single-sugar building blocks. As a result, the overall yield of this total synthesis might be problematic.<sup>4</sup>

Instead of building an entire oligosaccharide chain with one sugar molecule at a time, an alternative strategy using a different family of glycan-modifying enzymes, called endo- $\beta$ -N-acetylglucosaminidases or endoglycosidases (ENGase), seems to be much more convergent. In this method, the full-length or modified oligosaccharides are used as building blocks for ENGases to transfer to the glycoproteins, a process known as “transglycosylation”.<sup>89</sup> This strategy typically involves two major steps: (1) the release of the endogenous N-glycans from the heterogeneous antibody starting material (deglycosylation), and 2) the enzymatic formation of a new glycosidic linkage between the innermost GlcNAc residue of the deglycosylated protein and an activated N-glycan substrate using the catalytic activity of a mutant endoglycosidase (transglycosylation). The general concept of this strategy for glycoprotein and glycopeptide engineering is briefly illustrated in Figure 9.

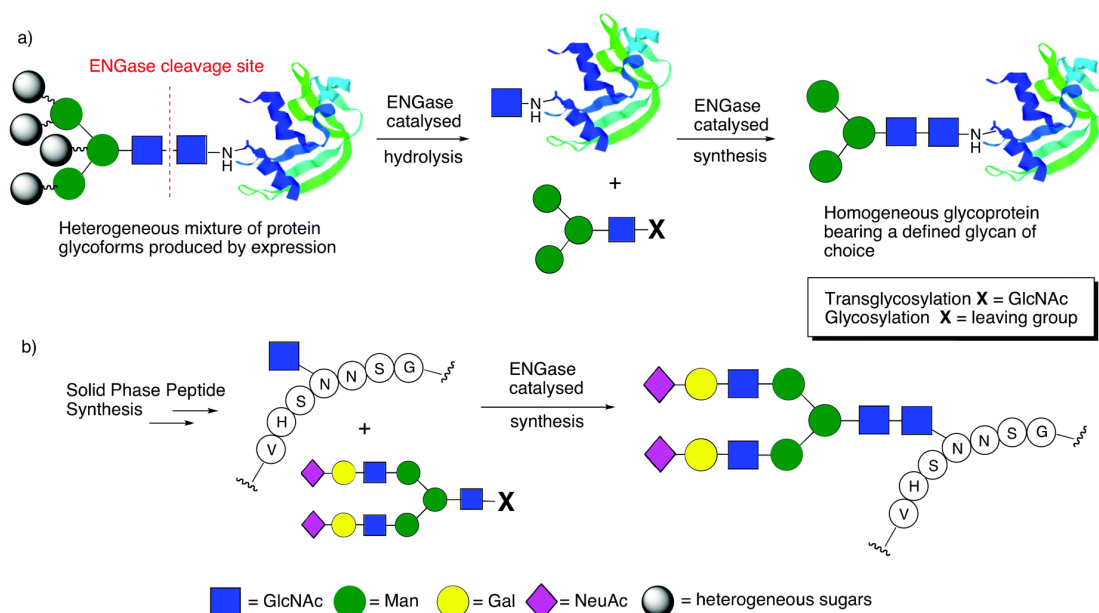


Figure 9. General concept of the ENGase-mediated glycosylation remodeling strategy of (a) glycoprotein and (b) glycopeptide.<sup>89</sup>

## 1. Introduction to endo- $\beta$ -N-acetylglucosaminidase (ENGase)

The endo- $\beta$ -N-acetylglucosaminidases (ENGases) or endohexosaminidases comprise a family of glycoside hydrolases (EC 3.2.1.96)<sup>90</sup> that catalyze the cleavage between the two GlcNAc residues within the diacetylchitobiose core of N-glycans.<sup>91</sup> The discovery of the first ENGase dates back to the early 1970's, and since then a large number of ENGases have been cloned from a series of organisms, such as bacteria, fungi, and higher organisms including mammals. Unlike other carbohydrate-modifying enzymes, ENGases possess the unique ability to hydrolyze N-glycans attached to other molecular structures, such as glycoproteins and glycolipids. All ENGases found in the Carbohydrate-Active enZYmes Database (CAZY) can be divided into two sub-classes based on their primary sequence features: the glycoside hydrolase family GH18 and GH85,<sup>91</sup> both sharing a conserved ( $\beta/\alpha$ )8-TIM-barrel fold

containing eight pairs of parallel  $\beta$ -sheets and  $\alpha$ -helices. The crystal structure of an typical bacterial ENGase of GH85 family called Endo-A from *Arthrobacter protophormia*, is shown in Figure 10, where the key residues conserved in the loop area of the  $(\beta/\alpha)_8$ -TIM-barrel domain are responsible for the glycoside hydrolytic activity (highlighted by the arrow).<sup>92</sup>

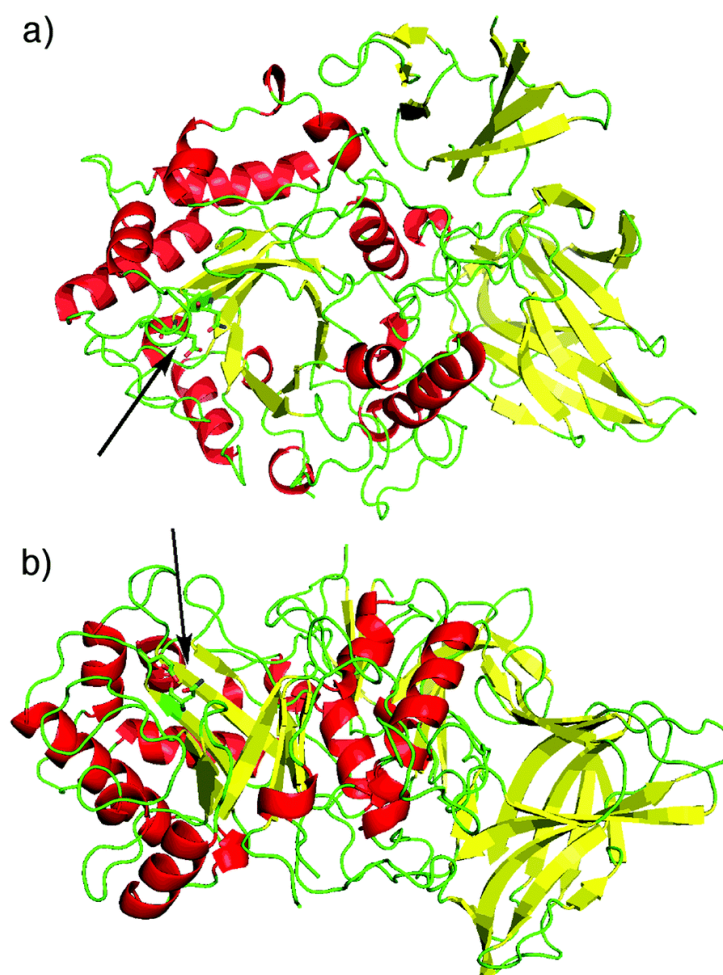


Figure 10. Crystal structure of endoglycosidase Endo-A (PDB: 3FHA) from two views. Parallel  $\beta$ -sheets and  $\alpha$ -helices are highlighted in yellow and red, respectively. The catalytic domain (residues 2–350) of Endo-A contains a  $(\beta/\alpha)_8$ -TIM-barrel structure. The active site region is marked by an arrow.<sup>92</sup>

## 2. Catalytic mechanism of ENGases and development of sugar oxazolines as activated glycan substrates for transglycosylation

Although by definition the dominant enzymatic activity of ENGase is to release the N-linked oligosaccharides from the protein/peptide backbone, leaving only a single GlcNAc residue attached at the glycosylation site, some ENGases also retain the ability to re-attach N-glycans back to the exposed GlcNAc residue through a reverse reaction<sup>93</sup>. The dual functionalities of ENGases form the basic principles of the highly convergent chemoenzymatic glycan remodeling strategy mentioned in the previous section (Figure 9), and this method can be applied to synthesize both the homogeneous glycoproteins and glycopeptides with highly controlled regio- and stereo-selectivity.<sup>94</sup>

Despite the diverse substrate specificities, all ENGases from the GH18 and GH85 families catalyze the hydrolysis of glycoproteins using two conserved acidic residues, a general acid-base and a nucleophile, in a two-step mechanism, as illustrated in Figure 11.<sup>89</sup> For the GH18 members, the two key residues in the active site are typically a glutamic acid and an aspartic acid, whereas the aspartic acid is replaced by an asparagine at the same position in the GH85 enzymes. A major difference between the reaction mechanisms of ENGases and other  $\beta$ -glycosidases is that the ENGases utilize neighboring group participation of the 2-acetamide from the second GlcNAc residue in catalysis.<sup>95</sup> Based on this unique substrate-assisted mechanism, an oxazolinium ion or oxazoline was identified as a transition-state intermediate formed during the hydrolytic reaction of ENGases. A critical discovery in the field was the use of chemically synthesized N-glycan oxazolines as high-energy

substrates to induce ENGases to catalyze the transglycosylation reaction. This is particularly useful as the activated glycan oxazolines may react with another GlcNAc residue of a different glycoprotein or glycopeptide to form a new glycosidic linkage in the final product.<sup>96</sup>

Realizing the potential of glycan oxazoline in transglycosylation, in 2001 Shoda and colleagues designed the first disaccharide oxazoline (Man $\beta$ 1-4GlcNAc) and used it as a probe to screen for potential transglycosylation activities of a library of ENGases.<sup>97</sup> Since then, the disaccharide oxazoline was used as substrate for several ENGases, including Endo-A and Endo-M, to catalyze the synthesis of some relatively simple compounds such as trisaccharides.<sup>98</sup> Although these earlier studies did not achieve efficient transglycosylation with more complicated glycosyl acceptors, such as glycopeptides or glycoproteins, they indeed laid the foundation for future use of more sophisticated oxazolines as the preferred substrates for the ENGase-mediated synthesis. One major advantage of this method was that the ENGases would not hydrolyze the product N-glycans containing truncated or modified sugar structures, which made it possible to achieve unidirectional synthesis of certain N-glycan conjugates.

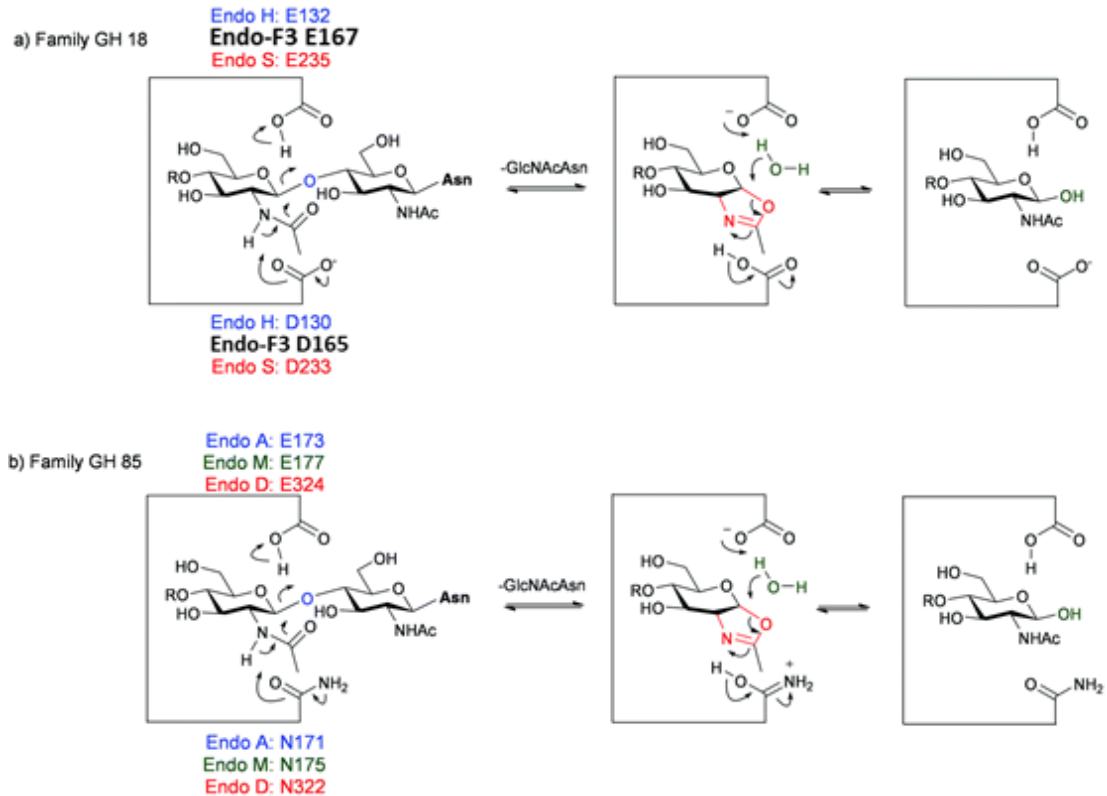


Figure 11. Catalytic mechanisms of ENGases showing key catalytic residues for some enzymes from: (a) family GH18; (b) family GH85.<sup>96</sup>

### 3. Glycosynthase mutants of ENGases for antibody glycan remodeling

Despite the fact that some modified N-glycans can be resistant to the intrinsic hydrolytic activity of ENGases, most full-length N-glycans of interest will still be rapidly hydrolyzed after they are transferred to the target glycoprotein-GlcNAc by the wild-type ENGases. This property greatly limited the application of ENGases in the general method of glycan remodeling. To solve this problem, Wang and Yamamoto investigated the possibility of using mutant ENGase generated by site-directed mutagenesis as “glycosynthase” enzymes specialized in protein transglycosylation.<sup>99</sup> Based on the catalytic mechanisms mentioned earlier (Figure 11), a second catalytic

residue known to be critical for the stabilization and deprotonation of the oxazolinium ion intermediate, an asparagine for GH85 or an aspartate for GH18, was selected as the site for mutation. Using this design, the first glycosynthase mutant of ENGases, developed together by Wang and Yamamoto, was generated by substituting the Asn-175 residue of Endo-M with an alanine residue (Figure 12a). The generated mutant showed much higher transglycosylation activity than the wild-type Endo-M. Systematic mutagenesis at this site and functional assays demonstrated that an N175Q mutant was the most efficient variant in terms of synthesizing glycopeptides using sugar oxazolines, and this mutant later became a commercially available product.<sup>100</sup>

Following this breakthrough, Wang and others applied this strategy to generate glycosynthase mutants of other members of GH18 family such as Endo-D<sup>101</sup> and Endo-A<sup>102</sup>, and these mutants proved to be useful for various synthetic purposes with distinct substrate specificities. Finally, studies by Wang and coworkers revealed that analogous mutations could be made at an aspartic acid in the active site of GH18 ENGases such as Endo-S<sup>103</sup> and Endo-F3<sup>85</sup> to generate novel glycosynthase mutants of this GH family. According to previous studies on the relative activities of ENGase mutants, alanine or glutamine substitution seemed to yield the most effective glycosynthase mutants from a given ENGase.<sup>89</sup> However, as a rapidly increasing number of new ENGases and mutants are being discovered and developed to expand the synthetic toolbox available, more systematic mutagenesis and functional studies are needed to verify whether other mutations at this catalytic N/D residue can yield more effective glycosynthase mutants than the previously reported A/Q substitutions. Finally, it is worth reiterating that these glycosynthase mutants of ENGases lack the

activity to utilize the glycopeptides containing full-length N-glycans as substrates for transglycosylation, as the initial step of N-glycan hydrolysis from the glycopeptides cannot happen without the participation of the second catalytic residue.<sup>104</sup> On the other hand, wild-type ENGases have the ability to catalyze such reactions but an enormous amount of glycopeptides are required to offset the dominant hydrolytic activity against the product.<sup>105</sup>

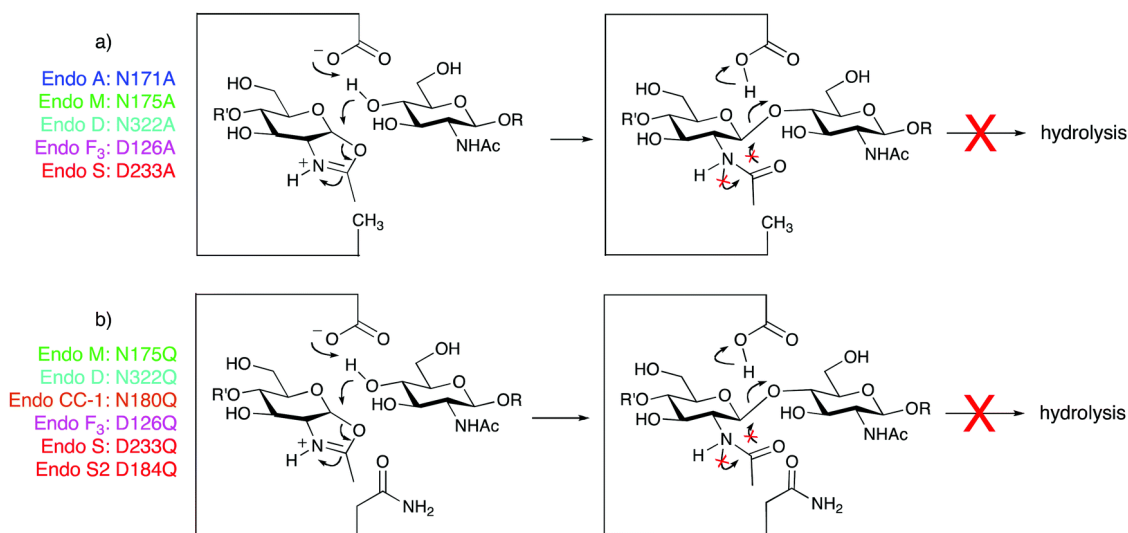


Figure 12. Mechanism-based design of mutant glycosynthases of the ENGases: (a) mutations of the catalytic base (family GH18: D, family GH85: N) to alanine; (b) mutations of the catalytic base (family GH18: D, family GH85: N) to glutamine.

#### 4. Examples of ENGase-mediated antibody glycoengineering

##### 4.1. A brief history of antibody glycoengineering using ENGases and mutants

In recent years the application of ENGase-mediated glycoengineering has made significant contributions to the synthesis of various antibody N-glycoforms, both naturally existing and artificially modified. One barrier to broad application of this strategy is that the majority of the IgG-Fc N-glycans produced in mammalian systems contains core fucose, which is not recognized by many ENGases. To circumvent this obstacle, Wang and colleagues in 2008 used a yeast expression platform to produce IgG-Fc fragment containing non-fucosylated oligomannose N-glycans as the starting glycoforms, which could be easily hydrolyzed by many commonly used ENGase such as Endo-H.<sup>106</sup> After deglycosylation, the truncated tetra- and hexa-saccharides were subsequently transferred to the exposed GlcNAc residue at Asn-297 by a bacterial ENGase Endo-A (Figure 13a). In this study, Endo-A demonstrated the ability to transfer truncated or modified full-length N-glycans to IgG-Fc under relatively mild conditions, and the resulting IgG-Fc glycoform library was used to test the specific functional roles of N-glycans including the bisecting GlcNAc. However, limitations were realized: Endo-A could not transfer intact complex-type bi- or tri-antennary N-glycans to IgG-Fc, and the related studies on Endo-M revealed the same restricted substrate specificities.<sup>107</sup>

The situation was improved when Wang and others discovered that another endoglycosidase called Endo-D from bacterium *Streptococcus pneumoniae* was able to use both the core fucosylated and non-fucosylated IgG-Fc fragments as substrates for transglycosylation reactions.<sup>101</sup> Based on this discovery, native antibodies

carrying the core-fucosylated N-glycans could be targeted for glycan remodeling. An example was demonstrated that the Endo-D N322Q mutant could transfer the simple core Man<sub>3</sub>GlcNAc glycan oxazoline to a commercial therapeutic antibody rituximab (Figure 13b). Nevertheless, neither Endo-A nor Endo-D could modify IgG-Fc with full-size complex type N-glycans. These limitations encouraged similar studies to be conducted on ENGases from the GH18 family such as Endo-S<sup>103</sup> and Endo-F3<sup>85</sup>, and very promising results were obtained with their glycosynthase mutants in terms of antibody glycoengineering.

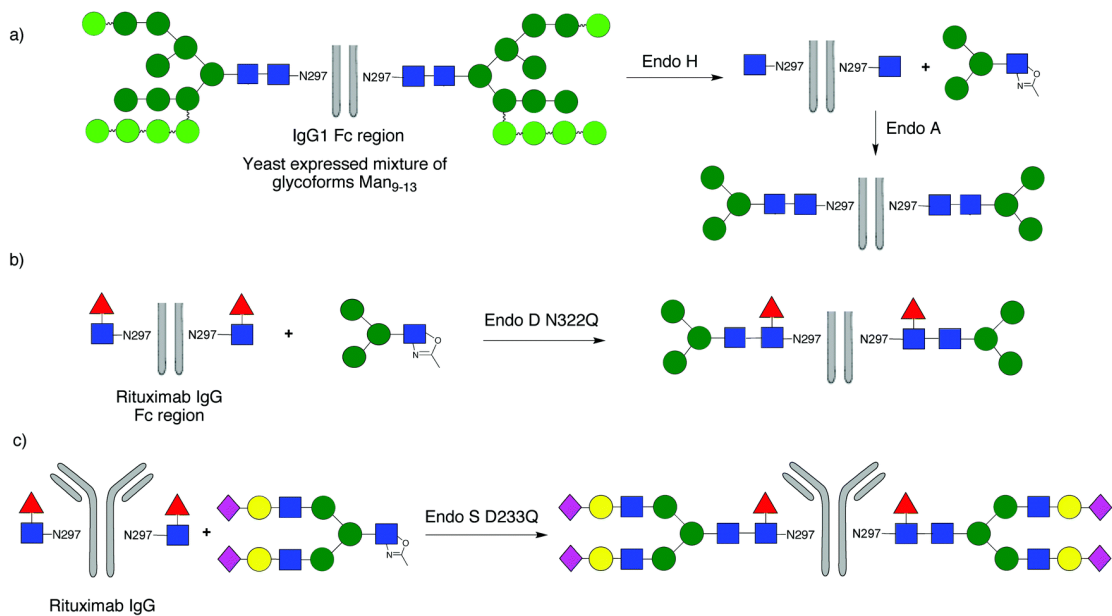


Figure 13. Selected examples of antibody glycan remodeling using ENGases: (a) Endo-A catalyzed attachment of a truncated core glycan to the non-fucosylated Fc region of human IgG; (b) Endo-D N322Q mutant catalyzed attachment of a truncated core glycan to the fucosylated Fc region of the mAb rituximab; (c) Endo-S D233Q mutant catalyzed attachment of a complex type biantennary glycan to the fucosylated intact rituximab.<sup>89</sup>

## 4.2. Chemoenzymatic glycan remodeling of intact IgG antibodies by GH18 ENGases

### Endo-S and End-F3

The first glycosynthase mutants of Endo-S, Endo-S D233A and D233Q, were developed by Wang and co-workers in 2012 and were subsequently applied to glycan remodeling of IgG antibodies with a series of complex biantennary N-glycans.<sup>103</sup> The Endo-S mutants in combination with activated sugar oxazolinium substrates enabled a highly efficient glycan remodeling of a therapeutic IgG antibody, rituximab, originally carrying a mixture of the G0F, G1F, and, G2F glycans at the Fc region (Figure 14). The homogeneous N-glycoforms produced include a fully sialylated S2G2F form that was proposed to provide anti-inflammatory activity, a completely de-fucosylated G2 form that would display an enhanced ADCC activity versus its G2F form, and an artificial N-glycoform linked with an azido group that could be further coupled to other functional groups via orthogonal chemistry.

Subsequent studies by other groups further demonstrated the applicability of Endo-S/Endo-S D233Q in preparing well-defined N-glycoforms of IgGs for various structural and functional purposes.<sup>42, 108, 109</sup> However, Endo-S mutants could not act on the high-mannose or tri-antennary N-glycan oxazolines for transglycosylation. In this regard, the Wang group explored the intrinsic transglycosylation activity of a unique GH18 ENGase Endo-F3 that exhibited the ability to process the triantennary N-glycans in the presence of the core fucose. A glycosynthase mutant of Endo-F3, Endo-F3 D165A, was found to be able to transfer both bi- and tri-antennary complex type N-glycans to the fucosylated IgG acceptor in a highly efficient manner.<sup>85</sup>

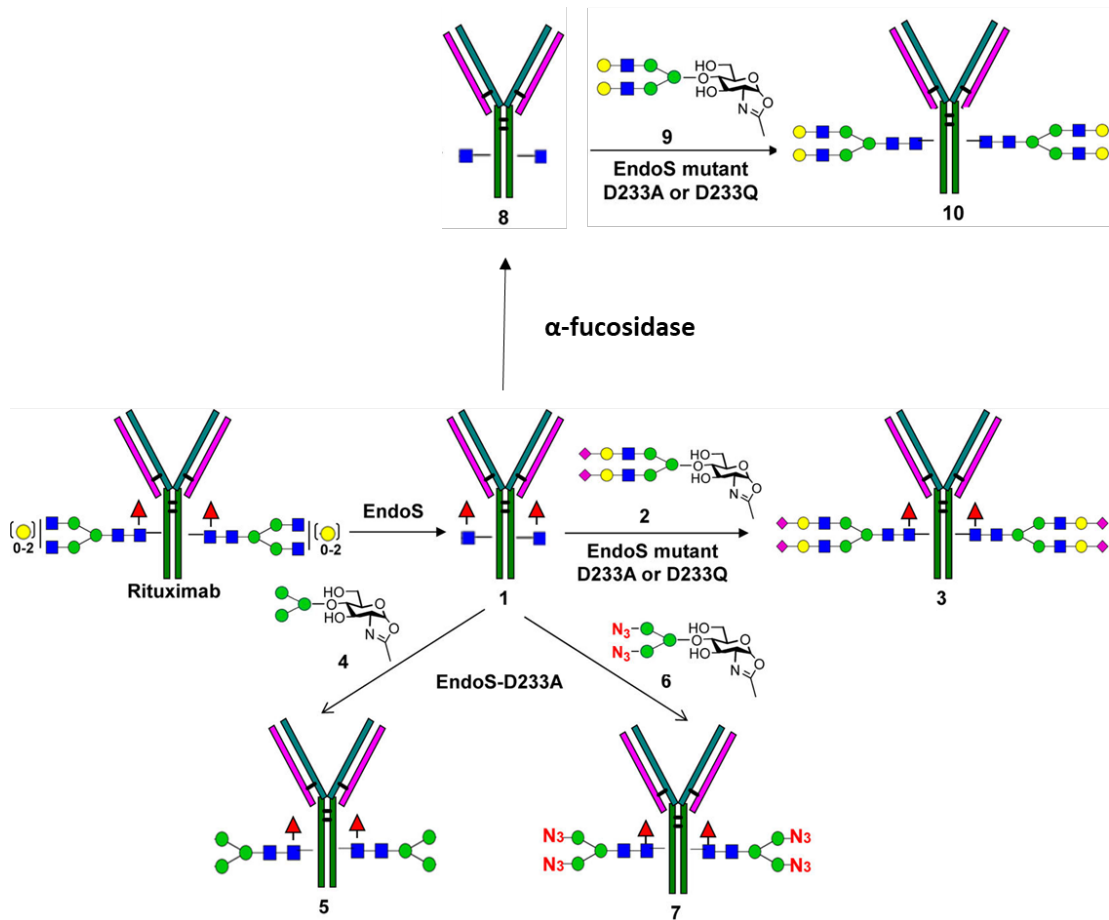


Figure 14. Glycosylation remodeling of IgG antibody rituximab using Endo-S and Endo-S glycosynthase mutants. Commercial therapeutic antibody rituximab was first deglycosylated using the wild-type Endo-S to generate fuc- $\alpha$ 1,6-GlcNAc-rituximab, from which the core fucose could be removed by an  $\alpha$ -1,6-fucosidase to generate the GlcNAc-rituximab. To the deglycosylated antibody with and without fucose, different N-glycans were transferred to the core GlcNAc by Endo-S D233A or D233Q in the presence of glycan oxazolines, generating homogeneous rituximab glycoforms.<sup>103</sup>

#### 4.3. Chemoenzymatic glycan remodeling of intact IgG antibodies by Endo-CC

A more recently discovered GH18 ENGase called Endo-CC from *Coprinopsis cinerea* was found to be able to act on both complex and high-mannose glycans.<sup>105, 110-112</sup> Inspired by the earlier studies, the glycosynthase mutants of Endo-CC were generated, and the mutant Endo-CC N180H was found to be most efficient in transferring the sialobiantennary complex N-glycan to various glycosyl acceptors. However, several aspects regarding the detailed catalytic properties of Endo-CC remain unclear. First, the substrates tested in Endo-CC transglycosylation were limited to the complex type N-glycans and glycoconjugates; therefore it is unknown whether Endo-CC and/or its glycosynthase mutants can react with the hybrid and high-mannose glycan structures. Secondly, current studies provided no experimental results concerning the tolerance of Endo-CC enzymes against the core fucose, which is a very important structural element in antibody glycosylation, as demonstrated in the previous section. Finally, the reported experiments related to the relative activities of Endo-CC mutants suggested that, among the 19 Endo-CC N180 mutants tested in the study, only two variants Endo-CC N180H and N180Q showed significant transglycosylation activities, which was not the case in many of the previously reported mutational studies of other ENGases. Additionally, it is still a question under debate whether the mutants of Endo-CC can independently catalyze the transfer of activated glycan oxazolines to the deglycosylated antibody.<sup>112</sup> A more detailed discussion for Endo-CC in antibody glycoengineering is given in Chapter 4 of this dissertation.

## **E. Scope and limitations of current chemoenzymatic antibody glycoengineering strategy mediated by ENGases**

Although the application of ENGases has proved very successful in producing homogeneous N-glycoproteins such as antibodies, there are still important functional limitations and unknown aspects associated with this glycoengineering strategy, which include the overall efficiency of the transglycosylation reactions by Endo-S, the restricted substrate specificities of Endo-S and other ENGases against additional N-glycans and acceptors, and the potential use of ENGases to remodel glycosylation of other antibody isotypes such as IgE and IgA.

### **1. Efficiency of transglycosylation catalyzed by the existing Endo-S glycosynthase mutants Endo-S D233Q and Endo-S D233A**

First, regarding the efficiency of the transglycosylation reactions catalyzed by the Endo-S mutants, only two glycosynthase mutants of Endo-S, D233Q and D233A, were generated and tested so far for their glycosylation efficiencies against N-glycan oxazolines. Similar studies on other ENGases such as Endo-M raised the question of whether substitutions of the catalytic residue Asp-233 with additional amino acids may lead to new glycosynthase mutants with further enhanced transglycosylation efficiency for antibody remodeling. More importantly, there has been no mechanistic information, such as the kinetic parameters of Endo-S enzymes, available to help understand how Endo-S and its mutants catalyze the reactions differently. Finally, despite the relatively high efficiency of the Endo-S D233Q and D233A mutants, an excess amount of glycan oxazoline substrate (approximately 20 molar equivalents to the accepting antibody) is required to ensure a nearly complete transfer of the glycan.

Novel ENGase mutants that can achieve a similar level of transglycosylation with less consumption of glycan substrates might be of great interest to facilitate more effective glycosylation remodeling of therapeutic antibodies.

## 2. Substrate specificity of current ENGases for different N-glycans

Although the Endo-S mutants could act on the biantennary complex type and truncated Man<sub>3</sub>GlcNAc glycans, they were unable to transfer the high-mannose and hybrid type N-glycans. The same restricted substrate specificity was observed for the Endo-F3 mutant D165A, which could not work on the non-fucosylated antibodies.<sup>85</sup> All these results indicated the need of a more versatile glycoengineering strategy with a relatively relaxed substrate selectivity. Adding to the limitations of the current glycan remodeling method is the fact that the antibody intermediate generated after each step of this multiple-reaction procedure needs to be purified from the reaction mixture before switching to the glycosynthase mutant. The concept of a potential “one-pot” method to optimize N-glycans of antibodies without the need of alternating enzymes and purifying intermediates might be worth pursuing to make this general strategy more effective.

## 3. Glycosylation remodeling of antibodies beyond the IgG isotype

So far all the ENGase-mediated glycan engineering efforts are focused on the IgG isotype of antibodies, and it remains unclear whether this general strategy using the chemoenzymatic modifications for glycan remodeling can be expanded to other antibody isotypes including IgA and IgE. This is becoming increasingly important as more studies are emerging to shed light on the functional significance of glycan

structures of IgE antibodies. For example, a recent report suggested that a unique oligomannose N-glycan is critical for the IgE-induced allergic reactions.<sup>113</sup> Access to synthetic IgE glycoforms with defined and modified glycan structures can potentially help us determine the IgE glycan participation in receptor binding and other cellular events related to anaphylaxis.

## **F. Organization of the dissertation**

The first chapter of this dissertation introduced the importance of antibody glycosylation and the basic concept of using chemoenzymatic glycoengineering to remodel the antibody N-glycans. A brief review of previous studies was also included to demonstrate how endoglycosidases were applied to synthesize homogeneous antibody glycoforms with well-defined glycan structures for various structural and functional studies.

The second chapter focuses on the study that was published in *Biochemistry* in 2018. In this work, several aspects of the ENGase-mediated glycan remodeling strategy were revisited to improve the overall efficiency of antibody glycosylation. Results of saturation mutagenesis on a previously identified ENGase Endo-S revealed additional glycosynthase mutants that could use glycan oxazolines as substrates for transglycosylation. A novel mutant Endo-S D233M was found to be more efficient in catalyzing the transfer of N-glycans than the previously identified Endo-S variants. Kinetic studies on selected Endo-S mutants provided new insight on the underlying mechanism of ENGases. A potent thiazoline-based inhibitor for Endo-S was also developed based on a unique substrate-assisted reaction mechanism. Finally, possible transglycosylation reactions using a reduced amount of glycan and the proposed non-enzymatic side reactions were also investigated to help improve the effectiveness of our strategy.

The third chapter describes our efforts in expanding the scope of the current glycosylation remodeling strategy beyond the restricted substrate specificity of some ENGases. Results of the mutational studies on another ENGase Endo-S2 identified

new glycosynthase mutants that could act on all three major types of N-glycans with higher efficiency than the previously reported Endo-S mutants. Furthermore, results on the unique substrate specificity of the wild-type Endo-S promoted us to develop a one-pot glycoengineering strategy to synthesize homogeneous high-mannose or hybrid glycoforms of antibody in a more effective fashion. The work about Endo-S2 mutants was published in the Journal of Biological Chemistry in 2016 and I made significant contribution to this work as a co-author. The work regarding the one-pot glycan remodeling of antibody was published in Bioorganic & Medicinal Chemistry in 2018.

The fourth chapter presents our study on a recently discovered ENGase Endo-CC. Previous studies on Endo-CC mutants indicated that only Endo-CC N180H and N180Q mutants showed significant transglycosylation activity with the complex-type glycan. Our results from substrate screening revealed that the Endo-CC mutants could transfer both the high-mannose and hybrid type glycans to the target glycopeptide. Core fucosylated substrates are resistant to the activity of both Endo-CC and mutants. In addition, comparison between the transglycosylation reaction time courses of different Endo-CC mutants demonstrated that, besides Endo-CC N180H and N180Q, other mutants of Endo-CC (N180Q, N180E and N180A) also retained the ability to use complex oxazoline for glycosylation reaction. Overall, these results improved our understanding of the catalytic properties of Endo-CC, which could be exploited for glycoengineering of glycopeptides and glycoproteins. The manuscript describing this work is in preparation.

The fifth chapter detailed our attempt to perform glycosylation remodeling on another class of antibody, IgE. Recent mutagenesis and cellular studies on IgE glycans revealed a single oligomannose N-glycan that was indispensable for IgE biological activity. Biophysical analysis on the synthetic IgE-Fc N-glycoforms generated by a combined method of *in vitro* enzymatic modifications and biosynthetic engineering revealed a relatively small but significant reduction of binding affinity to the FcεRs upon deglycosylation. Glycosylation remodeling of IgE-Fc with the complex type N-glycan is currently ongoing with the aim of developing a competitive inhibitor based on a glycoengineered IgE-Fc fragment to treat allergic disorders like asthma.

The final chapter summarizes the studies conducted in this research and their significance in optimizing the glycosylation states of monoclonal antibodies. Future studies regarding the mechanisms and applications of ENGases for glycoengineering will also be proposed in this chapter to further improve our understanding of ENGase catalysis and to expand the general concept of chemoenzymatic glycan remodeling strategy to other glycoproteins and glycopeptides.

## Chapter 2: Generation and comparative analysis of new glycosynthase mutants from endoglycosidase S (Endo-S) for antibody glycoengineering

### A. Introduction

The cellular process of attaching carbohydrate entities to proteins and lipids, also known as glycosylation, gives rise to a highly diverse repertoire of functionally important glycan structures that are critical for the survival of many organisms.<sup>25</sup> More than 50% of intracellular proteins and 90% of secreted proteins are glycosylated.<sup>33</sup> In particular, approximately 70% of the protein therapeutics currently on the market or in clinical trials are glycoproteins, and glycans are often found to be important for the pharmacokinetics and pharmacodynamics of therapeutic proteins, particularly monoclonal antibodies.<sup>69</sup> Recombinant antibodies typically carry a mixture of different glycan structures at multiple glycosylation sites, collectively described as antibody glycoforms, which are difficult to isolate or enrich in large quantities.<sup>86</sup> Because certain glycoforms of antibodies may confer unique biophysical properties and biological functions, such as mediating cellular killing and regulating anti-inflammatory activity, optimization of antibody glycosylation can potentially help develop more effective antibody therapeutics without altering the amino acid backbone.

The endo- $\beta$ -N-acetylglucosaminidase (ENGase)-catalyzed glycan remodeling mechanism has become an attractive strategy to optimize the heterogeneous glycosylation pattern of monoclonal antibodies.<sup>89</sup> As the initial step of antibody glycoengineering, the variable N-glycans of the starting antibodies are trimmed off by an ENGase that cleaves between the two GlcNAc residues within the chitobiose core

of N-linked oligosaccharides. Subsequent re-glycosylation or transglycosylation of antibody is achieved by the intrinsic ability of ENGase to catalyze the reverse reaction of glycan hydrolysis using a defined N-glycan in the form of activated oxazoline as substrate. The efficiency of this approach was significantly improved with the development of glycosynthase mutants of ENGases, such as End-M and Endo-D, which retained the transglycosylation activity for glycosyl oxazolines, with a much reduced tendency to hydrolyze the product, as discussed in the previous chapter.<sup>104</sup> However, none of the commonly available ENGases were able to transfer intact complex N-glycans to a fucosylated antibody acceptor, which promoted the search for new ENGases with broader substrate specificity and higher efficiency for antibody glycoengineering.

As part of our efforts to identify new ENGases for antibody glycosylation optimization, a family GH18 endoglycosidase Endo-S from the bacterial pathogen *Streptococcus pyogenes* was selected and studied for its ability to modify antibody N-glycans.<sup>114</sup> The intrinsic activity of this secreted Endo-S to specifically remove N-linked glycans from the Fc region of human IgG antibodies significantly improves the survival of *Streptococcus pyogenes* by helping evade the host immune surveillance, as the N-glycans are required for the optimal immunoregulatory functions of IgGs, such as receptor binding and complement activation.<sup>115</sup> Although Endo-S could process all four subclasses of IgG antibody (IgG<sub>1-4</sub>), it showed no significant hydrolytic activity against other antibody isotypes such as IgA and IgM, indicating that Endo-S recognizes specifically the protein structure of IgG antibodies for glycan hydrolysis. In addition to its substrate selectivity for the IgG antibody, only the

complex type N-glycoforms of IgGs are susceptible to the Endo-S-catalyzed hydrolysis, whereas the hybrid and high-mannose N-glycans of IgGs are unaffected by Endo-S treatment.<sup>114</sup> The strict substrate specificity of Endo-S for both the IgG-Fc domain and complex N-glycans makes it a suitable candidate for chemoenzymatic glycoengineering of antibodies with different complex N-glycoforms.

Inspired by previous studies on other ENGases, the first glycosynthase mutants of Endo-S, D233Q and D233A, were generated by Wang and colleagues through site-directed mutagenesis<sup>103</sup>. Using the activated glycan oxazoline as the glycosyl donor substrate, both mutants exhibited the remarkable activity to efficiently transfer a fully sialylated complex type glycan to the fucosylated intact IgG antibody without significant hydrolysis of the product (Figure 15). Such modifications could not be achieved by other ENGases such as Endo-A or Endo-D due to their restricted substrate specificities.<sup>104</sup> In addition, this work also demonstrated that, following the removal of N-glycans by Endo-S, the core fucose linked to the exposed GlcNAc at the glycosylation site of IgG-Fc could be subsequently released by an  $\alpha$ -fucosidase. Using this combined enzymatic process, Endo-S D233Q and D233A mutants could then transfer glycans to the non-fucosylated antibody to afford new glycoforms with no core fucose attached (Figure 16). Finally, the ability of Endo-S mutants to transfer the truncated and modified glycans to the deglycosylated antibody in a site-specific manner enabled further functionalization of the antibody molecules through orthogonal ligation chemistry, which could lead to the development of a new class of antibody therapeutics called antibody-drug conjugates.<sup>6</sup>

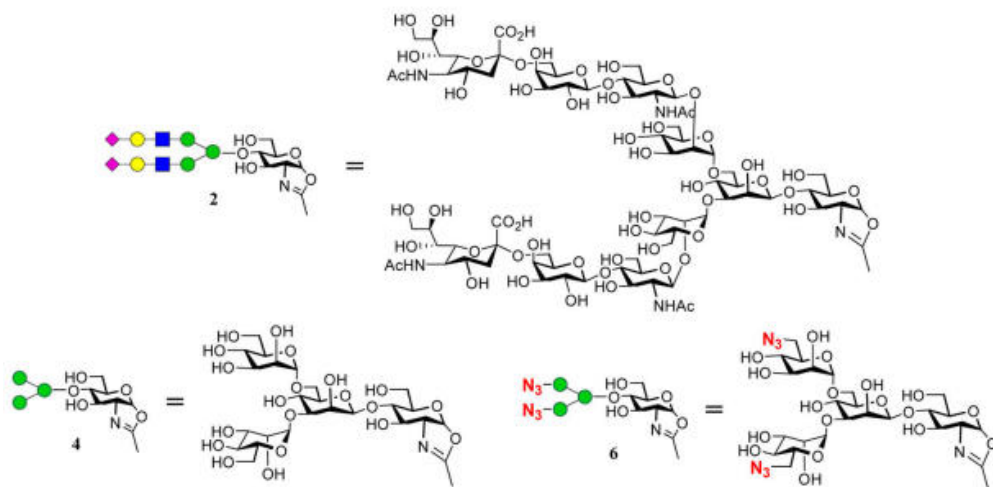
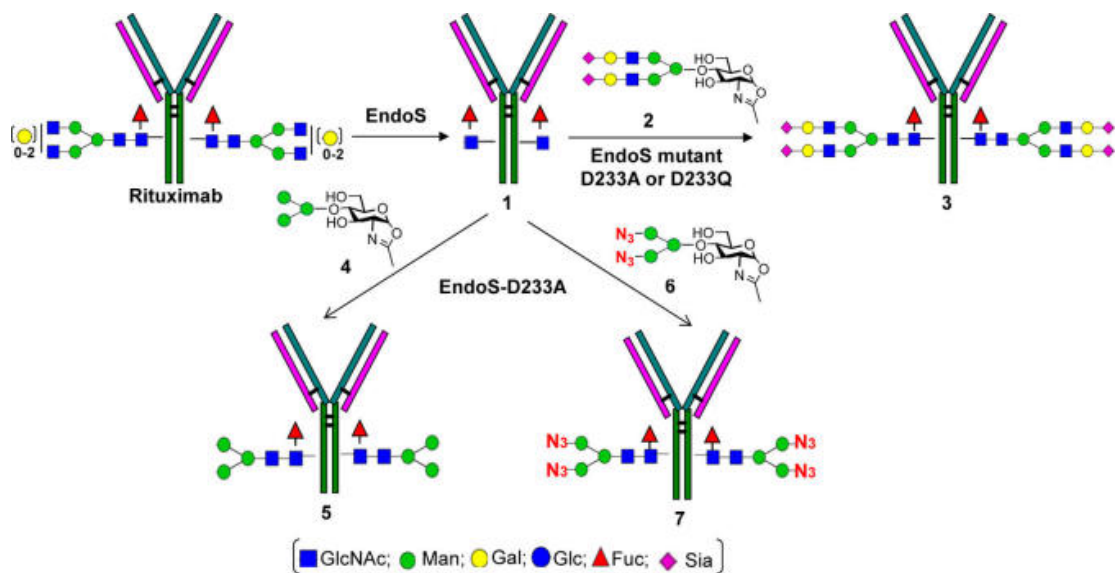


Figure 15. Glycoengineering of a core-fucosylated therapeutic antibody rituximab. Both natural and chemically modified N-glycan oxazolines were used to synthesize the homogeneous antibody N-glycoforms by Endo-S and its glycosynthase mutants Endo-S D233A and Endo-S D233Q. The detailed chemical structures of the glycan oxazoline substrates used in this procedure are shown here.<sup>103</sup>



Endo-S can lead to design of new glycosynthase mutants with distinctive hydrolytic and transglycosylation properties. Secondly, no mechanistic aspects of the catalysis of Endo-S and its mutants, such as kinetic properties, have been studied to date to help illustrate the molecular mechanism behind the different catalytic efficiencies among Endo-S mutants. Although the crystal structure of a truncated form of Endo-S (amino acid residues 98-995) was recently reported, no co-crystallized ligands were included in this structure and only limited information was provided to address the molecular mechanism by which the mutant Endo-S catalyzes the glycosylation of N-glycans.<sup>116</sup> A more in-depth understanding of Endo-S catalysis is needed to further improve the efficiency of the current antibody glycoengineering strategy.

Due to the important biological functions of glycoside hydrolases (GH), a large collection of the oligosaccharide-based small-molecule inhibitors have been developed as either molecular probes to dissect the cellular functions of GHs or as therapeutic interventions to target certain carbohydrate-related diseases.<sup>117</sup> Based on the substrate-assisted mechanism of ENGases (Figure 10), a class of thiazoline-based inhibitors were designed by replacing the anomeric oxygen of the sugar oxazolinium ion intermediate with a sulfur atom.<sup>118-121</sup> However, these inhibitors may possess promiscuous inhibitory activities against multiple ENGases or even other GH families within the cells due to the poor substrate selectivity. To date, there are no effective inhibitors that selectively target Endo-S over other ENGases. Therefore, the restricted substrate selectivity of Endo-S shown for the complex type N-glycans may provide a unique opportunity for the development of new selective thiazoline inhibitors for Endo-S and mutants.

Finally, it is worth noting that the non-enzymatic chemical ligation between glycan oxazolines and certain lysine residues of IgG antibodies has been reported as a competing side reaction during the ENGase-catalyzed transglycosylation. Davis and colleagues suggested that the non-selective glycosylation side reactions could happen when a large excess of oxazoline was used for transglycosylation.<sup>122</sup> Although Davis proposed a set of modified conditions to suppress these unwanted side reactions, the proposed method was relatively tedious and required multiple additions of oxazoline substrate in the presence of a high concentration of an Endo-S mutant. It is currently unclear whether these non-enzymatic glycosylation reactions may present a major issue for conventional remodeling of antibody glycosylation using Endo-S mutant and a reasonable amount of oxazoline (~10-20 molar equivalents to antibody), as typically used in our ENGase-mediated glycoengineering strategy.

In this chapter we describe a systematic mutagenesis study at the Asp-233 residue of Endo-S and evaluation of the relative catalytic activities of the resultant Endo-S mutants.<sup>123</sup> We found that substitution of Asp-233 with the other 19 canonical amino acids led to varied functional effects on the hydrolysis and transglycosylation activities of Endo-S, with the Endo-S D233M possessing the highest overall catalytic efficiency among the mutants studied, which was defined by the transglycosylation-to-hydrolysis activity ratio. Kinetic studies on the D233M mutant of Endo-S, as well as the previously identified D233A mutant, indicated that the enhanced overall catalytic efficacy of the Asp-to-Met mutant over that of the Asp-to-Ala mutant can be attributed mainly to two factors: the increased turnover number for the glycan oxazoline substrate and the enhanced affinity for the antibody substrate. These

findings provide a plausible mechanistic explanation for the enhanced catalytic activity of Endo-S D233M over the other mutants. In addition, based on the unique mechanism of Endo-S and other GH18 ENGases, we describe here a facile synthesis of a complex type N-glycan thiazoline analog as a new mechanism-based inhibitor for Endo-S and other complex glycan-specific ENGases.<sup>124</sup> Finally, investigation on the potential non-enzymatic side reactions between glycan oxazoline and antibody will be discussed. Collectively, these results elucidate key mechanistic aspects of Endo-S catalysis and can significantly improve the overall efficiency of the current Endo-S-mediated glycoengineering strategy.

## B. Results

### 1. Generation of additional glycosynthase mutants of Endo-S through site-directed saturation mutagenesis at the catalytic residue Asp-233.

To systematically screen for more efficient glycosynthase mutants of Endo-S, a library of Endo-S mutants was constructed by site-directed saturation mutagenesis at the previously identified catalytic residue Asp-233 (Figure 17). Previous studies have demonstrated that this aspartate residue is directly involved in stabilization and deprotonation of the oxazolinium ion intermediate during endoglycosidase-catalyzed hydrolysis. Replacement of this catalytic residue with a non-participating amino acid, could potentially render the mutant incapable of processing the intact glycoproteins or glycopeptides, but still allows the enzyme to retain the ability to transfer the glycan substrates to different acceptors if an activated sugar oxazoline is provided.

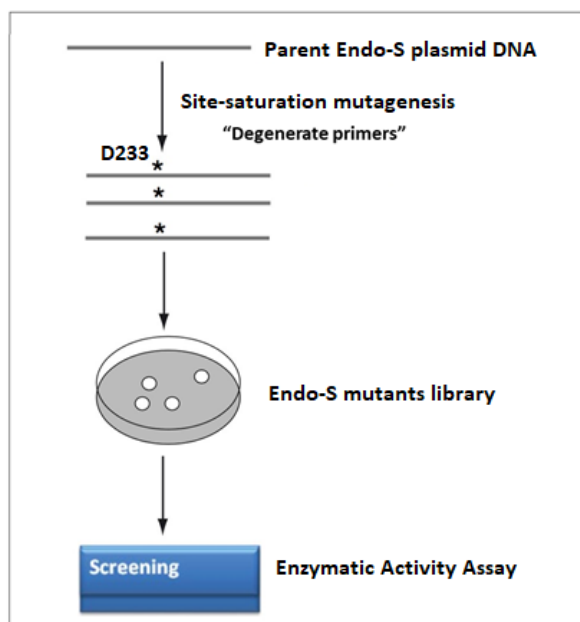


Figure 17. The general procedure of site-directed saturation mutagenesis of Endo-S using the degenerate primers.

For the subsequent comparative studies of their enzymatic activities, all Endo-S mutants were expressed and purified under the same conditions that were used for the expression of the wild-type Endo-S. The expression yield of Endo-S mutants was 15–30 mg/L of bacterial cell culture, which is comparable to the previously published expression yield of Endo-S and Endo-S D233A and D233Q mutants.<sup>103</sup> Endo-S and mutants were expressed as fusion proteins with a Glutathione S-transferase (GST) tag located at the C terminus to facilitate protein folding and affinity purification. To ensure that the GST domain does not perturb the normal enzymatic activity of Endo-S enzymes, the GST tag was removed by thrombin protease cleavage.<sup>125</sup> Comparison of the hydrolytic activities of the untagged and fusion proteins of Endo-S demonstrated the same level of enzymatic activity under previously reported reaction conditions.<sup>114</sup>

## 2. Transglycosylation and hydrolysis activities of Endo-S mutants

The specific activity of Endo-S and its glycosynthase mutants for hydrolysis of complex glycoforms of antibody was evaluated and quantified using a commercial therapeutic monoclonal antibody rituximab as model substrate. For assessing specific transglycosylation activities (Figure 18), the native N-glycan mixture (G0, G1 and G2) of rituximab was first removed by Endo-S, and the purified rituximab-GlcNAc was used as the glycosyl acceptor substrate for the subsequent transglycosylation assays. The full-sialylated complex type (S<sub>2</sub>G<sub>2</sub>) N-glycan was extracted from egg yolk and converted to the oxazoline donor substrate by chemical modifications.<sup>100</sup> The results of both activity tests are summarized in Table 1.

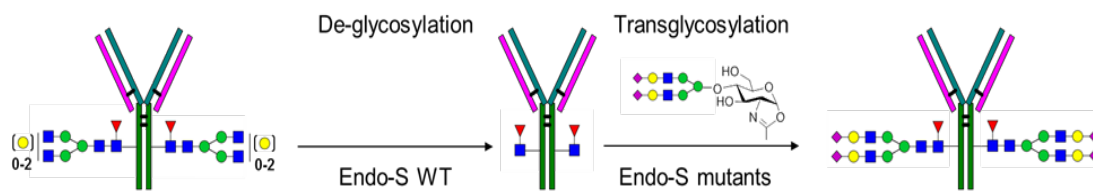


Figure 18. Schematic presentation of hydrolysis and transglycosylation reactions by Endo-S and its mutants using antibody rituximab as starting material. Complete deglycosylation of the original N-glycans of rituximab was confirmed by ESI-LS-MS analysis. The rituximab-GlcNAc intermediate was then purified via Protein-A affinity chromatography and was subsequently used for transglycosylation reactions catalyzed by the Endo-S mutants generated by site-directed mutagenesis.<sup>123</sup>

Comparison of the hydrolytic activities demonstrated that all mutants of Endo-S except Endo-S D233C showed significantly decreased tendency to hydrolyze the complex type N-glycans from the intact rituximab in comparison to the wild-type Endo-S. Specifically, the mutants D233F, D233G, D233H, D233K, D233R, D233L, D233M, D233P, D233W, and D233Y only possessed <1% of the intrinsic hydrolytic activity of the wild-type Endo-S. Endo-S D233C retained a significant capacity (~33% of the wild-type Endo-S) to hydrolyze the complex N-glycans attached at the Asn-297 glycosylation site located in the IgG-Fc region. Besides the mutants D233N, D233E, D233S and D233T, which showed only marginal activities, the D233G mutant also showed a relatively high hydrolytic activity towards rituximab despite the fact that the simple hydrogen functional group of glycine residue is typically considered incapable of participating in hydrogen bonding and many other interactions involved in enzyme catalysis.<sup>126</sup>

The transglycosylation assay revealed that most Endo-S mutants were still able to transfer the biantennary complex type glycan oxazoline to the deglycosylated rituximab with varied efficiencies. In particular, Endo-S D233C, D233E, D233G, D233M, D233N, and D233S exhibited the highest transglycosylation activities among the glycosynthase mutants tested here. However, via comparison of the overall transglycosylation efficiencies, most mutants with potent transglycosylation activities also possessed significant hydrolytic activities against antibody, a property less ideal for the glycoengineering application using ENGases. For instance, Endo-S D233C demonstrated the highest activities for both hydrolysis and transglycosylation among the 19 mutants studied here, but its overall catalytic efficiency for antibody glycoform remodeling (defined by the ratio of transglycosylation to hydrolysis, T/H) was found to be moderate. Interestingly, the Endo-S mutant D233M still retained a relatively high transglycosylation activity among the mutants with a remarkably low residual hydrolytic activity. Therefore, the highest overall catalytic efficiency makes D233M the most efficient glycosynthase mutant of Endo-S for antibody glycoengineering among all the mutants whose enzymatic activities were studied in this work.

On the basis of specific transglycosylation and hydrolytic activities by Endo-S mutants against antibody (Table 1), Endo-S D233M mutant showed an approximately 7- and 8-fold enhanced synthetic efficiency (T/H) versus those of D233Q and D233A, respectively. To directly demonstrate the enhanced catalytic efficiency of D233M for IgG glycosylation, we monitored the progression of three glycosylation reactions by mutants of Endo-S, D233M, D233Q, and D233A, under the same reaction condition. The parallel reactions were monitored by LC-ESI-MS (Figure 19). The comparison of

the time courses of all three reactions indicated that the mutant D233M was more efficient in catalyzing the glycosylation of rituximab than the previously identified Endo-S D233A and D233Q. According to this comparison, the D233M-catalyzed glycosylation reaction reached over 95% conversion of the rituximab N-glycoform within 30 min, while the Endo-S D233A- and D233Q-catalyzed reactions gave an approximately 60% conversion yield at 60 min under the same condition.

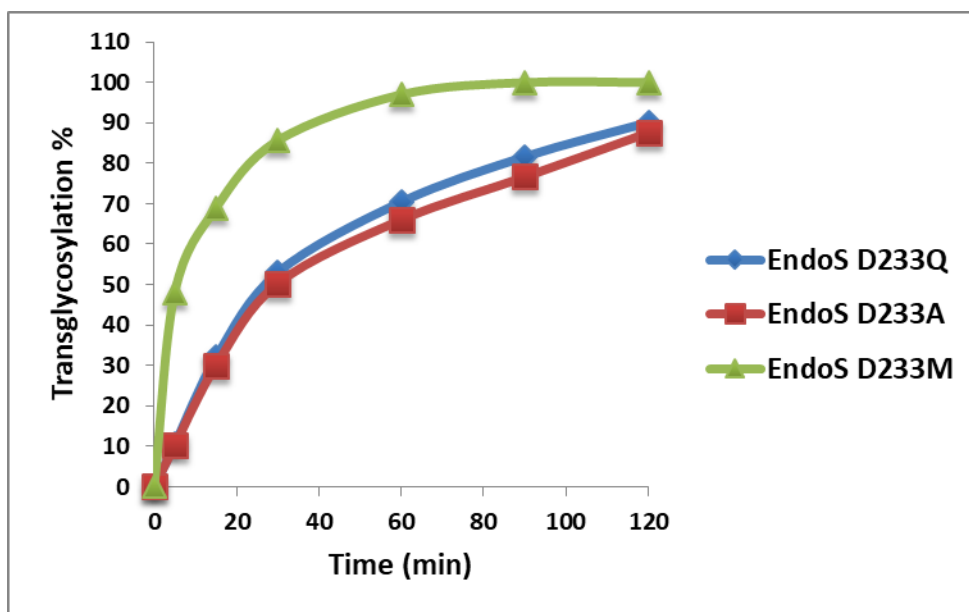


Figure 19. Comparison of transglycosylation reactions catalyzed by Endo-S D233M and previously reported Endo-S D233Q and D233A mutants. Fully sialylated complex glycan oxazoline SCT-Oxa was used as the glycosyl donor substrate. The reaction was conducted by incubating deglycosylated antibody (10 mg/mL) and SCT-Oxa with each mutant enzyme (0.05 mg/mL) in PBS buffer with a pH of 7.4 at 30°C. For each reaction, 20 molar equivalents of SCT-Oxa was added to the deglycosylated rituximab in the presence of Endo-S mutants. The data sets presented here are representative of three independent experiments.<sup>123</sup>

Table 1. Comparison of specific transglycosylation efficiencies of Endo-S mutants measured by LC-ESI-MS using a commercial antibody rituximab as substrate.<sup>123</sup>

Endo-S Mutants	Specific Hydrolysis Activity 100*( $\mu\text{mol}/\text{min}/\text{mg}$ )	Transglycosylation Activity 100*( $\mu\text{mol}/\text{min}/\text{mg}$ )	Transglycosylation/Hydrolysis Ratio T/H
WT	2.77 $\pm$ 0.64	25.9 $\pm$ 4.7	9.35
D233A	0.06 $\pm$ 0.01	1.06 $\pm$ 0.2	17.7
D233C	0.92 $\pm$ 0.16	21.3 $\pm$ 3.5	23.1
D233E	0.36 $\pm$ 0.09	9.45 $\pm$ 1.6	26.3
D233F	0.02 $\pm$ 0.01	0.16 $\pm$ 0.04	8.00
D233G	0.25 $\pm$ 0.04	3.13 $\pm$ 1.2	12.5
D233H	0.01 $\pm$ 0.01	0.00	0.00
D233K	0.01 $\pm$ 0.01	0.00	0.00
D233R	0.01 $\pm$ 0.01	0.00	0.00
D233I	0.04 $\pm$ 0.01	0.14 $\pm$ 0.05	3.50
D233L	0.02 $\pm$ 0.01	0.14 $\pm$ 0.03	7.00
D233M	0.02 $\pm$ 0.01	2.71 $\pm$ 0.4	136
D233N	0.43 $\pm$ 0.12	2.96 $\pm$ 1.3	6.88
D233P	0.02 $\pm$ 0.01	0.00	0.00
D233Q	0.05 $\pm$ 0.01	0.98 $\pm$ 0.2	19.6
D233S	0.36 $\pm$ 0.01	3.65 $\pm$ 0.6	10.1
D233T	0.21 $\pm$ 0.03	1.79 $\pm$ 0.3	8.50
D233V	0.21 $\pm$ 0.06	0.25 $\pm$ 0.08	1.20
D233W	0.01 $\pm$ 0.01	0.00	0.00
D233Y	0.01 $\pm$ 0.01	0.26 $\pm$ 0.1	26.0

<sup>a</sup>The specific hydrolysis activity of each enzyme was assayed by incubating the synthetic biantennary complex type rituximab with different mutants or wild-type Endo-S (0.01 mg/mL) in PBS pH 7.4 at 30 °C. To test the specific transglycosylation activity of each enzyme, the deglycosylated rituximab was used as the glycosyl acceptor and the complex type oxazoline (SCT) as the glycosyl donor substrate with a final concentration of enzymes at 0.01 mg/mL. The molar ratio of the glycosyl acceptor to donor substrate was 1:20. The experimental results shown here were collected from the average data of three independently repeated assays.

### 3. Enzyme kinetic analysis of Endo-S mutants D233M and D233A

The observed difference in the catalytic efficiency of mutants Endo-S D233M and D233A prompted us to perform kinetic measurements on the two mutants. Using a fully sialylated biantennary complex glycan oxazoline (SCT-Oxa) as the donor and the deglycosylated rituximab antibody as the acceptor substrate, we measured the kinetic profiles of Endo-S D233M and D233A mutants for both substrates. A mass spectrometry-based approach combined with an intact antibody internal standard was used to more accurately monitor the formation of the transglycosylation product in a quantitative manner. The results are summarized in Tables 2 and 3.

For the biantennary complex-type glycan oxazoline, the catalytic efficiency of Endo-S D233M ( $k_{\text{cat}}/K_{\text{M}} = 0.03 \text{ min}^{-1} \mu\text{M}^{-1}$ ) showed a 3-fold increase in comparison with that of Endo-S D233A ( $k_{\text{cat}}/K_{\text{M}} = 0.01 \text{ min}^{-1} \mu\text{M}^{-1}$ ) (Table 2 and Figure 20a). The apparent increase in the ( $k_{\text{cat}}/K_{\text{M}}$ ) of Endo-S D233M versus that of D233A was a result of an approximately 4-fold increase in the rate of turnover (as measured by  $k_{\text{cat}}$ ) and a 2-fold reduced substrate affinity for the oxazoline estimated by the  $K_{\text{M}}$  values, as a higher  $K_{\text{M}}$  is indicative of a lower substrate affinity. These results suggested that substitution with a methionine instead of an alanine at the Asp-233 residue enhanced the enzymatic turnover number of Endo-S for the glycan oxazoline substrate with a moderate decrease in the substrate affinity.

For the glycosyl acceptor substrate, the deglycosylated antibody, Endo-S D233M exhibited a substrate affinity much higher than that of Endo-S D233A. This was clearly supported by the Michaelis–Menten curves generated for the two mutants (Figure 20b), which demonstrated that Endo-S D233M was much easier to saturate

with the antibody substrate than Endo-S D233A was. The  $K_M$  value of D233M for the deglycosylated antibody was estimated to be 30  $\mu\text{M}$ , while the  $K_M$  value of D233A was projected to be higher than 200  $\mu\text{M}$  (Table 3). On the other hand, the catalytic turnover number ( $k_{cat}$ ) of Endo-S D233A for the antibody substrate could not be accurately measured due to the fact that the concentration of antibody required to saturate the enzyme exceeded the solubility of antibody under normal solution conditions.

Table 2. Kinetic parameters of Endo-S mutants D233M and D233A for SCT-Oxa.

Enzyme	$k_{cat}$ ( $\text{min}^{-1}$ )	$K_M$ ( $\mu\text{M}$ )	$k_{cat}/K_M$ ( $\text{min}^{-1} \mu\text{M}^{-1}$ )
Endo-S D233M	$5.0 \pm 0.9$	$195.4 \pm 7.2$	0.03
Endo-S D233A	$1.3 \pm 0.2$	$87.9 \pm 10.1$	0.01

Table 3. Kinetic parameters of Endo-S mutants D233M and D233A for rituximab.

Enzyme	$k_{cat}$ ( $\text{min}^{-1}$ )	$K_M$ ( $\mu\text{M}$ )	$k_{cat}/K_M$ ( $\text{min}^{-1} \mu\text{M}^{-1}$ )
Endo-S D233M	$5.5 \pm 1.9$	$30.2 \pm 7.2$	0.18
Endo-S D233A	-*	>200	-*

\*The catalytic turnover number of Endo-S D233A could not be accurately determined because the concentration required for the antibody substrate saturation could not be reached in the experiments under normal conditions.<sup>123</sup>

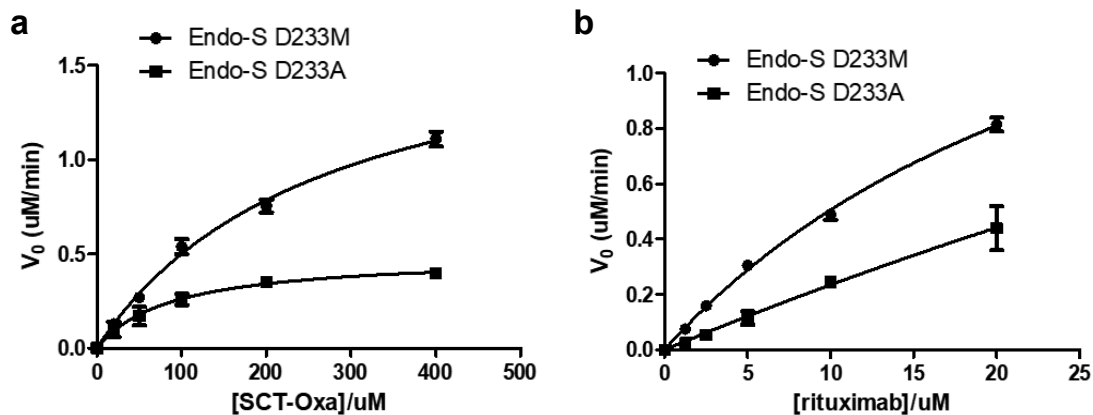


Figure 20. Michaelis-Menten plots of Endo-S D233M and Endo-S D233A. Kinetics for the two substrates were shown here: a) for the glycosyl donor, a gradient of SCT-Oxa (from 6.25 to 400  $\mu\text{M}$ ) was tested with a constant concentration of the deglycosylated rituximab (20  $\mu\text{M}$ ); b) for the glycosyl acceptor, a serial dilution of rituximab (0.32 to 20  $\mu\text{M}$ ) was tested with 400  $\mu\text{M}$  of SCT-Oxa. For both Endo-S D233M and D233A, the enzyme concentration was fixed at 0.01 mg/mL (0.067  $\mu\text{M}$ ). The data sets presented here are representative of three independent experiments.<sup>123</sup>

#### 4. Chemical synthesis of a complex glycan thiazoline inhibitor for Endo-S

The designed complex type glycan-based thiazoline inhibitor compound 2 was derived from the naturally existing sialylated biantennary complex type free glycan SCT 1 (Figure 21). The SCT free glycan was first released from the sialoglycopeptide (SGP) by the endoglycosidase Endo-M. The original SGP peptide was harvested and purified from commercial egg yolk powder according to our previously published procedure.<sup>127</sup> The released free SCT glycan then underwent a series of chemical modifications to afford the desired complex type glycan thiazoline 2.

The chemical synthesis of the thiazoline inhibitor presented in this work was achieved in collaboration with Dr. Chao Li from Prof. Lai-Xi Wang's group at the

Department of Chemistry and Biochemistry, University of Maryland, College Park. The work was published in Journal of Carbohydrate Chemistry in 2017.<sup>124</sup> Following our previously reported method Dr. Li was able to successfully convert the free SCT glycan **1** to the thiazoline-based inhibitor compound **2**.<sup>120, 128</sup> We performed the majority of chemical synthesis and purification experiments together, including the peracetylation of SCT glycan, synthesis of thiazoline derivative by the Lawesson's reagent, and purification of the final product by size-exclusion chromatography. Dr. Li and I also conducted the targeted enzymatic inhibition assays with the synthetic thiazoline inhibitor **2** together with assistance from other co-authors listed in the publication.<sup>124</sup>

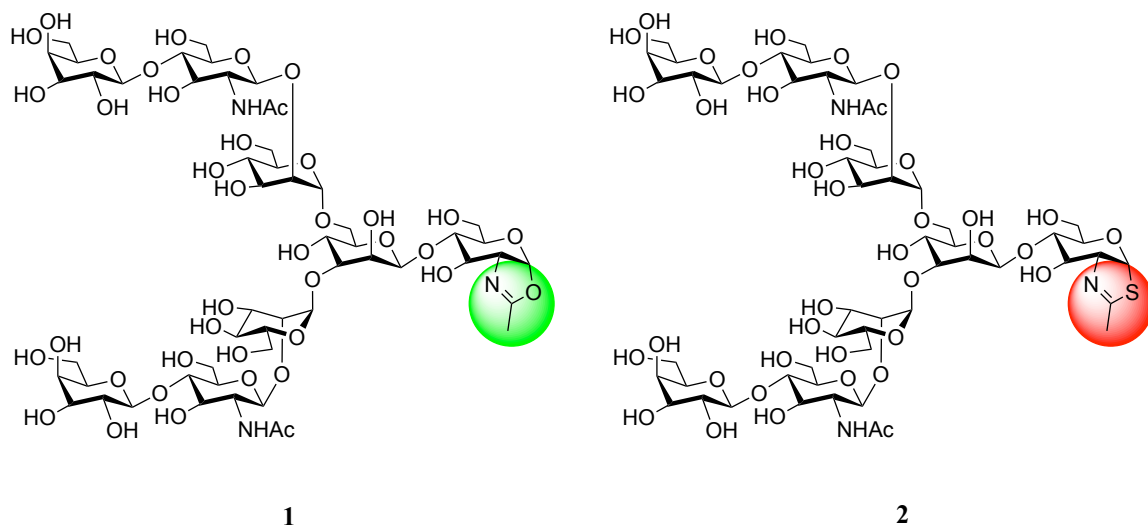


Figure 21. The chemical structure of the complex type N-glycan oxazoline (**1**) and the corresponding complex type N-glycan thiazoline (**2**).<sup>124</sup>

## 5. Inhibitory activity assays for the synthetic thiazoline-based inhibitor

The inhibitory activity of the synthetic thiazoline inhibitor compound **2** was examined against several commonly studied ENGases. To probe the specific inhibition of compound **2** against Endo-S, a fully sialylated and fucosylated complex N-glycoform of antibody rituximab (S<sub>2</sub>G<sub>2</sub>F-rituximab) was synthesized for use as starting material, following the previously reported glycoengineering strategy.<sup>103</sup> The relative abundance of the free glycans released by ENGases in the presence or absence of the inhibitor was monitored by high-performance anion-exchange chromatography coupled with pulsed amperometric detection instrument (Dionex HPAEC-PAD). It was found that glycan thiazoline **2** showed potent inhibitory activity against Endo-S, with an IC<sub>50</sub> of 1.4 μM (Figure 22A). To examine its inhibitory activity against Endo-M, sialoglycopeptide SGP was used as the substrate and the released glycans were also measured by HPAEC-PAD analysis. The results suggested that the glycan thiazoline **2** was also effective in inhibiting the hydrolase activity of Endo-M, and the IC<sub>50</sub> was 0.27 μM (Figure 22B). If the IC<sub>50</sub> value was taken as an indicator for the inhibition potency, the thiazoline inhibitor would be more active against Endo-M than Endo-S by approximately 5- and 2-fold, respectively. In addition, in comparison with the previously reported high-mannose type glycan-based thiazoline (Man<sub>9</sub>GlcNAc), which exhibited an IC<sub>50</sub> of 6 μM against Endo-M, the synthetic complex type N-glycan thiazoline was 22-fold more active.<sup>14</sup>

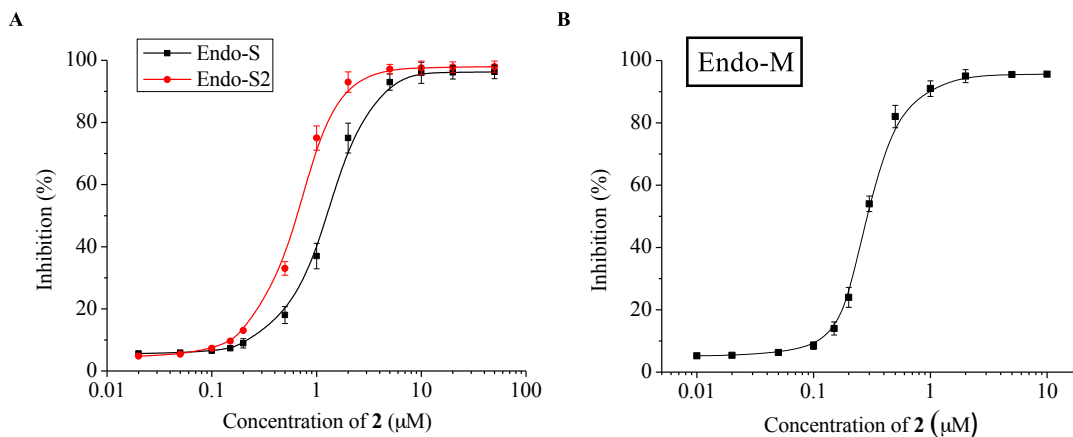


Figure 22. Inhibition effects of Endo-S, Endo-S2, and Endo-M by CT-thiazoline (**2**).

A) Inhibition of Endo-S and Endo-S2 by **2** using synthetic S<sub>2</sub>G<sub>2</sub>F-rituximab as substrate; B) Inhibition of Endo-M by **2**, using the protected glycan SCT-Fmoc as substrate.<sup>124</sup>

## 6. Investigation on non-enzymatic side reactions of glycan oxazoline

The formation of non-enzymatic glycosylation products between glycan oxazoline and antibody during transglycosylation was investigated here by carefully characterizing the chemical composition of the product antibody glycoform after each reaction. A typical transglycosylation reaction using Endo-S D233M and SCT-Oxa was carried out to validate the efficiency of this enzyme-assisted glycoengineering strategy. Non-enzymatic control experiments were conducted by directly incubating the deglycosylated antibody with a gradient of concentrations of glycan oxazolines in the absence of Endo-S enzymes. The nature of the glycosidic linkage formed after each reaction was verified by treating the product antibody with a unique amidase enzyme called PNGase F, which releases all N-linked glycans from glycoproteins including antibody.<sup>129</sup> Any oligosaccharides that remain attached to the amino acid

backbone after the PNGase F treatment are likely to be linked through a non-ENGase-catalyzed chemical linkage formed by the side reactions.

The standard transglycosylation reaction using the mutant Endo-S D233M and a reasonable amount of SCT-Oxa (20 molar equivalents to the antibody) achieved complete transglycosylation within 30-60 min (Figure 23). Analysis of the PNGase F-treated therapeutic antibody trastuzumab revealed no additional products besides the expected complex type antibody N-glycoform. On the other hand, control reactions with different glycan oxazoline concentrations (20, 40, 80, and 160 molar equivalents relative to the antibody) demonstrated that non-specific chemical ligation between the glycan oxazoline and antibody acceptor indeed occurred, but only when a large excess of oxazoline was used during a prolonged reaction time (Figure 24).

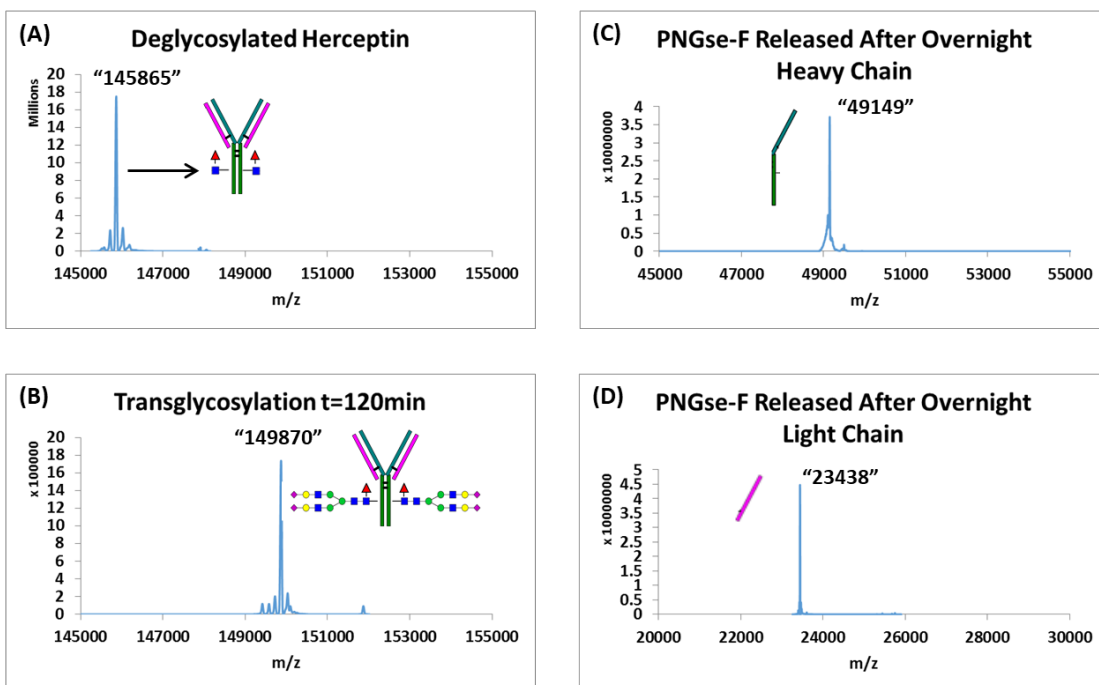


Figure 23. Mass spectrometry analysis of the antibody N-glycoforms generated by glycan remodeling of a therapeutic antibody trastuzumab (Herceptin). The reaction was performed by incubating deglycosylated antibody (10 mg/mL) and SCT-Oxa with a small amount of Endo-S D233M (0.05 mg/mL). The molar ratio of antibody to oxazoline was 1/20. Other reaction conditions followed the previously conducted transglycosylation reactions, as detailed in Figure 19. LC-MS analysis of the product glycoform revealed a single mass peak corresponding to the complex type trastuzumab N-glycoform (B), which confirmed complete transfer of complex glycan oxazoline. The product antibody after transglycosylation was subject to the PNGase F treatment, and heavy chain (C) and light chain (D) of the final product were analyzed separately by ESI-LC-MS under reducing conditions. The mass spectra that matches the mass of the PNGase F-treated heavy chain and light chain of antibody indicated that no significant non-enzymatic transfer of the complex glycan oxazoline under our conventional reaction condition.<sup>103</sup>

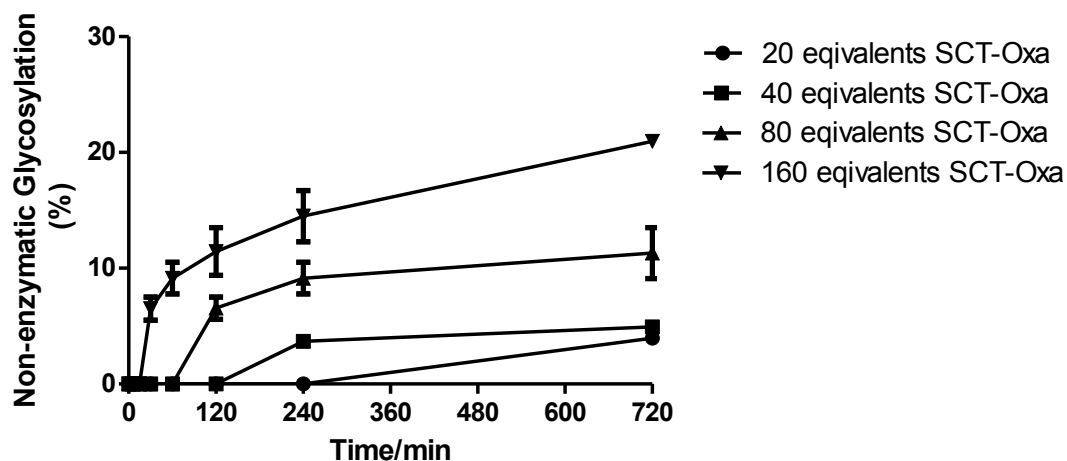


Figure 24. Non-enzymatic transfer of the sialylated complex type glycan oxazoline to the deglycosylated trastuzumab antibody in the absence of the Endo-S enzymes. The parallel reactions were conducted by incubating the deglycosylated trastuzumab and SCT-Oxa in a series of concentrations (20, 40, 80 and 160 equivalents to antibody) in PBS buffer with a pH of 7.4 at 30 °C. Other reaction conditions follow the previously stated transglycosylation reaction, as detailed in Figure 19 and experimental section. The product antibody of each control reaction was treated by PNGase F overnight, and the heavy chain and light chain of the final product were analyzed separately by ESI-LC-MS under reducing conditions. Selected raw data such as the mass spectra of antibody with the non-enzymatically transferred glycans are shown in the Supporting Information section.

### C. Discussion

We have previously identified two glycosynthase mutants of Endo-S, D233A and D233Q, which could transfer the intact and modified complex glycan oxazolines to Fc-deglycosylated IgG antibodies to afford homogeneous N-glycoforms. However, systematic mutagenesis study on Endo-S at the critical Asp-233 site had not been performed, and mechanistic insight into the different catalytic activities of these mutants is currently lacking.

In this study, we conducted a systematic mutagenesis analysis on Endo-S at Asp-233 and examined the hydrolytic and transglycosylation activities of the resulting mutants. The comparative studies revealed several glycosynthase mutants of Endo-S including D233M that demonstrated enhanced transglycosylation efficiencies compared to those of the previously identified Endo-S mutants. The kinetic data clearly indicated that the enhanced catalytic efficiency of the Endo-S D233M mutant versus that of the D233A mutant could be attributed to mainly two factors: the increased turnover number for the oxazoline donor substrate and the enhanced affinity for the antibody acceptor substrate. Nevertheless, the molecular basis behind this observed enhancement of the catalytic efficiency by the Asp-to-Met mutation remains to be elucidated by more detailed structural and mechanistic studies using additional biophysical approaches.

The first crystal structure of Endo-S was reported in 2014 by Sundberg and colleagues,<sup>116</sup> and more recently, the molecular structure of a full-length Endo-S bound with a complex free glycan was also solved by the same group.<sup>130</sup> In this co-crystallized structure, a functionally inactive double-mutant of Endo-S, in which both

the general acid/base residue Glu-235 and the key catalytic residue Asp-233 were substituted by leucine and alanine, respectively, was generated to abolish the intrinsic hydrolytic activity of Endo-S and to facilitate the crystallization process. The crystal structure provides a possible binding mode for the sugar residues of the complex type G2 glycan substrate by Endo-S, including the first GlcNAc (+1) residue. Molecular docking simulations suggest additional amino acids that make contact with the glycan. The side chain of T281 interacts with the O6 atom of GlcNAc (+1) through a hydrogen bond, whereas the N-acetamido group of the GlcNAc is also stabilized by the main chains of two “gating residues”, Q303 and Y305. In addition, hydrophobic interactions are implicated between GlcNAc (+1) and Y305 and W358 (Fig. 25b). Besides Y305, the structure also suggests that a D231 residue is involved in the interactions that stabilize the protonated D233-E235 network by providing a negative charge, and the transition state is stabilized by Y402 (Figure 25c).

Although these reported structures and related molecular simulations revealed important information about Endo-S overall conformation and how the non-reducing end oligosaccharides of the free glycan interact with specific amino acids at the active site of Endo-S, these existing crystal structures with the ground state N-glycans may not accurately display how the oxazolinium ring is recognized by the glycosidase domain of Endo-S. One potential solution is to determine the structure of Endo-S in complex with a stable, non-hydrolyzable glycan oxazoline analog, for example a glycan thiazoline<sup>101</sup>, which we recently synthesized and tested.<sup>124</sup> In addition to the glycan substrate, previous molecular simulations suggested that both Endo-S and IgG antibody would undergo significant conformational changes prior to the hydrolysis of

N-glycans.<sup>116</sup> Interestingly, kinetic analysis also indicated that the substrate affinity of Endo-S mutants for the IgG antibody is largely affected by the mutation at Asp-233 (Figure 19 and Table 3). Therefore, it would be of great interest to determine the molecular structure of an antibody-bound Endo-S to help understand the mechanism behind the enhanced substrate affinity for IgG due to the methionine substitution.

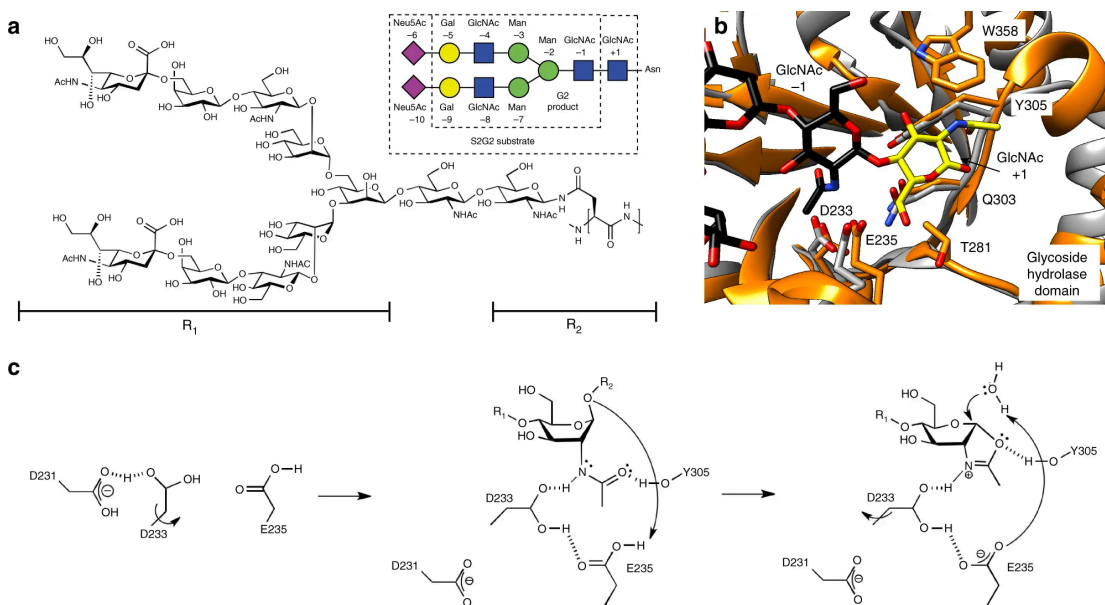


Figure 25. Molecular mechanism of Endo-S based on the co-crystallized structure with the G2 glycan substrate. a. Structure of the S2G2 glycan substrate based on molecular dynamic simulations. b. Structural alignment of the active site of Endo-F3 (gray) and Endo-S (orange). The residues of Endo-S are labeled with numbers. c. In the unbound form of Endo-S, no interactions can be observed between D233 and E235. In the first step of catalysis, structural displacement is found for both the GlcNAc (-1) residue and D233, making it possible for hydrogen bonding network between D233, E235 and the acetamido group. In the second step, E235 is protonated again and D233 was returned to its original position, facilitated by a deprotonated D231.<sup>130</sup>

To further study the mechanistic aspects of Endo-S and its mutants, a facile synthesis of a complex N-glycan thiazoline compound was achieved starting from the sialoglycopeptide (SGP) that can be obtained easily from the chicken egg yolks in large quantities.<sup>131</sup> This synthetic glycan thiazoline therefore represents a new type of mechanism-based inhibitor specially designed for the endoglycosidases with high selectivity for complex N-glycoproteins including antibodies. As mentioned above, this inhibitor may be useful as a transition state analog to form complexes with the ENGases during structural analysis. In addition, given the potential functional role of Endo-S in human infections by the pathogenic bacterium *Streptococcus pyrogenes*, this synthetic inhibitor may be further developed for its ability to control bacterial infections and pathogenesis as a potential therapeutic drug candidate.<sup>114</sup>

Despite the effectiveness of the Endo-S mutants for antibody glycosylation remodeling, the potential non-enzymatic ligation reaction occurring between glycosyl oxazoline and protein residues has been suggested as a major issue for the application of glycan oxazoline in large-scale glycoengineering.<sup>122, 132</sup> Previous studies using the tandem mass spectrometry (MS/MS) identified the amino groups (-NH<sub>2</sub>) of the lysine residues as potential chemical glycosylation sites for the activated glycan oxazolines. NMR spectroscopy also revealed that the oxazoline was chemically attached to the lysine residues of antibody through a different linkage from N-linked glycosylation, and this aberrant linkage is resistant to the PNGase F-catalyzed cleavage<sup>133</sup>. Here, by revisiting the nature of the glycosidic linkage formed in the product antibody glycoform, our results clearly demonstrated that, under our reported optimal conditions, glycoengineering of antibody using Endo-S D233M and SCT oxazoline

could achieve complete transfer of glycans in a timely fashion without the formation of any non-enzymatic side products. By comparing the levels of the non-selective glycosylation under different oxazoline concentrations in the absence of enzyme, we further concluded that this non-selective chemical ligation reaction occurred only if a relatively high concentration of glycan oxazoline was used in the transglycosylation reaction over an extended time of incubation, which is normally not required for the complete transfer of glycan by Endo-S mutants.

## **D. Conclusion**

The glycosynthase mutants of Endo-S D233Q and D233A are important biocatalysts for remodeling the glycosylation patterns of antibodies. The use of endoglycosidases to engineer antibody glycosylation is highly selective and efficient because of controlled stereo- and regio-selectivity by enzymes. Therefore, generation of more efficient Endo-S mutants for the transglycosylation reaction could improve the current glycoengineering strategy of antibody glycoforms, which could potentially be applied to enhance the efficacy of antibody therapeutics in clinic applications. Here, we presented several novel Endo-S mutants such as Endo-S D233M that demonstrated potent transglycosylation activity with diminished product hydrolysis. Kinetic studies on the new mutants Endo-S D233M and the previously reported Endo-S D233A revealed important mechanistic information that could help us understand the different catalytic behaviors of the two Endo-S mutants studied here in catalyzing the transglycosylation of the IgG antibody. In addition, a new mechanism-based inhibitor was designed for Endo-S and other ENGases that specifically target the complex type N-glycans. Further development of this inhibitor such as increasing its cell permeability could potentially lead to new therapeutic candidates for certain bacterial pathogenesis. Finally, the reported side reaction issue associated with the use of the activated glycan oxazoline was addressed in this chapter by characterizing the glycosylated antibody. In conclusion, the overall efficiency of transglycosylation process catalyzed by Endo-S glycosynthase mutants was significantly improved with the development of new glycosynthase mutants and the optimization of the reaction conditions.

## **E. Materials and Methods**

### **1. Chemicals and biochemical materials**

All chemicals and biochemical materials were qualified as reagent grade or above. The reduced glutathione stock solution (Sigma-Aldrich) was prepared in 50 mM Tris-HCl buffer at pH 8.0 and stored at 4°C. The diluted glutathione elution buffer was prepared immediately before affinity purification to minimize oxidation. The monoclonal therapeutic antibody rituximab and trastuzumab were purchased from Genentech Inc. (San Francisco, CA). The antibody materials were purified by Protein-A affinity chromatography to remove any storage additives and stored in phosphate-buffered saline (PBS, containing 137 mM NaCl, 2.7 mM KCl, 8 mM Na<sub>2</sub>HPO<sub>4</sub>, and 2 mM KH<sub>2</sub>PO<sub>4</sub>, pH 7.4) at 4°C. The fully sialylated complex-type glycan oxazoline was chemically synthesized according to the previously published procedure<sup>102</sup>. The concentration of antibody was measured on a NanoDrop 2000c by detecting absorbance at 280 nm using a molar extinction coefficient of 13700 M<sup>-1</sup>cm<sup>-1</sup>. High-performance anion-exchange chromatography with the pulsed amperometric detection (HPAEC-PAD) was performed on a Dionex ICS-5000 chromatography system (Fischer Scientific) equipped with an electrochemical detector (ED50) and an anion exchange column (PA200, 4 × 250 mm). The mobile phase (flow rate, 0.5 ml/min) was composed of 100 mM NaOH (eluent A) and 250 mM NaOAc in 100 mM NaOH (eluent B). The gradient used was as follows: 0 min, 100% eluent A; 20 min, 80% eluent A, 20% eluent B. The LC-ESI-MS was performed on an Exactive™ Plus Orbitrap Mass Spectrometer (Thermo Scientific) equipped with a Waters XBridge™ BEH300 C4 column (3.5 μm, 2.1 × 50 mm) and a C18 column (2.1 × 10 mm, 1.5 μm).

## 2. Mutagenesis, expression, and purification of Endo-S and mutants

The pGEX plasmid vector containing the coding sequence for the wild-type Endo-S was a gift from M. Collin (Lund University, Lund, Sweden). The Endo-S mutants were generated by PCR reactions using the Q5 site-directed mutagenesis kit (NEB) by the manufacturer's instructions. For systematic mutagenesis at the Asp-233 residue of Endo-S, two degenerate primers were used: 5' - CGTAAATTCGTGCTCAATNNAATATCTAGTCCATCGACACCACGATCAGTT-3' (forward) and 5'-AACTGATCGTGGTGTGCGATGGACTAGATATTNNNATTGAGCACGAATTTACG-3' (reverse). The corresponding mutations were verified by sequencing the coding sequence using T7 promoter and T7 terminator primers (Macrogen Inc., MD).

Each of the wild-type and mutant Endo-S protein was expressed using a widely used T7 expression *Escherichia coli* strain BL21/DE3 competent cell (NEB). The transformed competent cells were grown in 20 mL of 2YT pre-medium with 100 µg/mL carbenicillin antibiotic added. The pre-culture was incubated at 37 °C and induced with 0.5 mM isopropyl β-d-1-thiogalactopyranoside (IPTG) when the OD<sub>600</sub> reached 0.8–1.0. The induced cells were then incubated at 20 °C overnight and harvested by high-speed centrifugation (8000 rpm for 30 min). The cell were lysed using the bacterial cell lysis buffer (Gold Biotechnology, Inc.) following the manufacturer's instructions. After further centrifugation (2000 rpm for 30 min) the glutathione S-transferase (GST)-tagged proteins were purified using the GST affinity column GSTrap HP (GE Healthcare). The purified Endo-S proteins were diluted in phosphate-buffered saline (PBS) at pH 7.4 after buffer exchange using Amicon ultrafiltration units (10 kDa, Millipore). The purity of Endo-S proteins was shown to

be >90% by sodium dodecyl sulfate–polyacrylamide gel electrophoresis (SDS-PAGE), and the final concentration of each GST-tagged Endo-S variant was measured using a NanoDrop 2000c instrument at an absorbance of 280 nm using molar extinction coefficient of  $12200 \text{ M}^{-1}\text{cm}^{-1}$ .

### 3. Synthesis of deglycosylated antibody by wild-type Endo-S as acceptor substrate for transglycosylation

To generate the deglycosylated rituximab as the glycosyl acceptor substrate for the following transglycosylation assays, the commercial rituximab was treated with the wild-type Endo-S at a substrate/enzyme ratio of 1000/1 (w/w) for 30 min at 37 °C to release its native heterogeneous N-glycans. The complete release of the N-glycans attached to the glycosylation site at Fc region of rituximab was confirmed by the liquid chromatography–mass spectrometry (LC–MS) analysis. The resulting deglycosylated rituximab containing only the fucosylated innermost GlcNAc residue was purified using protein-A affinity chromatography following manufacturer's instructions (GE healthcare). The deconvoluted mass data (m/z) of the purified rituximab corresponds correctly with the calculated mass of (Fuc $\alpha$ 1,6)GlcNAc-rituximab molecule. LC-MS results: calculated for the heavy chain of (Fuc $\alpha$ 1,6)GlcNAc-rituximab, M = 49,420 Da; found (m/z), 49,412 (deconvoluted number).

#### 4. Synthesis of the S<sub>2</sub>G<sub>2</sub>F rituximab by mutant Endo-S D233Q as starting material for hydrolysis assays

Because native commercial rituximab displays heterogeneous compositions of various N-glycans attached at the conserved N-glycosylation site at Asn-297, a homogeneous antibody N-glycoform is required both for the hydrolysis assay and as the internal standard used for the quantification of the reaction product. A reaction mixture of 69  $\mu$ M (Fuc $\alpha$ 1,6)GlcNAc-rituximab and 1.38 mM SCT-oxa (20 eq.) was incubated with Endo-S2 D233Q (0.05 mg/mL) at 30 °C in Tris buffer (0.1 M, pH 7.4) for 4 h. The LC-MS analysis indicated completion of the glycosylation reaction after 2 h. The product glycoform S<sub>2</sub>G<sub>2</sub>F-rituximab was then purified by protein-A affinity chromatography. LC-MS results: calculated for the heavy chain of S<sub>2</sub>G<sub>2</sub>F-rituximab, M = 51,421 Da; found (m/z), 51,412 (deconvolution data).

#### 5. Liquid Chromatography-Mass Spectrometry (LC-ESI-MS) of antibodies

The LC-MS characterization of antibody N-glycoforms was conducted on an Exactive Plus Orbitrap instrument (Thermo Scientific). The reduced antibody sample was analyzed with a Waters XBridge™ BEH300 C4 column (3.5  $\mu$ m, 2.1  $\times$  50 mm). The program includes a 9 min linear gradient from 5 to 90% MeCN containing 0.1% formic acid at a flow rate of 0.4 mL/min. The original mass data of the heavy chain and light chain of antibody were then processed for deconvolution and integration using MagTran Software (Amgen).

## 6. Quantification of hydrolysis and transglycosylation reaction products using internal standard and a single-point normalization factor

To monitor hydrolysis and transglycosylation reactions in a more quantitative fashion, either of the following two glycan-modified antibody derivatives was used as the internal standards for the LC–MS analysis.<sup>134</sup> One standard was the completely deglycosylated rituximab antibody that was generated by treating the antibody with the peptide-N-glycosidase F (PNGase F), which could remove all Fc N-glycans from the N-glycoproteins and simultaneously introduced an Asn-to-Asp mutation at the conserved N-glycosylation site; the other standard was the fully sialylated glycoform, S<sub>2</sub>G<sub>2</sub>F-rituximab, which was synthesized according to the previously described procedure.<sup>103</sup> Serial dilutions containing a gradient of S<sub>2</sub>G<sub>2</sub>F-rituximab (0, 0.25, 0.5, 0.75, 1.0, 1.25, and 1.5  $\mu$ M) were mixed with a stock solution containing 0.67  $\mu$ M internal standard. The relative intensity of the reaction product and the standard peaks were then analyzed by the selected ion monitoring (SIM) to calculate a single-point normalization factor.<sup>135</sup> For each glycan remodeling reaction, the amount of the reaction product could be deduced from its relative abundance to the internal standard following the normalized mathematical algorithm.<sup>136</sup>

## 7. Transglycosylation and hydrolysis activity assays for Endo-S mutants

The specific hydrolytic activity of each Endo-S mutant and wild-type (0.01 mg/mL) was analyzed in Tris-HCl buffer (0.1 M, pH 7.4) at 30 °C with the synthetic biantennary sialo-complex-type rituximab (1.0 mg/mL, 6.9  $\mu$ M) as starting material. Each reaction was terminated at 5 min, and an aliquot was taken from the reaction mixture and dissolved in 0.1% formic acid to quench the reaction. The relative

quantity of the hydrolysis product was then calculated through deconvolution and integration of the selected MS peaks using the internal standard as a reference. The experimental details of product quantification using the LC–MS are described above. The specific transglycosylation activity of Endo-S mutants was measured in a similar fashion. The deglycosylated rituximab (10.0 mg/mL, 69  $\mu$ M) was incubated with SCT-Oxa (1.38 mM, 20 eq.) while being catalyzed by Endo-S enzymes (0.01 mg/mL) under the same condition that was used for the hydrolysis assay. The product S<sub>2</sub>G<sub>2</sub>F-rituximab was analyzed by LC-MS as mentioned above. Both enzyme activity assays were repeated twice for each mutant and the wild-type Endo-S, and the average activity is recorded in the Results section. For the transglycosylation assay, at least three time points ( $t = 5, 10,$  and  $15$  min) were sampled to ensure that the specific activity was measured as the initial rate of the transfer reaction without any potential product hydrolysis.

#### **8. Measurements of $K_M$ and $V_{max}$ of Endo-S mutants for SCT-oxa**

To measure the kinetic parameters of Endo-S D233M and D233A, serial dilutions with a total volume of 20  $\mu$ L reaction were prepared with a gradient of the SCT-Oxa concentrations and a constant deglycosylated antibody concentration mixed in PBS buffer at pH 7.4. Each reaction was initiated by adding 1  $\mu$ L of Endo-S mutant to give the final concentration of 0.1 mg/mL, and the reaction was conducted at 30  $^{\circ}$ C. The concentrations of SCT-Oxa were within the range of 6.25–400  $\mu$ M, whereas the concentration of the deglycosylated antibody was fixed at 20  $\mu$ M. For each reaction, three aliquots were taken at 1, 2, and 3 min of the same reaction, and the sampled reaction mixtures were immediately quenched in 100  $\mu$ L of 0.1% formic acid and

frozen at -20 °C. The quenched reaction samples were then characterized by ESI-LC-MS, and the concentration of the product was calculated using the normalization factor and the internal standard, as shown above. A linear progression curve was confirmed for each reaction by sampling at multiple early time points and plotting them in the same graph, which emphasized that the  $V_0$  measured indeed represented the initial rate of each reaction. The  $K_M$  and  $V_{max}$  values were deduced by fitting the initial velocities against the SCT-Oxa concentrations using the software GraphPad Prism7. The experiments were conducted in triplicate to determine the errors in each measurement. A control reaction without the enzyme added was set up for each of the transglycosylation reactions to confirm that non-enzymatic transfer of SCT-Oxa to the antibody did not occur, and the results obtained here indeed represent the specific transglycosylation activity of each Endo-S mutant.

#### **9. Measurements of $K_M$ and $V_{max}$ of Endo-S mutants for antibody**

The  $K_M$  and  $V_{max}$  values of Endo-S mutant D233M and D233A for the deglycosylated antibody substrate were measured in a fashion similar to that used for the measurements of SCT-Oxa. In the serial reactions, the deglycosylated antibody concentrations ranged from 0.313 to 20  $\mu$ M, whereas the SCT-Oxa concentration was fixed at 400  $\mu$ M. A similar control reaction was also performed for each antibody concentration to monitor the non-enzymatic side reactions.

#### **10. Chemical synthesis of complex glycan-based thiazoline inhibitor**

The SGP glycopeptide starting material was extracted and purified from hen's egg yolk according to the previously published method.<sup>127</sup> The crude glycopeptide

was enriched using the preparative HPLC to afford the pure SGP with a yield of 146 mg from 90 eggs. ESI-MS results: calculated mass for SGP,  $M = 2865.8$ . Found mass:  $2866.7 [M+H]^+$ . The sialylated N-glycan (50 mg, 50 mg/mL) was dissolved in buffer (pH 5.5, 5 mM  $\text{CaCl}_2$ , 50 mM NaOAc). The sialic acid was removed by incubating the glycan with  $\alpha 2-3,6,8$ -neuraminidase (80 U) at 37 °C overnight. Complete release of sialic acid was confirmed by LC-MS, and the intermediate was purified by Sephadex G-15 size exclusion chromatography. The asialylated glycan was then subject to peracetylation reaction to protect the hydroxyl functional groups of the compound. A solution of the glycan (50 mg, 0.035 mmol) in pyridine (5 mL) and acetic anhydride (5 mL) was stirred at 40 °C for 12 h until the TLC indicated that acetylation was complete. Finally, the peracetylated glycan was converted to thiazoline compound using the Lawesson's reagent following previously reported method<sup>121</sup>, and the structure of the final product was confirmed by  $^1\text{H}$  NMR ( $\text{CDCl}_3$ , 400 MHz).

## 11. Inhibition assays of thiazoline glycan inhibitor against ENGases

The inhibitory activity of the thiazoline glycan compound against Endo-S was measured by testing the hydrolytic activity of Endo-S in the presence or absence of serial dilutions of the thiazoline inhibitor. A solution of synthetic  $\text{S}_2\text{G}_2\text{F}$ -rituximab (10  $\mu\text{M}$ ) in PBS (100  $\mu\text{L}$ , 100 mM, pH 7.4) was incubated with the respective enzyme (5  $\mu\text{M}$ ) in the presence of serial dilutions (0.02 to 50  $\mu\text{M}$ ) of the N-glycan thiazoline. Reactions without any inhibitors added were carried out as a control. The mixture was incubated at 30 °C for 10 min and the reaction was quenched by 0.1% TFA solution. The enzyme-released free N-glycans were quantitated by HPAEC-PAD, which was

optimized for the analysis of oligosaccharides and related compounds. The inhibition assay against Endo-M was performed using the SGP glycopeptide as the substrate following the same procedure as that with Endo-S.

## 12. Comparison of non-enzymatic glycosylation reactions by enzyme treatment.

A standard transglycosylation reaction was carried out by incubating the deglycosylated (Fuc $\alpha$ 1,6)GlcNAc-rituximab (69  $\mu$ M) with 1.38 mM SCT-Oxa in the presence of 0.05 mg/mL Endo-S D233M mutant. The reaction mixture was incubated at 30 °C in Tris buffer (0.1 M, pH 7.4) for 60 min. The initial product was analyzed by ESI-LC-MS to confirm the corresponding mass for the S<sub>2</sub>G<sub>2</sub>F-rituximab and then purified from the reaction mixture by affinity chromatography. The fully glycosylated antibody was then reduced to the heavy chain and light chain fragments by incubating the antibody with 50 mM TCEP reducing agent overnight to break disulfide linkage. The light chain and heavy chain were then characterized independently by ESI-LC-MS, as the two fragments could be separated on the C4 column (Waters XBridge™ BEH300, 3.5  $\mu$ m, 2.1  $\times$  50 mm) prior to the mass analysis. To verify the glycosidic linkage, antibody fragments were diluted into 100  $\mu$ L of 1x Glycoprotein Denaturing Buffer (NEB) incubated with PNGase-F (20 mU, NEB) at 37°C overnight. Finally, the PNGase-F-treated antibody fragments were characterized by ESI-LC-MS as described above.

To study the non-enzymatic chemical ligation between the glycan oxazoline and antibody, the same amount of deglycosylated rituximab (69  $\mu$ M) was incubated with a serial dilutions of SCT-Oxa (1.38 to 11.0 mM) at 30 °C in Tris buffer (0.1 M, pH 7.4) for up to 12 h. Each reaction was sampled at 30, 60, 120, 240, 720 min. The

same processing and analyzing procedures for the reacted antibody fragments were used to analyze non-enzymatic reactions as those for the standard transglycosylation reactions, which were mentioned in the previous experimental sections.

## F. Supporting Information

MDKHLLVKRTLGCVCAATLMGAALATHHDSLNTVKAEKTVQVQKGLPSD  
SLHYLSENSKKEFKEELSKAGQESQKVKEILAKAQQADKQAQELAKMKIPEK  
IPMKPLHGPLYGGYFRTWHDKTSDPTEKDKVNSMGELPKEVDLAFIFHDWT  
KDYSLFWKELATKHVPKLNKQGTRVIRTIPWRFLAGGDNSGIAEDTSKYPNT  
PEGNKALAKAIVDEYVYKYNLDGLDVDVEHDSIPKVDKKEDTAGVERSIQVF  
EEIGKLIGPKGVDKSRLFIMDSTYMADKNPLIERGAPYINLLLQVYGSQGEK  
GGWEPVSNRPEKTMEERWQGYSKYIRPEQYMIGFSFYEENAQEGNLWYDIN  
SRKDEDKANGINTDITGTRAERYARWQPKTGGVKGGIFSYAIDRDGVAHQPK  
KYAKQKEFKDATDNIFHSDYSVSKALKTVMLKDKSYDLIDEKDFPDKALRE  
AVMAQVGTRKGDLEFNGTLRLDNPAIQSLEGLNKFKKLAQLDLIGLSRITK  
LDRSVLPANMKPGKDTLETVLETYKKDNKEEPATIPPVSLKVSGLTGLKELD  
LSGFDRETLAGLDAATLTSLEKVDISGNKLDLAPGTENRQIFDTMLSTISNHV  
GSNEQTVKFDKQKPTGHYPDTYGKTSRLRPVANEKVDLQSLLFGTVTNQG  
TLINSEADYKAYQNHKIAGRSFVDSNYHYNNFKVSYENYTVKVTDSTLGTTT  
DKTLATDKEETYKVDFVSPADKTKAVHTAKVIVGDEKTMMVNLAEGATVIG  
GSADPVNARKVFDGQLGSETDNISLGWDSKQSIIFKLKEDGLIKHWRFFNSA  
RNPETTNKPIQEASLQIFNIKDYNDLNLENPNKFDDEKYWITVDTYSAQGER  
ATAFSNTLNNITSKYWRVVFDTKGDRYSSPVPELQILGYPLPNADTIMKTVT  
TAKELSQQKDKFSQKMLDELKIKEMALETSLNSKIFDVTAINANAGVLKDCIE  
KRQLLK

Supplementary Figure 1. Sequence of Endo-S (Genbank entry: AF296340).

## Chapter 3: Development of alternative antibody glycoengineering methods with relaxed substrate specificity for different glycan structures

### A. Introduction

Although the glycosynthase mutants of Endo-S have been applied by many groups to synthesize homogeneous N-glycoforms of antibody for different research purposes,<sup>108, 111, 137</sup> the currently known mutants of Endo-S, including D233M and D233Q, can only utilize the biantennary complex type or truncated Man<sub>3</sub>GlcNAc core glycan structures for antibody glycan remodeling. Other N-glycan structures such as the high-mannose or hybrid N-linked oligosaccharides were generally not susceptible to Endo-S-mediated transglycosylation. In terms of the narrow substrate specificity of the current glycoengineering strategy, a major breakthrough was made in 2016 by Wang and colleagues, who developed a new class of glycosynthase mutants for another GH18 family endoglycosidase F3 (Endo-F3). The glycosynthase mutants of Endo-F3, including Endo-F3 D165A, demonstrated the ability to transfer triantennary glycans to the deglycosylated antibody acceptor.<sup>85</sup> However, Endo-F3 mutants only act on the core fucosylated glycosyl acceptors for transglycosylation and did not exhibit any transfer activities towards non-fucosylated substrates. These studies collectively suggest that the glycosynthase mutants currently used in antibody glycoengineering still have major limitations in terms of their substrate specificity and transglycosylation efficiency.<sup>89</sup>

To further improve the current glycan remodeling strategy for monoclonal antibodies, Endo-S2, another GH18 family endoglycosidase also harvested from the

pathogenic bacterium *Streptococcus pyogenes* of serotype M49 was investigated for its potential glycan-remodeling activities. Sequence alignment analysis revealed approximately 37% amino acid sequence identity between Endo-S and Endo-S2. Comparative hydrolytic assays on serum antibodies by the two enzymes suggested that Endo-S2 possessed a more relaxed substrate selectivity for the N-glycans attached at the Fc region of antibodies, although it remained a mystery whether Endo-S2 was capable of transferring N-glycans to any glycosyl acceptors for transglycosylation reactions.<sup>138</sup> By analogy to previous studies conducted on Endo-S, potential glycosynthase mutants of Endo-S2 could also be generated through site-directed mutagenesis and studied for their transglycosylation activities based on a possible substrate-assisted mechanism. In particular, the functional variants of Endo-S2 could potentially act on additional N-glycan oxazoline structures for transglycosylation, which might expand the scope of the current ENGase-mediated glycosylation method. Therefore, systematic mutational study was performed on Endo-S2 at the catalytic amino acid residue Asp-184, which was selected based on sequence alignment between Endo-S/S2 and other ENGases. The hydrolytic and transglycosylation activities of the generated Endo-S2 mutants were tested and compared in order to screen for more efficient glycosynthase mutants for antibody glycoengineering.<sup>139</sup> The generation and comparison of Endo-S2 mutants was conducted using a similar experimental method to those on Endo-S, as described in Chapter 2. The results indicated that Endo-S2 did show both potent hydrolytic and transglycosylation activities, and saturation mutagenesis study successfully identified multiple glycosynthase mutants of Endo-S2, including Endo-S2 D184M and D184Q,

which exhibited significant oxazoline-transferring activities with much diminished hydrolytic tendencies against the product antibody glycoforms. More importantly, the glycosynthase variants of Endo-S2 showed flexible substrate specificity using three different types of N-glycan oxazoline structures (complex, high-mannose, and hybrid) for transglycosylation onto a deglycosylated antibody. Comparative functional assay between Endo-S and Endo-S2 mutants revealed that the Endo-S2 D184M was more efficient than the previous Endo-S D233Q in catalyzing transglycosylation reactions. In addition, we demonstrated that a significantly reduced amount of glycan oxazoline (only 2.5 molar equivalents for each Fc monomer glycosylation site) was required to achieve complete glycosylation of the deglycosylated IgG-Fc fragment, which is significantly more efficient than the Endo-S D233M (10 molar equivalents each) in terms of substrate consumption and reaction completion time. Finally, similar to the mechanistic analyses on Endo-S mutants, the kinetic parameters of Endo-S2 D184M and D184A were measured and compared with those of Endo-S. Comparison between the kinetics of Endo-S2 D184M and D184A demonstrated similar patterns to Endo-S mutants. Interestingly, the combined results collectively suggested that the enhanced catalytic efficiencies of Endo-S2 D184M over Endo-S D233M for both glycan and antibody substrates were due to increased catalytic turnover numbers ( $k_{cat}$ ), whereas the substrate affinities ( $K_M$ ) did not change significantly.<sup>123</sup>

Despite successful applications of Endo-S2 and mutants in glycoengineering, one drawback of this general method still persisted that the wild-type enzyme (either Endo-S or Endo-S2) was required to release the native heterogeneous N-glycans from the starting antibody prior to the transfer of new N-glycan structures. Therefore, the

wild-type Endo-S/S2 must to be removed from the reaction mixture after the deglycosylation step in order to prevent the wild-type enzymes from hydrolyzing the final product, and an additional step of antibody purification was needed after the transglycosylation step. The necessary switching between the wild type and mutant enzymes in addition to the tedious antibody purification procedure would present a major issue for the cost-effectiveness of this method in large-scale industrial applications.<sup>109</sup> To circumvent this problem, we re-evaluated the substrate specificity of Endo-S with a broader range of substrates including different N-glycan oxazolines and antibody N-glycoforms. Interestingly, our results clearly demonstrated that the wild-type Endo-S displayed promiscuous activities against multiple glycan structures for transglycosylation, which included hybrid and high-mannose glycan oxazolines. However, the product hybrid and high-mannose N-glycoforms of antibody are highly resistant to Endo-S-catalyzed hydrolysis. These selective catalytic properties of Endo-S, combined with its highly efficient hydrolytic activity against the native N-glycans of conventional antibodies, allowed us to develop a one-pot glycoengineering method for IgG antibodies to synthesize additional target antibody N-glycoforms. Using this one-pot strategy, removal of the wild-type enzymes was no longer necessary since deglycosylation and transglycosylation of the antibody were catalyzed simultaneously by Endo-S. Finally, we applied this single-step method to the remodeling of a therapeutic antibody rituximab with a chemically modified N-glycan. As mentioned in Introduction section, an azido-functionalized N-glycoform of therapeutic antibody could be used as molecular handle for the bioorthogonal ligation chemistry to develop new classes of antibody-drug conjugates.<sup>140</sup>

## B. Results

### 1. Cloning, expression, and characterization of Endo-S2

The DNA sequence coding Endo-S2 (38–819) was cloned into a pET22b-CPD vector, which contains a C-terminal cysteine protease domain (CPD) derived from the *Vibrio cholerae* MARTX toxin with a 10-histidine tag.<sup>141</sup> We recently reported that a high-level, soluble expression of Endo-F3 and its mutants could be achieved using this vector<sup>85</sup>. Following a similar strategy, Endo-S2 was successfully expressed in BL21 (DE3) *Escherichia coli* competent cells and was purified using immobilized metal ion affinity chromatography to obtain the soluble enzyme with a yield of more than 20 mg/liter. The recombinant Endo-S2 showed significant hydrolysis activity against the intact IgG antibody as demonstrated by its rapid deglycosylation of commercial rituximab, which was monitored by LC-MS analysis.

### 2. Generation of glycosynthase mutants of Endo-S2

We have previously generated glycosynthase mutants from endoglycosidases of both GH85 and GH18 families by site-directed mutation at a key residue that is responsible for promoting the formation of the oxazolinium ion intermediate during hydrolysis, which proceeds in a substrate-assisted mechanism. These include a key asparagine residue for endoglycosidases Endo-A (Asn-171), Endo-M (Asn-175), and Endo-D (Asn-322) of the GH85 family, or a key aspartic acid residue for the GH18 family endoglycosidases Endo-S (Asp-233) and Endo-F3 (Asp-165). Sequence alignment of Endo-S2 and Endo-S revealed that the Asp-184 of Endo-S2 was the residue equivalent to the Asp-233 of Endo-S essential for promoting oxazolinium ion

formation in hydrolysis (Figure. 26). To generate glycosynthase mutants from Endo-S2, we systematically replaced the Asp-184 with other 19 natural amino acid residues using site-directed mutagenesis. The resulting 19 Asp-184 mutants of Endo-S2 were expressed as soluble proteins in pET22b-CPD vector and purified using immobilized metal ion affinity chromatography, in the same way as demonstrated for the wild-type Endo-S2. The expression of mutant Endo-S2 enzymes gave comparable yields (15–20 mg/liters) as the expression of the wild type enzyme.

```

Endo S2      WHDRASTGIDGKQQHPENTMAEVPKEVDILFVFDHTASDSPFWSELKDSYVHKLHQQGT 133
Endo S       WHDKTSDPT---EKDKVNSMGELPKEVDLAFIFHDWTKDYSLFWKELATKHVPKLNKQGT 177
             ***:::*          ::.  *:*.*:*****: *:*** * . * **.*** .:* **.:***

Endo S2      ALVQTIGVNELNGR-----TGLSKDYPDTPEGNKALAAAIVKAFVTDRGVDGLDIDIEHE 188
Endo S       RVIRTIPWRFLAGGDNSGIAEDTSKYPNTPEGNKALAKAIVDEYVYKYNLDGLDVIDVEHD 237
             :::** . * *          :  :..**:*:***** ***. :* . :****:*:**:

Endo S2      FTKRTPPEE----DARALNVFKEIAQLIGKNGSDKSKLLIMDTTILSVENNPFKGIAEDL 244
Endo S       SIPKVDKKEDTAGVERSIQVFEEIGKLIGPKGVDKSRLFIMDSTYMADKNPLIERGAPYI 297
             *      :*          *:::**:*.*:*** :* ***:**:*:* * .:***::: * :

```

Figure 26. Sequence alignment of Endo-S2 and Endo-S. The aspartic acid residue (Asp 233 of Endo-S and Asp-184 of Endo-S2) critical for promoting the oxazolinium ion formation in hydrolysis and the catalytic general acid/base residue (Glu-235 of Endo-S and Glu-186 of Endo-S2) are highlighted.

### 3. Generation and comparative studies on the hydrolytic and transglycosylation activities of the 19 glycosynthase mutants and wild-type enzyme of Endo-S2

The hydrolysis activities on the IgG-Fc N-glycans in an intact antibody and the transglycosylation activities with glycan oxazoline were assessed following the scheme shown in Figure 27. The results indicate that most of the mutants at Asp-184 residue led to significantly reduced or completely diminished hydrolysis activities on the IgG-Fc N-glycan. Among them, D184F, D184H, D184K, D184R, and D184W

mutants were completely devoid of hydrolytic activity, whereas several other mutants, including D184C, D184E, D184G, D184N, D184S, D184Y, were found to still retain significant hydrolysis activity (Table 4). On the other hand, the evaluation of transglycosylation indicated that almost all the mutants possessed transglycosylation activity when using the deglycosylated rituximab as the acceptor and a biantennary complex type glycan oxazoline as the donor substrate, but the activities varied significantly among different mutants (Table 5). Among others, D184C, D184M, D184G, D184E, D184Y, D184S, and D184A were found to be the most active mutants. However, D184C, D184G, D184E, D184Y, D184S, and D184A also demonstrated significant residual hydrolytic activity. The most interesting mutant is Endo-S2 D184M, which retained only marginal hydrolytic activity but showed high transglycosylation activity (only second to D184C), making the best glycosynthase mutants to choose for the glycosylation remodeling of antibody.

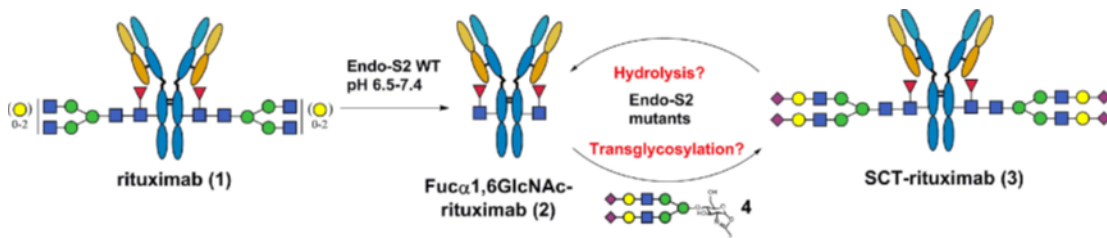


Figure 27. Schematic presentation of hydrolysis and transglycosylation by Endo-S2 and its mutants using rituximab as the substrate. The fucosylated GlcNAc-rituximab, the deglycosylated rituximab carrying the core-fucosylated GlcNAc moiety at the glycosylation site; SCT-rituximab (S<sub>2</sub>G<sub>2</sub>), the sialylated complex type glycoform of rituximab.

Table 4. Comparison of the specific hydrolytic activities of Endo-S2 D184 mutants using the synthetic complex type rituximab (S<sub>2</sub>G<sub>2</sub>-rituximab) as the starting material.<sup>a</sup>

Mutant	Specific hydrolysis activity	Percentage of specific hydrolysis activity
	<i>*100 (umole/min/mg)</i>	%
WT	11.185	100.000
D184A	0.750	6.701
D184C	1.386	12.392
D184E	0.879	7.855
D184F	0.000	0.000
D184G	1.249	11.168
D184H	0.000	0.000
D184K	0.000	0.000
D184R	0.000	0.000
D184I	0.033	0.295
D184L	0.045	0.405
D184M	0.158	1.410
D184N	0.842	7.526
D184P	0.340	3.043
D184Q	0.049	0.441
D184S	1.387	12.398
D184T	0.212	1.899
D184V	0.409	3.659
D184W	0.000	0.000
D184Y	5.526	49.406

<sup>a</sup>The specific hydrolysis activity of each enzyme was assayed by incubating the synthetic biantennary complex type rituximab antibody with each of the mutants or the wild-type Endo-S2 (0.01 mg/mL) in PBS pH 7.4 at 30 °C.

Table 5. Comparison of specific transglycosylation activity of Endo-S2 D184 mutants using glycan oxazoline as donor and deglycosylated rituximab as acceptor.<sup>a</sup>

Mutants	Specific transglycosylation activity <i>*10 (umol/min/mg)</i>	Percentage of specific transglycosylation activity %
WT	1.712	44.31
D184A	1.023	26.46
D184C	3.864	100.00
D184E	2.006	51.907
D184F	0.044	1.14
D184G	2.270	58.73
D184H	0.026	0.68
D184K	0.021	0.54
D184R	0.022	0.57
D184I	0.066	1.71
D184L	0.099	2.55
D184M	2.866	74.18
D184N	0.879	22.75
D184P	0.160	4.13
D184Q	0.383	9.92
D184S	1.164	30.13
D184T	0.828	21.42
D184V	0.147	3.79
D184W	0.046	1.20
D184Y	1.198	30.99

<sup>a</sup>To test the specific transglycosylation activity of each enzyme, the deglycosylated rituximab antibody was used as the glycosyl acceptor and the SCT oxazoline as the glycosyl donor substrate with a final concentration of enzymes at 0.01 mg/mL. The molar ratio of the glycosyl acceptor to donor substrate was 1:20. The experimental results obtained here were representative from three independently conducted experiments.

#### 4. Enzyme kinetic parameters of Endo-S2 D184M and Endo-S2 D184A

To evaluate the nature of the enhanced catalytic efficiency of Endo-S2 mutant, we measured the kinetic parameters of the D184M and D184A mutants of Endo-S2. For the sugar oxazoline, the Endo-S2 methionine mutation significantly enhanced its catalytic efficiency ( $k_{\text{cat}}/K_{\text{M}}$ ) in comparison with that seen for the alanine mutation, and an approximately 10-fold increase in  $k_{\text{cat}}/K_{\text{M}}$  was observed for the D184M mutant over the D184A mutant of Endo-S2 (Table 6 and Figure 28a). In analogy to Endo-S, the increased  $k_{\text{cat}}/K_{\text{M}}$  value for D184M mutant was caused by a >15-fold increase in the catalytic turnover number ( $k_{\text{cat}}$ ) and a <2-fold decrease in the substrate affinity ( $K_{\text{M}}$ ) for the glycan oxazoline substrate.

For the deglycosylated antibody, like the Endo-S D233M mutant, the Endo-S2 D184M mutant also showed an affinity for the antibody substrate significantly higher than that of the D184A mutant. The  $K_{\text{M}}$  of Endo-S2 D184A was estimated to be >20 times higher than that of the Endo-S2 D184M mutant. Similar to the case of Endo-S, Michaelis–Menten curves indicated that the Endo-S2 D184A mutant showed no sign of saturation within the range of antibody concentrations tested. Therefore, the catalytic turnover number of Endo-S2 D184A also could not be accurately measured because of the difficulty of saturating the antibody substrate (Table 7 and Figure 28b).

Interestingly, for both the sugar oxazoline and the antibody substrate, Endo-S2 D184M demonstrated a catalytic turnover number significantly higher than that of Endo-S D233M, whereas substrate affinity for both substrates proved to be comparable between the two mutants. Therefore, the overall catalytic efficiency ( $k_{\text{cat}}/K_{\text{M}}$ ) of Endo-S2 D184M was found to be higher than that of Endo-S D233M.

Table 6. Kinetic parameters of Endo-S2 mutants D184M and D184A for SCT-Oxa.

Enzyme	$k_{cat}$ ( $\text{min}^{-1}$ )	$K_M$ ( $\mu\text{M}$ )	$k_{cat}/K_M$ ( $\text{min}^{-1} \mu\text{M}^{-1}$ )
Endo-S2 D184M	$167.8 \pm 20.5$	$229.1 \pm 34.8$	0.73
Endo-S2 D184A	$10.2 \pm 2.4$	$121.3 \pm 17.1$	0.08

Table 7. Kinetic parameters of Endo-S2 mutants D184M and D184A for rituximab.

Enzyme	$k_{cat}$ ( $\text{min}^{-1}$ )	$K_M$ ( $\mu\text{M}$ )	$k_{cat}/K_M$ ( $\text{min}^{-1} \mu\text{M}^{-1}$ )
Endo-S2 D184M	$29.8 \pm 9.3$	$32.6 \pm 6.7$	0.91
Endo-S2 D184A	-*	N.D.	-*

\*The catalytic turnover number of Endo-S2 D184A was not determined because the concentration of antibody substrate required to saturate the enzyme could not be used in the experiments under normal conditions.

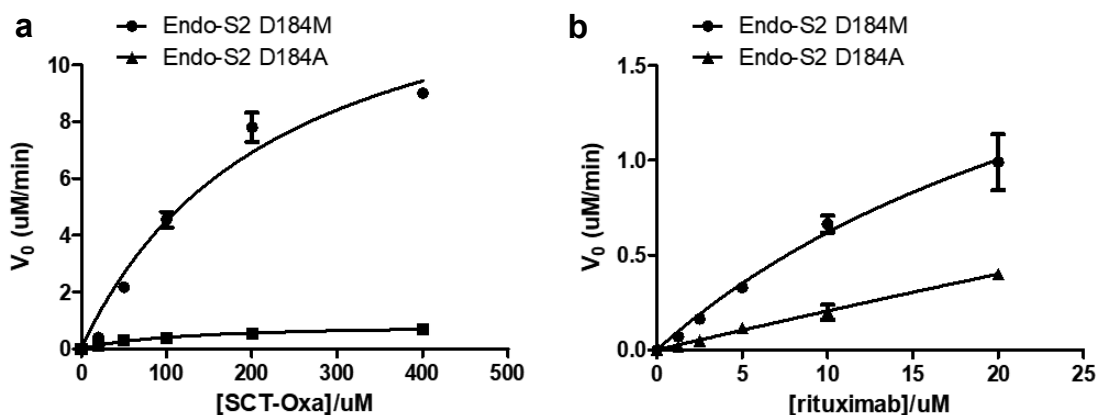


Figure 28. Michaelis-Menten curves of the Endo-S2 mutants (D184M and D184A): a) for glycosyl donor, a gradient of SCT-Oxa (6.25 to 400  $\mu\text{M}$ ) was tested with a constant concentration of rituximab (20  $\mu\text{M}$ ); b) for glycosyl acceptor, a serial dilution of antibody (0.32 to 20  $\mu\text{M}$ ) was tested with 400  $\mu\text{M}$  of SCT. For both Endo-S2 D184M and D184A, the enzyme concentration was controlled at 0.01 mg/mL (0.067  $\mu\text{M}$ ). The data sets presented here are representative of three independent experiments.

## 5. Endo-S2 D184M showed relaxed glycan substrate specificity

Rituximab, a therapeutic monoclonal antibody, was selected as the model to examine the transglycosylation activity of the Endo-S2 Asp-184 mutants. The major N-glycans of the commercial rituximab are the core-fucosylated biantennary complex oligosaccharides containing 0–2 galactose residues, namely G0F, G1F, and G2F glycoforms, respectively. The glycosylation remodeling approach is shown in Fig. 29 and the identity of antibody products were assessed by LC-MS analysis. Treatment of rituximab with wild-type Endo-S2 resulted in complete deglycosylation of the native rituximab. The Fuc-1,6GlcNAc-rituximab was then purified away from the wild-type endoglycosidase and the released glycans by Protein-A affinity chromatography and used as the acceptor in the following transglycosylation reactions. We demonstrated that Endo-S2 D184M was able to efficiently transfer the sialylated biantennary complex glycan to the acceptor antibody with 20 molar eq (i.e. 10 molar equivalents per monomeric Fc domain) of the glycan oxazoline. The reaction yield was estimated by LC-MS analysis to be over 95% as almost no starting material was detected, which confirmed the completion of the transglycosylation.

In addition to the complex type N-glycan, the specificity of Endo-S2 was further tested with high-mannose type (HM) Man<sub>9</sub>GlcNAc oxazoline and the sialylated hybrid type (Hyb) Neu<sub>5</sub>AcGalGlcNAcMan<sub>5</sub>GlcNAc oxazoline as the donor substrate in the transglycosylation reactions. The reactions led to formation of corresponding antibody N-glycoforms. Under the same conditions, we found that the previously reported Endo-S mutants, including D233A and D233Q mutants of Endo-S, showed only marginal transglycosylation activity with high-mannose and hybrid

type N-glycans, although they could efficiently transfer biantennary complex type N-glycan. In addition, the recently reported D165A mutant of Endo-F3 was unable to transfer the high-mannose or hybrid type N-glycans but could work on the bi- and triantennary complex type sugars. Thus, these Endo-S2-derived mutants represent the first glycosynthases that can efficiently transfer high-mannose and hybrid type N-glycans to the core-fucosylated GlcNAc acceptor in an intact antibody. It should be mentioned that the Endo-A mutant (N171A and N171Q) could transfer high-mannose N-glycan to the GlcNAc-Fc domain, but they were unable to use core-fucosylated GlcNAc-Fc as acceptor. These studies also show that combined use of wild type Endo-S2 and Endo-S2 glycosynthase mutants provides an efficient glycosylation remodeling approach to homogeneous glycoforms of antibodies starting from a single precursor glycoform.

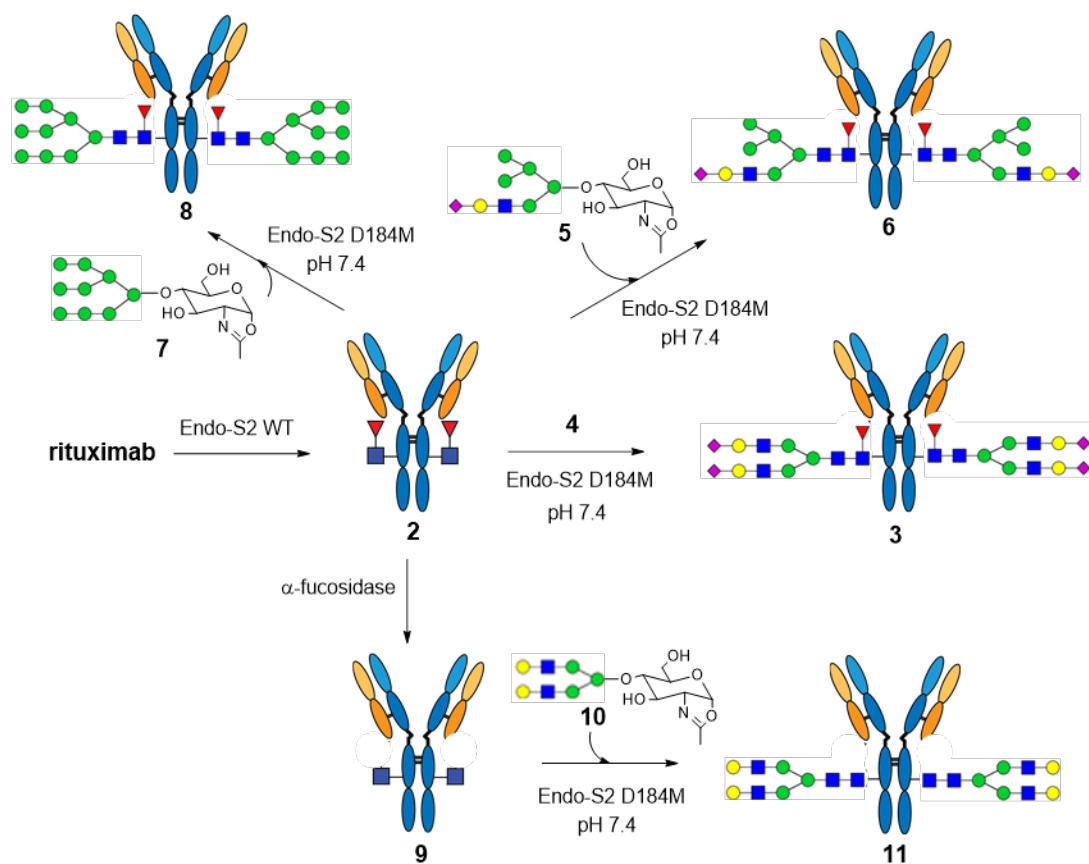


Figure 29. Evaluation of substrate specificity of Endo-S2 D184M on different glycans (HM, CT, and Hyb type). GlcNAc-rituximab, the rituximab glycoform carry only first GlcNAc moiety at the glycosylation site; 1,6GlcNAc-rituximab, the deglycosylated rituximab carrying the core-fucosylated GlcNAc moiety at the glycosylation site; SCT-rituximab, the sialyl complex type glycoform of rituximab; HM-rituximab, the high-mannose type glycoform of rituximab; Hyb-rituximab, the hybrid type glycoform of rituximab.

## 6. Transglycosylation of different N-glycan structures by Endo-S2 D184M

To further characterize the N-glycan substrate preference of Endo-S2 D184M, parallel transglycosylation reactions were carried out with the N-glycan oxazolines of complex (SCT) type, high-mannose (HM) type, and hybrid (Hyb) type, respectively. The reaction progresses were monitored by LC-MS analysis of reaction aliquots taken at multiple time points and the results were summarized in Figure. 30. Under the same reaction conditions, the transglycosylation reaction with SCT-oxazoline (**4**) was completed within 20 min to give the full sialylated S<sub>2</sub>G<sub>2</sub>F-rituximab (**3**), whereas the transglycosylation with HM-oxazoline (**7**) and Hyb-oxazoline (**5**) were much slower. These results confirm that Endo-S2 D184M prefers the complex type over the high-mannose and hybrid type N-glycans despite having a remarkably relaxed N-glycan specificity.

The semipreparative synthesis of antibody N-glycoforms by Endo-S2 D184M was conducted in collaboration with Dr. Tiezheng Li from Prof. Lai-Xi's group at the Department of Chemistry and Biochemistry, University of Maryland, College Park. This work was published in *Journal of Biological Chemistry* in 2016.<sup>139</sup> The mutational studies and enzyme activity assays were performed by Xin Tong and Dr. Li and other authors. The large-scale glycosylation remodeling and purification of antibody glycoforms were achieved primarily by Dr. Li.

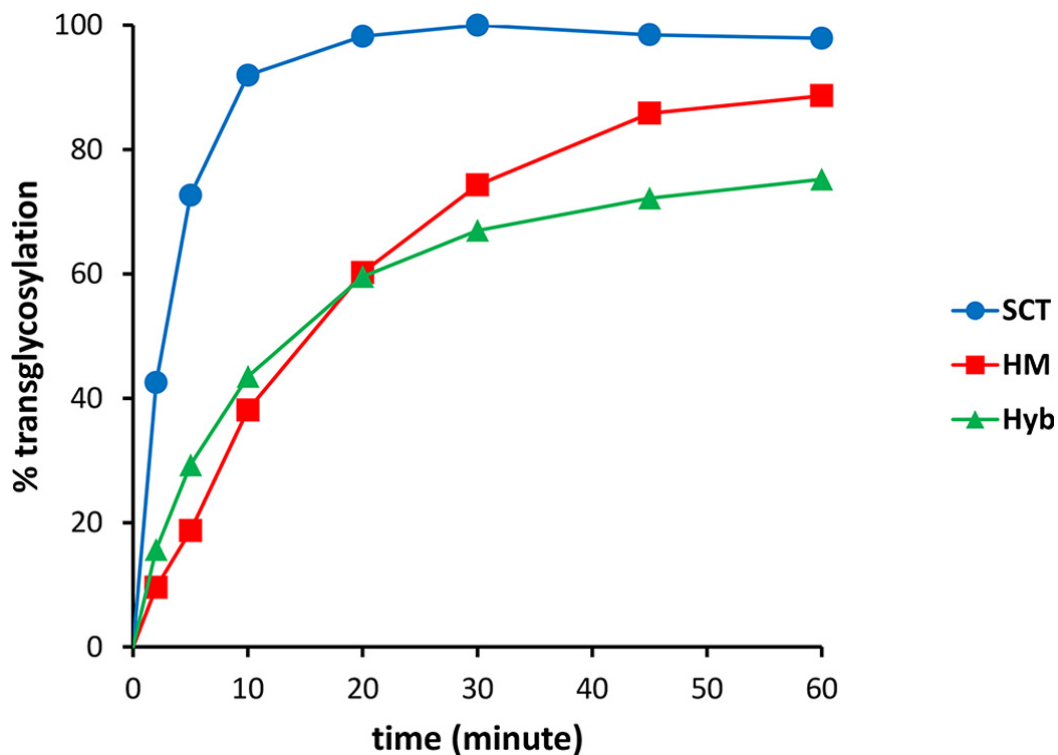


Figure 30. Comparison of transglycosylation reactions by Endo-S2 D184M with different N-glycans. Transglycosylation reaction was carried out using deglycosylated rituximab **2** as the acceptor and different types of glycan oxazolines as the donor substrate under the catalysis of Endo-S2 D184M (0.05 mg/ml). The molar ratio of donor to acceptor was 20:1. The data presented here are representative of two independent experiments.

#### 7. Transglycosylation efficiencies of selected Endo-S2 and Endo-S mutants.

We previously generated the first Endo-S glycosynthase mutants D233Q and D233A that transglycosylate rituximab efficiently with the complex type N-glycan oxazoline.<sup>103</sup> The Endo-S Asp-233 mutants have been recently used by us and other groups to generate homogeneous monoclonal antibodies for structural and functional studies.<sup>20</sup> To compare the transglycosylation efficiency of the glycosynthase mutants

from both Endo-S2 and Endo-S, we selected to use the Endo-S D233Q mutant, the corresponding Endo-S2 D184Q mutant, and the Endo-S2 D184M mutant to catalyze three parallel transglycosylation reactions. The time course of each transglycosylation reaction was monitored by LC-MS analysis and summarized in Figure 31. Under the same reaction conditions, the D184M mutant of Endo-S2 showed remarkably potent transglycosylation activity, and reached completion of the glycan transfer within 10 min. The other Endo-S2 mutant could also transfer the glycan smoothly and reached the completion within 1 h. However, the corresponding Endo-S mutant (D233Q) was much less efficient, reaching about 10% of transglycosylation at 1 h under the same conditions (Figure 31). As demonstrated in a separate experiment, more (10-fold) Endo-S D233Q mutant and a larger excess of the glycan oxazoline were required to achieve the same level of the transglycosylation catalyzed by the Endo-S2 D184Q mutant, and the D184M mutant of Endo-S2 was even much more efficient than the D184Q mutant. These studies suggest that some newly discovered Endo-S2 Asp-184 mutants are superior to the previously reported Endo-S Asp-233 mutants for antibody glycosylation remodeling in both efficiency of reactions and the breadth of substrate diversity.

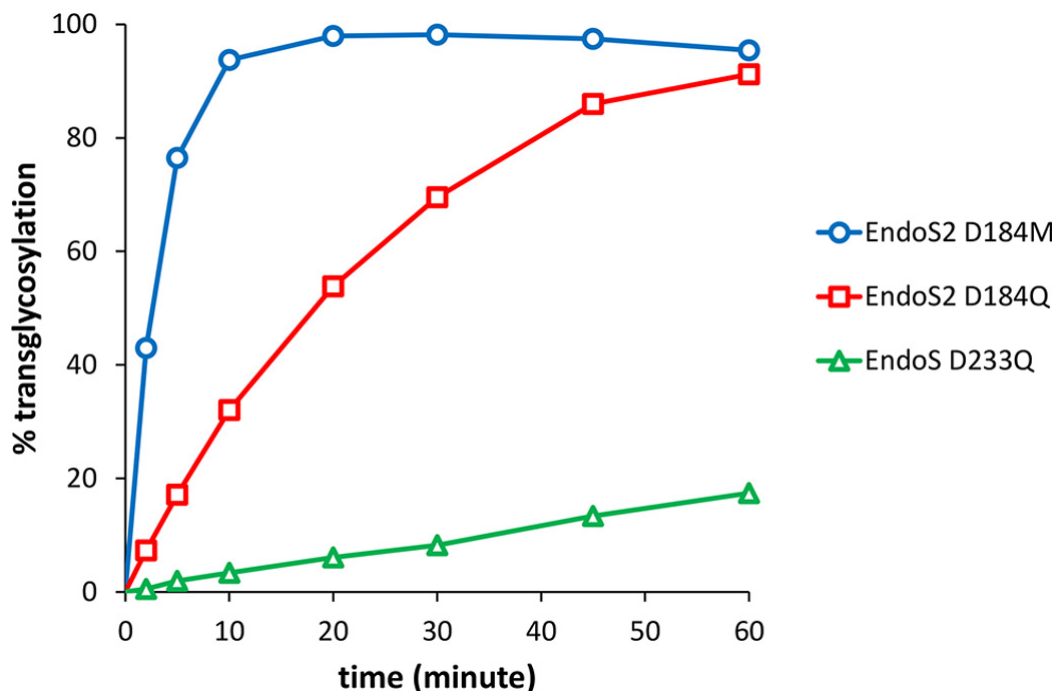


Figure 31. Comparison of transglycosylation reactions catalyzed by selected mutants Endo-S2 D184Q, Endo-S2 D184M, and Endo-S D233Q. The transglycosylation was performed using deglycosylated rituximab **2** as the acceptor and SCT glycan oxazoline **4** as the donor substrate under the catalysis of different endoglycosidase mutants at a fixed concentration of 0.05 mg/ml. The molar ratio of donor to acceptor was 20:1. The data presented here are representative of two independent experiments.

#### 8. Antibody transglycosylation using a reduced amount of glycan oxazoline.

To investigate whether it would be possible to achieve the same level of antibody glycosylation by Endo-S2 mutants with reduced oxazoline consumption, we performed the routine transglycosylation reactions by Endo-S2 D184M with only five molar equivalents of SCT-Oxa per antibody under conventional reaction conditions. As demonstrated in Figure 32, depending on the concentration of Endo-S2 D184M used, the glycosylation of antibody could be completed at different rates. It is worth

mentioning that hydrolysis was observed when the enzyme concentration was high (0.25 mg/mL), emphasizing the importance of controlling the enzyme concentration of glycosynthase mutants used to minimize the product hydrolysis. Nevertheless, all three concentrations of Endo-S2 D184M reached complete transglycosylation within 4 hours using only 5 equivalents of SCT-Oxa per antibody, which was significantly less than the previously reported amount. This discovery provides another advantage of using the End-S2 mutant such as Endo-S2 D184M for the glycan remodeling of antibody, particularly for the large scale manufacturing of antibody N-glycoforms.

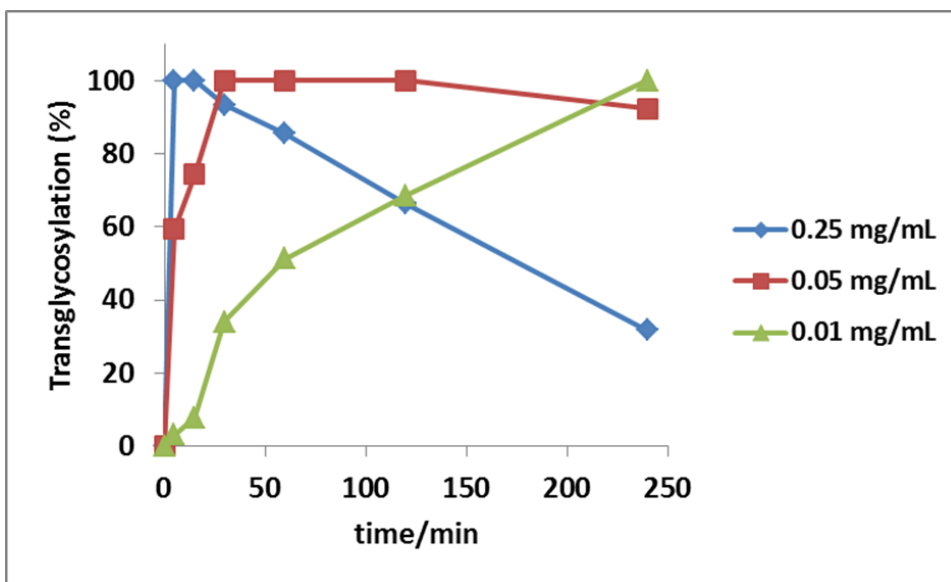


Figure 32. Transglycosylation of antibody with a reduced oxazoline substrate at different Endo-S D184M concentrations. Only five molar equivalents of SCT-Oxa substrate per antibody were used for the transglycosylation of antibody in the PBS buffer (pH 7.4) at 30 °C. The transglycosylation yield (%) of each reaction was monitored by LC-MS and estimated using previously described methods.<sup>139</sup>

## 9. Endo-S-catalyzed hydrolysis of antibody glycoforms and N-glycan oxazolines

Previously, Collin and co-workers have reported that Endo-S and Endo-S2 hydrolyze the Fc glycans of therapeutic antibodies with different selectivities.<sup>138</sup> While Endo-S2 can release all three major types of N-glycans from the Fc domain of several therapeutic antibodies including cetuximab, Endo-S is only efficient for releasing bi-antennary complex type N-glycans from the antibodies. To further confirm the substrate selectivity of the wild-type Endo-S, we performed side-by-side comparison of Endo-S-catalyzed hydrolysis reactions for the selected homogeneous glycoforms of rituximab, as well as various synthetic N-glycan oxazolines (Figure 33).

We first tested three different homogeneous glycoforms of rituximab, namely, the sialylated complex type (**1**), the high-mannose (Man<sub>9</sub>GlcNAc<sub>2</sub>) type (**2**), and the hybrid type (**3**) (Figure 34). These homogeneous glycoforms (**1-3**) were synthesized following our recently published method, using the Endo-S2 glycosynthase mutant (EndoS2-D184M) as a key enzyme for transglycosylation.<sup>139</sup> The enzymatic reactions were monitored by LC-ESI-MS analysis. We found that Endo-S could hydrolyze the biantennary complex form of rituximab (**1**) fast, resulting in over 90% hydrolysis within 2 h under the reaction condition. However, only marginal hydrolysis (less than 5%) of the high-mannose and hybrid glycoforms (**2** and **3**) was observed under the same reaction condition (Figure 34A). A prolonged (overnight) incubation resulted in about 10% hydrolysis of the high mannose glycoform (**2**) and approximately 15% of the hybrid glycoform (**3**), respectively (data not shown). These data confirm that the high-mannose and hybrid type Fc glycoforms of antibodies are largely resistant to Endo-S-catalyzed hydrolysis although residual hydrolytic activity was detected, and

the bi-antennary complex type glycoform is an excellent substrate for the wild-type Endo-S.

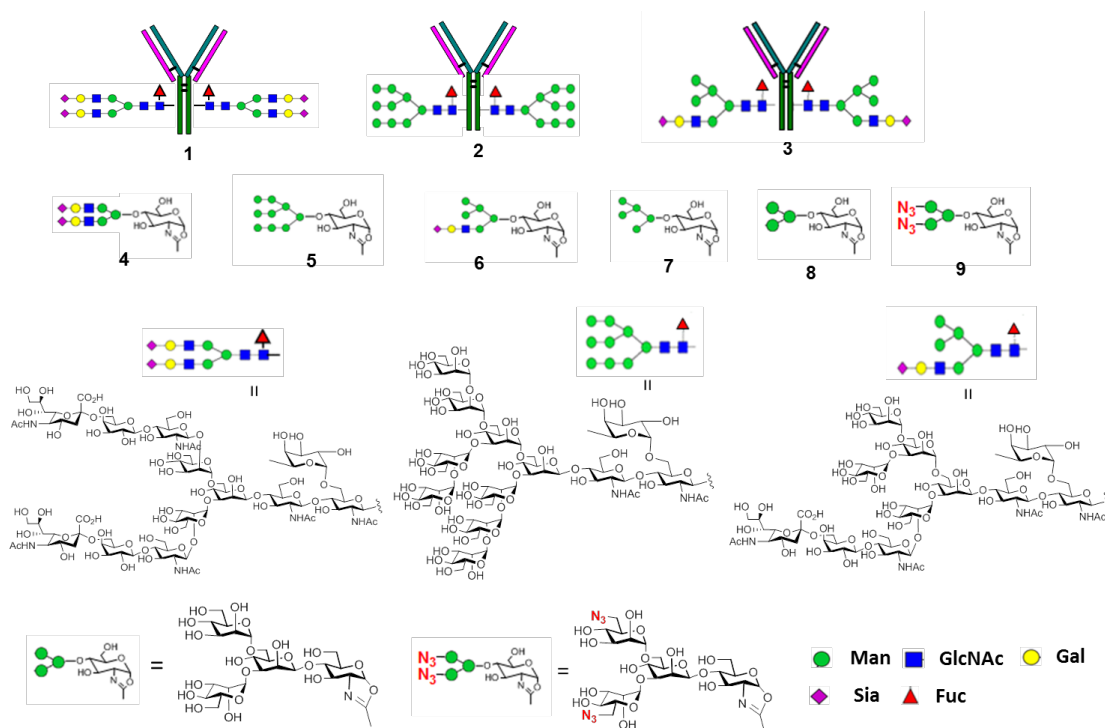


Figure 33. Structures of different rituximab N-glycoforms and N-glycan oxazolines used for the assessment of Endo-S activity.

Next, we compared the Endo-S WT-catalyzed hydrolysis of various synthetic N-glycan oxazolines. Synthetic glycan oxazolines, the mimics of the oxazolinium intermediate during the endoglycosidase-catalyzed reaction in a substrate-assisted mechanism, are the key donor substrates for the endoglycosidase-catalyzed transglycosylation used for glycoprotein remodeling. Thus, it is important to know whether the glycan oxazolines will be hydrolyzed and how fast they will be hydrolyzed by the enzyme of interest. Various glycan oxazolines were incubated with Endo-S WT in PBS buffer, and the hydrolysis products (free glycans) were monitored

and quantitated by HPAEC-PAD (high performance anion exchange chromatography coupled with pulsed amperometric electrochemical detection). As illustrated in Figure 33B, the complex type glycan oxazoline (**4**) was rapidly hydrolyzed by Endo-S WT. In contrast, the high-mannose type N-glycans oxazolines, including Man9 oxazoline (M9-Oxa **5**) and the Man5 glycan oxazoline (Man5-Oxa **7**), were shown to be rather resistant to Endo-S hydrolysis. The hybrid oxazoline (Hyb-Oxa **6**) showed moderate hydrolysis by Endo-S. Interestingly, the Man3 oxazoline (M3-Oxa **8**), corresponding to the shared N-glycan core, was also hydrolyzed very rapidly by Endo-S. However, chemical modifications at the two outer mannose moieties led to reduction of the enzymatic hydrolysis, as demonstrated by azide-Man3 glycan oxazoline (AzideM3-Oxa **9**) (Figure 34B). These results clearly indicate that wild-type Endo-S possesses distinct enzymatic activities towards different glycan oxazolines, as well as different glycoforms of antibodies.

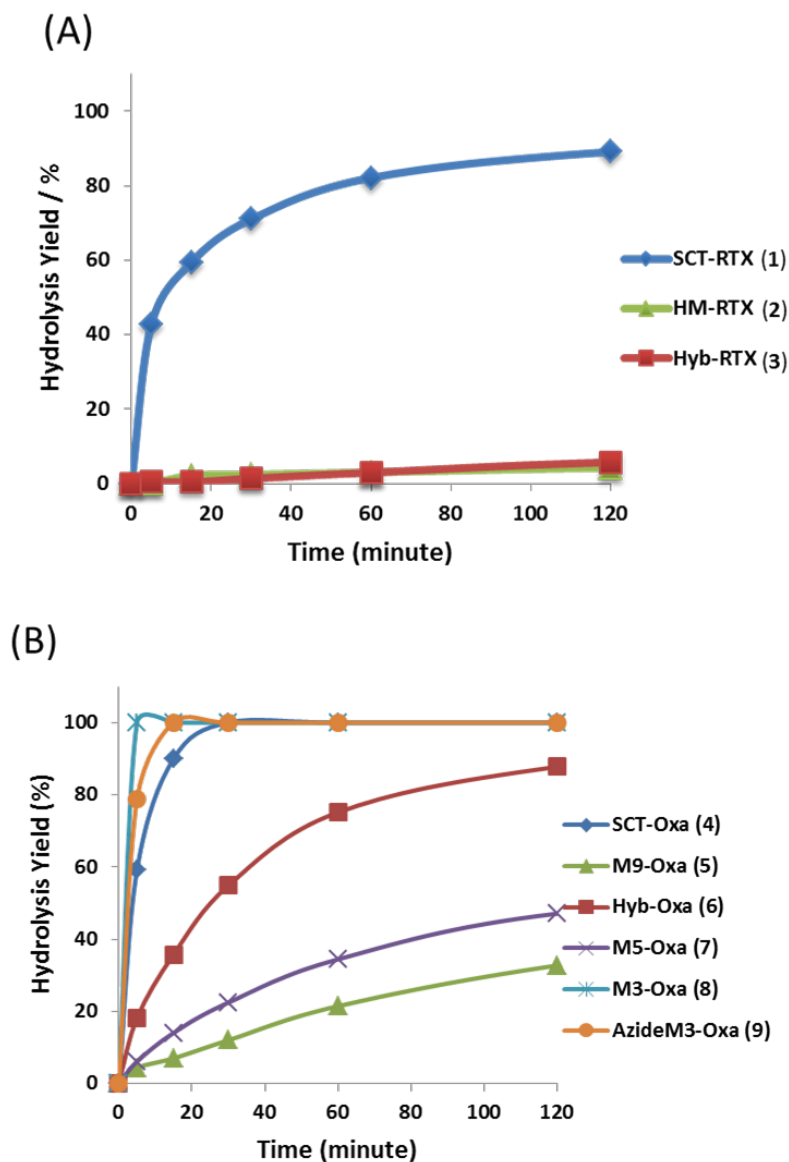


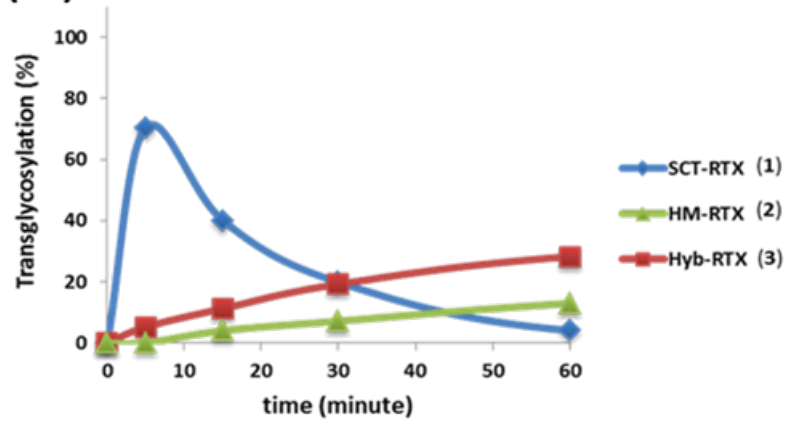
Figure 34. Hydrolytic activity of Endo-S WT on different rituximab N-glycoforms and oxazolines; A) Comparison of the hydrolytic activity of Endo-S WT towards the complex (1), hybrid (2) and high-mannose (3) type synthetic N-glycoforms of rituximab; B) Comparison of the hydrolytic activity of Endo-S WT towards various N-glycan oxazolines to the free N-glycans. The results shown here are representative of three independently conducted experiments.

## 10. Endo-S-catalyzed transglycosylation of antibody with additional oxazolines

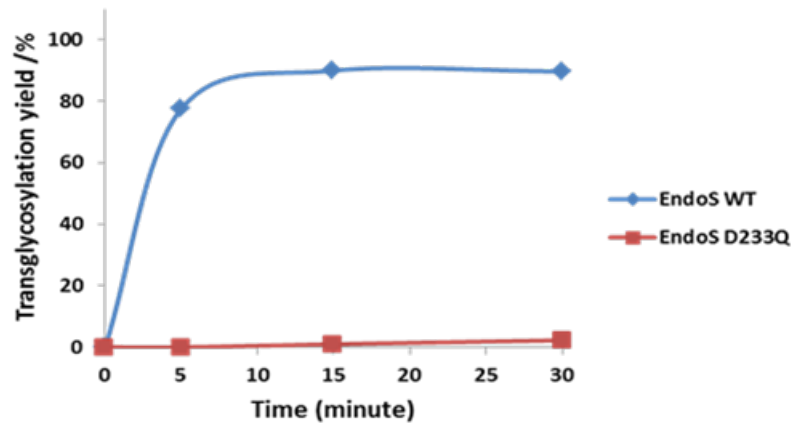
The unique substrate specificity of Endo-S towards the different antibody N-glycoforms and glycan oxazolines prompted us to examine the wild-type Endo-S-catalyzed transglycosylation with the three major Fc N-glycans oxazolines, complex (SCT-Oxa **4**), Man9 (HM-Oxa **5**), and Hybrid (Hyb--Oxa **9**), to the deglycosylated rituximab (GlcNAc-rituximab, **10**) (Figure 35). The Fuc1,6GlcNAc-rituximab (**10**) was prepared by deglycosylation of rituximab with Endo-S, following our previously published procedure.<sup>103</sup> We found that the wild-type Endo-S showed a significant transglycosylation activity with the complex type N-glycan oxazoline (**4**) to form the transglycosylation product (**1**) (Figure 35A). However, the product was quickly hydrolyzed by the enzyme, as the resultant complex type N-glycoform turned out to be an excellent substrate for Endo-S-catalyzed hydrolysis. This result was consistent with our previous observations.<sup>114</sup> We also observed that, under the same condition, wild-type Endo-S was also able to transfer the high-mannose glycan oxazoline (**5**) and hybrid glycan oxazoline (**6**), but at a much lower reaction rate than that with the complex type glycan oxazoline (**4**). Nevertheless, since the transglycosylation products (**2** and **3**) were largely resistant to Endo-S catalyzed hydrolysis, the transglycosylation products could thus be accumulated. Previously we have generated novel Endo-S mutants, including EndoS-D233Q, which are glycosynthases that can use glycan oxazolines for transglycosylation but lack the activity to hydrolyze the product.<sup>103</sup> The EndoS-D233Q mutant was efficient for transferring complex type N-glycan oxazolines to the deglycosylated antibody; however, it was not clear how the glycosynthase mutant would act on the high-mannose and hybrid type N-glycan

oxazolines for transglycosylation. Here we tested EndoS-D233Q with oxazolines **5** and **6** for glycoengineering. Surprisingly, we found that the Endo-S mutant EndoS-D233Q was unable to act on either the high-mannose glycan oxazoline (**5**) or the hybrid glycan oxazoline (**6**) for transglycosylation with the Fuc1,6GlcNAc-rituximab (**10**), while under same condition the wild-type Endo-S could achieve over 85% transglycosylation to form the corresponding antibody glycoforms (Figure 35B and Figure 35C). In comparison with the wild-type enzyme, the D233Q mutation reduced both the hydrolysis and transglycosylation activities of the enzyme, thus, resulting in the decreased efficiency toward the less favorable glycan oxazoline substrates, while it was still reactive enough towards the complex type N-glycan oxazoline (**4**), as shown in the previous publications.<sup>98</sup> These new experimental data suggest that the wild-type Endo-S is complementary to the mutant Endo-S in terms of their substrate specificities, and the Endo-S WT will be particularly useful for the synthesis of high-mannose and hybrid N-glycoforms of antibodies, which could not be achieved by the previously reported Endo-S mutants.

(A)



(B)



(C)

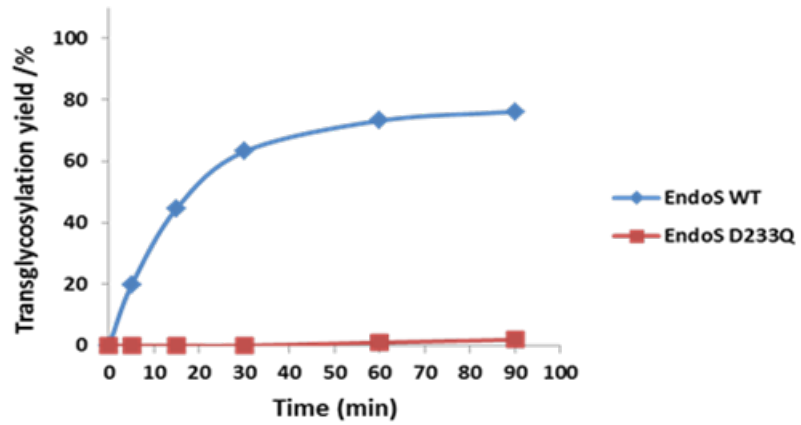


Figure 35. Endo-S-catalyzed transglycosylation reactions with oxazolines SCT-Oxa **4**, HM-Oxa **5**, Hyb-Oxa **6** of deglycosylated rituximab **10**; A) Comparison of the transglycosylation activity of Endo-S WT towards oxazolines SCT-Oxa **4**, HM-Oxa **5**, Hyb-Oxa **6**; B) Comparison of the transglycosylation activity of Endo-S WT and Endo-S D233Q mutant towards the high mannose-type oxazoline (HM-Oxa **5**); C) Comparison of transglycosylation activity of Endo-S WT and Endo-S D233Q mutant towards the hybrid-type oxazoline (Hyb-Oxa **6**). The detailed reaction conditions are shown in Materials and Methods section. The results shown here are representative of three independently conducted experiments.

#### 11. One-pot glycosylation remodeling of rituximab via the wild-type Endo-S

The potent transglycosylation activity of Endo-S WT with the hybrid and high-mannose type oxazolines, together with its efficient hydrolysis of the complex-type N-glycans from the commercial antibody rituximab, prompted us to examine the possibility of remodeling antibody glycosylation in a one-pot fashion (Figure 36). Thus, a mixture of the commercial rituximab, glycan oxazoline (**5** or **6**), and the wild-type Endo-S was incubated at room temperature. The reaction was monitored by LC-ESI-MS analysis. As expected, the Endo-S-catalyzed deglycosylation of rituximab took place rapidly and was completed within 5 min under the reaction condition, even before any significant transglycosylation could occur (data not shown). Then the transglycosylation product (**2** or **3**) was steadily formed over time without apparent hydrolysis, reaching about 80% within 2 hours (Figure 37A and 37B). It was also observed that the transglycosylation with the hybrid type glycan oxazoline (**6**) went faster than that of the high-mannose type glycan oxazoline (**5**) under the same

reaction condition. The mass spectrometry profiles of the antibody products formed after transglycosylation are shown in Figure 37C and 37D. The experimental data indicated that the free N-glycans in the medium released from the deglycosylation step did not interfere with the transglycosylation process, and the one-pot approach was able to transform the heterogeneous rituximab into homogenous high-mannose or hybrid glycoforms without the need of separating the deglycosylated intermediate or changing the catalyzing enzyme. It should be pointed out that this transformation could be optimized to push the reactions to completion by adding more glycan oxazolines and/or enzyme with prolonged incubation time.

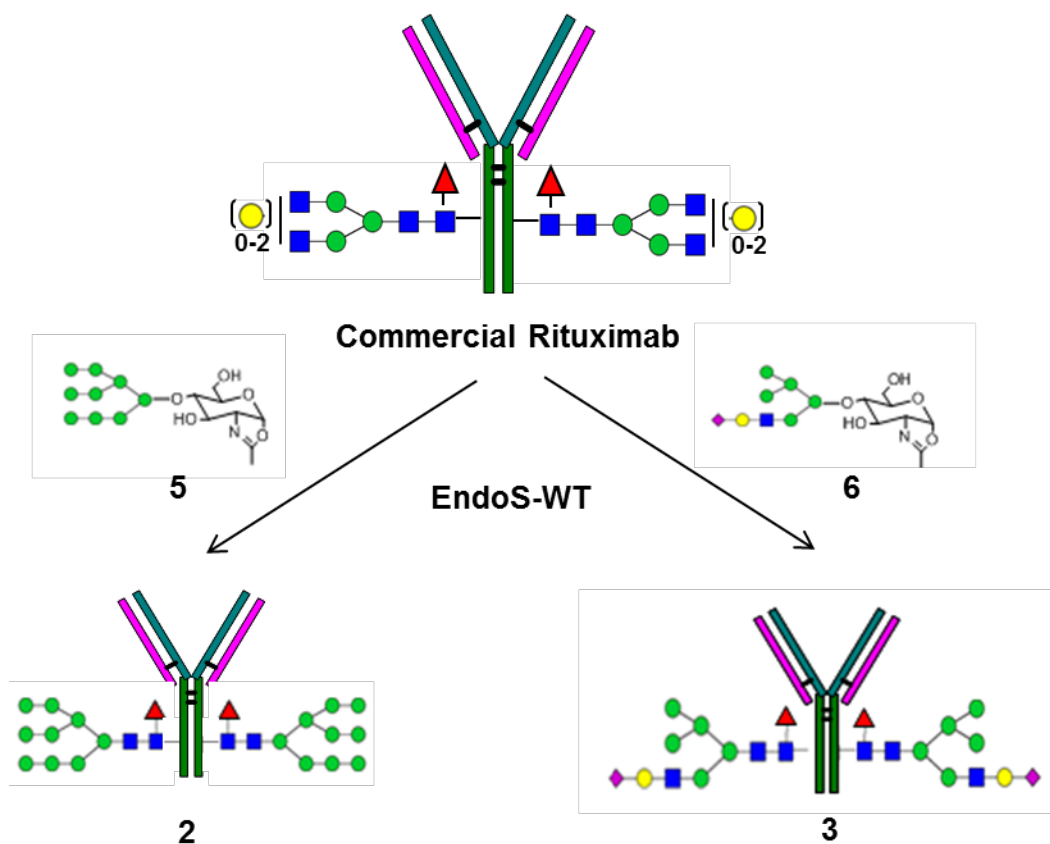


Figure 36. One-pot N-glycosylation remodeling of commercial rituximab to give rise to hybrid and high-mannose rituximab N-glycoforms, Hyb-RTX 2 and HM-RTX 3.

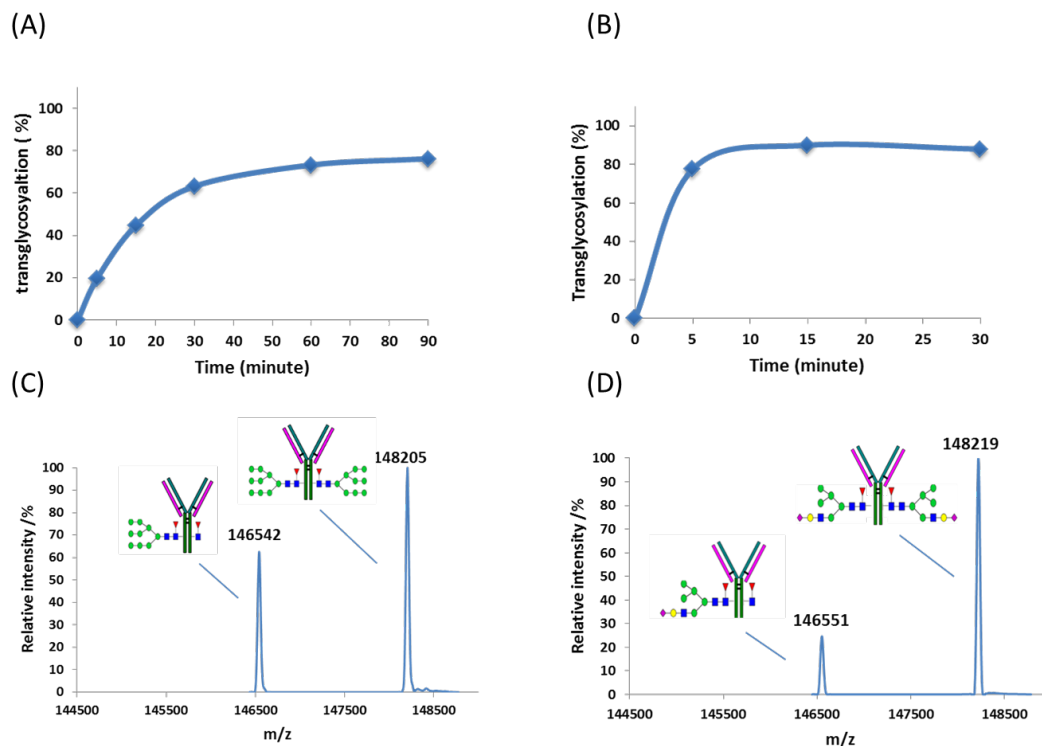


Figure 37. Endo-S WT-catalyzed one-pot transglycosylation reaction with mannose (HM-Oxa **5**) and hybrid (Hyb-Oxa **6**): A) Transglycosylation with HM-Oxa **5** reached over 70% completion within 90 min; B) Transglycosylation with Hyb-Oxa **6** reached about 90% completion in 30 min; C) LC-MS spectrum of the transglycosylation product with HM-Oxa **5** showed two product species at 146542 and 148205; D) LC-MS spectrum of transglycosylation product with Hyb-Oxa **6** showed two product species at 146551 and 148219. The results shown here are representative of two independently conducted experiments.

## 12. One-pot glycosylation remodeling of commercial antibody with modified glycan oxazolines by wild-type Endo-S

In addition to the hybrid and high mannose type N-glycans, we also tested the ability of Endo-S to act on the modified azido-tagged azide-Man<sub>3</sub>GlcNAc oxazoline (AzideM3-Oxa, **9**) for Fc glycan remodeling of rituximab in a one-pot manner (Figure 38). Following the same one-pot reaction protocol described above, we found that the conversion took place relatively slowly, but the transglycosylation product, the azide-tagged glycoform of rituximab was formed steadily. Within 6 h, nearly 40% conversion was achieved (Figure 38B). We also tested the Man<sub>3</sub>-glycan oxazoline (M3-Oxa **8**). Interestingly, only marginal level of transglycosylation product was detected by LC-MS analysis in the case of using the Man<sub>3</sub>-glycan oxazoline (Figure 38A). This result is consistent with our previous comparative studies on the Man<sub>3</sub> glycan oxazoline using the Endo-S D233Q mutant and the wild-type Endo-S, where only transitional formation of the transglycosylation product was observed by SDS-PAGE analysis when the wild-type Endo-S was used, and significant conversion was only achieved using EndoS-D233Q mutant. Indeed, as shown in the oxazoline hydrolysis experiment described above (Figure 34B), Man<sub>3</sub>-glycan oxazoline was hydrolyzed rapidly by the wild-type Endo-S. In addition, the transglycosylation product was also hydrolyzed quickly by the wild-type Endo-S. Thus it was not a surprise that only transitional transglycosylation product could be detected during the reaction. It should be pointed out that Davis and co-workers previously reported the Endo-S-catalyzed transglycosylation with the same Man<sub>3</sub>-glycan oxazoline to the deglycosylated IgG antibody, but no detailed quantitative characterization of the

transglycosylation product was reported except the MS analysis of the released N-glycans. In the present case of the azide-Man<sub>3</sub> glycan oxazoline (**9**), our enzymatic oxazoline hydrolysis experiment showed that the chemical modification increased to some extent its resistance toward the Endo-S-catalyzed hydrolysis (Figure 38B), which could partially explain the moderate transglycosylation activity using azide-Man<sub>3</sub>-glycan oxazoline. It is expected that this one-pot enzymatic glycan remodeling method might be extended to other modified glycan oxazolines to prepare selectively functionalized antibody glycoforms for various structural and functional purposes such as development of antibody-drug conjugates.

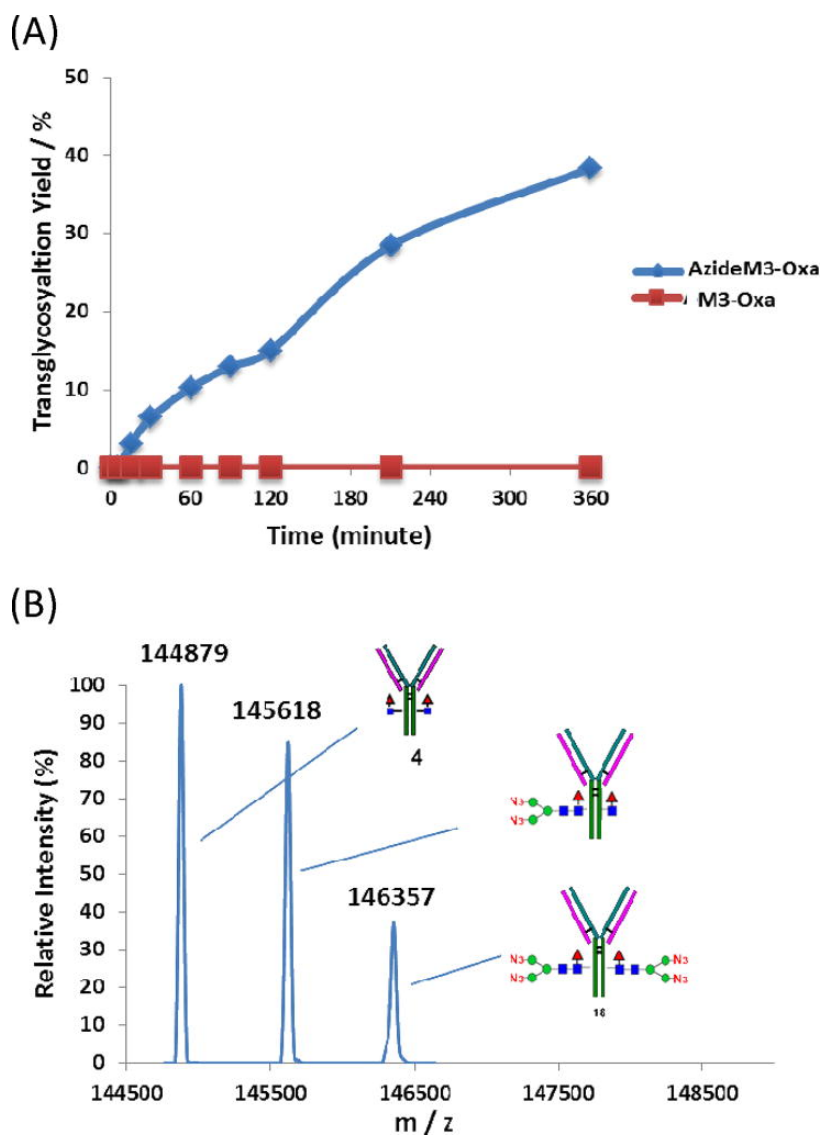


Figure 38. Endo-S WT-catalyzed one-pot transglycosylation reactions with chemically modified glycan oxazoline: A) transglycosylation with reached almost 40% completion within 360 min, whereas reaction with the Man3 core glycan (M3-Oxa **8**) showed no detectable level of transglycosylation under the same condition; B) The LC-MS spectrum of the transglycosylation product with AzideM<sub>3</sub>-Oxa, **9** showed the two product species at mass 145618 and 146357, and a significant percentage of the starting material was still present in the reaction mixture after 360 min. The results shown here are representative of two independently conducted experiments.

### C. Conclusion

We describe in this paper the discovery of a new class of glycosynthases derived from an endoglycosidase (Endo-S2) of the *S. pyogenes* M49 serotype, which showed broader substrate specificity and more potent transglycosylation activity for antibody glycosylation remodeling than the previously reported glycosynthases, such as those derived from Endo-A, Endo-M, and Endo-S. These findings were enabled by systematic mutagenesis at the critical residue Asp-184, coupled with comparative analysis of the hydrolysis and transglycosylation activities of the resulting 19 mutants. Our experimental data also revealed a remarkable difference in both the hydrolysis and transglycosylation activities among the 19 mutants, which would be difficult to predict without this comparative study. Several interesting mutants, including Endo-S D184M and D184Q, were identified that showed high transglycosylation activities for glycosylation remodeling but retained only marginal hydrolysis activity. Comparison of the hydrolysis and transglycosylation activities of Endo-S2 mutants reveals several interesting features. First, most of the mutants that showed high transglycosylation activities, including D184C, D184G, D184E, D184Y, D184S, and D184A mutants, also possessed relatively high residual hydrolysis activities. An exception is Endo-S2 D184M, which demonstrated remarkable transglycosylation activity but retained a very low level of hydrolytic activity, making it the most efficient glycosynthase for glycosylation remodeling. Second, most of Endo-S2 mutants at the Asp-184 residue being replaced by amino acids with positively charged side chains (Lys, Arg, and His) or bulky hydrophobic side chains (Ile, Leu, Phe, and Trp) showed very low activities in both transglycosylation and hydrolysis. However, interestingly, the D184Y mutant

retained the highest hydrolytic activity among all the mutants and also possessed a relatively high transglycosylation activity. A detailed understanding of the molecular mechanism behind these observations may rely on structural studies of the Endo-S2 mutants and their complex with respective substrates.

Another important discovery is the broader substrate specificity of Endo-S2-derived glycosynthase mutants than the previously reported Endo-S glycosynthases. We found that the D184M and D184Q mutants, two notable Endo-S2 glycosynthases identified, were able to efficiently transfer all three major types of N-glycans including the high-mannose, complex, and hybrid type, in antibody glycosylation remodeling. In addition, the Endo-S2 glycosynthases could recognize both the core-fucosylated and non-fucosylated GlcNAc moieties at the Fc domain as an acceptor for transglycosylation. These findings significantly expand the scope of the glycosylation remodeling strategy. For example, the previously reported Endo-S and Endo-F3 are specific for the complex type N-glycans and are unable to efficiently transfer the high-mannose and hybrid type N-glycans, and Endo-F3 is effective only for the core-fucosylated GlcNAc acceptor.<sup>85</sup> A direct comparison of the transglycosylation activities of the typical Endo-S2 and Endo-S glycosynthase mutants reveals that the Endo-S2 mutants are generally much more active than the corresponding Endo-S mutants. By an estimate of the initial rate, the D184Q mutant of Endo-S2 was at least 10-fold more efficient than the corresponding D233Q mutant of Endo-S, and the most efficient Endo-S2 mutant, D184M, was estimated to be 100-fold better than Endo-S D233Q mutant in glycosylating the deglycosylated rituximab.

It is expected that these highly efficient glycosynthases of Endo-S2 with the remarkably relaxed substrate specificity, will find a wide range of applications for producing various types of homogeneous glycoforms of antibodies in research and for developing more effective antibody-based therapeutics as well.

We have demonstrated that the wild-type Endo-S possesses promiscuous hydrolysis and transglycosylation activities on different glycan oxazolines and antibody glycoforms, using therapeutic monoclonal antibody rituximab as a model system. The potent activity of Endo-S to deglycosylate the recombinant complex type N-glycoforms of antibodies, the promiscuous transglycosylation activity on the high-mannose and hybrid type N-glycan oxazolines, and yet the lack of hydrolysis activity on the “ground-state” high-mannose and hybrid type glycoforms collectively enabled us to develop an efficient one-pot N-glycan remodeling of heterogeneous glycoforms of rituximab to give homogenous high-mannose or hybrid type glycoforms, without the need of intermediate separation and enzyme switching. This one-pot enzymatic glycan remodeling method should be applicable to other therapeutic antibodies for obtaining specific N-glycoforms for various applications.

## D. Materials and Methods

### 1. Chemical and biochemical materials

Monoclonal antibody, rituximab, was purchased from Genentech Inc., (South San Francisco, CA). The complex (SCT) (**4**) and high-mannose type (HM) oxazoline (**5**) were harvested and synthesized from egg yolk and soybean flour, respectively, following previously described methods.<sup>127</sup> The hybrid-type (Hyb) oxazoline (**6**) was converted from Man<sub>5</sub>GlcNAc structure (**7**) via a multi-step enzymatic treatment using a series of previously described enzymes, including  $\beta$ -1,2-GlcNAc transferase,  $\beta$ -1,4-galactosyltransferase, and sialyltransferase. The Man<sub>3</sub> (M3-Oxa **8**) and azide-tagged Man<sub>3</sub>-(AizdeM<sub>3</sub>-Oxa **9**) oxazolines were synthesized following previous publication.<sup>106</sup> All oxazolines (**4-9**) were then converted from their corresponding free glycans using a one-pot transformation procedure.<sup>121</sup>

### 2. Expression and purification of recombinant Endo-S WT and Endo-SD233Q

The pGEX plasmid vector encoding the wild-type Endo-S was a gift from Dr. M. Collin (Lund University, Sweden). Site-directed mutagenesis was conducted as described in the previous publication to generate Endo-S D233Q mutant DNA.<sup>103</sup> The plasmid DNA encoding both the wild-type Endo-S and the Endo-S D233Q mutant was transformed in *E. coli* BL21 (DE3) cells for overexpression. For purification of all Endo-S enzymes, the transformed cells were grown in 1L 2YT media with 100  $\mu$ g/mL Carbenicillin added. Cells were incubated at 37 °C and induced with 0.5 mM isopropyl  $\beta$ -D-1-thiogalactopyranoside (IPTG) when the cell density reached an OD<sub>600</sub> of 0.8-1.0. The induced cells were incubated at 20 °C overnight and harvested

by high-speed centrifugation. The cell lysates were collected after treating with the bacterial cell lysis buffer (Gold Biotechnology, Inc.) following the manufacturer's instructions. The GST-tagged proteins were purified using the GST resin (Thermo). The purified proteins were diluted into PBS at pH 7.4 after buffer exchange using Amicon ultra filtration units (10 kDa, Millipore). The purity of Endo-S proteins was over 90% on SDS-PAGE and the final concentration was recorded on a NanoDrop 2000c at absorbance 280 nm.

### 3. Mutagenesis, expression, and purification of recombinant Endo-S2 and mutants

The cDNA encoding amino acids 38 – 819 of Endo-S2 from *S. pyogenes* NZ131 (serotype M49) was amplified by standard PCR and cloned into pCPD-Lasso vector (a pET22b-CPD derivative). For saturation mutagenesis of Asp-184 residue, a forward primer, 5'-CGTAAATTCGTGCTCAATNNNAATATCTAGTCCATCGA-CACCACGATCAGTT-3', and a reverse primer, 5'-AACTGATCGTGGTGTCG-ATGGACTAGATATTNNNATTGAGCACGAATTTACG-3', were used. Mutations were confirmed by DNA sequencing. The plasmids containing the mutated Endo-S2 genes were transformed into *E. coli* BL21 (DE3). For simultaneous production of 20 Endo-S2 Asp-184 variants, the transformants were cultured in 20 ml of 2YT broth media supplemented with 100 µg/ml of carbenicillin. Cultures were grown at 37 °C until cells reached an absorbance  $A_{600}$  of 0.8–1.0. Then 0.5 mM isopropyl-D-1-thio-galactopyranoside (IPTG) was added to the culture to induce protein overproduction at 20 °C. After 24 h the cells were harvested by centrifugation. The cell pellets were then lysed by Bacterial Cell Lysis Buffer (Gold Biotechnology, Inc.) following the manufacturer's instructions. The His<sub>10</sub>-tagged Endo-S2/CPD fusion proteins were

purified with nickel-nitrilotriacetic acid spin columns (Qiagen). The purified Endo-S2 proteins were desalted into PBS (pH 7.4) buffer using centrifugal diafiltration with Amicon Ultrafiltration (10 kDa, Millipore). The purity was confirmed by SDS-PAGE analysis and the concentration was measured on a NanoDrop 2000c using absorbance at 280 nm. For large-scale purification of selected Endo-S2 variants, 1 liter of culture was used. The cell lysate was applied to a HisTrap HP column (GE Healthcare) and washed with 0.5 M NaCl and 20 mM imidazole added (pH 7.4). Bound His-tagged protein was eluted with a gradient of 0 –250 mM imidazole in PBS buffer. The eluted fractions containing Endo-S2 proteins were pooled, concentrated, and further purified by size exclusion chromatography using HiPrep 16/60 Sephacryl S-200 HR column (GE Healthcare).

#### 4. Liquid Chromatography Mass Spectrometry (LC-ESI-MS) analysis

Antibody N-glycoforms were studied using an Exactive Plus Orbitrap instrument equipped with a HPLC system and an ESI source. The capillary temperature and the spray voltage were set according to previous publications.<sup>134 135</sup> Approximately 25  $\mu$ L of the intact rituximab solution was injected and separated via a Waters XBridge™ BEH300 C4 column (3.5  $\mu$ m, 2.1 x 50 mm) at a flow rate of 0.4 mL/min. The program includes a 9 min linear gradient of 5-90% MeCN containing 0.1 % formic acid. The starting material deglycosylated rituximab (m/z 144879) and transglycosylation products were measured using selected ion monitoring (SIM). The signal intensities of the target ions were optimized by automatic tuning function and the same optimized conditions were used in all LC-MS quantifications. The MagTran Software (Amgen) was used to analyze the data from the exported chromatogram

results. An average of scans was analyzed through deconvolution to give a spectrum list for each analyzed sample. Integration of the deconvoluted spectrum shows the relative abundance of the analyzed ions. Total peak intensities within 0.7 mass units surrounding the center of the target ion peak were used to determine the ratio of the starting material and the product species. This relative ratio can be used to calculate the reaction yield of each hydrolysis and transglycosylation reaction with the concentration of the starting material known.

## 5. HPAEC-PAD analysis of glycans and oxazolines

High-performance anion-exchange chromatography coupled with pulsed amperometric detection (HPAEC-PAD) analysis was conducted on a DIONEX chromatography system (DIONEX Corporation, Sunnyvale, CA) using an anion exchange column (CarboPac PA200, 3 × 250 mm). The sample was delivered with a mobile phase consisting of deionized water (eluent A), 0.2 M NaOH (eluent B), 0.1M M NaOH (eluent C) and 0.1M M NaOH with 0.25M NaOAc (eluent D). The program for the complex and hybrid type glycans and oxazolines used a gradient as follows: 0 min, 0% eluent A, 0% eluent B, 100% eluent C and 0% eluent D; 5.0 min, 0% eluent A, 0% eluent B, 100% eluent C and 0% eluent D; and 25.0 min, 0% eluent A, 0% eluent B, 60% eluent C and 40% eluent D at a flow rate of 1.0 mL/min. The program for oligomannose type glycans and oxazolines (Man9, Man5, Man3 and Azide-Man3) were analyzed using a different program: 0 min, 0% eluent A, 0% eluent B, 100% eluent C and 0% eluent D; 5.0 min, 0% eluent A, 0% eluent B, 100% eluent C and 0% eluent D; and 25.0 min, 0% eluent A, 0% eluent B, 80% eluent C and 20% eluent D

with a flow rate of 1.0 mL/min. The relative abundance of each glycan and oxazoline was calculated from the integrated spectrum.

#### 6. Comparison of hydrolytic activity of Endo-S against rituximab N-glycoforms

The rituximab N-glycoforms, SCT-RTX 1, HM-RTX 2 and Hyb-RTX 3 were synthesized according to previously published protocol.<sup>139</sup> In three parallel reactions, each of the three N-glycoforms (0.01 mg, 6.9  $\mu$ M) was incubated with Endo-S WT (5 mg/mL) at 30 °C in 20  $\mu$ l of PBS buffer (pH 7.4) for a given amount of time. Each reaction was quenched by adding 20  $\mu$ l of 0.1% formic acid and the sample was placed at -20 °C. The hydrolysis yield was measured by calculating the ratio of the hydrolyzed product versus the starting material using LC-ESI-MS as shown above.

#### 7. Comparison of hydrolytic activity of Endo-S WT towards different oxazolines

In parallel reactions, SCT-Oxa 4, HM-Oxa 5, Hyb-Oxa 6, M5-Oxa 7, M3-Oxa 8 and AzideM<sub>3</sub>-Oxa 9 oxazolines (1 mM) was incubated with Endo-S (0.05 mg/ml) at 30 °C in a total of 25  $\mu$ l of PBS buffer (pH 7.4). Aliquots of reaction mixture (1  $\mu$ l) was sampled at the same time intervals and diluted in 100 mM NaOH solution to quench the reaction. All reactions were monitored by HPAEC-PAD and the relative percentage of the hydrolyzed oxazolines (free glycans) was quantified from the integrated spectrum as detailed in previous experimental section.

#### 8. Evaluation of transglycosylation activity of Endo-S on deglycosylated rituximab using SCT-Oxa 4, HM-Oxa 5 and Hyb-Oxa 6 as glycosyl donors.

The ability of Endo-S WT to transfer three different N-glycan oxazolines SCT-Oxa 4, HM-Oxa 5 and Hyb-Oxa 6 to the deglycosylated rituximab 10 in a

conventional two-step transglycosylation reaction was compared under the same reaction conditions. First, the commercial rituximab underwent deglycosylation by incubation with a catalytic amount of Endo-S WT (0.01 mg/mL) at 30 °C for a short period of time. Once the complete deglycosylation was confirmed, the deglycosylated rituximab antibody was subsequently purified through Protein-A chromatography for further modification. The following transglycosylation reaction was performed using the deglycosylated rituximab 10 (10 mg/mL) as the glycosyl acceptor and N-glycan oxazolines as glycosyl donors with a catalytic amount of Endo-S WT (0.05 mg/mL) at 30 °C in 20 µl of PBS buffer (pH 7.4). The molar ratio of the donor substrate to the glycosyl acceptor was set to be 40 : 1.

9. Evaluation of transglycosylation activities of Endo-S WT and Endo-S D233Q towards deglycosylated rituximab antibody using HM-Oxa 5 and Hyb-Oxa 6 as glycosyl donors.

The transglycosylation efficiency of Endo-S WT and Endo-S D233Q towards the deglycosylated rituximab was compared separately for HM-Oxa 5 and Hyb-Oxa 6. For reaction with either oxazoline, the deglycosylated rituximab (10 mg/mL) was incubated with each enzyme (0.5 mg/mL) at 30 °C in 20 µl of PBS buffer (pH 7.4). The molar ratio of the donor substrate to the glycosyl acceptor was also 40 : 1. The transglycosylation products were analyzed and quantified as mentioned previously.

**10.** Transglycosylation of rituximab with Hyb-Oxa and HM-Oxa by Endo-S WT in a one-pot manner.

Commercial Rituximab (0.1 mg, 69  $\mu$ M) was dissolved in PBS buffer (pH 7.4) and was mixed with 40 equivalents of hybrid and high mannose oxazolines HM-oxa **5** (2.8 mM) and Hyb-oxa **6** (2.8 mM), respectively. The reactions were initiated by adding a catalytic amount of Endo-S WT (0.5 mg/ml) and incubated in PBS at 30°C (pH 7.4). For the product quantification, the concentration of the product glycoform carrying two N-glycans, 148205 Da for HM-RTX and 148219 Da for Hyb-RTX (deconvoluted mass), were counted twice as each antibody carries two glycosylation sites. The N-glycoform carrying only one N-glycan for each oxazoline was only counted once as the product formed. The same quantification method using LC-ESI-MS was used for the similar experiments conducted in this study.

**11.** Transglycosylation of commercial Rituximab with M<sub>3</sub>-Oxa and AzideM<sub>3</sub>-Oxa by Endo-S WT in a one-pot fashion.

Commercial rituximab (0.1 mg, 69  $\mu$ M) was incubated in PBS at 30°C (pH 7.4) with 40 equivalents of oxazolines M<sub>3</sub>-Oxa **8** (2.8 mM) and AzideM<sub>3</sub>-Oxa **9** (2.8 mM), respectively. To initiate the reaction, a fixed amount of Endo-S WT (0.5 mg/ml) was added into the reaction mixture at t = 0 min. The reactions with the M<sub>3</sub>-Oxa and AzideM<sub>3</sub>-Oxa oxazolines were maintained for a prolonged period of time to allow the accumulation of transglycosylation product. Additional 40 equivalents of oxazolines were added to each reaction at t = 120 min. Transglycosylation with AzideM<sub>3</sub>-Oxa **9** showed three species at 144879 Da (starting material), 145618 Da (antibody product



## Chapter 4: Revisiting the substrate specificity of endoglycosidase Endo-CC and its mutants in hydrolysis and transglycosylation

### A. Introduction

The Endo- $\beta$ -*N*-acetylglucosaminidase (ENGase) (EC 3.2.1.96) belongs to a family of glycoside hydrolases (GH) that catalyze the cleavage of the  $\beta$ -1,4-glycosidic linkage within the innermost *N,N'*-diacetylchitobiose core of the asparagine-linked oligosaccharides.<sup>98</sup> The unique ability of ENGases to process the N-glycan structures with stringent stereo- and regio-selectivity has made them important tools for analysis and synthesis of the homogeneous glycoproteins and oligosaccharides. Besides their hydrolytic activities, we and others have previously reported that many ENGases also possessed the capability to re-attach the released glycans to different acceptors by forming a new glycosidic linkage, a process also known as transglycosylation.<sup>89, 93, 94</sup> Several such ENGases, including Endo-A from *Arthrobacter protophormiae*<sup>102</sup>, Endo-M from *Mucor hiemali*<sup>99</sup>, and Endo-D from *Streptococcus pneumoniae*<sup>101</sup>, exhibit the remarkable activity to transfer various N-linked oligosaccharides to the GlcNAc-containing peptides *en bloc* to afford new glycopeptides and glycoproteins. Importantly, those ENGases exhibit distinct substrate specificities. Whereas multiple ENGases such as Endo-A and Endo-H could act on the high mannose type N-glycans, Endo-M was found to be particularly interesting, as it has displayed relatively broad substrate specificity towards all three major types of N-glycans (complex, hybrid, and high-mannose type) for both hydrolysis and transglycosylation.<sup>100</sup> However, the application of Endo-M in large-scale glycoengineering of glycoproteins is hindered by technical obstacles such as the difficulties to produce the active Endo-M enzymes

in large quantities<sup>142</sup>. To overcome these problems with the existing ENGases, new unknown ENGases with broad substrate specificity and high catalytic efficiency are still being actively searched.

Recently, the discovery of a new ENGase, namely Endo-CC from the fungus *Coprinopsis cinerea*, has attracted much attention in the glycoengineering field due to its ability to hydrolyze both the complex and high-mannose N-glycans.<sup>142</sup> Using simple fluorescence-labeled oligosaccharides as standard substrates, Takegawa and colleagues demonstrated that Endo-CC was able to hydrolyze multiple types of Pyridylamino (PA)-labeled-glycans with relatively high efficiencies. Subsequently, multiple glycoproteins with different N-glycans, including the ribonuclease B (RNase B), human transferrin and fetuin, were tested with Endo-CC to study its substrate specificity for hydrolysis. The results suggested similar substrate selectivity between Endo-CC and Endo-M, both of which exhibited potent hydrolytic activities against the biantennary complex and high-mannose type N-glycans, although unlike Endo-M, Endo-CC displayed no activities against the bisecting GlcNAc. In addition, neither Endo-CC nor Endo-M were able to act on the triantennary or tetra-antennary N-linked oligosaccharides. However, it remains to be investigated whether the fucosylated glycoproteins and glycopeptides are subject to hydrolysis by Endo-CC.<sup>89</sup>

Following similar studies on other ENGases, a library of glycosynthase mutants from Endo-CC were generated by site-directed mutagenesis at a previously identified catalytic key residue Asn-180. Functional studies further demonstrated that mutant Endo-CC N180H was the most efficient glycosynthase variant of Endo-CC to transfer the biantennary complex type N-glycan to the deglycosylated RNase B.<sup>110</sup>

The reported comparative studies suggested that, unlike previously studied of Endo-S<sup>123</sup>, Endo-S2<sup>139</sup>, and Endo-F3<sup>85</sup>, among the 19 mutants generated at Asn-180 residue of Endo-CC, only two mutants Endo-CC N180H and N180Q showed significant transglycosylation activities using both the sialoglycopeptide (SGP) and the activated glycan oxazolines as the donor substrates. A following study revealed that Endo-CC N180H can transfer complex glycan to a range of acceptors including the monoclonal antibody, although a large excess amount of SGP instead of glycan oxazoline was used as donor substrate for the transglycosylation of antibody. In addition, Endo-CC N180H was also applied in combination with other ENGases such as Endo-S D233Q to improve the transglycosylation efficiency of antibody.<sup>111</sup>

Despite successful application of Endo-CC enzymes in the chemoenzymatic synthesis of glycoproteins, there are still several unknown aspects regarding the substrate specificities and catalytic efficiency of Endo-CC and its mutants: A) The reported expression yield of the original Endo-CC construct was less than 0.5 mg/L of bacterial cell culture. It is unclear whether an alternative purification strategy utilizing any peptide or protein fusion tags could increase the production of Endo-CC and potentially enhance its stability; B) The glycosyl donor substrates tested for Endo-CC transglycosylation were limited to the complex type glycans only, thus it is currently unknown whether Endo-CC and/or its glycosynthase mutants could use other glycan oxazolines, such as the hybrid and the high-mannose glycans, for transglycosylation reactions; C) The previous studies provided no experimental data concerning the substrate selectivity of Endo-CC and its mutants for the core-fucosylated glycans and glycoconjugates; D) The reported experiments detailing transglycosylation activities

of Endo-CC mutants did not show complete reaction progressions for Endo-CC N180 mutants except for Endo-CC N180H and N180Q. Additional functional assays might be required to identify Endo-CC mutants that possess a different catalytic landscape from the known N180H and N180Q; E) Whether Endo-CC and/or its mutants could independently transfer activated glycan oxazoline instead of sialylglycopeptide (SGP) to the deglycosylated antibody is still a question under debate.

To improve our understanding of the substrate specificity of Endo-CC and its mutants, we first created a new version of Endo-CC containing a C-terminal 6xHis-tagged fusion protein called the “Cysteine Protease Domain (CPD)” tag to improve solubility and expression yield<sup>143</sup>. The expression yield of the soluble Endo-CC using the new construct was estimated to be higher than 4 mg/L of *E. coli* culture and the CPD-tagged Endo-CC and Endo-CC N180H exhibited the same level of activity as the untagged enzymes. Next, we performed further substrate selectivity test on Endo-CC and its glycosynthase mutants with a variety of substrates for both hydrolysis and transglycosylation. It was discovered that the Endo-CC N180H could potentially transfer additional glycan oxazolines, such as the high-mannose and hybrid type glycans, to afford new homogeneous glycopeptides and glycoproteins. Furthermore, side-by-side comparative studies on the fucosylated and non-fucosylated substrates, including SGP, Erythropoietin (EPO) and IgG antibodies, revealed that core-fucosylation of glycoconjugates is not tolerated by Endo-CC and its mutants. Finally, we performed additional enzyme activity assays on the selected mutants of Endo-CC and demonstrated that several Endo-CC mutants besides N180H and N180Q exhibited significant transglycosylation activity towards a CD52-GlcNAc peptide

using the complex glycan oxazoline as the donor substrate. However, the relative catalytic efficiency of these mutants varied significantly over prolonged reaction time. Interestingly, Endo-CC N180A, in contrast to several other Endo-CC mutants, demonstrated a relatively slow but persistent transglycosylation activity over a long period of reaction time.

## B. Results and Discussions

### 1. Cloning, expression, and comparison of recombinant Endo-CC and Endo-CC fusion protein (CPD)

The DNA sequence encoding Endo-CC was initially synthesized (GenScript) and cloned into a pET-41b (+) vector, which contains a 7-histidine tag at C terminus. It was previously reported that soluble expression of Endo-CC and mutants could be achieved using leaky expression without any induction.<sup>105</sup> Following a similar expression protocol, Endo-CC was successfully expressed in *Escherichia coli* and purified via the immobilized metal ion affinity chromatography with the expected yield (~400 µg/L). The Endo-CC DNA was also cloned into a pET22b-CPD vector, which contained an additional C-terminal fusion tag (CPD) harvested from the *Vibrio cholerae* MARTX toxin.<sup>141</sup> Consistent with our previous studies on the expression of ENGases,<sup>85, 144</sup> the CPD fusion protein significantly increased the expression yield of the soluble Endo-CC by approximately 10 folds (~ 4 mg/L). Using the ribonuclease B as the standard substrate, the hydrolytic activities of Endo-CC and CPD-tagged Endo-CC were found to be comparable. Both versions of Endo-CC were able to rapidly hydrolyze the high-mannose N-glycans of RNase B under mild reaction conditions (Figure 39).

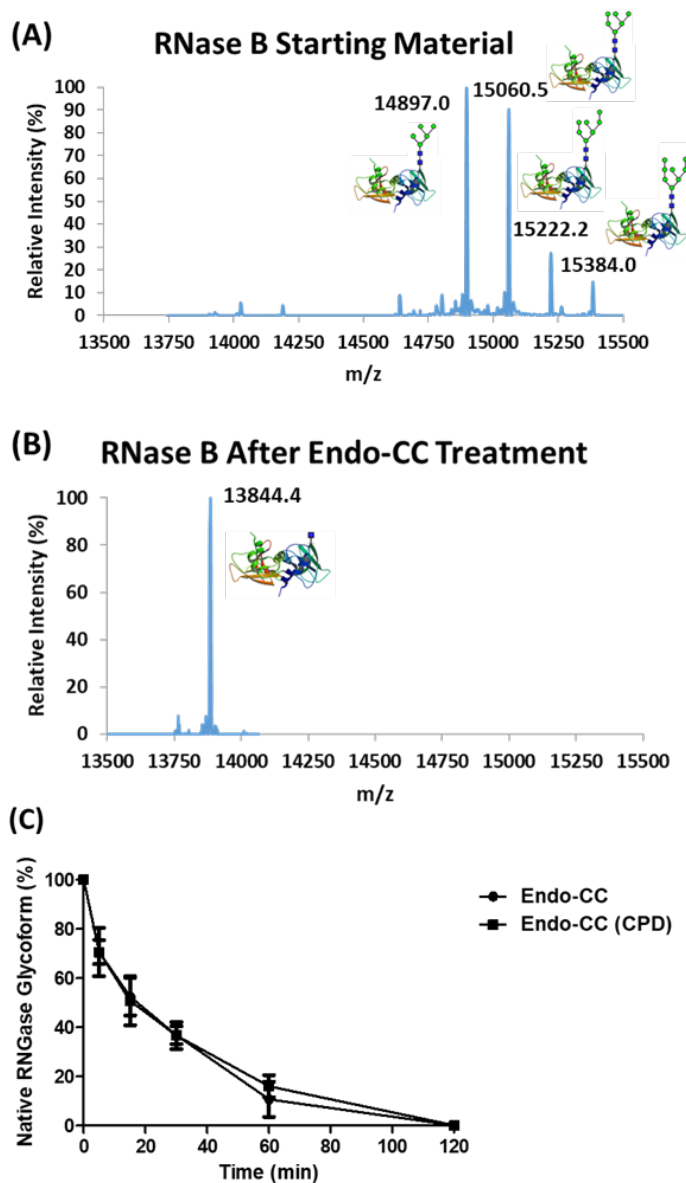


Figure 39. Hydrolysis of RNase B by recombinant Endo-CC and Endo-CC (CPD). MS analysis of (A) RNase B and (B) Deglycosylated RNase B-GlcNAc. (C) Comparison of hydrolytic activities of untagged and CPD-tagged Endo-CC enzymes. A total of 10 mg/mL of RNase B was incubated with 0.1 mg/mL of both recombinant Endo-CC (+/- CPD) at 37 °C in Tris buffer at pH 7.4. At t = 2 h, oligomannose glycans of RNase B were completely hydrolyzed by both versions of Endo-CC. The reactions were monitored by SDS-PAGE densitometry and the final products were

confirmed by LC-MS (B). The schematic structure of RNase B was based on the published crystal structure (1RBB)<sup>145</sup>.

## 2. Generation of glycosynthase mutants from recombinant Endo-CC

Takegawa and co-workers have previously generated glycosynthase mutants of Endo-CC through site-directed mutagenesis at a key amino acid residue that is critical for the formation of the oxazolinium ion intermediate according to a substrate-assisted mechanism.<sup>105</sup> Based on previous studies on other endoglycosidases, such as Endo-M<sup>99</sup>, Endo-A<sup>92</sup>, Endo-S<sup>123</sup> and Endo-S2<sup>139</sup>, several mutants of Endo-CC were generated via site-directed mutagenesis at the same key residue Asn-180, including N180A, N180H, N180M, N180Q and N180E, to study their transglycosylation activities in real-time reaction courses. These mutants were expressed and purified following the same protocol as for the wild-type Endo-CC with a comparable yield and purity, which were confirmed by SDS-PAGE.<sup>105</sup> In particular, the CPD-tagged Endo-CC N180H mutant was also tested for its glycosylation activity in parallel to the original Endo-CC construct, and the results indicated that both versions of Endo-CC N180H displayed similar transfer activities towards the deglycosylated RNase B using the sialylated complex glycan oxazoline (SCT-Oxa) as substrate (Figure 40). Nevertheless, like the wild-type Endo-CC, the expression yield of the CPD-tagged Endo-CC N180H (~ 5.0 mg/L) was significantly higher than that of the non-CPD mutant (0.5 mg/L).

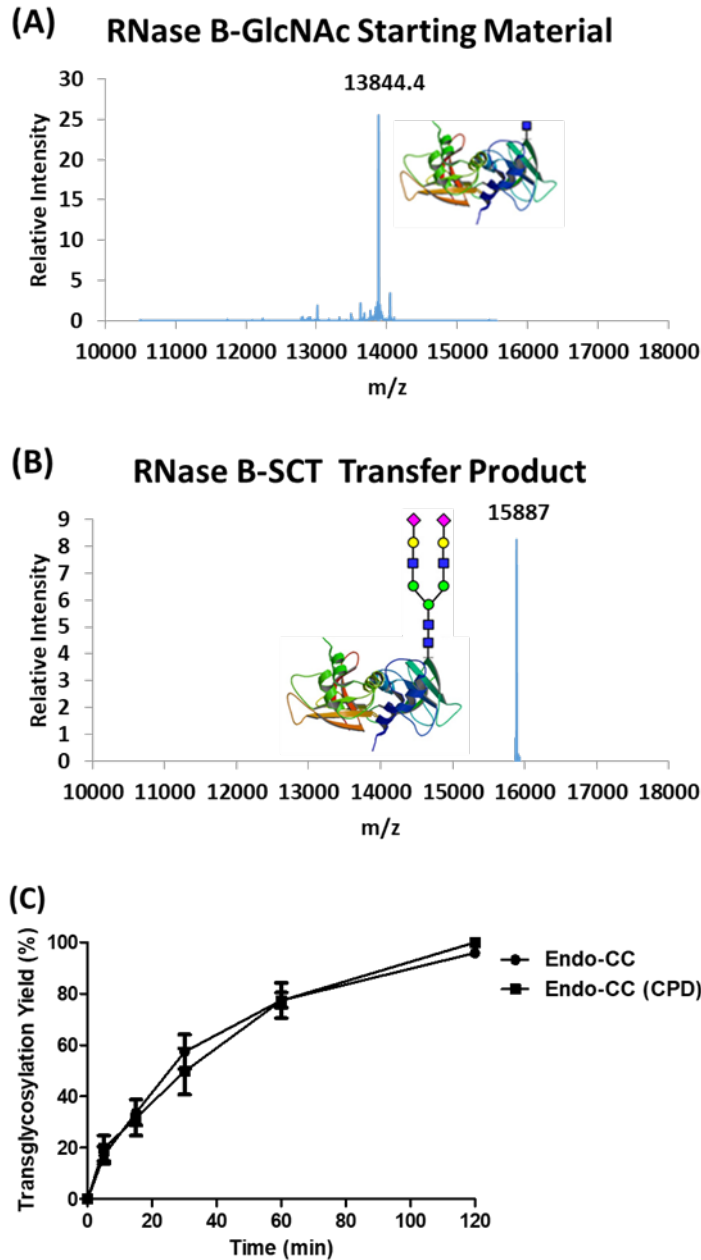


Figure 40. Transglycosylation of deglycosylated RNase B by recombinant Endo-CC and Endo-CC (CPD). LC-MS analysis of (A) N-glycoforms of RNase B-GlcNAc and (B) RNase B-SCT by Endo-CC N180H. (C) Comparison of the transglycosylation reactions on RNase B-GlcNAc by the untagged and CPD-tagged Endo-CC N180H mutants. A total concentration of 10 mg/mL of RNase B-GlcNAc was incubated with

0.5 mg/mL of both recombinant Endo-CC N180H (+/- CPD) at 30 °C in Tris buffer at pH 7.4. At t = 2 h, the sialylated complex form of RNase B was synthesized by both version of Endo-CC with similar catalytic efficiencies. The reactions were monitored by SDS-PAGE densitometry and the final products were confirmed by LC-MS (B). The schematic structure of RNase B was based on the published crystal structure (1RBB)<sup>145</sup>.

### 3. Substrate specificity of Endo-CC in hydrolysis of glycoproteins: core-fucosylation of glycosyl acceptor substrates is not tolerated by Endo-CC

Despite that sequence alignment between Endo-CC and Endo-M revealed significant sequence similarity (approximately 46%), it is currently unknown whether Endo-CC can process the core-fucosylated glycoproteins as suitable substrates for glycan hydrolysis.<sup>142</sup> Here, a number of commonly studied glycoproteins in both their core-fucosylated and non-fucosylated forms were tested for their susceptibility to the Endo-CC-catalyzed hydrolysis of N-glycans, including the sialoglycoprotein (SGP), erythropoietin (EPO) and monoclonal IgG antibody N-glycoforms. As shown in Figure 41, the complex type N-glycans attached to the non-fucosylated SGP was completely released by Endo-CC after 4 h, whereas the core-fucosylated SGP peptide was resistant to Endo-CC-mediated hydrolysis after the overnight reaction.

To more clearly reflect the substrate selectivity of Endo-CC against the core fucose, a glycoengineered protein erythropoietin (EPO), a therapeutic glycoprotein hormone that stimulates erythropoiesis, was prepared by an engineered mammalian expression system to carry a mixture of the core-fucosylated and non-fucosylated complex N-glycoforms (Figure 42A).<sup>146</sup> Treatment of EPO N-glycoforms by Endo-

CC revealed that all non-fucosylated EPO N-glycans were hydrolyzed by Endo-CC in as early as  $t = 2$  h, whereas the core-fucosylated EPO glycoforms remained unaffected after overnight incubation (Figure 42B).

Similarly, both the core-fucosylated and non-fucosylated complex-type IgG N-glycoforms (namely IgG-S<sub>2</sub>G<sub>2</sub>F and IgG-S<sub>2</sub>G<sub>2</sub>) were synthesized and compared for their susceptibilities to the Endo-CC-catalyzed deglycosylation. As the comparative results demonstrated (Figure 43), although neither IgG glycoforms were completely hydrolyzed by Endo-CC after overnight, the IgG-S<sub>2</sub>G<sub>2</sub>F form was distinctively more resistant to Endo-CC hydrolysis in comparison with the IgG-S<sub>2</sub>G<sub>2</sub>. Interestingly, the high-mannose form of IgG (IgG-HM) was also synthesized<sup>139</sup> and tested as a control glycoform. Under the same reaction conditions, the majority of the high-mannose N-glycans of IgG-HM were released by Endo-CC with only a small portion of the mono-glycosylated species present on the mass spectrometry (MS) profile after the reaction. These unexpected results suggested that the high-mannose N-glycans of IgG are more susceptible to the Endo-CC-mediated hydrolysis in comparison to the fucosylated and non-fucosylated complex type N-glycans.

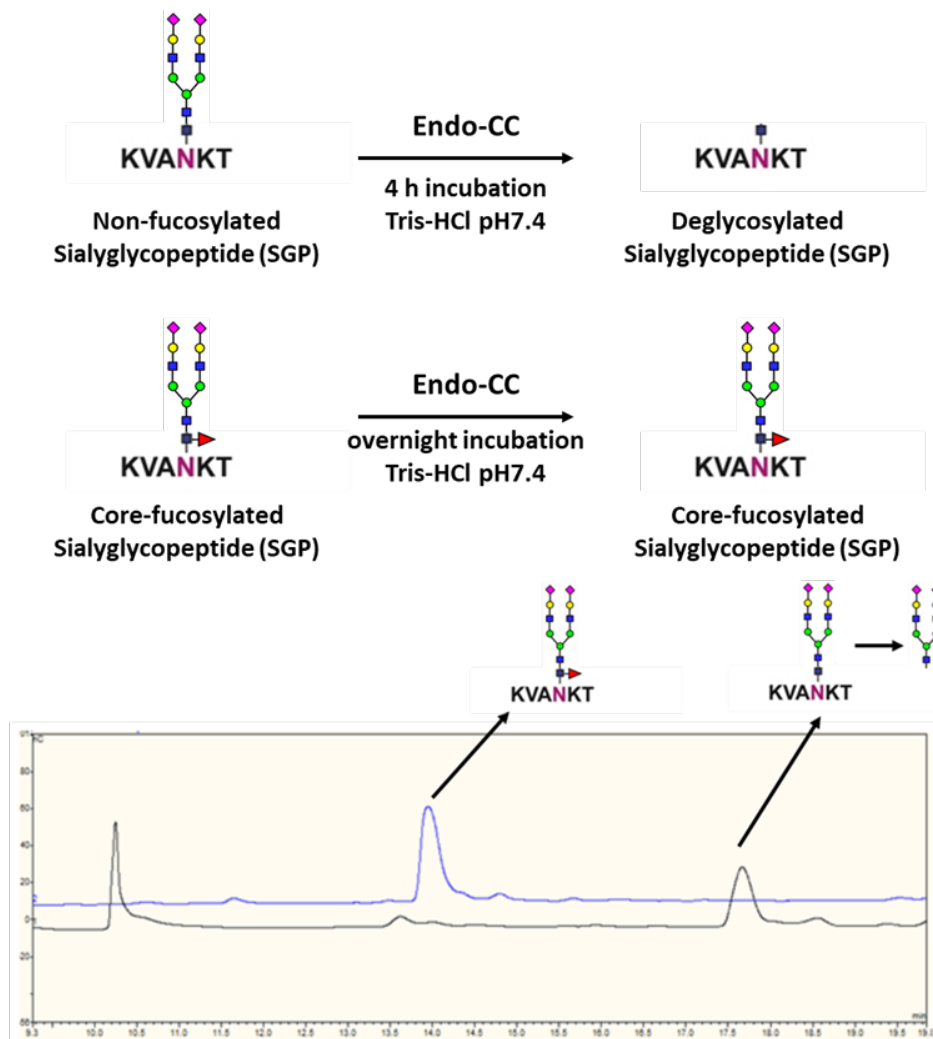


Figure 41. Comparison of Endo-CC-catalyzed hydrolysis against fucosylated and non-fucosylated sialoglycoprotein (SGP). The concentration of both forms of SGP was maintained at 50 mg/mL and samples were incubated with 0.1 mg/mL recombinant Endo-CC at 37 °C in PBS buffer at pH 7.4. The hydrolytic reactions were monitored by HPAEC-PAD analysis. At  $t = 4$  h, the non-fucosylated SGP (bottom curve) was completely hydrolyzed by Endo-CC, whereas core-fucosylated SGP (top curve) remained unchanged after overnight incubation, supported by the different retention times of SGP and the hydrolyzed SCT free glycan, respectively.

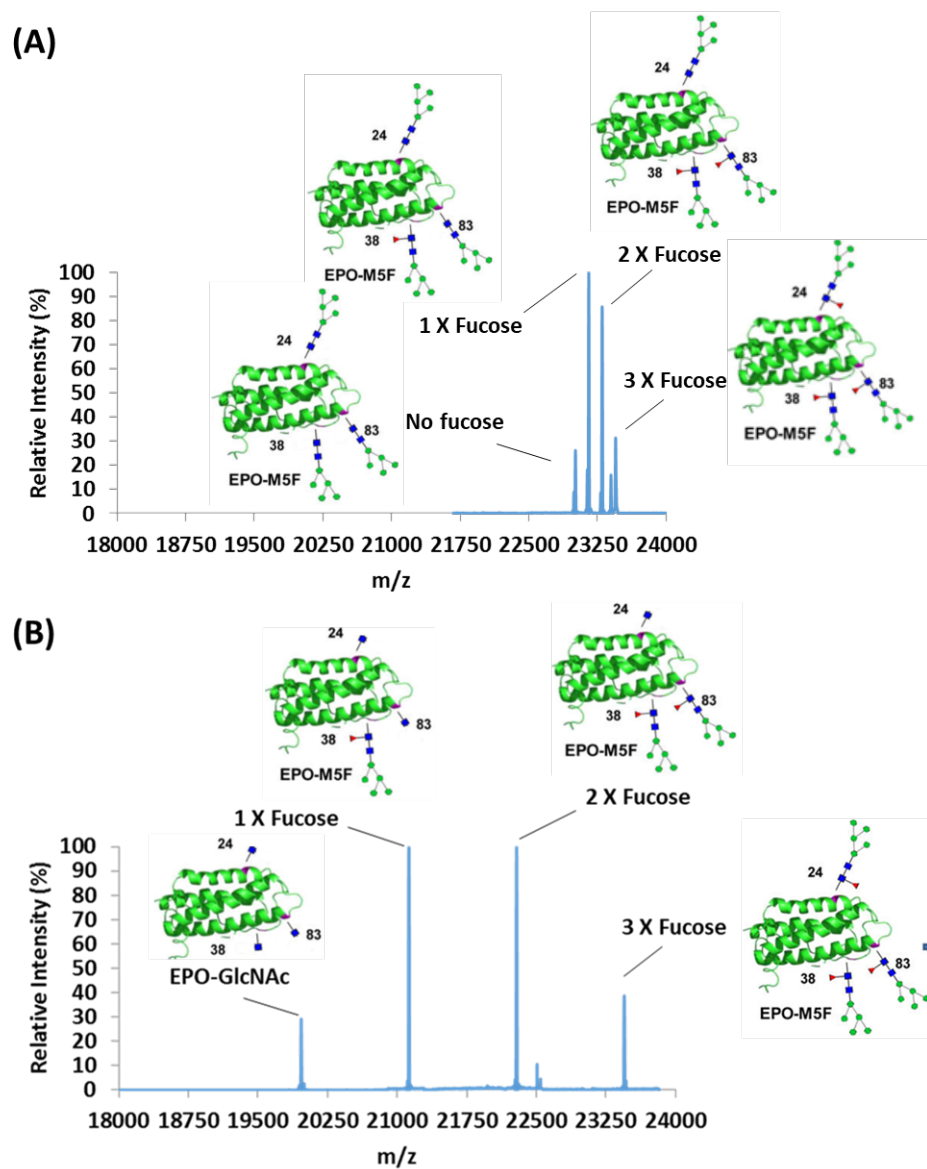


Figure 42. Selective deglycosylation of non-fucosylated N-glycans by Endo-CC from the heterogeneous N-glycoforms of erythropoietin (EPO). A total concentration of 0.5 mg/mL of EPO (A) with a mixture of fucosylated and non-fucosylated oligomannose N-glycans was incubated with 0.01 mg/mL Endo-CC at 37 °C in PBS buffer at pH 7.4. The reaction was quenched at  $t = 2$  h and analyzed by LC-MS. (B) After deglycosylation, only the non-fucosylated N-glycans were completely released, while the fucosylated N-glycans remained unaffected.

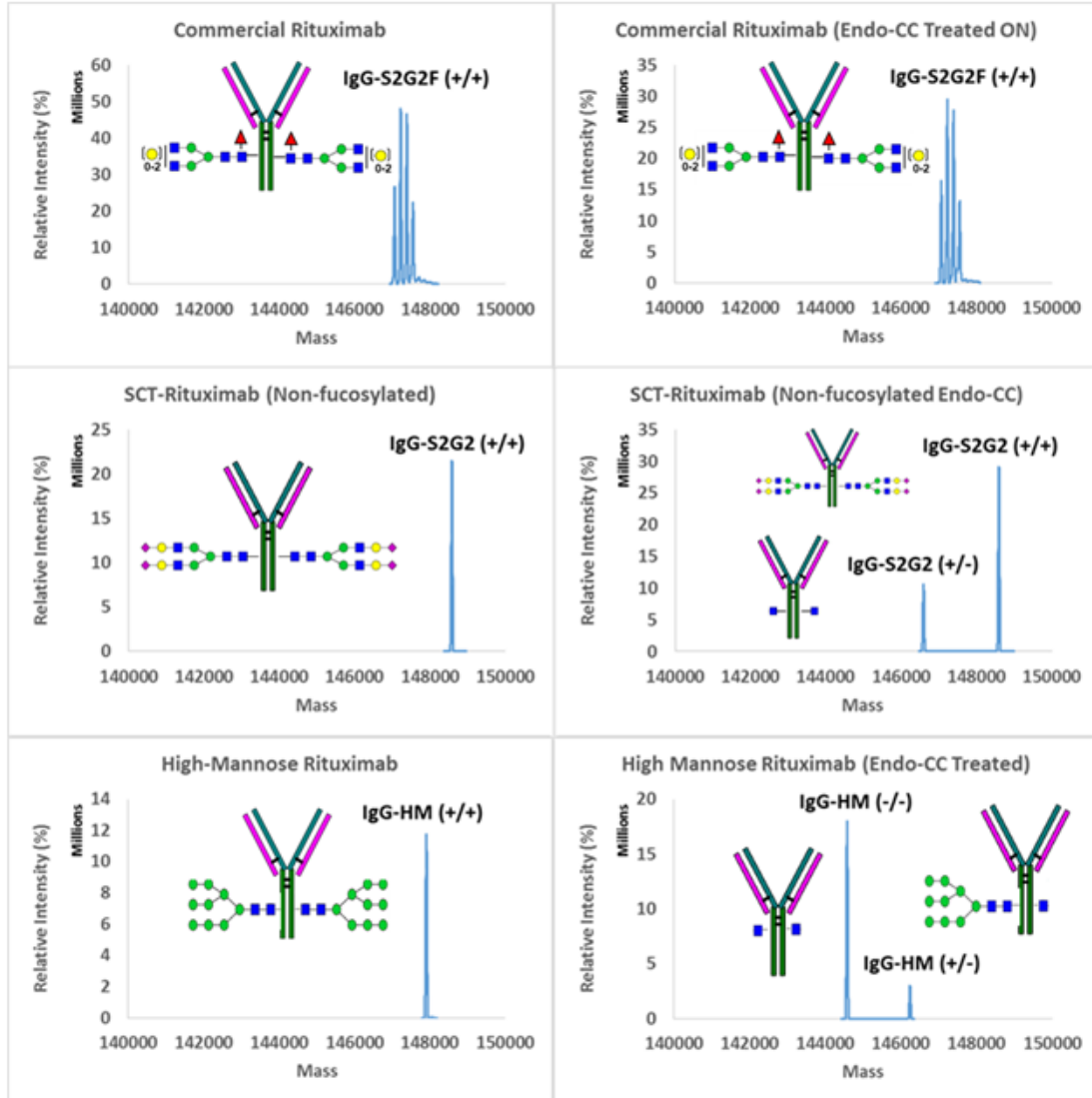


Figure 43. Selective removal of fucosylated and non-fucosylated IgG N-glycans by Endo-CC. A total concentration of 5 mg/mL of IgG N-glycoforms was incubated with 0.05 mg/mL Endo-CC at 37 °C in the Tris-HCl buffer at pH 7.4. For the fucosylated IgG-S<sub>2</sub>G<sub>2</sub>F glycoform (upper row), no hydrolysis was observed, whereas a small percentage of the non-fucosylated complex IgG-S<sub>2</sub>G<sub>2</sub> underwent deglycosylation (middle row). After overnight incubation, nearly complete release of N-glycans was achieved by Endo-CC for the high-mannose IgG glycoform (IgG-HM, bottom row). The deglycosylation reactions were monitored by ESI-LC-MS.

#### 4. Studies on the substrate specificity of Endo-CC in transglycosylation:

##### 4.1. Transglycosylation of high-mannose, hybrid and complex type glycan oxazolines by mutant Endo-CC D180H

To further understand the substrate specificity of Endo-CC N180H mutant against other types of N-glycans besides the complex type, three N-glycan oxazoline substrates derived from the complex (SCT), hybrid (Hyb) and high-mannose (HM) glycans were tested for transglycosylation by Endo-CC N180H towards the GlcNAc-containing peptide (CD52-GlcNAc) to provide the side-by-side comparison for the substrate specificity of Endo-CC N180H mutant. The transfer reactions were assayed at multiple time points and the products were analyzed by the analytical HPLC and characterized by mass spectrometry. The results are summarized in Figure 44. Under the same reaction condition, the transglycosylation yield by Endo-CC N180H with HM-Oxa reached approximately 70% within 480 min to afford the CD52-HM, whereas the reactions with Hyb-Oxa and SCT-Oxa were relatively slower but still significant. These results demonstrated that mutant Endo-CC N180H possessed broad substrate selectivity against all three major N-glycan types for transglycosylation, despite that the transfer efficiency varied depending on the type of N-glycan, as the transfer for HM-Oxa was relatively more efficient than those for the SCT-Oxa and Hyb-Oxa by comparison.

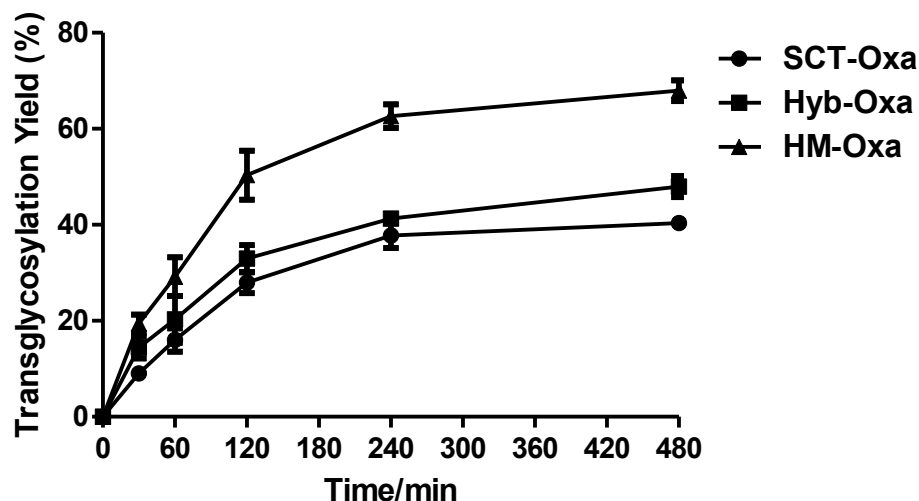


Figure 44. Comparison of transglycosylation efficiency of Endo-CC N180H for three major types of glycan oxazolines (high-mannose, hybrid and biantennary complex). The transglycosylation reactions were conducted using the purified CD52-GlcNAc (5 mg/mL) as the glycosyl acceptor and different glycan oxazolines as the glycosyl donor substrates at 37 °C in Tris-HCl buffer at pH 7.4. The final concentration of Endo-CC N180H was 0.125 mg/mL. The molar ratio of oxazoline to peptide was 5:1. The results presented here are representative of two independent sets of experiments.

#### 4.2. Comparative studies on the transglycosylation activities of Endo-CC mutants

Previous systematic mutagenesis studies on other ENGases such as Endo-S<sup>123</sup>, Endo-S2<sup>139</sup> and Endo-M<sup>100</sup> suggested that substitution of the catalytic residue (D233, D184 and N175, respectively) with methionine (M), glutamine (Q), alanine (A) and glutamate (E) all led to generation of more efficient glycosynthase mutants for transglycosylation with glycan oxazolines. However, the previous mutational studies on Endo-CC indicated that only N180H and N180Q showed significant transfer

activities against SGP and SCT-Oxa. Here, we performed similar mutagenesis on the Asn-180 residue of Endo-CC and expressed several Endo-CC mutants, including EnN180A, N180H, N180M and N180E and N180Q. The transglycosylation activities of these mutants were assayed using the CD52-GlcNAc glycopeptide as glycosyl acceptor substrate and the complex type glycan oxazoline (SCT-Oxa) as the glycosyl donor. The progression of each transfer reaction was monitored by the analytical HPLC followed by MS characterization (Figure 45). Side-by-side comparison of the progression patterns catalyzed by each mutant under the same reaction condition indicated that the N180H mutant indeed demonstrated the highest transglycosylation yield in the first 4 hours of the reaction, which was consistent with the previous publication<sup>110</sup>. However, the accumulation of the product by Endo-CC N180H stopped at  $t = 4$  h, and the product CD52-SCT underwent significant hydrolysis during the rest of the reaction time. Similarly, the N180E mutant exhibited the second highest reaction yield within the first 8 hours before product hydrolysis. The behaviors of these mutants were consistent with several other ENGase mutants, as mentioned above.

On the other hand, additional mutants, namely Endo-C N180M, N180A, and N180Q, were found to exhibit relatively slow but highly persistent product formation with no significant product hydrolysis observed in the first 24 hours of the reaction. Interestingly, the N180A mutant exhibited continuous accumulation of the transfer product for at least 24 hours without any sign of product hydrolysis. Therefore, at  $t = 24$  h, the overall transglycosylation yield of the N180A mutant was the highest among all the mutants tested here, as a large percentage of the transfer product formed by

N180H and N180E was hydrolyzed. The wild-type Endo-CC was also included as a control to demonstrate the dominant hydrolytic activity of the wild-type enzyme and, as a result, no accumulation of the transfer product under the presented condition. Unlike the D233M and D184M mutant of Endo-S and Endo-S2, respectively, the Endo-CC N180M did not achieve a high level of transglycosylation in comparison with N180Q and N180A. However, the minimal tendency of Endo-CC N180M to hydrolyze the product was partially consistent with the behavior of Endo-S D233M Endo-S2 D184M.<sup>123, 139</sup>

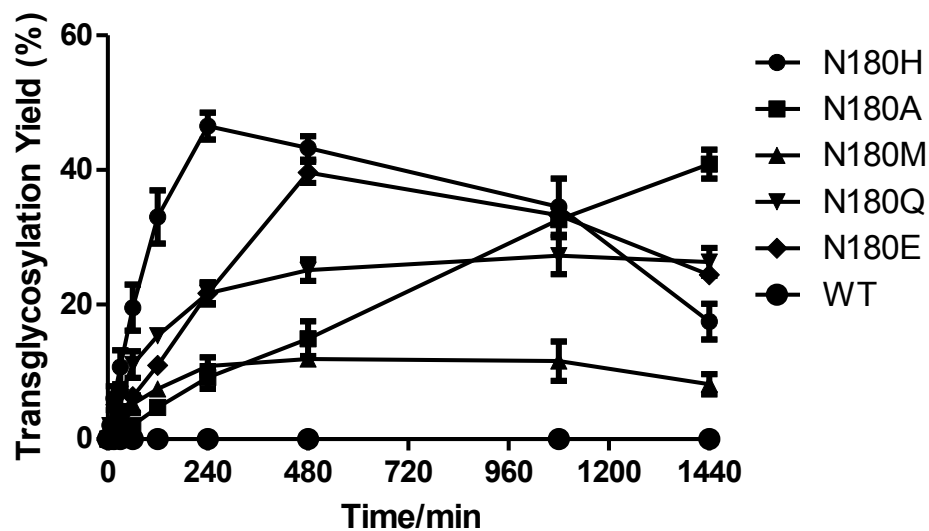


Figure 45. Comparison of the transglycosylation reactions catalyzed by selected Endo-CC mutants. The reaction was carried out using CD52-GlcNAc (2 mg/mL) as the glycosyl acceptor and SCT-Oxa as the glycosyl donor substrate at 30 °C in Tris-HCl buffer at pH 7.4. The final concentration of mutant/wild-type enzyme was 0.125 mg/mL. The molar ratio of SCT-Oxa to CD52-GlcNAc was 5: 1. The results presented here are representative of two independent sets of experiments.

5. Glycosylation remodeling of a therapeutic antibody rituximab using Endo-CC and Endo-CC N180H with glycan oxazoline as glycosyl donor substrate

Finally, glycoengineering of antibody was also attempted in this work using either the wild-type Endo-CC or Endo-CC mutant and the complex type glycan oxazoline (SCT-Oxa) as substrate. Similar studies have been conducted by Ito and others to generate the homogeneous antibody N-glycoforms using Endo-CC enzymes.<sup>111, 112</sup> However, these studies involved a combination of two enzymes, Endo-CC and Endo-S mutants, and a large excess of SGP (approximately 25000 molar equivalents to antibody) used as the glycosyl donor substrate. How Endo-CC and its mutants alone catalyze the transglycosylation of the deglycosylated antibody using the glycan oxazoline as donor substrate remains a question to be answered in more detail. Here, glycosylation remodeling was performed on rituximab, which has been prescribed for breast cancer treatment.<sup>63</sup> The process of glycan remodeling of antibody was illustrated by a two-step chemoenzymatic strategy. First, the mixture of the native N-glycans of rituximab was removed by immobilized Endo-S2 to produce the deglycosylated antibody acceptor. The intermediate was then purified and used as glycosyl acceptor for the following transglycosylation reaction. The transfer reactions were conducted by incubating the deglycosylated antibody with a moderate amount of activated SCT-Oxa (20 molar equivalents to antibody) in the presence of varying concentrations of both Endo-CC and Endo-CC N180H. The relative reaction yield for transglycosylation by each enzyme was estimated by LC-MS following our previously described protocol.<sup>123</sup> As shown in Figure 46, Endo-CC and Endo-CC N180H at concentration 0.05 mg/mL did not show significant transfer of SCT glycan

oxazoline to the antibody after a prolonged incubation time. However, wild-type Endo-CC at a reduced concentration (0.01 mg/mL) indeed demonstrated nearly 40% conversion of antibody glycan at  $t = 4$  h, although the same result was not observed for mutant Endo-CC N180H at the same low concentration. These results are supported by previous reports that a low concentration of the wild-type ENGase could be used for transglycosylation of certain substrates with moderate efficiency, although further optimization might be required to achieve a near-completion level of transglycosylation, especially with complex substrates like antibody.<sup>99</sup>

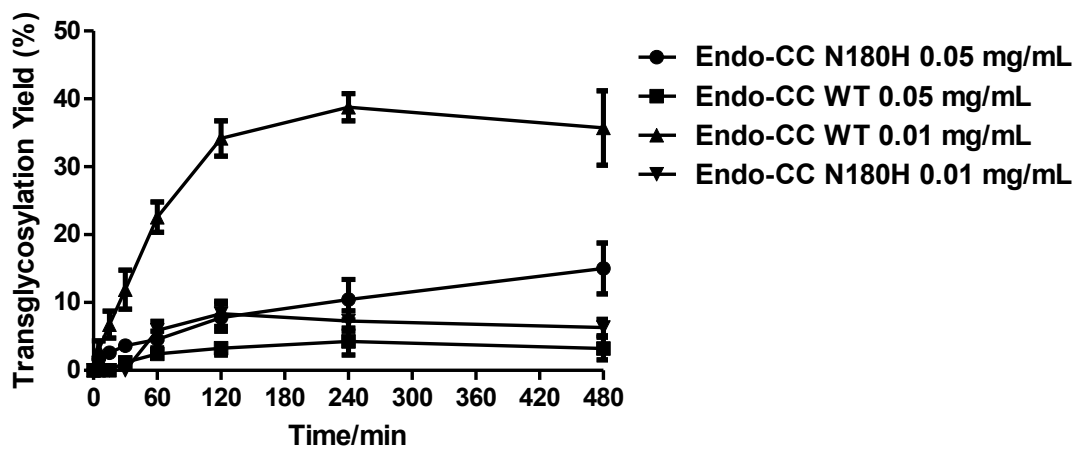


Figure 46. Transglycosylation reactions for deglycosylated antibody by Endo-CC and Endo-CC N180H enzymes at varied concentrations. The reactions were performed by adding 20 molar equivalents of SCT-Oxa to the deglycosylated trastuzumab (10 mg/mL) in the presence of 0.01 mg/mL and 0.05 mg/mL Endo-CC or Endo-CC N180H at 30 °C in 100 mM Tris-HCl at pH 7.4. The experimental data presented here are representative of three independent sets of experiments.

### **C. Conclusion**

The substrate specificity of Endo-CC and mutants for hydrolysis and transglycosylation was re-evaluated in this work. The substrate requirement of Endo-CC for the glycan composition was determined that it could not recognize the core-fucosylated glycoproteins and glycopeptides for glycan hydrolysis. Furthermore, the transglycosylation experiments demonstrated that, besides complex N-glycans, the high-mannose and hybrid type glycan oxazolines could also serve as donor substrates for glycosynthase mutants of Endo-CC for transglycosylation. Finally, based on the previous mutagenesis studies, selected Endo-CC mutants, including N180H, N180Q, N180E, N180A and N180M, were tested for their transglycosylation activities. The functional assays revealed that all these mutants exhibited different but significant levels of abilities to transfer complex type oxazolines to the glycopeptide acceptor. In particular, Endo-CC N180A mutant exhibited highly persistent transfer activity over time in contrast to the other mutants. Moreover, the enzyme and its transfer mutants have been overexpressed with a good yield in *E. coli* as a CPD fusion protein. This study re-visits the substrate selectivity of Endo-CC and its mutants and provides important functional information for future work involving applications of Endo-CC for glycoengineering of various target glycopeptides and glycoproteins.

## D. Materials and Methods

### 1. Chemical and biochemical materials

All reagents, chemicals, and solvents used in this work were purchased from Sigma-Aldrich unless otherwise stated. Monoclonal antibody rituximab was purchased from Premium Health Services Inc. (Columbia, MD). The sialylated complex type glycan oxazoline (SCT-Oxa) was prepared as described in the previously published protocol.<sup>92</sup> The hybrid type (Hyb) glycan was synthesized by sequential glycosylation reaction on a Man5GlcNAc intermediate using enzymes including  $\alpha$ 1,2-GlcNAc transferase (GnT1),  $\alpha$ 1,4-galactosyltransferase and  $\alpha$ 2,6-sialyltransferase.<sup>127</sup> The details concerning the synthetic method are summarized elsewhere. The high-mannose type (HM) glycan was extracted from soybean flour based on a previously described method. All glycan oxazolines were synthesized according to the previously detailed one-pot conversion strategy.<sup>121</sup> The endoglycosidase Endo-S2 used for deglycosylation was expressed and purified following our previous publication<sup>123</sup>. Analytical reverse-phase high-performance liquid chromatography (HPLC) was conducted using a Waters 626 HPLC instrument connected with an XBridge BEH130 C18 column (3.5  $\mu$ m, 4.6  $\times$  250 mm). The elution of glycopeptide was achieved using a linear gradient of acetonitrile (0–30%, v/v) in water containing TFA (0.1%) in 35 min at a flow rate of 0.5 mL/min under UV wavelength at 214 nm. The high-performance anion-exchange chromatography with pulsed amperometric detection (HPAEC-PAD) was performed on a Dionex ICS-5000 chromatography system (Fischer Scientific) connected to an electrochemical detector (ED50) and an anion exchange column (CarboPac PA10 4  $\times$  250 mm). The

elution on the PA10 column was achieved by a constant solvent containing 100 mM NaOH in water with a flow rate of 1.0 mL/min. Liquid chromatography-electrospray mass spectrometry (LC-ESI-MS) was used to characterize glycoproteins including ribonuclease B and antibody rituximab. MS analysis was conducted using an Exactive Plus Orbitrap Mass Spectrometer (Thermo Scientific) and a C18 column (proZap Expedite MS C18, 2.1 × 10 mm, 1.5 μm, P.J. Cobert Associates, Inc.) for analysis of glycopeptides, a C8 column (Poroshell 300SB-C8, 1.0 × 75 mm, 5 μm, Agilent) for glycoproteins such as RNase B (RNase B) and EPO, and an C-4 column (XBridge BEH300 C4, 2.1 × 50 mm, 3.5 μm, Waters) for antibody analysis.

## 2. Mutagenesis, expression, and purification of recombinant Endo-CC

The plasmid DNA encoding recombinant Endo-CC from *Coprinopsis cinerea* was synthesized (GenScript) and cloned into pET-41b (+) vector, which contains a 7 histidine tag at C terminus. For site-directed mutagenesis at Asn-180 residue (N180H, N180Q, N180A, N180E, and N180M), a forward primer, 5'-TTGGCTGCTC NNGTTGAGATTG-3', and a reverse primer, 5'-CCATCGAATCCACGCTCG-3' were used. The site-directed mutagenesis was conducted using a Q5 Site-Directed Mutagenesis Kit (NEB, Inc.) Selected mutations were confirmed by DNA sequencing (Macrogen, MD). The plasmid was then transformed into *E. Coli* BL21 competent cell (DE3), and a 20 mL LB preculture was inoculated by the transformant containing 100 μg/mL of carbenicillin. The preculture was incubated 37°C for 12 h before inoculated into a 1L of LB and cultured at 30°C for another 12 h. The cells were harvested by centrifugation at 8000 x g for 20 min at 4°C, and the pelleted cells were lysed in 20 mL Bacterial Lysis Buffer (Gold Biotechnology, Inc.) following the

manufacturer's instructions. The His-tagged protein was purified from the centrifuged supernatant using HisTrap HP column (GE Healthcare) following the manufacturer's protocol. The resultant Endo-CC was buffer-exchanged into 1x PBS (pH 7.4) using dialysis tubing (Sigma). The purity of the protein was confirmed by SDS-PAGE and the concentration was estimated on a Nanodrop 2000c instrument at the absorbance 280 nm.

### 3. Transglycosylation using wild-type Endo-CC and its mutants

The transglycosylation reactions catalyzed by each of the wild-type Endo-CC and mutants (0.125 mg/mL) was conducted in 50 mM Tris-HCl buffer (pH 7.4, 50  $\mu$ L) at 30 °C using the synthetic CD52-GlcNAc peptide (2 mg/mL) as the starting material. Each reaction was initiated by adding 5 molar equivalents of SCT-Oxa, and the reaction was sampled at 0, 5, 15, 30, 60, 120, 240, 480, 1080 and 1440 min. For each time point, an aliquot of reaction mixture was quenched in 0.1% formic acid and frozen at – 20 °C. To monitor the reaction in a quantitative manner, each reaction mixture was subject to reverse phase HPLC for separation and MS for mass confirmation, and the transglycosylation yield was calculated from the integrated data.

### 4. Transglycosylation by Endo-CC N180H with different N-glycan oxazolines

Comparative studies on the transglycosylation efficiency of Endo-CC N180H against three major types of N-glycan oxazolines were carried out at 30 °C in Tris-HCl buffer at pH 7.4. The synthetic glycopeptide CD52-GlcNAc (5 mg/mL) was incubated with 7.5 equivalents of each of the glycan oxazolines. The concentration of

Endo-CC N180H was 0.125 mg/mL. The reactions were sampled at 0, 30, 60, 120, 240 and 480 min, and the quenched reaction was separated by reverse phase HPLC followed by MS analysis.

#### 5. Enzymatic deglycosylation of ribonuclease B

The mutant enzyme Endo-CC N180H (0.1mg/mL) was incubated with 10 mg/mL of the native ribonuclease B protein at 37 °C in PBS buffer at pH 7.4. After 2 hours of incubation, the enzyme-treated RNase B was subject to LC-ESI-MS analysis and the resultant mass spectrum was presented after deconvolution in Results.

#### 6. Enzymatic deglycosylation of sialylglycopeptide with and without core fucose

The native sialylglycopeptide (SGP) was extracted from egg yolk power as described in the previous publication. The fucosylated form of SGP was synthesized by an  $\alpha$ 1,6-fucosidase mutant from *L.casei* (AlfC). The details of the synthesis were reported in the previous report.<sup>147</sup> During deglycosylation process, an equal amount of SGP (+/- core fucose, 50 mg/mL) was incubated with a relatively small amount of Endo-CC (0.1 mg/mL) at 37 °C in PBS buffer at pH 7.4. The progress of hydrolysis was monitored by the high-performance anion-exchange chromatography coupled with pulsed electrochemical detection (HPAEC-PAD). A major shift of the peak representing the starting material (SGP) was detected after 4 hours of incubation, and a new glycan peak characteristic of the hydrolyzed SCT free glycan was observed for the non-fucosylated SGP, but not the fucosylated SGP.

7. Differential deglycosylation of erythropoietin (EPO) containing a mixture of core-fucosylated and non-fucosylated N-glycans.

It has been reported that the core-fucosylated GlcNAc-EPO intermediate can be produced using a HEK293S GnT I knockout and FUT8 overexpressing cell line.<sup>146</sup> Using this intermediate, a sialylated glycoform of EPO containing a mixture of fucosylated and non-fucosylated HM glycans was prepared to test the substrate specificity of Endo-CC. A final concentration of 0.5 mg/mL EPO was treated by 0.01 mg/mL recombinant Endo-CC. At  $t = 2$  h, the reaction was quenched and injected to LC-ESI-MS for characterization.

8. Differential deglycosylation of antibody glycoforms with core-fucosylated, non-fucosylated complex type, and high-mannose N-glycans.

Previous glycan analysis of commercial IgG antibodies has demonstrated that nearly all N-glycoforms of rituximab are core-fucosylated. The homogeneous non-fucosylated  $S_2G_2$  and HM rituximab glycoforms were generated based on a previously published protocol.<sup>139</sup> For all three types of rituximab glycoforms, a final concentration of 5 mg/mL antibody was incubated with 0.05 mg/mL Endo-CC in PBS buffer (pH 7.4) at 37 °C overnight. The glycosylation patterns of the resultant rituximab were analyzed by LC-ESI-MS.

**9. Differential transglycosylation of deglycosylated antibody by wild-type Endo-CC and Endo-CC N180H**

The transglycosylation activity of Endo-CC and its mutant Endo-CC N180H at different concentrations was measured by incubating the deglycosylated rituximab (10.0 mg/mL, 69  $\mu$ M) and the complex-type glycan oxazoline SCT-Oxa (1.38 mM, 20 equivalents) in 50 mM Tris-HCl (pH 7.4, 20  $\mu$ L) at 30 °C. The concentration of the wild-type Endo-CC was fixed at 0.01 mg/mL and 0.05 mg/mL. The concentration of the mutant Endo-CC N180H was 0.05 mg/mL. The reaction was sampled at 0, 5, 15, 30, 60, 120, 240, and 480 min. For each sampled reaction mixture, an aliquot was quenched in 0.1% formic acid and subject to LC-ESI-MS analysis. To monitor the transglycosylation reaction in a quantitative manner, the reaction yield was estimated by LC-MS using an internal standard and a single-point normalization factor. SDS-PAGE densitometry data were also obtained to support the reaction progression by the relative intensity of peaks.

### **E. Supporting Information**

MPIAGKKFHPRALPEFWRTFREMDEWRATQTGPQARPAEGILKYVPRKIRPA  
DIAGKGRLLVSHDYKGGYVEDPFSKSYSFNWWFSTDSFNYFAHHRITIPPE  
WINAAHRQGVPI LGTIIFEGGSDEDILRMVIGKTPGSTSNFHAERNAEYTPVVS  
SYAELFADLAVERGFDGWLLNVEIGLQGGSEQARGLAAWVALLQQEVLK  
KVGPHGLVIWYDSVTVRGDLWWQDRLNAFNLPFFLNSSGIFTNYWWYNDA  
PQKQIDFLSRVDPNLTGQTAEPHQYNLQKTIQDIYIGVDVWGRGSHGGGGFG  
AYKAIEHADPKGLGFSVALFAQGWTWETEEKPGWNWAQFWDYDSKLWV  
GPPGVVEAPDHTVKPGEYPCVHGPFQPISSFFLTYPDPDLDPFYTNFCPGIG  
DAWFVEGKEVFRSETGWTMDKQTTVGDLVWPRPKIYDLPSQNASQATLN  
AAFNFNDAWNGGNSLQINLTVPGGATTYGAYWVPIQTFTFSSRRQYEASIVY  
KPGLSGKTRFDAKYEVGIRTITGEDQGKIISNTTTEVGNGWRKVHILFEIETPV  
EGGSIIVPSSIGLVIAVSNVSTTEQFEFPFLVGQITIHPHLPDRYKEFKPALLWLL  
FTPSAGTNSLDGTLTWDVVA AIERPPPVEINNPDDAQIPWNLQPTKQEWFPDF  
LYFNVYVLELLDGGGQGPQWIGTTGYDGEKKRFFIYDESLPPTSGLRRFTFQ  
IEGVLETGESTHWYDAPAAPSATAGGEQKRTRRTSLKSVLSPLRRKKS KGDIS  
VAK

Supplementary Figure 3: amino acid sequence of Endo-CC1 (XP\_001839402).

## Chapter 5: Glycosylation remodeling of IgE antibody and effects of Fc N-glycans on FcεR binding

### A. Introduction

Although immunoglobulin E (IgE) represents the least abundant class of antibody found in human circulation,<sup>148</sup> it provides an important immune defense mechanism against venom toxins and parasites.<sup>149</sup> IgE is also the major antibody responsible for mediating various atopic and allergic disorders such as asthma and hayfever.<sup>150</sup> The effector functions of IgE to activate allergic responses have attracted tremendous attention due to an increasing global onset of asthma and chronic allergies in childhood and adults.<sup>151</sup> More recently, the unique immunoregulatory properties of IgE allowed development of novel IgE-based therapeutic interventions against cancers and other disease targets of interest. A first-in-class anticancer therapeutic IgE antibody called MOv18 was administered to patients with advanced solid tumors in a phase I clinic trial for the first time.<sup>152</sup>

The effector functions of IgE are mainly dependent on interactions with two principle IgE-Fc receptors (FcεRs), which include the high-affinity FcεRI and the low-affinity FcεRII/CD23.<sup>153</sup> Compared with other antibodies and related receptors, IgE exhibited a remarkably high affinity for FcεRI ( $K_D \sim 0.1-1$  nM). Thus, the majority of IgE is constantly bound to the surface of mast cells and basophiles, and a minimal amount of allergen is sufficient to initiate an acute hypersensitivity response by cross-linking the IgE-bound FcεRIs and subsequently triggering cell degranulation.<sup>18</sup> Although the affinity of IgE for the monomeric CD23 receptor ( $K_D \sim$

1.0 - 10  $\mu$ M) is significantly lower than that for the high-affinity Fc $\epsilon$ RI, a high avidity can be achieved between IgE-Fc and trimeric CD23 via multivalent interactions.<sup>154</sup> CD23 is involved in allergen presentation and transport of the IgE-captured allergen complexes, and functional interplay between IgE and CD23 on B cells plays an important role in regulating IgE homeostasis in mammalian systems.<sup>154-156</sup>

Among all antibody isotypes, IgE is the most heavily glycosylated with seven potential N-glycosylation sites located in the heavy chain, and there is a considerable level of heterogeneity in the N-glycosylation patterns of IgE in terms of both the occupancy of the glycosylation sites and the specific glycan compositions.<sup>50, 53, 157</sup> Among the potential glycosylation sites of IgE, the Asn-394 site is highly conserved and is structurally homologous to the Asn-297 residue of IgG antibodies.<sup>158</sup> Unlike other glycosylation sites located in the C $\epsilon$ 2 and C $\epsilon$ 3 domains, which all contain complex type N-glycans, a unique oligomannose N-glycan is associated with the Asn-394 residue in the IgE Fc fragment (Figure 46). Structural analysis on IgE-Fc homodimers suggest that these heterogeneous high-mannose glycans at Asn-394 are involved in extensive non-covalent interactions with the C $\epsilon$ 3 and C $\epsilon$ 4 domains and may stabilize the two heavy chains by making contacts with each other.<sup>159-161</sup> In contrast to IgG in which the complex N-glycan at Asn-294 is critical for binding to Fc $\gamma$ Rs and biological functions,<sup>25</sup> it is less clear whether the N-glycosylation of IgE affects its binding activity towards the Fc $\epsilon$ RI and CD23 receptors. Previous studies indicated that the non-glycosylated IgE-Fc fragments produced from bacterial and mammalian systems were able to bind IgE receptors with comparable affinities to the native IgE-Fc.<sup>162, 163</sup> However, a recent study demonstrated that the single

oligomannose N-glycan at Asn-394 is indispensable for IgE to elicit its biological activities in mediating anaphylaxis *in vitro* and *in vivo*.<sup>113</sup>

To improve our understanding about the effect of N-glycosylation on IgE biology, we here describe a combined chemoenzymatic strategy to remodel the N-glycosylation profile of IgE and the IgE-Fc fragment in a site-specific manner. For full-length IgE antibody, the oligomannose N-glycans were removed by Endo-H, an endoglycosidase that specifically releases the mannose-rich N-glycans but does not alter the fucosylated complex type glycan structures. Thus, other complex type N-glycans remained unaffected and analysis on this partially deglycosylated IgE revealed a 2-4-fold reduction in binding affinity to the high-affinity IgE-Fc receptor FcεRI, which may lead to more significant impact on the biological functions of IgE *in vivo*.

According to the previous studies on IgE glycosylation, only the Asn-394 N-glycan of IgE was found to be necessary for receptor binding and biological functions.<sup>113</sup> Therefore, we generated a mutant IgE-Fc that lacks all N-glycosylation sites except for Asn-394 by the site-directed mutagenesis. This IgE-Fc variant known as IgE-Fc-Asn394only was then expressed in mammalian cells and the binding assays confirmed that the intact IgE and IgE-Fc-Asn394only exhibited similar levels of binding affinity for the immobilized FcεRI. Using this IgE-Fc variant as a model protein, we applied a combined method of mammalian expression and enzymatic modifications to generate a panel of IgE-Fc N-glycoforms and analyzed their binding affinities to FcεRI and CD23. The results clearly suggested that the deglycosylated IgE-Fc fragment showed a 4-fold reduction in its binding affinity to FcεRI, whereas

other oligomannose IgE-Fc glycoforms retained the same affinities as the native IgE-Fc glycoform. Similarly, the IgE-Fc/CD23 interactions were also affected by the glycoengineering, and, like FcεRI, a 2-3-fold decrease of IgE-Fc binding to CD23 was observed upon the removal of the Asn-394 N-glycans. Finally, following a highly efficient chemoenzymatic glycan remodeling strategy developed by Wang and others,<sup>103</sup> a complex N-glycan was transferred to the Asn-394 residue of IgE-Fc using IgE-Fc-Asn394only-GlcNAc as glycosyl acceptor and chemically activated glycosyl oxazoline (G2-CT-Oxa) as the donor substrate. The effective transglycosylation was catalyzed by a recently reported glycosynthase mutant Endo-CC N180H.<sup>105</sup> The successful glycosylation of a complex glycan to IgE altered its binding properties to the high-affinity receptor FcεRI, and this study clearly demonstrated the possibility of further glycosylation remodeling of IgE antibody with additional natural or artificial N-glycan structures for future structural and functional studies.

The development of mammalian expression system for IgE-Fc glycoforms was assisted by Dr. Qiang Yang from Prof. Lai-Xi's group at the Department of Chemistry and Biochemistry, University of Maryland, College Park. The enzymatic treatments of IgE-Fc N-glycoforms by multiple mannosidases were conducted by Xin Tong and Dr. Yang together. The mass spectrometry analysis of the released N-glycans from IgE-Fc N-glycoforms was assisted by Dr. Zong and other co-authors involved in this study.

## B. Results and Discussion

### 1. Selective glycosylation remodeling of commercial and recombinant full-length IgE antibodies and binding analyses on the product IgE N-glycoforms

The full-length human IgE contains seven conserved N-glycosylation sites in its primary sequence.<sup>50</sup> Among all potential sites, only the Asn-394 site is exclusively glycosylated with the oligomannose N-glycans, whereas other sites can be either unoccupied or associated exclusively with the complex type oligosaccharides.<sup>157</sup> Interestingly, this unique oligomannose glycan in the Cε3 domain of IgE was found by Shade and colleagues to be obligatory for FcεRI receptor binding and the ability of IgE to promote anaphylaxis.<sup>113</sup> However, in this study, binding between IgE and FcεRI was analyzed in a cell-based functional assay using the fluorescence-activated cell sorting technique (FACS), and information regarding the *in vitro* binding kinetics of the glycoengineered full-length IgE antibodies with FcεRI is lacking.

To evaluate the functional effects of the previously studied N-glycans at the Asn-394 site, we first performed site-specific deglycosylation at Asn-394 of two full-length IgE antibodies, a commercially available human IgE (Abcam-hIgE, Abcam, UK) and a recombinant ovalbumin (OVA)-specific human IgE antibody (OVA-hIgE). Ovalbumin is a well-established model allergen extracted from chicken eggs and has been frequently used to artificially induce the acute IgE-mediated pulmonary allergic response in experimental animals.<sup>153</sup> The biological activity of the anti-OVA IgE to induce asthma are often studied using the OVA challenge model system.<sup>164</sup> To selectively remove this oligomannose glycan from IgE without affecting the other complex N-glycans, the antibodies were treated with Endo-H, an endoglycosidase

that specifically cleaves between the two GlcNAc residues in the diacetylchitobiose core of the high-mannose and hybrid N-linked oligosaccharides with no hydrolytic activities against the bystander complex N-glycans.<sup>165</sup> Treatment of the intact IgE antibodies by Endo-H led to the release of the oligomannose N-glycans from IgE antibodies, as confirmed by sodium dodecyl sulfate polyacrylamide gel electrophoresis (SDS-PAGE) analysis (Figure 47).

To assess the change in the binding affinity between IgE-Fc and FcεRI caused by partial deglycosylation, we covalently immobilized the soluble domain of the high-affinity IgE receptor (FcεRIa) on a standard CM5 sensor chip, and then injected the site-selectively deglycosylated IgE antibodies through the channel to monitor the specific binding events between IgE and FcεRIa using the Surface Plasmon Resonance (SPR) technique (Figure 48). As illustrated in Figure 48 and Table 8, for both the commercial and recombinant IgE antibodies, a roughly 4-fold reduction in binding affinity to the high-affinity receptor FcεRI was observed after the oligomannose N-glycan was removed. In addition, all antibodies displayed binding affinities within the nM range to FcεRI, which were consistent with the previous reported affinities of both the full-length IgE antibodies and IgE-Fc fragments to the high-affinity receptor.<sup>166</sup>

In the previous study by Shade and others, the human IgE was treated with an alternative endoglycosidase F1 (EndoF1) that selectively removes the oligomannose N-glycans without affecting the other complex N-glycans.<sup>113</sup> Their results indicated that Endo-F1 treatment abolished the IgE interactions with FcεRI in cell-based assays using flow cytometry and saturation binding analysis. Comparing the two studies, it

remains unclear why selective removal of the oligomannose N-glycan by Endo-H showed a less dramatic impact on FcεRI binding in our *in vitro* experiments in comparison with those shown in the previous cell-based assays. It is worth noting that, in the previous publication, the IgE antibodies were treated with Endo-F1 at 37 °C for 72 hours prior to the cell-based binding assays. Whether a prolonged incubation of IgE at certain temperature could cause instability of antibody and loss of binding activity remains a question to be answered.

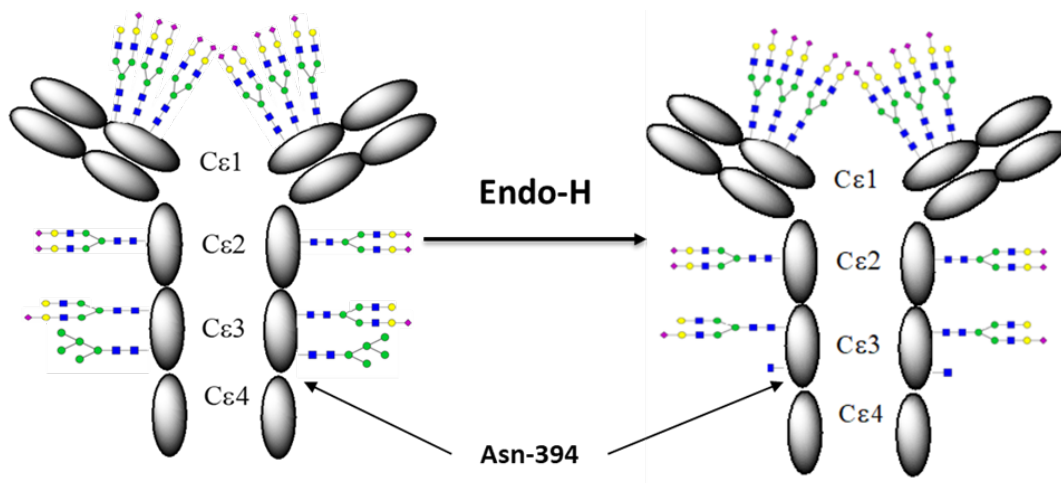


Figure 47. Site-selective N-glycosylation remodeling of full-length human IgE antibodies using endoglycosidase Endo-H. The oligosaccharide composition of all occupied N-glycosylation sites are based on the previously published site-specific glycosylation analysis on IgE antibodies.<sup>50</sup> Only the previously described Asn-394 site contains an oligomannose N-glycan, whereas all the other N-linked carbohydrate chains attached to IgE are complex type N-glycans. The position of the key N-glycosylation site Asn-394 was highlighted.

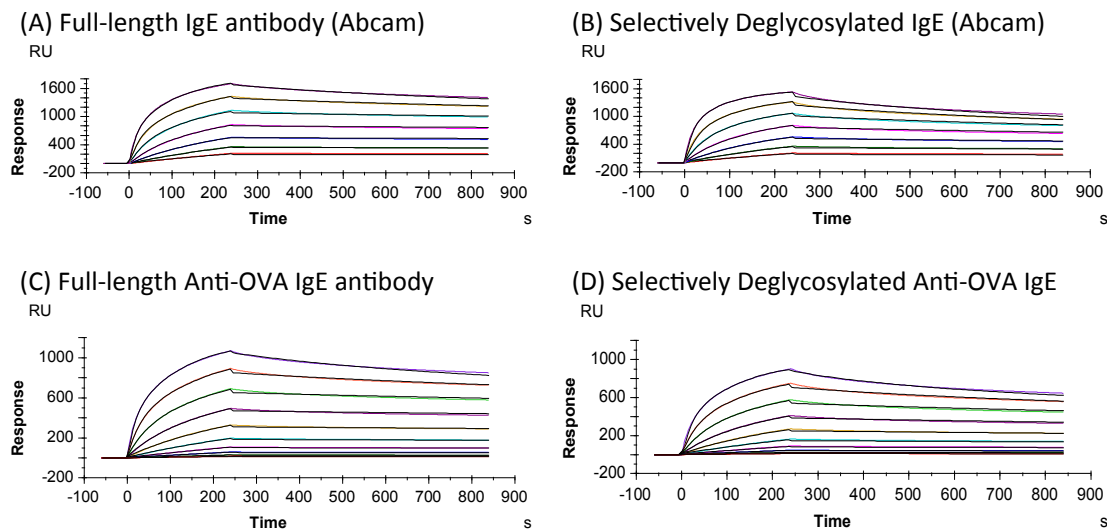


Figure 48. Surface plasmon resonance (SPR) representative sensorgrams of binding between full-length IgE antibodies and immobilized soluble domain of high-affinity IgE receptor  $Fc\epsilon RI$ , (A) commercial IgE (Abcam, UK) and (B) selectively deglycosylated commercial IgE (IgE-Asn394-GlcNAc) (C) recombinant anti-OVA IgE, and (D) selectively deglycosylated recombinant anti-OVA IgE (IgE-Asn394-GlcNAc). Eight concentrations of IgE antibodies (400 – 3.125 nM) were tested in the standard SPR buffer, and a global monovalent fitting was applied to determine the kinetic parameters shown in Table 8.

Table 8. Kinetic parameters and binding affinities of commercial IgE antibody and recombinant anti-OVA IgE binding to the immobilized FcεRIα obtained from SPR analysis<sup>a</sup>

Native Full-length IgE	$k_a$ (1/Ms)	$k_d$ (1/s)	$K_D$ (M) <sup>b</sup>
IgE (Abcam)	$(1.35 \pm 0.07) \times 10^{+5}$	$(2.41 \pm 0.02) \times 10^{-4}$	$(1.78 \pm 0.21) \times 10^{-9}$
IgE-Asn394-GlcNAc <sup>c</sup>	$(0.78 \pm 0.05) \times 10^{+5}$	$(5.13 \pm 0.04) \times 10^{-4}$	$(7.81 \pm 0.17) \times 10^{-9}$
Anti-OVA IgE	$(1.20 \pm 0.04) \times 10^{+5}$	$(2.96 \pm 0.01) \times 10^{-4}$	$(2.46 \pm 0.32) \times 10^{-9}$
IgE-Asn394-GlcNAc <sup>d</sup>	$(0.91 \pm 0.01) \times 10^{+5}$	$(8.71 \pm 0.02) \times 10^{-4}$	$(9.57 \pm 0.09) \times 10^{-9}$

<sup>a</sup>Kinetics for binding between native IgE antibodies and FcεRIα were measured in Standard SPR buffer at 20 °C and the obtained data were analyzed using global monovalent fitting model (BiaEvaluation). The parameters are average ± SD of experiments conducted in triplicate. The binding activity of the immobilized FcεRIα was confirmed by standard IgE binding assay prior to each of the repeated binding experiments to ensure that the CM5 chip-immobilized FcεRIα did not lose activity during storage.

<sup>b</sup>The dissociation constant  $K_D$  was deduced as  $(k_d/k_a)$ .

IgE-Asn-394-GlcNAc<sup>c</sup> represents the selectively deglycosylated full-length IgE N-glycoform generated from the commercial human native IgE (Abcam, UK), where only the oligomannose N-glycan at Asn-394 was removed by Endo-H treatment.

IgE-Asn-394-GlcNAc<sup>d</sup> is the selectively deglycosylated full-length IgE N-glycoform derived from the recombinant anti-OVA IgE antibody, and the Asn-394 site contains only the innermost GlcNAc residue after the Endo-H-mediated hydrolysis.

2. Generation of mutant IgE-Fc containing only one oligomannose glycosylation site at Asn-394 with comparable FcεRI-binding capacity to full-length IgE antibodies.

The ability of IgE to mediate allergic responses are primarily regulated through interactions with IgE receptors FcεRI and FcεRII/CD23.<sup>150</sup> Structural studies and functional assays revealed that the Fc (crystallizable) domain of IgE consisting of Cε2, Cε3, and Cε4 domains alone was sufficient to bind both IgE receptors with comparable affinities as full-length IgE antibodies.<sup>51</sup> Furthermore, as described in a previous publication,<sup>113</sup> only a single glycan at Asn-394 in the Cε3 domain of IgE-Fc was required for IgE to interact with FcεRI and to promote allergic reactions.<sup>113</sup> Based on these studies, we designed a construct of the IgE-Fc fragment selectively lacking all the conserved N-glycosylation sites except for Asn-394 by mutating asparagine (N) to glutamine (Q). This unique human IgE-Fc fragment (IgE-Fc-Asn394only) was successfully expressed in HEK294 cell with only one glycosylation site preserved at the Asn394 residue of the Cε3 domain. Mass spectrometry analysis on released glycans from this IgE-Fc antibody fragment confirmed that the majority of the N-linked glycans found were oligomannose oligosaccharides containing five (-Man<sub>5</sub>, majority) to nine (-Man<sub>9</sub>, minority) mannose residues (Figure 50A), which was consistent with reported site-specific analysis of human IgE N-glycosylation.<sup>50</sup> After confirming that this IgE-Fc variant (IgE-Fc-Asn394only-HM) bound to FcεRI with similar kinetics and affinities to full-length IgE antibodies (Table 9), we used this IgE-Fc-Asn394only N-glycoform as starting material for further glycoengineering to study the impact of N-glycosylation remodeling on IgE binding with both the high-affinity IgE receptor FcεRI and the low-affinity IgE receptor FcεRII/CD23.

3. Generation of homogeneous IgE-Fc oligomannose glycoforms using enzymatic modifications and biosynthetic engineering and their binding properties to FcεRI.

To further dissect the functional role of oligosaccharide compositions at Asn-394 of IgE-Fc, a panel of IgE-Fc-Asn394only N-glycoforms were generated through enzymatic modifications and biosynthetic inhibitor (Figure 49). The identity of the modified N-glycan associated with each IgE-Fc glycoform was confirmed by matrix-assisted laser desorption/ionization time-of-flight (MALDI-TOF) mass spectrometry analysis on the released glycans from IgE after treatment with amidase enzyme peptide-N-glycosidase F (PNGase F).

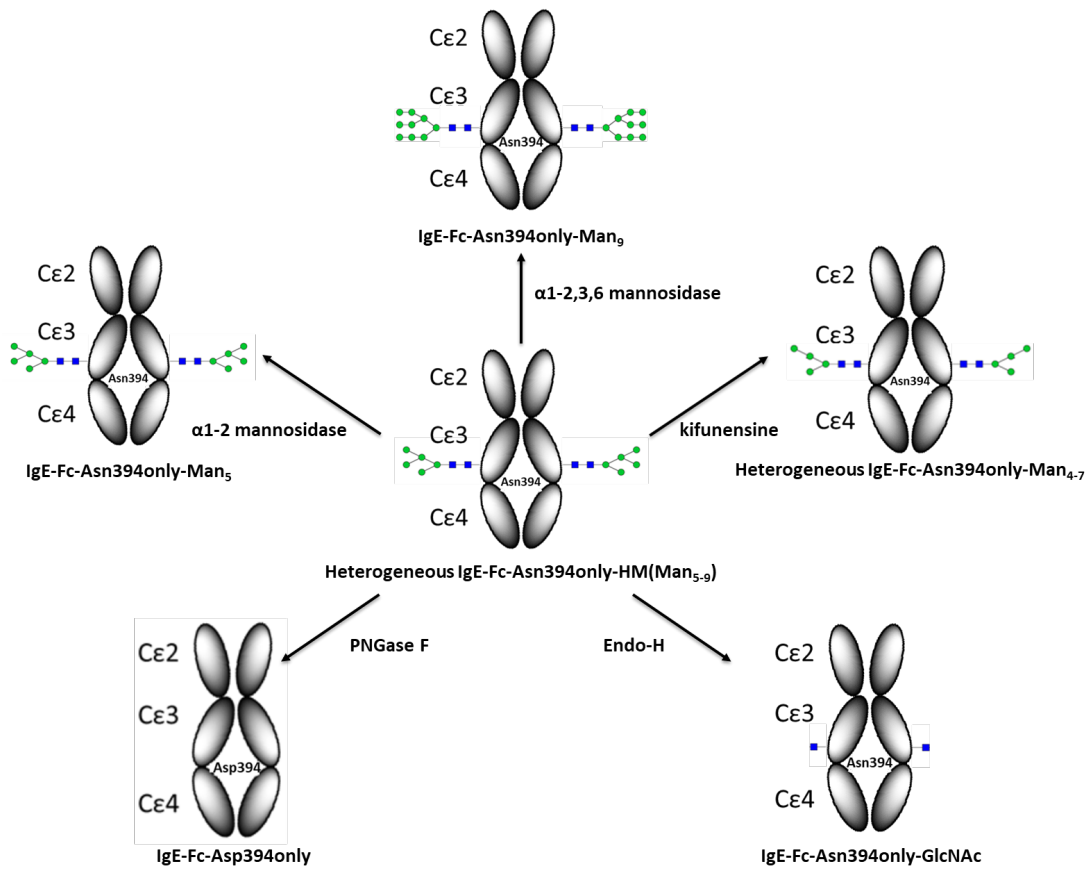


Figure 49. Glycan remodeling of heterogeneous high-mannose N-glycoforms of IgE-Fc-Asn394only-HM (Man<sub>5-9</sub>) using a combination of glycan remodeling strategies, including  $\alpha$ 1-2 and  $\alpha$ 1-2, 3, 6 mannosidases, endoglycosidase (Endo-H), peptide-N-glycosidase (PNGase F), and biosynthetic N-glycan inhibitor kifunensine. For the N-glycoforms that contain a mixture of glycans such as IgE-Fc-Asn394only-HM and IgE-Fc-Asn394only-Man<sub>4-7</sub>, only the most abundant species is illustrated here.

### 3.1. Deglycosylation of IgE-Fc-Asn394only-HM N-glycoform by Endo-H reduced the Fc $\epsilon$ RI-binding affinity to the same extent as for full-length IgE antibodies

As demonstrated on the full-length IgE antibodies, the IgE-Fc-Asn394only-HM N-glycoform was treated with the high-mannose-specific Endo-H to remove the native oligomannose glycans to afford deglycosylated IgE-Fc-Asn394only-GlcNAc N-glycoform, which was subsequently tested for its binding affinity to Fc $\epsilon$ RI using the same conditions as in the previous binding studies. Interestingly, for the high-affinity IgE receptor Fc $\epsilon$ RI, the binding kinetics of IgE-Fc-Asn394only-HM and IgE-Fc-Asn394only-GlcNAc displayed the same patterns as for the full-length glycoforms (Table 8 and Table 9), where the removal of the high-mannose N-glycans caused an approximately 4-fold reduction in binding affinity to Fc $\epsilon$ RI. In addition, binding of IgE-Fc-Asn394only-HM were shown to be comparable to full-length IgE antibodies, which confirmed that IgE-Fc carrying only a single N-glycan at Asn-397 was sufficient to provide high-affinity binding to Fc $\epsilon$ RI. Therefore, it would be plausible to use our mutant IgE-Fc fragment as model protein for following glycoengineering and functional studies.

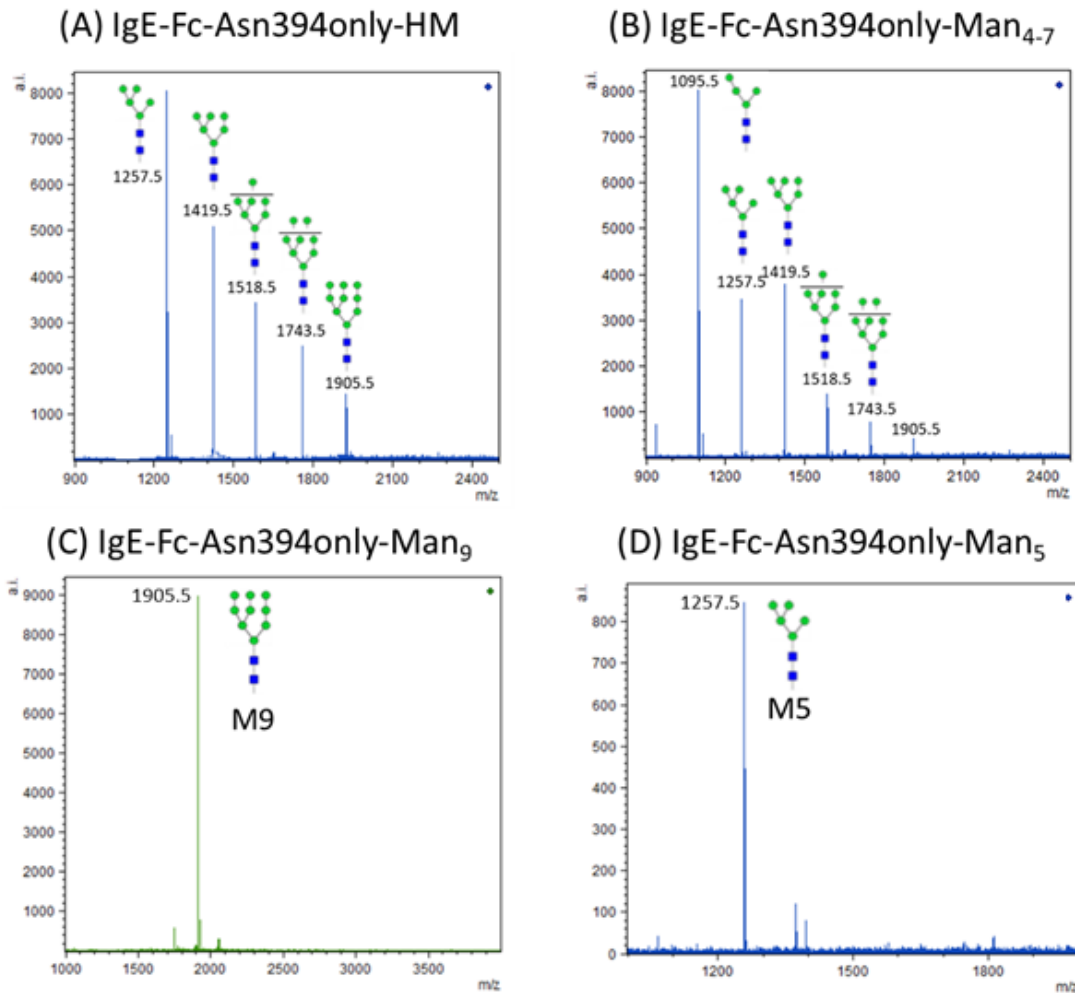


Figure 50. MALDI-TOF mass spectrometry identification of the released N-glycans from the IgE-Fc-Asn394only N-glycoforms generated through glycan remodeling: (A) IgE-Fc-Asn394only-HM produced under native expression conditions in HEK 293T cell line; (B) IgE-Fc-Asn394only-Man<sub>4-7</sub> generated by the  $\alpha$ 1-2, 3, 6 mannosidase processing; (C) IgE-Fc-Asn394only-Man<sub>9</sub> expressed under the effect of 40  $\mu$ M of kifunensine in HEK 293T; (D) IgE-Fc-Asn394only-Man<sub>5</sub> generated by the  $\alpha$ 1-2 mannosidase treatment.

### 3.2. Biosynthetic glycoengineering of IgE-Fc-Asn394only-HM glycoform to generate homogeneous IgE-Fc-Asn394only-Man<sub>9</sub>.

In parallel to enzymatic modification, the IgE-Fc-Asn394only fragment was expressed in a HEK293-derived cell line in the presence of mannosidase inhibitor kifunensine to minimize the processing of oligomannose N-glycans, which gave rise to a homogeneous high-mannose N-glycoform containing a total of nine mannose residues, IgE-Fc-Asn394only-Man<sub>9</sub>. Kifunensine is a monosaccharide-based inhibitor derived from plant alkaloid. This mannose analogue serves as a competitive inhibitor for Type-1 endoplasmic reticulum (ER) and Golgi  $\alpha$ -mannosidases during early stage of N-glycan biosynthesis and it can effectively disrupt the normal processing of Man<sub>9</sub>GlcNAc<sub>2</sub> intermediate to Man<sub>5</sub>GlcNAc<sub>2</sub>.<sup>146</sup> As a result, a high concentration of kifunensine could efficiently control the processing of N-glycans during biosynthesis and produce recombinant glycoproteins with homogeneous high-mannose N-glycans. Indeed, MALDI-TOF analysis revealed a single peak on mass spectrum corresponding to the Man<sub>9</sub>GlcNAc<sub>2</sub> glycan (Figure 50C). Binding analysis further confirmed that the affinities of IgE-Fc-Asn394only-Man<sub>9</sub> ( $K_D = 2.13 \pm 0.09$  nM) and IgE-Fc-Asn394only-HM ( $K_D = 2.41 \pm 0.12$  nM) to Fc $\epsilon$ RI were nearly identical, which suggested that addition of mannose residues to the native high-mannose N-glycans (Man<sub>5</sub>GlcNAc<sub>2</sub> as the major N-glycoform) did not significantly alter the binding affinity between IgE-Fc and Fc $\epsilon$ RI.

### 3.3. Enzymatic modifications on IgE-Fc-Asn394only-HM to generate additional IgE-Fc-Asn394only N-glycoforms.

In order to remove the mannose residues off the IgE-Fc-Asn394only-HM N-glycoform and to afford the homogeneous Man<sub>5</sub>GlcNAc<sub>2</sub> N-glycan, the expressed IgE-Fc fragment was treated with  $\alpha$ 1-2 mannosidase to remove all  $\alpha$ 1-2 linked mannoses from the high-mannose N-glycans without affecting the  $\alpha$ 1-3 and  $\alpha$ 1-6 linked mannoses, as shown in Figure 51. The glycan analysis confirmed that the released N-glycan from the resultant IgE-Fc-Asn394only-Man<sub>5</sub> glycoform displayed the expected mass values according to the MALDI-TOF analysis (Figure 50D).

To further trim IgE-Fc-Asn394only-Man<sub>5</sub> to paucimannose N-glycoforms, which contain mainly Man<sub>3-4</sub>GlcNAc<sub>2</sub> N-glycans, the starting Man<sub>5</sub> N-glycoform was incubated with an alternative  $\alpha$ 1-2, 3, 6 mannosidase harvested from the Jack Bean (*Canavalia ensiformis*) seeds, which possesses a broad substrate selectivity than the  $\alpha$ 1-2 mannosidase for all terminal  $\alpha$ 1-2,  $\alpha$ 1-3 and  $\alpha$ 1-6 linked mannose residues of N-glycans (Figure 51). Treatment of the IgE-Fc-Asn394only-Man<sub>5</sub> glycoform by this mannosidase provided a paucimannose N-glycoform of IgE-Fc, which contained a mixture of Man<sub>4-7</sub>GlcNAc<sub>2</sub> N-glycans, and the Man<sub>4</sub>GlcNAc<sub>2</sub> N-glycan was found to be the most abundant species among the released N-glycans, as demonstrated by MALDI-TOF analysis. The resistance of the innermost  $\alpha$ 1-4 and  $\alpha$ 1-6 mannoses (Man<sub>1-3</sub>GlcNAc<sub>2</sub>) to enzymatic treatment was suggested in a previous structural study concerning N-linked carbohydrates of human IgE antibodies. The X-ray crystallographic structures indicated that the high-mannose N-glycans of IgE-Fc at Asn-394 was buried between the two C $\epsilon$ 3 domains and the adjacent C $\epsilon$ 2 domains

were found to be blocking access of the intracellular mannosidases during IgE N-glycan biosynthesis.<sup>155</sup> This phenomenon was also observed for high-mannose N-glycans of IgY-Fc found in avian species.<sup>167</sup> Nevertheless, the kinetic parameters measured by SPR analysis (Table 9) suggested that the  $\text{Man}_{1-3}\text{GlcNAc}_2$  core structure alone was able to maintain the same level of  $\text{Fc}\epsilon\text{RI}$  binding capacity as the original IgE-Fc-Asn394only-HM glycoform, since IgE-Fc-Asn394only- $\text{Man}_9$ , IgE-Fc-Asn394only- $\text{Man}_5$ , IgE-Fc-Asn394only- $\text{Man}_{4-7}$ , and IgE-Fc-Asn394only-HM all exhibited similar binding affinities to the immobilized  $\text{Fc}\epsilon\text{RI}$  ( $\sim 2$  nM). Because only IgE-Fc-Asn394only-GlcNAc showed significantly reduced binding affinity ( $\sim 9$  nM) to  $\text{Fc}\epsilon\text{RI}$ , the innermost  $\text{Man}_{1-3}\text{GlcNAc}_2$  glycan core is suggested to be the minimal structural requirement for the optimal binding of IgE-Fc fragment to  $\text{Fc}\epsilon\text{RI}$ .

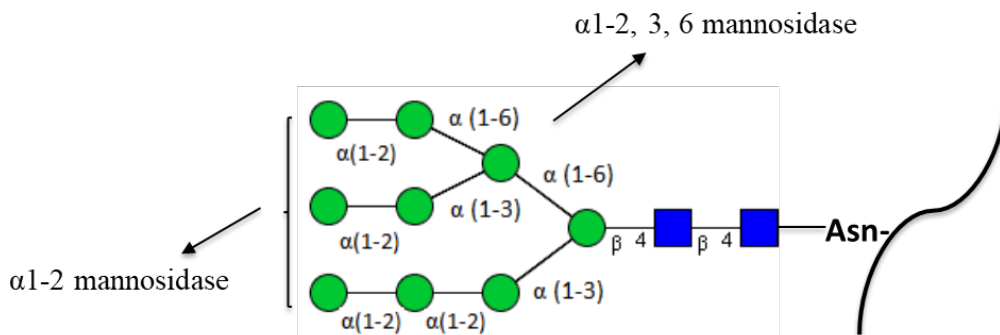


Figure 51. Schematic representation of the substrate specificity of  $\alpha(1-2)$  and  $\alpha(1-2, 3, 6)$  mannosidase against differentially linked mannose residues of the high-mannose Asn-linked oligosaccharides in glycoproteins. This figure is created based on the reported glycosidic linkage selectivities of commercial  $\alpha(1-2)$  and  $\alpha(1-2, 3, 6)$  mannosidase.<sup>168</sup>

3.4. Complete removal of N-glycans from the native IgE-Fc glycoform by PNGase F caused further reduction of FcεRI binding affinity.

Finally, the native high-mannose type N-glycans of IgE-Fc-Asn394only were completely released from the conserved asparagine residue using a bacterial endoglycosidase-like amidase enzyme called peptide-N-glycosidase F (PNGase F). Unlike endoglycosidase, PNGase F catalyzes the cleavage between the asparagine residue and the innermost GlcNAc of all types of N-linked oligosaccharides and deaminates the asparagine residue to an aspartate in the process.<sup>129</sup> To maintain the structural integrity of the resultant IgE-Fc protein, the deglycosylation reaction was performed under the non-denaturing condition, and other glycoproteins including ribonuclease B (RNase B) and IgG antibody were also treated with PNGase F to provide side-by-side controls for the reaction.<sup>94</sup> A complete deglycosylation of IgE-Fc-Asn394only-HM was confirmed by SDS-PAGE, where a clear shift of protein bands was observed after PNGase F treatment.

Similar to all the other IgE-Fc-Asn394only N-glycoforms, the binding affinity of resulting IgE-Fc-Asp394 protein to FcεRI was measured and compared with other IgE-Fc N-glycoforms. The comparative data (Figure 52 and Table 9) clearly revealed a further reduction of IgE-Fc-Asp394 binding to FcεRI [ $K_D = (19.1 \pm 0.31) \times 10^{-9} \text{ M}^{-1}$ ] in comparison to the Endo-H-treated IgE-Fc-Asn394only-GlcNAc form [ $K_D = (8.64 \pm 0.09) \times 10^{-9} \text{ M}^{-1}$ ]. These results may also suggest a functional role of the  $\text{Man}_{1-3}\text{GlcNAc}_2$  core structure for IgE-Fc binding to FcεRI. However, it is important to take into consideration the fact that PNGase F treatment introduces an Asn-to-Asp mutation at the N-glycosylation site (Asn394) due to deamination. It remains unclear

whether the decreased binding affinity could also be caused by the rearrangement of the local secondary structure of IgE as a result of glycan remodeling. Indeed, a previous study on murine IgG antibodies demonstrated that deglycosylation of the homologous complex type N-glycan from IgG-Fc at Asn-297 caused a significant conformational change that negatively impacts Fc $\gamma$ R binding.<sup>169</sup> Furthermore, Shade and colleagues also investigated the contribution of Asn-394 N-glycans to the secondary structure of human IgE by circular dichroism (CD).<sup>113</sup> In their study, a relatively small but significant shift in CD spectra was observed for Endo-F1-treated IgE antibody, which could indicate delicate changes in the overall conformation of human IgE causing variations in receptor binding properties. Therefore, further structural analysis such as CD and X-ray crystallography on the remodeled IgE-Fc N-glycoforms described in this study are needed to shed light on the molecular mechanism behind the altered Fc $\epsilon$ RI binding capacity due to N-glycoengineering.

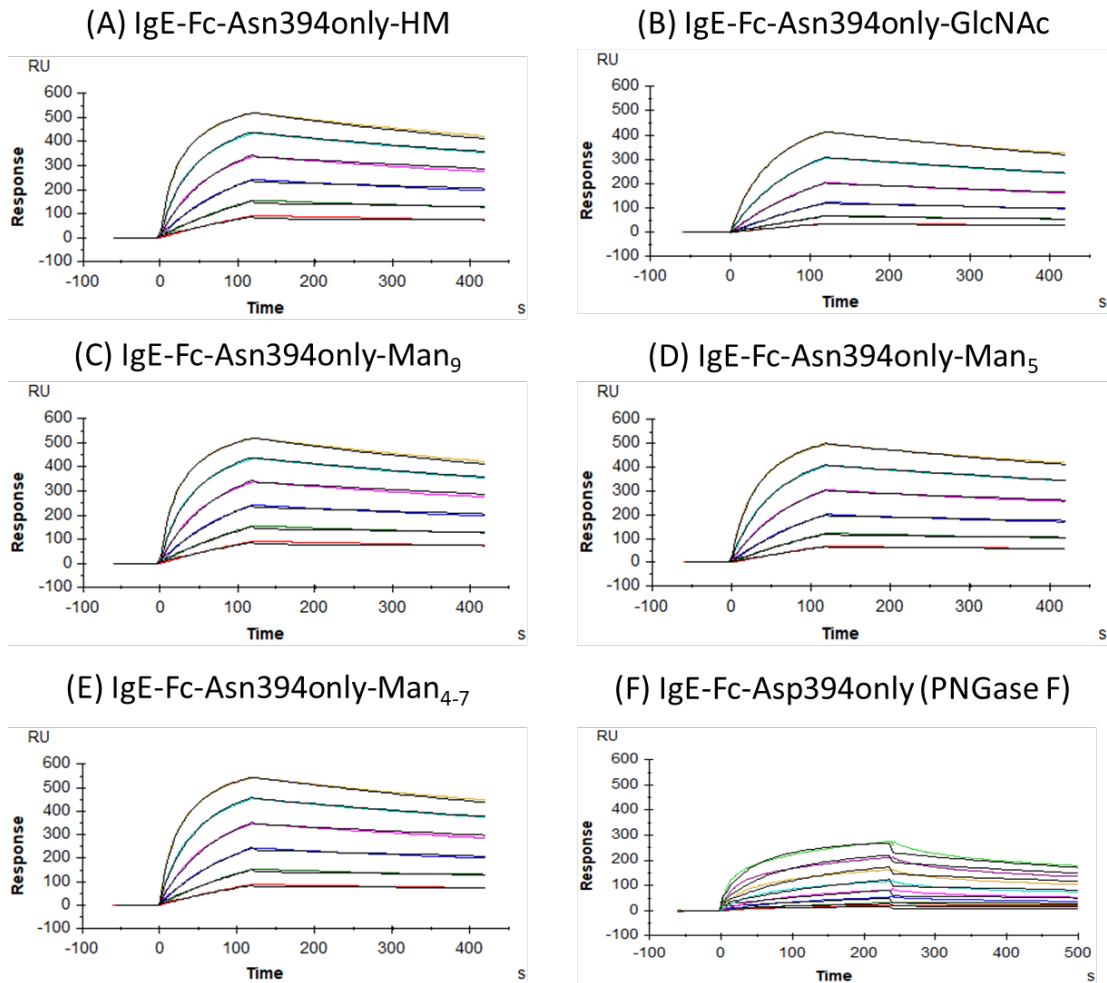


Figure 52. Surface plasmon resonance (SPR) representative sensorgrams of binding events analyzed between remodeled IgE-Fc-Asn394only glycoforms and immobilized soluble domain of high-affinity IgE receptor FcεRI, (A) the native IgE-Fc-Asn394only-HM containing a mixture of Man<sub>5-9</sub> oligomannose N-glycans, (B) Endo-H-treated IgE-Fc-Asn394only-GlcNAc, (C) IgE-Fc-Asn394only-Man<sub>9</sub>, (D) IgE-Fc-Asn394only-Man<sub>5</sub>, (E) IgE-Fc-Asn394only-Man<sub>4-7</sub>, and (F) PNGase F-treated IgE-Fc-Asp394. Six concentrations of IgE antibodies (100–3.125 nM) were measured in the standard SPR buffer, and a global monovalent fitting was applied to determine the kinetic parameters shown in Table 9.

Table 9. Kinetic parameters and binding affinities of IgE-Fc N-glycoforms for FcεRI.<sup>a</sup>

IgE-Fc N-glycoforms	$k_d$ (1/Ms)	$k_d$ (1/s)	$K_D$ (M) <sup>b</sup>
IgE-Fc-Asn394only-HM	$(1.01 \pm 0.01) \times 10^{+5}$	$(2.79 \pm 0.03) \times 10^{-4}$	$(2.76 \pm 0.15) \times 10^{-9}$
IgE-Fc-Asn394only-Man <sub>9</sub>	$(1.75 \pm 0.05) \times 10^{+5}$	$(4.08 \pm 0.04) \times 10^{-4}$	$(2.33 \pm 0.09) \times 10^{-9}$
IgE-Fc-Asn394only-Man <sub>5</sub>	$(1.35 \pm 0.04) \times 10^{+5}$	$(3.46 \pm 0.02) \times 10^{-4}$	$(2.56 \pm 0.13) \times 10^{-9}$
IgE-Fc-Asn394only-Man <sub>4-7</sub>	$(1.57 \pm 0.01) \times 10^{+5}$	$(3.78 \pm 0.02) \times 10^{-4}$	$(2.41 \pm 0.21) \times 10^{-9}$
IgE-Fc-Asn394only-GlcNAc	$(1.05 \pm 0.01) \times 10^{+5}$	$(9.65 \pm 0.02) \times 10^{-4}$	$(9.19 \pm 0.18) \times 10^{-9}$
IgE-Fc-Asp394only	$(5.21 \pm 0.09) \times 10^{+4}$	$(9.91 \pm 0.11) \times 10^{-4}$	$(1.90 \pm 0.32) \times 10^{-8}$

<sup>a</sup>The data were measured by SPR from a panel of glycoengineered IgE-Fc glycoforms containing a single N-glycosylation site at Asn-394. These IgE-Fc glycoforms were generated by enzymatic modifications and biosynthetic glycan manipulation. Kinetic parameters for binding between FcεRIα and glycoengineered IgE-Fc-Asn394only N-glycoforms were obtained in Standard SPR buffer at 20 °C and the obtained raw data were then analyzed using global monovalent 1 : 1 fitting model (BiaEvaluation). The parameters were means ± SD of experiments conducted in triplicate and the optimal binding capacity of the immobilized FcεRIα domain was confirmed by standard IgE binding assay prior to each of the repeated binding experiments to ensure that the CM5 chip-immobilized FcεRIα did not loss activity during storage.

<sup>b</sup>The dissociation constant  $K_D$  was defined as  $(k_d/k_a)$  and calculated using the monovalent fitting model of BiaEvaluation software.

4. Glycosylation remodeling of IgE-Fc-Asn394 only showed no significant impact on binding capacity to low-affinity immunoglobulin E (IgE) receptor, CD23 (FcεRII)

While most studies regarding IgE glycosylation and receptor binding focus on the high-affinity IgE receptor, FcεRI, there is limited discussion about the potential effects of N-glycans on the ability of IgE antibodies to interact with the low-affinity IgE receptor, CD23/FcεRII. Because the CD23 signaling is critical for many allergy-associated immune functions, including maintaining the IgE homeostasis, facilitating allergen recognition, and transporting allergens across airway and gut membranes<sup>51</sup>, interaction between IgE-Fc and CD23 has become a promising target for therapeutic intervention. An anti-CD23 antibody (lumiliximab) was developed as an anti-asthma therapy and exhibited the ability to effectively reduce the IgE level in human serum<sup>170</sup>. Regarding the functional relationship between IgE-Fc N-glycosylation and CD23-binding capacity, an early study by Gould and others demonstrated that glycosylation was not necessary for IgE to bind B cells through CD23,<sup>171</sup> as the enzymatically deglycosylated IgE-Fc ε-domain fragments displayed comparable or even increased binding to CD23. However, only a series of recombinant ε-chain peptide fragments expressed in bacteria instead of mammalian systems were tested in their study and no detailed glycan analysis was performed on the resulting IgE-Fc fragments during the deglycosylation process. Given the controversial results about the exact glycosylation requirement for human IgE to bind FcεRI and trigger allergic response, as discussed in previous sections, it is of great interest to investigate whether any alterations in the N-glycosylation profile of the IgE-Fc fragments produced in mammalian systems can also affect binding to CD23 and the associated B cell signaling pathways.

Using the homogeneous IgE-Fc-Asn394only N-glycoforms described in the previous section, including IgE-Fc-Asn394only-Man<sub>9</sub>, IgE-Fc-Asn394only-Man<sub>5</sub>, IgE-Fc-Asn394only-GlcNAc, and IgE-Fc-Asp394, we compared the binding properties of these four IgE-Fc glycoforms to the monomeric soluble domain of CD23 immobilized on sensor surface using a similar experimental setup as for FcεRIa. The representative sensorgrams and their binding kinetics are summarized in Figure 53 and Table 10. Analogous to the results from FcεRIa binding, comparison between binding kinetics of oligomannose (-Man<sub>9</sub>) and deglycosylated IgE N-glycoforms (-GlcNAc and PNGase F-treated -Asp394) revealed an approximately 2-fold difference in binding affinities to CD23, which was mainly due to higher association rates of high-mannose N-glycoforms. As shown in Table 10, the IgE-Fc-Asn394only-Man<sub>9</sub> and IgE-Fc-Asn394only-Man<sub>5</sub> associates with CD23 faster than both IgE-Fc-Asn394only-GlcNAc and IgE-Fc-Asp394, which are supported by higher association constants [ $k_a = (6.91 \pm 0.09) \times 10^4 \text{ Ms}^{-1}$  for IgE-Fc-Asn394only-Man<sub>9</sub> and  $k_a = (2.35 \pm 0.01) \times 10^4 \text{ Ms}^{-1}$  for IgE-Fc-Asp394]. A small difference in CD23 binding affinities was observed between the two mannose-rich N-glycoforms, including IgE-Fc-Asn394only-Man<sub>9</sub> [ $K_D = (3.14 \pm 0.08) \times 10^{-8} \text{ M}^{-1}$ ] and IgE-Fc-Asn394only-Man<sub>5</sub> [ $K_D = (5.89 \pm 0.15) \times 10^{-8} \text{ M}^{-1}$ ], which were due to variations in both  $k_a$  and  $k_d$ . Unlike previous studies regarding FcεRI binding, no further reduction of IgE-Fc binding toward CD23 was observed after the complete removal of the N-glycans by PNGase F, as binding kinetics and affinities of IgE-Fc-Asn394only-GlcNAc and IgE-Fc-Asp394 were comparable [ $K_D = (6.76 \pm 0.07) \times 10^{-8} \text{ M}^{-1}$  for IgE-Fc-Asn394only-GlcNAc and  $K_D = (7.95 \pm 0.14) \times 10^{-8} \text{ M}^{-1}$  for IgE-Fc-Asp394].

Although low-affinity IgE receptor CD23 is structurally categorized as a lectin, which represents a superfamily of carbohydrate-binding proteins, early structural study demonstrated that CD23 recognized IgE-Fc through protein-protein interactions that did not involve any carbohydrate determinants<sup>171</sup>. Adding to this point, a separate structural analysis on possible CD23/carbohydrate interactions suggested that soluble domain of CD23 did not show any carbohydrate-specific binding activities<sup>172</sup>. In this study, the abilities of simple carbohydrates such as glucose, galactose, lactose, mannose, and N-acetylglucosamine to bind to recombinant CD23 protein were tested using NMR chemical shift perturbation titrations. The results showed that none of these carbohydrates exhibited any specific binding to CD23 even at the highest concentrations. A recently published crystal structure of IgE-Fc in complex with CD23 showed that IgE binding sites for CD23 and FcεRI were located at the opposite faces of Cε3 domain and the Asn-394 N-glycan was found to be in proximity to FcεRI binding site but not to the CD23 binding site, which suggested that a change of IgE glycosylation may only impact CD23 binding through long-range interactions or allosteric effects<sup>154</sup>. Interestingly, comparison of the IgE-Fc structures in complex with either CD23 or FcεRI demonstrated that binding events with the two receptors displayed an allosteric effect and were mutually exclusive<sup>173</sup>. Since several structural studies showed that removal of Asn-394 N-glycans did result in small conformational changes to the IgE-Fc domain and reduced its binding to FcεRI, the same molecular mechanism may also contribute to the observed decrease of CD23-binding activity caused by deglycosylation. Nevertheless, similar to the previous studies on FcεRI,

further structural and biophysical studies on IgE-Fc N-glycoforms in complex with CD23 are needed to help explain the varied binding kinetics observed in this study.

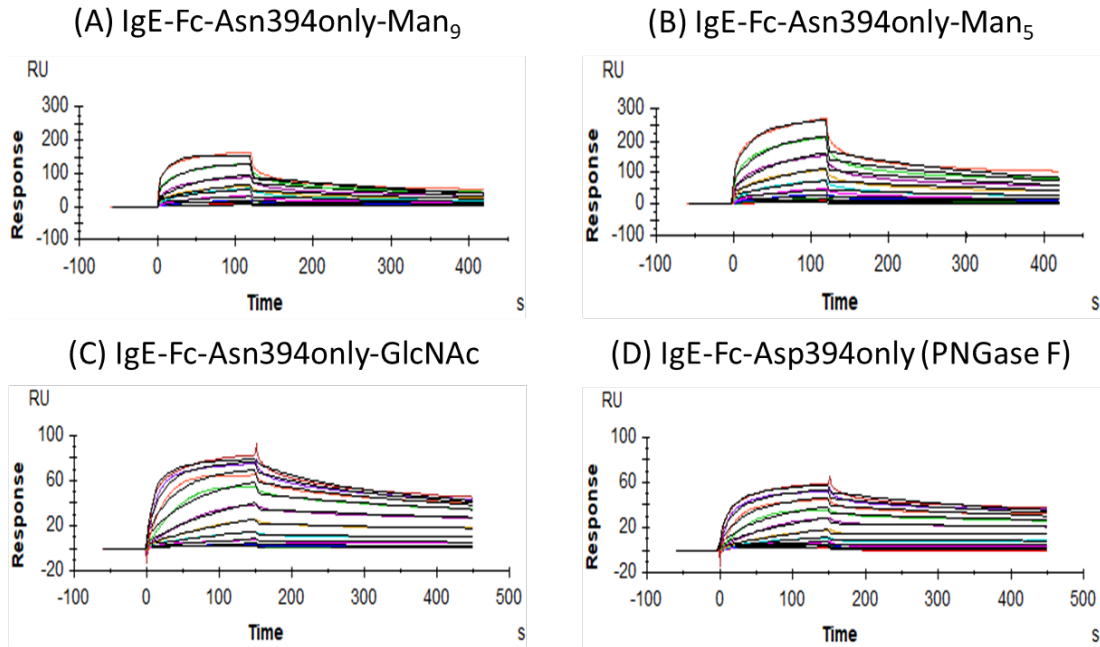


Figure 53. Representative surface plasmon resonance (SPR) sensorgrams of interactions between the homogeneous IgE-Fc-Asn394only N-glycoforms and the immobilized soluble domain of the IgE-Fc low-affinity receptor CD23/ FcεRII, (A) IgE-Fc-Asn394only-Man<sub>9</sub>, (B) IgE-Fc-Asn394only-Man<sub>5</sub>, (C) Endo-H-released IgE-Fc-Asn394only-GlcNAc, and (D) PNGase F-released IgE-Fc-Asp394. A total of eight IgE-Fc concentrations (400 – 3.125 nM) were tested in the standard SPR buffer at 20 °C, and a global monovalent fitting model was used to measure the kinetic parameters shown in Table 10.

Table 10. Kinetic parameters of IgE-Fc-Asn394only glycoforms with the immobilized soluble domain of IgE-Fc low-affinity receptor CD23 measured by SPR<sup>a</sup>.

IgE-Fc N-glycoforms	$k_a(1/Ms)$	$k_d(1/s)$	$K_D(M)^b$
IgE-Fc-Asn394only-Man <sub>9</sub>	$(6.91 \pm 0.09) \times 10^{+4}$	$(2.17 \pm 0.01) \times 10^{-3}$	$(3.14 \pm 0.08) \times 10^{-8}$
IgE-Fc-Asn394only-Man <sub>5</sub>	$(5.78 \pm 0.04) \times 10^{+4}$	$(3.40 \pm 0.05) \times 10^{-3}$	$(5.89 \pm 0.15) \times 10^{-8}$
IgE-Fc-Asn394only-GlcNAc	$(2.86 \pm 0.01) \times 10^{+4}$	$(1.93 \pm 0.02) \times 10^{-3}$	$(6.76 \pm 0.07) \times 10^{-8}$
IgE-Fc-Asp394only	$(2.35 \pm 0.11) \times 10^{+4}$	$(1.87 \pm 0.17) \times 10^{-3}$	$(7.95 \pm 0.14) \times 10^{-8}$

<sup>a</sup>Kinetic parameters for binding events between CD23 and glycoengineered IgE-Fc-Asn394only N-glycoforms were measured in Standard SPR buffer at 20 °C and the obtained kinetic parameters were then analyzed using a global monovalent fitting algorithm (BiaEvaluation). The experiments were performed in triplicate and the optimal binding capacity of the immobilized CD23 receptor was confirmed by the standard IgE binding assay prior to each of the binding experiments to ensure that the CM5 chip-immobilized CD23 did not loss its binding capacity during storage at 4 °C.

<sup>b</sup>The dissociation constant  $K_D$  was defined as  $(k_d/k_a)$  and calculated using the monovalent fitting model of BiaEvaluation software.

5. Chemoenzymatic N-glycosylation remodeling of IgE-Fc with complex N-glycan using the active glycosyl oxazoline and glycosynthase mutants

The glycoengineering studies in previous sections with the heterogeneous IgE-Fc-Asn394only-HM were successful in producing the uniformly glycosylated variants IgE-Fc-Asn394only-Man<sub>9</sub> and IgE-Fc-Asn394only-Man<sub>5</sub> by enzymatic modifications and biosynthetic inhibitor. However, the oligomannose core of the native N-glycans attached at Asn-394 of IgE-Fc makes it intrinsically difficult to convert the original IgE N-glycans to a completely different glycoform such as IgE-Fc with complex type N-glycan. As discussed extensively in the previous chapters, a conserved complex type N-glycan associated with Asn-297 residue in the IgG-Fc region can critically modulate the biological functions of different subclasses of IgG antibodies.<sup>20</sup> Taking advantage of the different substrate specificities of various endoglycosidases, we and other groups have developed a collection of endoglycosidases and corresponding glycosynthases for glycoengineering of glycoproteins, including Endo-S, Endo-S2, and Endo-CC. These enzymes in combination with the activated glycosyl oxazolines have been highly successful in producing many glycopeptides and glycoproteins with desired N-glycan structures including IgG antibodies. Therefore, it will be of great interest to apply this strategy on IgE antibody with the goal of generating novel IgE-Fc N-glycoforms that could not be obtained using the existing techniques. Generation of such atypical fully-processed complex type N-glycoforms of IgE at Asn-394 may lead to IgE glycovariants with distinct structural and functional properties from the wild type

IgE-Fc, which can be exploited as potential therapeutic interventions against asthma and other allergic diseases.<sup>156, 174</sup>

### 5.1. Selection of suitable endoglycosidases for IgE-Fc glycosylation remodeling

In order to screen for potential endoglycosidases that can efficiently transfer the complex type N-glycans to IgE-Fc, we used the engineered IgE-Fc-Asn394only-HM as starting material to test hydrolytic activities of a number of endoglycosidases that have been previously studied for this purpose, including Endo-M<sup>100</sup>, Endo-S<sup>103</sup>, Endo-S2<sup>139</sup>, and Endo-CC<sup>110</sup> (Figure 54). Our initial results in Figure 55 indicated that treatment of IgE-Fc-Asn394only-HM with Endo-M and Endo-S2 led to only marginal hydrolysis of the IgE-Fc N-glycans even when a high concentration of enzyme and an extended incubation time were applied. In addition, enzyme Endo-S did not show any hydrolytic activities against native IgE-Fc glycoforms after an overnight reaction. These results are consistent with our previous observations that conserved Asn-394 glycosylation site of IgE-Fc was not largely accessible by enzymatic modifications such as  $\alpha$ -mannosidase.<sup>162</sup> The inability of Endo-S to process high-mannose N-glycans from IgE was expected due to its restricted substrate selectivity for the complex type N-glycans only.<sup>130</sup> Although Endo-S2 indeed possesses a broad substrate specificity for all three major types of N-glycans found in IgG antibodies (complex, hybrid, and high-mannose) and is efficient in processing the IgG N-glycans, many structural and functional studies suggested that both Endo-S and Endo-S2 were highly selective for the IgG class of antibody and exhibited only marginal hydrolytic activities against other commonly studied glycoproteins such as

ribonuclease B.<sup>138</sup> In contrast to Endo-S/S2, Endo-M was able to process the high-mannose N-glycans of a large number of glycopeptides and glycoproteins, but the enzyme did not demonstrate any enzymatic activities toward the IgG antibody, as illustrated in previous study.<sup>89</sup> Interestingly, the recently discovered endoglycosidase Endo-CC from fungus *Coprinopsis cinerea*, as characterized in Chapter 4, was found to be able to efficiently remove the indigenous N-glycans from the IgE-Fc-Asn394only-HM form (Figure 55). This was supported by the results shown in Chapter 4 that Endo-CC displayed a relatively relaxed substrate selectivity for both the carbohydrate structures and protein framework of various glycoconjugates<sup>112</sup>.

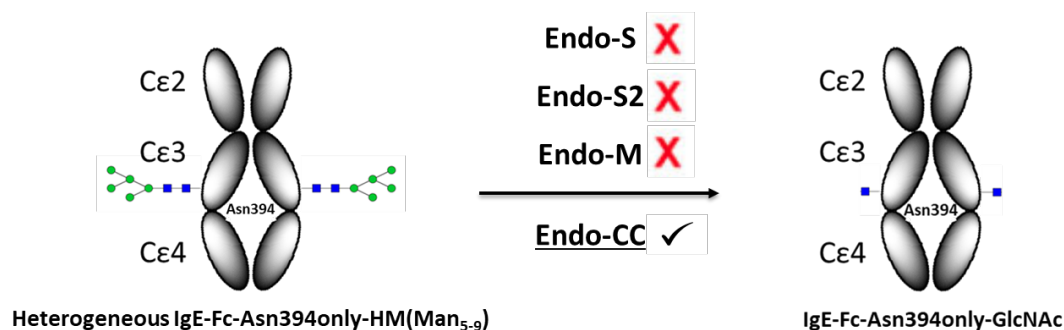


Figure 54. Hydrolytic selectivity of Endo-S, Endo-S2, Endo-M and Endo-CC against the high-mannose IgE-Fc-Asn394only-HM (Man<sub>5-9</sub>) N-glycoforms. For Endo-CC, rapid deglycosylation was observed against IgE-Fc N-glycoform, whereas Endo-S/S2 and Endo-M did not show significant hydrolysis of the native N-glycans associated with the heterogeneous IgE-Fc fragment. Comparative hydrolysis assay is shown in Figure 54.

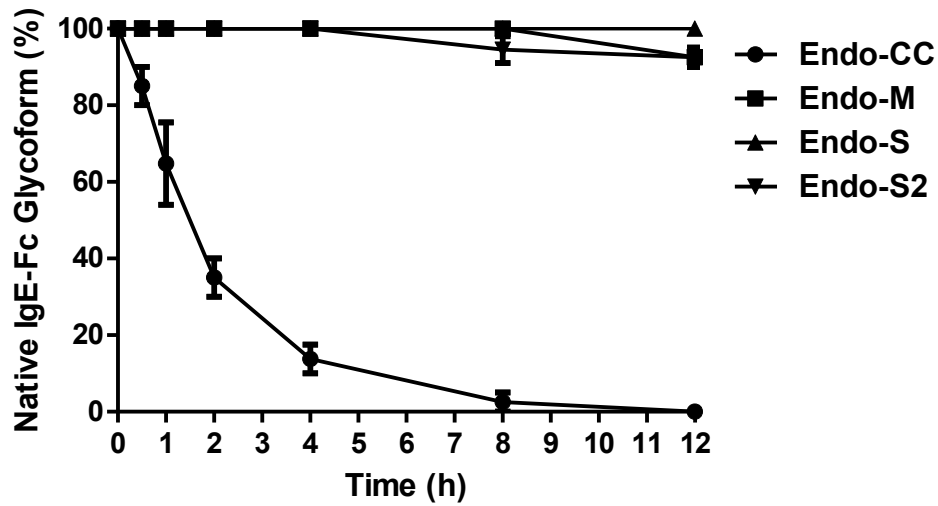


Figure 55. Comparison of enzymatic hydrolysis on native IgE-Fc-Asn394only-HM (Man<sub>5-9</sub>) N-glycoforms by the recombinant Endo-CC, Endo-M, Endo-S, and Endo-S2. A total concentration of 2 mg/mL of original IgE-Fc starting material was incubated with 0.1 mg/mL of all four enzymes 37 °C in the Tris buffer at pH 7.4. The reaction was checked by SDS-PAGE and the relative hydrolysis of the IgE-Fc was quantified using densitometry analysis of the protein bands corresponding to the native and the deglycosylated IgE-Fc fragments. Each reaction was conducted in duplicate.

## 5.2.Generation of a non-fucosylated complex type IgE-Fc-Asn394only N-glycoform using mutant Endo-CC N180 glycosynthase-catalyzed transglycosylation and CT (G2) glycan oxazoline

Having confirmed that Endo-CC was able to efficiently hydrolyze the native N-glycans associated with IgE-Fc, we then performed transglycosylation reactions on the IgE-Fc-Asn394only-GlcNAc acceptor using the Endo-CC glycosynthase mutant Endo-CC N180H and a fully galactosylated glycan oxazoline (G2-CT-Oxa) as the

donor substrate (Figure 56). A number of reaction conditions such as oxazoline molar equivalent and enzyme concentration were tested to maximize the transglycosylation yield and to minimize any non-enzymatic side reactions (data not shown). The final results demonstrated that treatment of IgE-Fc-Asn394only-GlcNAc with a total of 50 molar equivalents of G2-CT-Oxa (25 equivalents per each glycosylation site of IgE-Fc monomer) and 0.1 mg/mL of CPD-tagged recombinant Endo-CC N180H for 4 hours resulted in a homogeneous IgE-Fc-CT N-glycoform that appeared as a single band on the SDS-PAGE (Figure 57A). The molecular weight of the product band was estimated to be about 2 kDa (approximately the size of a G2-CT glycan per one IgE-Fc monomer) larger than the starting material. The band of a lower-molecular-weight species corresponding to the starting material was not seen after the reaction, suggesting a complete conversion of IgE-Fc. Again, MALDI-TOF mass spectrometry analysis on the PNGase F-released N-glycans of the reaction product revealed a major mass species of 1663.3 Da, which corresponds to the released G2-CT glycan (calculated M.W. 1664, Figure 57B). A minor species with a M.W. of 1257.4 was also present in the released glycan profile possibly due to incomplete deglycosylation of the native high-mannose N-glycans from the previous step. The product was subsequently treated with both Endo-CC and PNGase F to confirm that the transferred complex type N-glycan was not linked to IgE-Fc through non-enzymatic chemical ligation.<sup>122</sup> Therefore, a highly efficient and regioselective chemoenzymatic glycosylation modeling of the IgE antibody with the novel complex type glycan oxazoline was achieved.

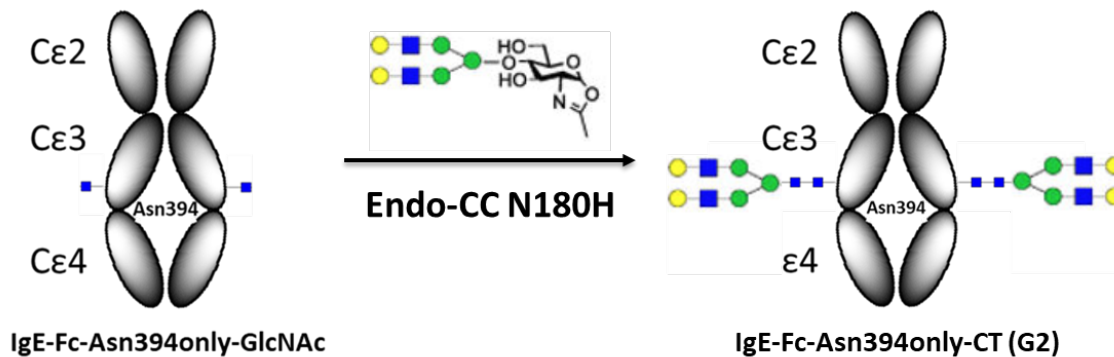


Figure 56. Transglycosylation of IgE-Fc-Asn394only-GlcNAc with the galactosylated complex type glycan oxazoline (CT-Oxa) using glycosynthase Endo-CC N180H.

### 5.3. Glycoengineered complex type IgE-Fc-Asn394only-CT displayed distinct binding properties from those of the oligomannose IgE-Fc N-glycoforms

The binding kinetics of the remodeled IgE-Fc glycoform for the high-affinity IgE receptor FcεRI was measured by surface plasmon resonance (SPR). Following the previously described procedure, serial dilutions of both the product glycoform IgE-Fc-Asn394only-CT and starting glycoform IgE-Fc-Asn394only-GlcNAc were analyzed as analytes and compared for their binding kinetics. As expected, the deglycosylated IgE-Fc exhibited an expected binding affinity for FcεRI [ $K_D = (9.47 \pm 0.08) \times 10^{-9} \text{ M}^{-1}$ ] prior to transglycosylation. On the other hand, the  $K_D$  value of the complex IgE-Fc glycoform (IgE-Fc-Asn394only-CT) to FcεRI was found to slightly higher than that of the deglycosylated IgE-Fc [ $K_D = (1.28 \pm 0.01) \times 10^{-8} \text{ M}^{-1}$ ] (Figure 57C and 57D), although the difference was not dramatic statistically. However, the kinetic parameters of the two IgE-Fc glycoforms studied here revealed to be significantly different. The association rate constant  $k_a$  of the glycoengineered IgE-Fc-Asn394only-CT [ $k_a = (6.79 \pm 0.06) \times 10^5 \text{ Ms}^{-1}$ ] was approximately 5-fold higher

than that of the deglycosylated glycoform [ $k_a = (1.25 \pm 0.01) \times 10^5 \text{ Ms}^{-1}$ ], whereas the relationship was reversed for the dissociation rate constant, as the IgE-Fc-Asn394only-CT [ $k_d = (8.69 \pm 0.11) \times 10^4 \text{ s}^{-1}$ ] dissociates from FcεRI faster than IgE-Fc-Asn394only-GlcNAc [ $k_d = (1.18 \pm 0.03) \times 10^3 \text{ s}^{-1}$ ]. These results suggest a significant change of IgE-Fc binding kinetics to FcεRI caused by the remodeling of the complex type N-glycan. In addition to the CT-Oxa, previous studies on Endo-CC N180H substrate specificities showed that the mutant was also able to transfer the fully sialylated complex type glycan oxazoline (SCT-Oxa) to different glycosyl acceptors including the therapeutic IgG antibody<sup>112</sup>, which suggested that other complex glycan structures could potentially be transferred to IgE antibody as well. Therefore, this chemoenzymatic glycoengineering strategy discussed here can provide additional homogeneous IgE N-glycoforms that might be useful for structural and functional studies as well as development for novel anti-allergic therapies.

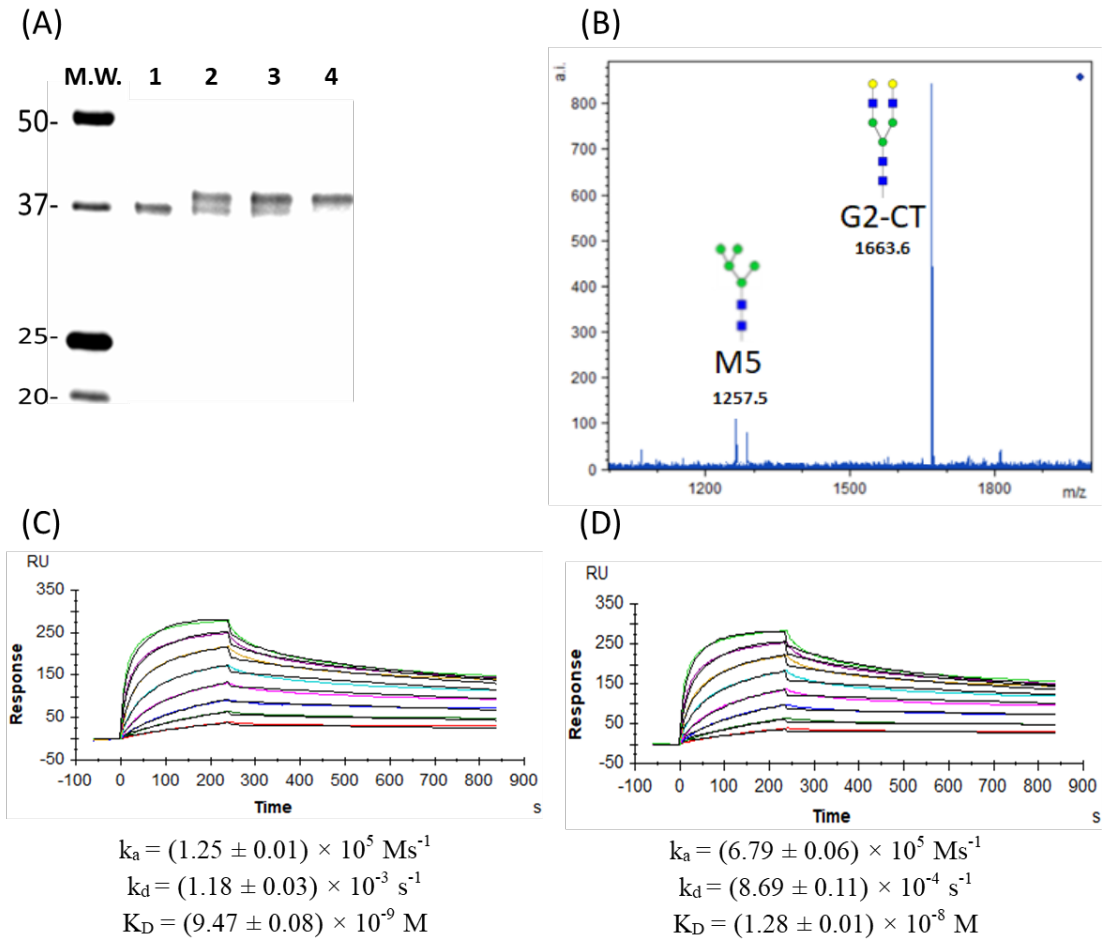


Figure 57. Glycan remodeling of IgE-Fc-Asn394only-CT (G2) N-glycoform and its binding properties for the high-affinity receptor FcεRI. (A) SDS-PAGE analysis to monitor transglycosylation of IgE-Fc by Endo-CC N180H: Lane 1, IgE-Fc-Asn394only-GlcNAc; Lane 2, reaction at t = 1 h; Lane 3, reaction at t = 2 h; Lane 3, reaction at t = 4 h and final product of IgE-Fc-Asn394only-CT. (B) MALDI-TOF MS analysis of the released N-glycans from the remodeled IgE-Fc-Asn394only-CT. (C) and (D) SPR sensorgrams of the binding between FcεRI and (C) IgE-Fc-Asn394only-GlcNAc or (D) IgE-Fc-Asn394only-CT, respectively. Eight concentrations of IgE-Fc N-glycoform (400–3.125 nM) were injected as analytes and the kinetic data was analyzed using a monovalent fitting model.

### C. Conclusion

A combined glycosylation remodeling strategy of enzymatic modification and biosynthetic perturbation for intact IgE antibodies and IgE-Fc fragments is described in this work. This method enabled the generation of a series of homogeneous IgE-Fc N-glycoforms, and binding properties of these IgE glycoforms to both the high- and low-affinity IgE receptors FcεRI and CD23 were characterized. To our knowledge, this study represents the first investigation on the functional role of N-glycans in regulating the binding between IgE-Fc expressed in mammalian cells and the low-affinity CD23 receptor, which is important for mediating IgE homeostasis in human. Although the sugar composition did not display any dramatic impact on IgE binding to either receptor, the presence of the native N-glycans and, for the first time, the remodeling of a novel complex N-glycan at the critical Asn-394 residue did show changes to the binding properties of IgE-Fc glycoforms. These adequately combined approaches greatly expand the scope of the chemoenzymatic glycoengineering strategy beyond the IgG antibody and opened the avenue for further remodeling of other human antibodies such as IgA and IgE, using endoglycosidases and additional oxazoline structures, such as the sialylated (S2G2-CT) and agalactosylated (G0-CT) glycoforms, which are difficult to produce using current techniques. In addition, recent structural studies suggested that anti-IgE antibodies such as omalizumab<sup>175</sup> and 8D6<sup>155</sup> provide effective amelioration of asthma-like allergic diseases by targeting a mixed protein-carbohydrate epitope including Asn-394 N-glycan at IgE-Fc. Therefore, glycoengineering of IgE-Fc N-glycans may further our understanding of the structural

mechanism behind IgE/anti-IgE recognition and potentially facilitate the development of novel therapeutic interventions against allergic disorders.

## D. Materials and Methods

### 1. Mammalian cell culture: cell lines, strains and expression conditions

The plasmid DNA expressing the high-mannose IgE-Fc-Asn394only-HM fragment was designed with asparagine-to-glutamine (N-to-Q) mutations at all conserved N-glycosylation sites except for Asn-394 (Genscript). The IgE-Fc DNA was transfected into the HEK293T cells by transient transfection with 20 µg/ml of kifunensine (Cayman Chemical, Ann Arbor, Michigan) added as an inhibitor for mannosidases. The mammalian HEK293T cells were grown in FreeStyle F17 Expression Medium in the presence of 2 mM GlutaMax (Thermo Fisher Scientific). All cell lines were subject to 150 rpm shaking at 37 °C with 8% CO<sub>2</sub>. The detailed protocol for transfection and purification of the IgE-Fc protein was described in a previous publication.<sup>176</sup>

### 2. Expression, purification and characterization of recombinant endoglycosidases Endo-CC, Endo-M, Endo-S and Endo-S2 and their glycosynthase mutants in bacterial cell culture

The detailed protocol for the expression and purification of endoglycosidases and their related glycosynthase mutants, including Endo-CC (Chapter 4), Endo-S (Chapter 1), and Endo-S2 (Chapter 3), were described in the experimental sections of previous Chapters. The recombinant CPD-tagged Endo-M was generated following a previous published protocol<sup>99</sup>.

### 3. Site-specific glycan remodeling of full-length IgE antibodies

To selectively release the oligomannose N-glycan at Asn-394 without removing the other complex N-glycans attached at the heavy chain of the full-length IgE antibodies, 50 µg of both the commercial human IgE antibody (Abcam, UK) and the recombinant ovalbumin (OVA)-specific IgE antibody were treated with 1000 units of recombinant Endo-Hf (New England Biolabs, NEB) in a total volume of 50 µl PBS buffer (pH 7.4) at 37°C for overnight incubation. The commonly used Glycoprotein Buffer 3 (New England Biolabs, NEB) was not used in this study because the deglycosylation were found to be efficient without adding any additional buffer components. Removal of N-glycans from IgE were monitored and confirmed by SDS-PAGE analysis with a shift of bands corresponding to the differentially glycosylated heavy chains of IgE antibody. The anti-OVA IgE antibody was provided by Dr. Robert Anthony's group at Harvard University, MA.

### 4. Deglycosylation of starting high-mannose IgE-Fc-Asn394only-HM to afford IgE-Fc-Asn394only-GlcNAc acceptor intermediate and IgE-Fc-Asp394 intermediate

The expressed heterogeneous IgE-Fc-Asn394only-HM N-glycoforms were dialyzed into PBS at pH 7.4 and purified using an anion exchange chromatography (GE Healthcare) following the manufacturer's instruction. For the deglycosylation of IgE-Fc by endoglycosidase Endo-H, a total of 500 µg IgE-Fc-Asn394only-HM was treated with 1000 units of commercial Endo-Hf enzyme (New England Biolabs, NEB) in 50 µl of PBS buffer (pH 7.4) at 37°C for 4 hours. The completely deglycosylated IgE-Fc-Asp394 was prepared in a similar fashion by incubating 200 µg IgE-Fc-Asn394only-HM with 20 units of PNGase F (New England Biolabs, NEB) in 100 µl

of PBS buffer (pH 7.4) at 37°C for overnight reaction. Removal of N-glycans were monitored and confirmed by SDS-PAGE densitometry followed by MALDI-TOF mass spectrometry characterization of Fc-Asn394only-GlcNAc and IgE-Fc-Asp394.

#### 5. Generation of N-glycoforms IgE-Fc-Asn394only-Man<sub>5</sub> and IgE-Fc-Asn394only-Man<sub>4-7</sub> N-glycoforms by enzymatic modifications

For each N-glycoform, 500 µg IgE-Fc-Asn394only-HM was treated with 20 units (RU) of either commercial  $\alpha$  1-2 or  $\alpha$  1-2, 3, 6 mannosidase (New England Biolabs, NEB) in 50 µl of PBS buffer (pH 7.4) at 37°C for overnight reaction. One overnight of  $\alpha$  1-2, 3, 6 mannosidase showed little progress of mannose removal and additional 20 units of  $\alpha$  1-2, 3, 6 mannosidase was added to the reaction mixture and incubated for additional 12 h. The final glycoforms of modified IgE-Fc were analyzed by SDS-PAGE and MALDI-TOF analysis on the released N-glycans by PNGase F.

#### 6. MALDI-TOF mass spectrometry

The N-glycans were released from the IgE-Fc proteins by overnight incubation with a small amount of commercial PNGase F (20 units) at 37 °C for up to 12 hours. The released glycans were then characterized using a Bruker UltrafleXtreme MALDI-TOF/TOF mass spectrometer. The instrument was set to the positive reflectron mode. A solution of 2,5-dihydroxybenzoic acid (DHB, Sigma-Aldrich) was formulated by adding 100mg of DHB into 1mL of 50% acetonitrile (ACN) and used as the MALDI-TOF matrix for released N-glycans. To improve the detection sensitivity for some N-glycans studied here, N,N-dimethylaniline (DMA, Sigma-Aldrich) was also added to the sample mixture prior to analysis.

## 7. Surface Plasmon Resonance (SPR)

The interactions between different N-glycoforms of IgE-Fc-Asn394only proteins and both the high- and low-affinity IgE receptors, FcεRI and CD23, were studied using a BIAcore T200 system (GE Healthcare Life Sciences) at 25 °C. The soluble domain of both FcεRI and CD23 were immobilized on the CM5 sensor chip (GE Healthcare Life Sciences) using the amine coupling kit according to the manufacturer's instruction. For each IgE receptor, a 1000 response unit (RU) of immobilization was achieved by pH scouting. A reference channel was also prepared by blocking the active functional groups on the CM5 chip. The IgE-Fc analytes were prepared in serial dilutions in HBS-P buffer (GE Healthcare Life Sciences). A total of 6-8 concentrations of each IgE-Fc samples were injected across the sensor surface at a flow rate of 40 μL/min, and the CM5 surface was regenerated after each analysis using 20 mM HCl solution at pH 2.4 (GE Healthcare Life Sciences). The obtained binding parameters were analyzed using a global monovalent fitting model (BiaEvaluation) to calculate the binding affinity constant ( $K_D$ ). The results were collected from three independently conducted binding experiments.

## 8. Assay for hydrolytic activities of Endo-CC, Endo-S, Endo-S2 and Endo-M against recombinant IgE-Fc-Asn394only-HM

For each hydrolysis reaction, a total of 100 μg IgE-Fc-Asn394only-HM was incubated with a final concentration of 0.5 mg/mL of each enzyme in 50 μl PBS buffer (pH 7.4) at 37°C. The reaction was sampled at multiple time points up to  $t = 12$

h. Hydrolysis of high-mannose N-glycans from IgE-Fc was estimated by SDS-PAGE densitometry analysis. The experiments were performed in duplicate.

**9. Glycan remodeling of the deglycosylated IgE-Fc-Asn394only to a homogenous galactosylated complex type (G2-CT) N-glycoform**

In the first step of glycan remodeling, 100  $\mu$ g of IgE-Fc-Asn394only-HM was treated with Endo-H to provide the deglycosylated IgE-Fc glycosyl acceptor. 75  $\mu$ g of this IgE-Fc-Asn394only-GlcNAc intermediate was mixed with 3  $\mu$ g of CPD-tagged recombinant Endo-CC N180H, and 50  $\mu$ g of G2-Oxa, in 20 mM Tris-HCl buffer, at pH 7.4, which was reported to be the optimal reaction condition for Endo-CC N180H transglycosylation.<sup>110</sup> The reaction temperature was set to 30 °C.<sup>89</sup> Additional 50  $\mu$ g of G2-Oxa and 1 $\mu$ g of Endo-CC N180H were added to increase the reaction yield. Aliquot was collected at the 1, 2, and 4 h time points to monitor the transfer of the complex N-glycan by both SDS-PAGE and MALDI-TOF analysis. After 4 hours, the transglycosylation reaction was complete and further incubation did not show any improvements of total reaction yield. The biantennary galactosylated complex glycan oxazoline (G2-Oxa) was prepared following the previously reported protocol.<sup>99</sup>

## E. Supporting Information

**GT**MGWSCILFLVATATGVHSSVCSRDFTPPTVKILQSSCDGGGHFPPTIQLLC  
LVSGYTPGTIQITWLEDGQVMDVDLSTASTTQEGELASTQSELTLSQKHWLS  
DRTYTCQVTYQGHTFEDSTKKCADSNPRGVSAYLSPSPFDLFIKRSPTITCLV  
VDLAPSKGTVQLTWSRASGKPVQHSTRKEEKQR**N**GTLTVTSTLPGTRDWIE  
GETYQCRVTHPHLPRALMRSTTKTSGPRAAPEVYAFATPEWPGSRDKRTLAC  
LIQNFMPEDISVQWLHNEVQLPDARHSTTQPRKTKGSGFFVFSRLEVTRAEW  
EQKDEFICRAVHEAASPSQTVQRAVSVNPGK

Supplementary Figure 4: Amino acid sequence of the mutated IgE-Fc fragment IgE-Fc-Asn394only. A CD5 signal peptide is inserted at the beginning of the sequence. The Asn394 is highlighted in red. All glycosylation sites (N) of this IgE-Fc construct are mutated to glutamine (Q) except for Asn-394.

## Chapter 6: Summary and future directions

The major focus of this dissertation is to develop and improve the current chemoenzymatic remodeling method for antibody glycosylation using various endoglycosidases and glycosynthases. The glycosylation patterns of monoclonal antibodies, both naturally existing and recombinantly expressed, are typically complex and highly heterogeneous in their carbohydrate compositions and can critically determine the structural and biological properties of antibody molecules.<sup>4, 10, 16, 34</sup> To more effectively control and optimize the structural diversity of antibody glycans, an efficient *in vitro* chemoenzymatic glycoengineering strategy was developed based on the unique hydrolysis and transglycosylation activities of endoglycosidases and glycosynthases, respectively.<sup>20, 99, 103, 106</sup>

In Chapter 2, systematic site-directed mutagenesis analysis at the key catalytic residue Asp-233 of Endo-S (*Streptococcus pyogenes*) identified many glycosynthase mutants of Endo-S including Endo-S D233M that exhibited higher transglycosylation efficiencies than the previously reported D233Q and D233A.<sup>123</sup> Quantitative determination of antibody glycosylation was achieved using the electrospray ionization (ESI) mass spectrometry and an antibody-based internal standard.<sup>136</sup> Kinetic analyses of Endo-S D233M and D233A indicated that the Asp-to-Met mutation at Asp-233 led to the increased enzyme turnover number for the glycan donor substrate and enhanced substrate affinity for the glycan acceptor substrate. The potential occurrence of the non-enzymatic chemical glycosylation of glycan oxazolines to random residues of antibody was investigated by comparing the reaction conditions and characterizing the chemical composition of the antibody

products formed after glycoengineering. The comparative results suggested that such unwanted side reactions did not occur under the optimized reaction conditions commonly used for the antibody glycosylation by endoglycosidases. Potential chemical ligation of glycan oxazolines with antibody acceptor residues only became significant when a large excess of glycan substrate was used.<sup>109, 122, 132</sup>

In Chapter 3, similar to studies on glycosynthase mutants of Endo-S, systematic mutagenesis on another endoglycosidase Endo-S2 led to the first antibody-specific glycosynthases that could efficiently catalyze transglycosylation of IgG antibodies with additional N-glycans such as the N-linked hybrid and high-mannose oligosaccharides. Kinetic studies on the Endo-S2 mutants D184M and D184A revealed highly similar enzyme behaviors to glycosynthase mutants of Endo-S, including an enhanced affinity for antibody and a faster turnover number for glycan oxazoline. The superior catalytic activities of Endo-S2 D184M over other ENGases promoted the synthesis of antibody N-glycoforms with more diverse sugar structures. In collaboration with my colleague Dr. Tiezheng Li in Prof. Lai-Xi Wang's lab and Prof. Jeffrey Ravetch from the Rockefeller University, a comprehensive library of IgG N-glycoforms were generated using mutant Endo-S2 D184M, and both *in vitro* and *in vivo* functional assays on the resulting library identified the core fucosylation as a major determinant of the antibody activity in modulating the immune response.<sup>177</sup>

In Chapter 4, substrate specificity analyses of the wild-type Endo-S revealed promiscuity for additional N-glycan substrates, and demonstrated that, unlike Endo-S mutants, the wild-type Endo-S was capable of recognizing both the high-mannose and

hybrid glycans for antibody glycosylation with a minimal level of product hydrolysis. A highly efficient “one-pot” glycan remodeling method was developed based on the relaxed substrate selectivity of Endo-S to modify different antibody glycoforms and glycan oxazolines, which also included a chemically modified azido-tagged N-glycan. Because of its ability to convert antibody N-glycosylation without the need of purifying the deglycosylated intermediate or switching enzymes, this method could be potentially useful in large-scale antibody manufacturing in terms of lowered cost due to reduced producing steps.<sup>178</sup>

The scope and limitations related to the catalytic properties of Endo-CC and its glycosynthase mutants were investigated using a series of glycoprotein and N-glycan oxazolines as substrates. Parallel transglycosylation reactions indicated that the mutant Endo-CC N180H could potentially utilize several types of N-glycan substrates for transglycosylation in addition to complex oxazoline. Competitive functional assays confirmed that core fucosylation was not recognized by Endo-CC in terms of glycosyl acceptor substrate selectivity. In addition, the relative activities of Endo-CC mutants were re-evaluated in a quantitative assay, which revealed additional mutants that showed significant transglycosylation activities over a long period of reaction time. This study introduced an alternative endoglycosidase with broad substrate selectivity for the protein acceptor part in the glycan remodeling procedure.

Finally, a combined strategy of both enzymatic modifications and biosynthetic inhibition was applied to another isotype of antibody known as IgE. Surface binding assays using these generated IgE N-glycoforms revealed significant change of

receptor binding affinities caused by alteration in IgE glycan structures attached at Fc region. Furthermore, chemoenzymatic glycosylation remodeling of IgE successfully gave rise to a novel complex type IgE-Fc glycoform with a distinct receptor binding profile from the deglycosylated and native glycoforms of IgE antibody. The results collectively suggested that further remodeling of IgE antibodies with additional glycan structures, such as terminal sialylation and core fucosylation, is possible through glycosynthase-catalyzed transglycosylation reactions using different activated glycosyl oxazolines.

Together, studies in this dissertation greatly improved the scope of the current chemoenzymatic glycan remodeling strategy of antibody and other glycoconjugates. Nevertheless, there are still limitations and challenges associated with the application of this method in other systems. Future work is needed to improve our understanding of the catalytic mechanisms of endoglycosidases and to help us design more efficient glycan-remodeling enzyme tools for various structural and functional purposes.

First, the molecular mechanism behind the different behaviors of Endo-S and Endo-S2 and their glycosynthase mutants in glycan remodeling of antibody is still not clear. Structural analyses reported by other groups on Endo-S and Endo-S2 both in their native forms and in complex with free glycans revealed some molecular information on how the branches of N-linked oligosaccharide were recognized by a number of loops located in the glycoside hydrolase (GH) domain conserved in both enzymes.<sup>116, 130, 179</sup> However, based on the general catalytic mechanism of endoglycosidases, the ground-state glycan in the crystal structure may not accurately reflect the interactions between catalytic residues and oxazolinium ion intermediates

during glycosylation. In order to explain the different turnover numbers of Endo-S and Endo-S2 mutants for the glycan oxazoline substrate observed in our kinetic results,<sup>123, 139</sup> a non-participating thiazoline glycan analogue<sup>124</sup> can be applied in the future crystallographic analysis of Endo-S and Endo-S2 to help understand how the oxazoline is recognized by both enzymes. Our kinetic analyses on glycosynthase mutants of both enzymes also clearly indicated that a single mutation at Asp-233 and Asp-184 of Endo-S and Endo-S2, respectively, exhibited profound effects on substrate affinities for the antibody acceptor. Therefore, structural analysis on Endo-S/S2 mutant interacting with a deglycosylated Fc fragment of IgG antibody by either co-crystallization or molecular simulations can be helpful in understanding the mechanisms behind this observation. Together, these structural and functional studies can help design possible chimeric endoglycosidase or glycosynthase variants with more customizable glycan remodeling abilities in glycoengineering.

Another structural feature of the complex and hybrid N-glycans that has not been addressed in this work is the “bisecting” N-acetylglucosamine (GlcNAc) residue that is associated with core  $\beta$ -mannose of N-glycans. Unlike other GlcNAc structures found in N-glycans, the bisecting GlcNAc demonstrated several unique functional properties in N-glycan biosynthesis and has been implicated in neurodegenerative disorders such Alzheimer’s disease.<sup>180</sup> In terms of antibody N-glycosylation, the bisecting GlcNAc-containing N-glycan has been regarded as one of the critical quality attributes (CQA) for therapeutic antibodies<sup>181</sup> and has been associated with the physiological state of individuals including human longevity.<sup>182</sup> The unique properties of bisecting N-glycoforms of antibody made it of interest to study the

structural-functional relationships of this specific sugar residue in antibody. However, like other N-glycans, it has been difficult to isolate or enrich the pure bisecting N-glycoforms of antibody from natural sources given the relatively low abundance of such antibodies in animal serum.<sup>36</sup> To address this problem, the chemoenzymatic glycan modeling method can be tested for its compatibility with the bisecting glycan substrates. The glycosynthase mutant Endo-S2 D180M can be a promising candidate enzyme for transferring the bisecting N-glycans to the antibody acceptor because a previous study already demonstrated that the wild-type Endo-S2 was able to efficiently remove a wide range of N-glycans from human antibodies including the bisecting glycans.<sup>183</sup> Generation of the homogeneous bisecting N-glycoforms of antibodies may further our understanding of the disease-associated variations related to antibody glycosylation.

Finally, considering the universal distribution of N-glycans across all antibody isotypes<sup>59</sup>, it might be interesting to investigate the potential application of this method in other antibody isotypes such as IgE and IgA. Binding analyses on IgE N-glycoforms revealed distinct interaction patterns between IgE-Fc and its related immune receptors. However, the available IgE-Fc glycoforms studied in this work are still limited to the oligomannose and basic complex forms without any additional modifications such as terminal sialic acid or core fucose. Since extensive studies have suggested that both terminal sialylation and core fucosylation can dramatically affect IgG interactions with immune receptors, we hypothesize that glycoengineering of IgE antibody with these structural features might lead to novel IgE N-glycoforms with interesting biophysical and immunoregulatory properties. Glycan remodeling with

sialylated N-glycans can be experimented using the same Endo-CC N180H mutant, as our results in Chapter 4 clearly indicated that Endo-CC could recognize a wide range of N-glycan substrates including the sialylated complex type. For the core fucosylated N-glycans, a recently reported mutant of an  $\alpha$ 1,6-fucosidase can be used to attempt direct core fucosylation on IgE-Fc or intact IgE antibodies. The ability of this mutant to efficiently transfer the modified fucose substrates to a variety of glycopeptides and glycoproteins has been demonstrated in several previous studies.<sup>94, 147, 184</sup> In conclusion, generation of possible IgE-Fc N-glycoforms with improved binding affinities to both IgE receptors Fc $\epsilon$ RI and CD23 may allow us to design novel competitive inhibitors for the anaphylactic IgE antibodies *in vivo* and facilitate the development of new therapeutics for allergic disorders such as asthma.

Glycosylation remodeling of IgE antibodies can also affect the recognition of allergic IgE antibodies by anti-IgE therapeutics. Interestingly, structural and functional studies suggest that IgE-neutralizing IgG antibodies such as 8D6<sup>155</sup> and MEDI4212<sup>185</sup> target the pathogenic IgE antibodies through a mixed protein-carbohydrate epitope, which involves the critical oligomannose glycan located at Asn-394 that we discussed in Chapter 5. Removal or modifications of this N-glycan from IgE-Fc domain is likely to affect recognition of IgE by these anti-IgE antibodies. However, such modifications might not dramatically affect normal binding of IgE-Fc with the low-affinity receptor CD23, as indicated by our results of our IgE glycoengineering and binding studies in Chapter 5. These studies may contribute to the development of new anti-IgE therapies, as one of the major problems associated with the current anti-IgE therapeutics is the disruption of normal IgE antibody

homeostasis due to lack of IgE/CD23 signaling.<sup>155</sup> Therefore, a potential glycoengineered IgE-Fc fragment with no functionality to trigger the allergic response due to lack of the allergen-binding Fab domain may serve as a therapeutic intervention in combination with the conventional anti-IgE antibodies to treat long-term allergic disorders (Figure 58). Such IgE-Fc N-glycoforms may help maintain the normal homeostasis of circulating IgE antibodies through binding to the CD23 receptors on B cell surface, yet it may be less likely to be recognized and sequestered by the anti-IgE antibodies due to its changed glycan epitope at Fc region. Similar IgE combination therapies have already been experimented in previous studies using alternative strategies to disrupt anti-IgE/IgE recognition such as mutagenesis.<sup>186</sup>

## Allergic IgE Antibodies

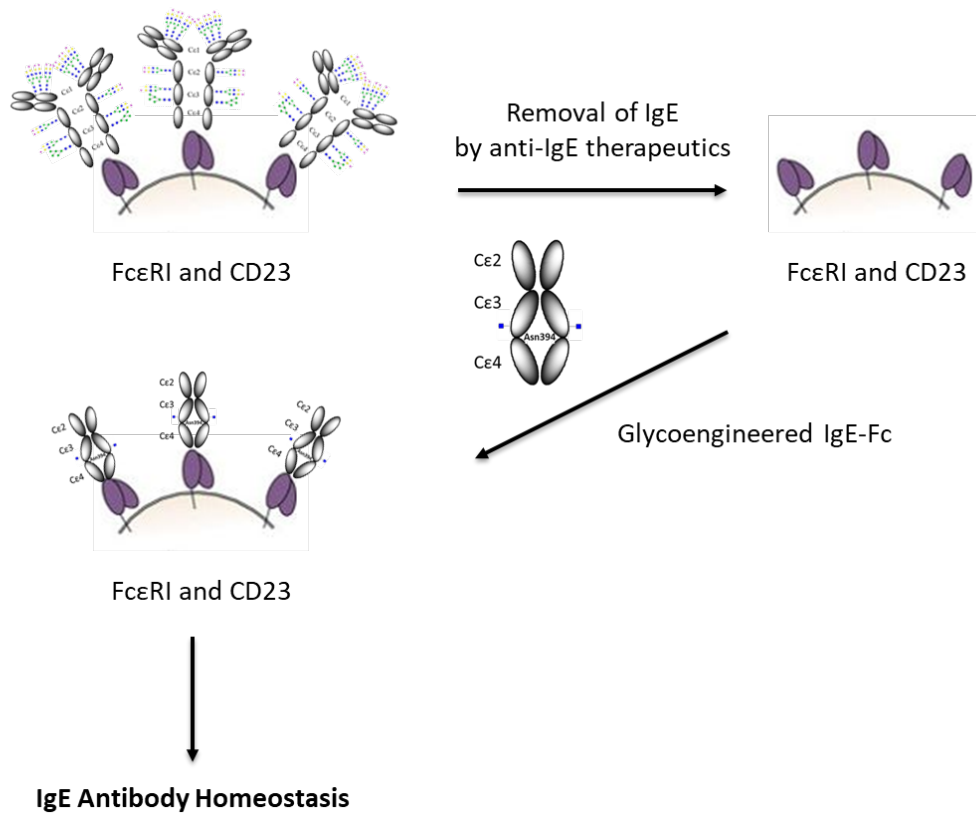


Figure 58. Design for therapeutic intervention as IgE replacement therapy using a combination of anti-IgE antibodies and glycoengineered IgE-Fc. Briefly, the native allergic IgE antibody is sequestered from the immune cell surface by high-affinity anti-IgE antibodies. The receptors are then bound by IgE-Fc N-glycoforms with similar binding affinities to maintain the homeostasis of serum IgE level. Modifications on IgE-Fc N-glycans at Asn-394 and/or other glycosylation sites may reduce the recognition by anti-IgE antibodies on the cell surface.

## Bibliography

- [1] Kaplon, H., and Reichert, J. M. (2018) Antibodies to watch in 2018, *Mabs-Austin* 10, 183-203.
- [2] Burk, M. L., and Matuszewski, K. A. (1997) Muromonab-CD3 and antithymocyte globulin in renal transplantation, *The Annals of pharmacotherapy* 31, 1370-1377.
- [3] Grilo, A. L., and Mantalaris, A. (2019) The increasingly human and profitable monoclonal antibody market, *Trends in Biotechnology* 37, 9-16.
- [4] Mastrangeli, R., Palinsky, W., and Bierau, H. (2019) Glycoengineered antibodies: towards the next-generation of immunotherapeutics, *Glycobiology* 29, 199-210.
- [5] Elgundi, Z., Reslan, M., Cruz, E., Sifniotis, V., and Kayser, V. (2017) The state-of-play and future of antibody therapeutics, *Advanced Drug Delivery Reviews* 122, 2-19.
- [6] Su, D., Kozak, K. R., Sadowsky, J., Yu, S. F., Fourie-O'Donohue, A., Nelson, C., Vandlen, R., Ohri, R., Liu, L., Ng, C., He, J., Davis, H., Lau, J., Del Rosario, G., Cosino, E., Cruz-Chuh, J. D., Ma, Y., Zhang, D., Darwish, M., Cai, W., Chen, C., Zhou, H., Lu, J., Liu, Y., Kaur, S., Xu, K., and Pillow, T. H. (2018) Modulating antibody-drug conjugate payload metabolism by conjugation site and linker modification, *Bioconjugate Chemistry* 25, 21-50.
- [7] Almagro, J. C., Daniels-Wells, T. R., Perez-Tapia, S. M., and Penichet, M. L. (2018) Progress and challenges in the design and clinical development of antibodies for cancer therapy, *Frontiers in Immunology* 8, 31-45.
- [8] Elvin, J. G., Couston, R. G., and van der Walle, C. F. (2013) Therapeutic antibodies: market considerations, disease targets and bioprocessing, *International Journal of Pharmaceutics* 440, 83-98.
- [9] Schroeder, H. W., Jr., and Cavacini, L. (2010) Structure and function of immunoglobulins, *The Journal of Allergy and Clinical Immunology* 125, S41-S52.
- [10] Jennewein, M. F., and Alter, G. (2017) The Immunoregulatory Roles of Antibody Glycosylation, *Trends in Immunology* 38, 358-372.
- [11] Williams, A. F., and Barclay, A. N. (1988) The immunoglobulin superfamily--domains for cell surface recognition, *Annual Review of Immunology* 6, 381-405.
- [12] Harpaz, Y., and Chothia, C. (1994) Many of the immunoglobulin superfamily domains in cell-adhesion molecules and surface-receptors belong to a new structural set which is close to that containing variable domains, *Journal of Molecular Biology* 238, 528-539.
- [13] Smith, K. A., Nelson, P. N., Warren, P., Astley, S. J., Murray, P. G., and Greenman, J. (2004) Demystified ... recombinant antibodies, *Journal of Clinical Pathology* 57, 912-917.
- [14] Matthias, P., and Rolink, A. G. (2005) Transcriptional networks in developing and mature B cells, *Nature Reviews. Immunology* 5, 497-508.
- [15] Jazwinska, E. C., Dunckley, H., Propert, D. N., Gatenby, P. A., and Serjeantson, S. W. (1988) Gm typing by immunoglobulin heavy-chain gene RFLP analysis, *American Journal of Human Genetics* 43, 175-181.

- [16] Cymer, F., Beck, H., Rohde, A., and Reusch, D. (2018) Therapeutic monoclonal antibody N-glycosylation - Structure, function and therapeutic potential, *Biologicals : Journal of the International Association of Biological Standardization* 52, 1-11.
- [17] Normansell, D. E. (1987) Human immunoglobulin subclasses, *Diagnostic and Clinical Immunology* 5, 115-128.
- [18] Kraft, S., and Kinet, J. P. (2007) New developments in Fc epsilon RI regulation, function and inhibition, *Nature Reviews Immunology* 7, 365-378.
- [19] Torres, M., and Casadevall, A. (2008) The immunoglobulin constant region contributes to affinity and specificity, *Trends in Immunology* 29, 91-97.
- [20] Wang, L. X., Tong, X., Li, C., Giddens, J. P., and Li, T. (2019) Glycoengineering of antibodies for modulating functions, *Annual Review of Biochemistry* 88, 433-459.
- [21] Schroeder, H. W., and Cavacini, L. (2010) Structure and function of immunoglobulins, *Journal of Allergy and Clinical Immunology* 125, S41-S52.
- [22] Kurosu, M. (2019) Structure-based drug discovery by targeting N-glycan biosynthesis, dolichyl-phosphate N-acetylglucosaminyltransferase, *Future Medicinal Chemistry*, in press.
- [23] Piirainen, M. A., Salminen, H., and Frey, A. D. (2019) Tailoring N-Glycan biosynthesis for production of therapeutic proteins in *Saccharomyces cerevisiae*, *Methods in Molecular Biology* 1923, 227-241.
- [24] Bieberich, E. (2014) Synthesis, Processing, and Function of N-glycans in N-glycoproteins, *Advances in Neurobiology* 9, 47-70.
- [25] Arnold, J. N., Wormald, M. R., Sim, R. B., Rudd, P. M., and Dwek, R. A. (2007) The impact of glycosylation on the biological function and structure of human immunoglobulins, *Annual Review of Immunology* 25, 21-50.
- [26] Stanley, P., Taniguchi, N., and Aebi, M. (2015) N-Glycans, In *Essentials of Glycobiology* (rd, Varki, A., Cummings, R. D., Esko, J. D., Stanley, P., Hart, G. W., Aebi, M., Darvill, A. G., Kinoshita, T., Packer, N. H., Prestegard, J. H., Schnaar, R. L., and Seeberger, P. H., Eds.), pp 99-111, Cold Spring Harbor (NY).
- [27] Liu, H., Bulseco, G. G., and Sun, J. (2006) Effect of posttranslational modifications on the thermal stability of a recombinant monoclonal antibody, *Immunology Letters* 106, 144-153.
- [28] Natsume, A., Wakitani, M., Yamane-Ohnuki, N., Shoji-Hosaka, E., Niwa, R., Uchida, K., Satoh, M., and Shitara, K. (2005) Fucose removal from complex-type oligosaccharide enhances the antibody-dependent cellular cytotoxicity of single-gene-encoded antibody comprising a single-chain antibody linked the antibody constant region, *Journal of Immunological Methods* 306, 93-103.
- [29] Sazinsky, S. L., Ott, R. G., Silver, N. W., Tidor, B., Ravetch, J. V., and Wittrup, K. D. (2008) Aglycosylated immunoglobulin G1 variants productively engage activating Fc receptors, *Proceedings of the National Academy of Sciences of the United States of America* 105, 20167-20172.
- [30] Siberil, S., de Romeuf, C., Bihoreau, N., Fernandez, N., Meterreau, J. L., Regenman, A., Nony, E., Gaucher, C., Glacet, A., Jorieux, S., Klein, P., Hogarth, M. P., Fridman, W. H., Bourel, D., Beliard, R., and Teillaud, J. L.

- (2006) Selection of a human anti-RhD monoclonal antibody for therapeutic use: Impact of IgG glycosylation on activating and inhibitory Fc gamma R functions, *Clinical Immunology* 118, 170-179.
- [31] Albert, H., Collin, M., Dudziak, D., Ravetch, J. V., and Nimmerjahn, F. (2008) In vivo enzymatic modulation of IgG glycosylation inhibits autoimmune disease in an IgG subclass-dependent manner, *Proceedings of the National Academy of Sciences of the United States of America* 105, 15005-15009.
- [32] Miranda, L. R., Duval, M., Doherty, H., Seaman, M. S., Posner, M. R., and Cavacini, L. A. (2007) The neutralization properties of a HIV-specific antibody are markedly altered by glycosylation events outside the antigen-binding domain, *Journal of Immunology* 178, 7132-7138.
- [33] Clerc, F., Reiding, K. R., Jansen, B. C., Kammeijer, G. S. M., Bondt, A., and Wuhrer, M. (2016) Human plasma protein N-glycosylation, *Glycoconjugate Journal* 33, 309-343.
- [34] Giorgetti, J., D'Atri, V., Canonge, J., Lechner, A., Guillaume, D., Colas, O., Wagner-Rousset, E., Beck, A., Leize-Wagner, E., and Francois, Y. N. (2018) Monoclonal antibody N-glycosylation profiling using capillary electrophoresis - Mass spectrometry: Assessment and method validation, *Talanta* 178, 530-537.
- [35] Deisenhofer, J. (1981) Crystallographic refinement and atomic models of a human Fc fragment and its complex with fragment B of protein A from *Staphylococcus aureus* at 2.9- and 2.8-Å resolution, *Biochemistry* 20, 2361-2370.
- [36] Malhotra, R., Wormald, M. R., Rudd, P. M., Fischer, P. B., Dwek, R. A., and Sim, R. B. (1995) Glycosylation changes of IgG associated with rheumatoid arthritis can activate complement via the mannose-binding protein, *Nature Medicine* 1, 237-243.
- [37] Gomes, M. M., Wall, S. B., Takahashi, K., Novak, J., Renfrow, M. B., and Herr, A. B. (2008) Analysis of IgA1 N-glycosylation and its contribution to FcαRI binding, *Biochemistry* 47, 11285-11299.
- [38] Saphire, E. O., Parren, P. W., Pantophlet, R., Zwick, M. B., Morris, G. M., Rudd, P. M., Dwek, R. A., Stanfield, R. L., Burton, D. R., and Wilson, I. A. (2001) Crystal structure of a neutralizing human IgG against HIV-1: a template for vaccine design, *Science* 293, 1155-1159.
- [39] Lewis, G. K., Pazgier, M., Evans, D. T., Ferrari, G., Bournazos, S., Parsons, M. S., Bernard, N. F., and Finzi, A. (2017) Beyond viral neutralization, *AIDS Research and Human Retroviruses* 33, 760-764.
- [40] Kanda, Y., Yamada, T., Mori, K., Okazaki, A., Inoue, M., Kitajima-Miyama, K., Kuni-Kamochi, R., Nakano, R., Yano, K., Kakita, S., Shitara, K., and Satoh, M. (2007) Comparison of biological activity among nonfucosylated therapeutic IgG1 antibodies with three different N-linked Fc oligosaccharides: the high-mannose, hybrid, and complex types, *Glycobiology* 17, 104-118.
- [41] Chen, C. L., Hsu, J. C., Lin, C. W., Wang, C. H., Tsai, M. H., Wu, C. Y., Wong, C. H., and Ma, C. (2017) Crystal Structure of a homogeneous IgG-Fc glycoform with the N-Glycan designed to maximize the antibody dependent cellular cytotoxicity, *ACS Chemical Biology* 12, 1335-1345.

- [42] Tsai, T. I., Li, S. T., Liu, C. P., Chen, K. Y., Shivatare, S. S., Lin, C. W., Liao, S. F., Lin, C. W., Hsu, T. L., Wu, Y. T., Tsai, M. H., Lai, M. Y., Lin, N. H., Wu, C. Y., and Wong, C. H. (2017) An effective bacterial fucosidase for glycoprotein remodeling, *ACS Chemical Biology* 12, 63-72.
- [43] Quast, I., Keller, C. W., Maurer, M. A., Giddens, J. P., Tackenberg, B., Wang, L. X., Munz, C., Nimmerjahn, F., Dalakas, M. C., and Lunemann, J. D. (2015) Sialylation of IgG Fc domain impairs complement-dependent cytotoxicity, *The Journal of Clinical Investigation* 125, 4160-4170.
- [44] Arnold, J. N., Wormald, M. R., Suter, D. M., Radcliffe, C. M., Harvey, D. J., Dwek, R. A., Rudd, P. M., and Sim, R. B. (2005) Human serum IgM glycosylation: identification of glycoforms that can bind to mannan-binding lectin, *The Journal of Biological Chemistry* 280, 29080-29087.
- [45] Campbell, I. K., Miescher, S., Branch, D. R., Mott, P. J., Lazarus, A. H., Han, D., Maraskovsky, E., Zuercher, A. W., Neschadim, A., Leontyev, D., McKenzie, B. S., and Kasermann, F. (2014) Therapeutic effect of IVIG on inflammatory arthritis in mice is dependent on the Fc portion and independent of sialylation or basophils, *Journal of immunology* 192, 5031-5038.
- [46] Bruckner, C., Lehmann, C., Dudziak, D., and Nimmerjahn, F. (2017) Sweet SIGNS: IgG glycosylation leads the way in IVIG-mediated resolution of inflammation, *International Immunology* 29, 499-509.
- [47] Hachiya, A., Kobayashi, N., Matsuzaki, S., Takeuchi, Y., Akazawa, Y., Shigemura, T., Motoki, N., Masumoto, J., and Agematsu, K. (2018) Analysis of biomarker serum levels in IVIG and infliximab refractory Kawasaki disease patients, *Clinical Rheumatology* 37, 1937-1943.
- [48] Seite, J. F., Cornec, D., Renaudineau, Y., Youinou, P., Mageed, R. A., and Hillion, S. (2010) IVIg modulates BCR signaling through CD22 and promotes apoptosis in mature human B lymphocytes, *Blood* 116, 1698-1704.
- [49] Schwab, I., Seeling, M., Biburger, M., Aschermann, S., Nitschke, L., and Nimmerjahn, F. (2012) B cells and CD22 are dispensable for the immediate antiinflammatory activity of intravenous immunoglobulins *in vivo*, *European Journal of Immunology* 42, 3302-3309.
- [50] Plomp, R., Hensbergen, P. J., Rombouts, Y., Zauner, G., Dragan, I., Koeleman, C. A., Deelder, A. M., and Wuhler, M. (2014) Site-specific N-glycosylation analysis of human immunoglobulin E, *Journal of Proteome Research* 13, 536-546.
- [51] Sutton, B. J., and Davies, A. M. (2015) Structure and dynamics of IgE-receptor interactions: Fc epsilon RI and CD23/Fc epsilon RII, *Immunological Reviews* 268, 222-235.
- [52] Mackay, G. A., Hulett, M. D., Cook, J. P. D., Trist, H. M., Henry, A. J., McDonnell, J. M., Beavil, A. J., Beavil, R. L., Sutton, B. J., Hogarth, P. M., and Gould, H. J. (2002) Mutagenesis within human Fc epsilon RI alpha differentially affects human and murine IgE binding, *Journal of Immunology* 168, 1787-1795.
- [53] Shade, K. T. C., Platzer, B., Washburn, N., Mani, V., Bartsch, Y. C., Conroy, M., Pagan, J. D., Bosques, C., Mempel, T. R., Fiebiger, E., and Anthony, R.

- M. (2015) A single glycan on IgE is indispensable for initiation of anaphylaxis, *Journal of Experimental Medicine* 212, 457-467.
- [54] Shade, K. T., and Anthony, R. (2018) Breaking the allergic cascade by modulating IgE glycosylation, *Glycobiology* 28, 1060-1060.
- [55] Butler, M., Quelhas, D., Critchley, A. J., Carchon, H., Hebestreit, H. F., Hibbert, R. G., Vilarinho, L., Teles, E., Matthijs, G., Schollen, E., Argibay, P., Harvey, D. J., Dwek, R. A., Jaeken, J., and Rudd, P. M. (2003) Detailed glycan analysis of serum glycoproteins of patients with congenital disorders of glycosylation indicates the specific defective glycan processing step and provides an insight into pathogenesis, *Glycobiology* 13, 601-622.
- [56] Parekh, R., Roitt, I., Isenberg, D., Dwek, R., and Rademacher, T. (1988) Age-related galactosylation of the N-linked oligosaccharides of human serum IgG, *Journal of Experimental Medicine* 167, 1731-1736.
- [57] Jefferis, R., Lund, J., Mizutani, H., Nakagawa, H., Kawazoe, Y., Arata, Y., and Takahashi, N. (1990) A comparative study of the N-linked oligosaccharide structures of human IgG subclass proteins, *The Biochemical Journal* 268, 529-537.
- [58] Wormald, M. R., Rudd, P. M., Harvey, D. J., Chang, S. C., Scragg, I. G., and Dwek, R. A. (1997) Variations in oligosaccharide-protein interactions in immunoglobulin G determine the site-specific glycosylation profiles and modulate the dynamic motion of the Fc oligosaccharides, *Biochemistry* 36, 1370-1380.
- [59] Zauner, G., Selman, M. H., Bondt, A., Rombouts, Y., Blank, D., Deelder, A. M., and Wuhrer, M. (2013) Glycoproteomic analysis of antibodies, *Molecular & Cellular Proteomics : MCP* 12, 856-865.
- [60] Stadlmann, J., Weber, A., Pabst, M., Anderle, H., Kunert, R., Ehrlich, H. J., Schwarz, H. P., and Altmann, F. (2009) A close look at human IgG sialylation and subclass distribution after lectin fractionation, *Proteomics* 9, 4143-4153.
- [61] Wuhrer, M., Stam, J. C., van de Geijn, F. E., Koeleman, C. A. M., Verrips, C. T., Dolhain, R. J. E. M., Hokke, C. H., and Deelder, A. M. (2007) Glycosylation profiling of immunoglobulin G (IgG) subclasses from human serum, *Proteomics* 7, 4070-4081.
- [62] Clausen, H., Wandall, H. H., Steentoft, C., Stanley, P., and Schnaar, R. L. (2015) Glycosylation Engineering, In *Essentials of Glycobiology* (rd, Varki, A., Cummings, R. D., Esko, J. D., Stanley, P., Hart, G. W., Aebi, M., Darvill, A. G., Kinoshita, T., Packer, N. H., Prestegard, J. H., Schnaar, R. L., and Seeberger, P. H., Eds.), pp 713-728, Cold Spring Harbor (NY).
- [63] Giddens, J. P., and Wang, L. X. (2015) Chemoenzymatic Glyco-engineering of monoclonal antibodies, *Glyco-Engineering: Methods and Protocols* 1321, 375-387.
- [64] Yamane-Ohnuki, N., and Satoh, M. (2009) Production of therapeutic antibodies with controlled fucosylation, *Mabs-Austin* 1, 230-236.
- [65] von Horsten, H. H., Ogorek, C., Blanchard, V., Demmler, C., Giese, C., Winkler, K., Kaup, M., Berger, M., Jordan, I., and Sandig, V. (2010) Production of non-fucosylated antibodies by co-expression of heterologous GDP-6-deoxy-D-lyxo-4-hexulose reductase, *Glycobiology* 20, 1607-1618.

- [66] Shinkawa, T., Nakamura, K., Yamane, N., Shoji-Hosaka, E., Kanda, Y., Sakurada, M., Uchida, K., Anazawa, H., Satoh, M., Yamasaki, M., Hanai, N., and Shitara, K. (2003) The absence of fucose but not the presence of galactose or bisecting N-acetylglucosamine of human IgG1 complex-type oligosaccharides shows the critical role of enhancing antibody-dependent cellular cytotoxicity, *Journal of Biological Chemistry* 278, 3466-3473.
- [67] Yver, A., Homery, M. C., Fuseau, E., Guemas, E., Dhainaut, F., Quagliaroli, D., Beliard, R., and Prost, J. F. (2012) Pharmacokinetics and safety of roledumab, a novel human recombinant monoclonal anti-RhD antibody with an optimized Fc for improved engagement of FCgammaRIII, in healthy volunteers, *Vox Sang* 103, 213-222.
- [68] Sharman, J. P., Farber, C. M., Mahadevan, D., Schreeder, M. T., Brooks, H. D., Kolibaba, K. S., Fanning, S., Klein, L., Greenwald, D. R., Sportelli, P., Miskin, H. P., Weiss, M. S., and Burke, J. M. (2017) Ublituximab (TG-1101), a novel glycoengineered anti-CD20 antibody, in combination with ibrutinib is safe and highly active in patients with relapsed and/or refractory chronic lymphocytic leukaemia: results of a phase 2 trial, *British Journal of Haematology* 176, 412-420.
- [69] Ferrara, C., Brunker, P., Suter, T., Moser, S., Puntener, U., and Umana, P. (2006) Modulation of therapeutic antibody effector functions by glycosylation engineering: influence of Golgi enzyme localization domain and co-expression of heterologous beta1, 4-N-acetylglucosaminyltransferase III and Golgi alpha-mannosidase II, *Biotechnology and Bioengineering* 93, 851-861.
- [70] Ratner, M. (2014) Genentech's glyco-engineered antibody to succeed Rituxan, *Nature Biotechnology* 32, 6-7.
- [71] Ureshino, H., Kamachi, K., and Kimura, S. (2019) Mogamulizumab for the Treatment of Adult T-cell Leukemia/Lymphoma, *Clinical Lymphoma, Myeloma & Leukemia*, in press.
- [72] Louie, S., Haley, B., Marshall, B., Heidersbach, A., Yim, M., Brozynski, M., Tang, D., Lam, C., Petryniak, B., Shaw, D., Shim, J., Miller, A., Lowe, J. B., Snedecor, B., and Misaghi, S. (2017) FX knockout CHO hosts can express desired ratios of fucosylated or afucosylated antibodies with high titers and comparable product quality, *Biotechnology and Bioengineering* 114, 632-644.
- [73] von Horsten, H. H., Ogorek, C., Blanchard, V., Demmler, C., Giese, C., Winkler, K., Kaup, M., Berger, M., Jordan, I., and Sandig, V. (2010) Production of non-fucosylated antibodies by co-expression of heterologous GDP-6-deoxy-D-lyxo-4-hexulose reductase, *Glycobiology* 20, 1607-1618.
- [74] Okeley, N. M., Alley, S. C., Anderson, M. E., Boursalian, T. E., Burke, P. J., Emmerton, K. M., Jeffrey, S. C., Klussman, K., Law, C. L., Sussman, D., Toki, B. E., Westendorf, L., Zeng, W., Zhang, X., Benjamin, D. R., and Senter, P. D. (2013) Development of orally active inhibitors of protein and cellular fucosylation, *Proceedings of the National Academy of Sciences of the United States of America* 110, 5404-5409.
- [75] Allen, J. G., Mujacic, M., Frohn, M. J., Pickrell, A. J., Kodama, P., Bagal, D., San Miguel, T., Sickmier, E. A., Osgood, S., Swietlow, A., Li, V., Jordan, J. B., Kim, K. W., Rousseau, A. C., Kim, Y. J., Caille, S., Achmatowicz, M.,

- Thiel, O., Fotsch, C. H., Reddy, P., and McCarter, J. D. (2016) Facile Modulation of Antibody Fucosylation with Small Molecule Fucostatin Inhibitors and Cocrystal Structure with GDP-Mannose 4,6-Dehydratase, *ACS Chemical Biology* 11, 2734-2743.
- [76] McKenzie, N. C., Scott, N. E., John, A., White, J. M., and Goddard-Borger, E. D. (2018) Synthesis and use of 6,6,6-trifluoro-L-fucose to block core-fucosylation in hybridoma cell lines, *Carbohydrate Research* 465, 4-9.
- [77] Hossler, P., Chumsae, C., Racicot, C., Ouellette, D., Ibraghimov, A., Serna, D., Mora, A., McDermott, S., Labkovsky, B., Scesney, S., Grinnell, C., Preston, G., Bose, S., and Carrillo, R. (2017) Arabinosylation of recombinant human immunoglobulin-based protein therapeutics, *Mabs-Austin* 9, 715-734.
- [78] Iizuka, M., Ogawa, S., Takeuchi, A., Nakakita, S., Kubo, Y., Miyawaki, Y., Hirabayashi, J., and Tomita, M. (2009) Production of a recombinant mouse monoclonal antibody in transgenic silkworm cocoons, *The FEBS Journal* 276, 5806-5820.
- [79] Cox, K. M., Sterling, J. D., Regan, J. T., Gasdaska, J. R., Frantz, K. K., Peele, C. G., Black, A., Passmore, D., Moldovan-Loomis, C., Srinivasan, M., Cuison, S., Cardarelli, P. M., and Dickey, L. F. (2006) Glycan optimization of a human monoclonal antibody in the aquatic plant *Lemna minor*, *Nature Biotechnology* 24, 1591-1597.
- [80] Ward, M., Lin, C., Victoria, D. C., Fox, B. P., Fox, J. A., Wong, D. L., Meerman, H. J., Pucci, J. P., Fong, R. B., Heng, M. H., Tsurushita, N., Gieswein, C., Park, M., and Wang, H. (2004) Characterization of humanized antibodies secreted by *Aspergillus niger*, *Applied and Environmental Microbiology* 70, 2567-2576.
- [81] Wildt, S., and Gerngross, T. U. (2005) The humanization of N-glycosylation pathways in yeast, *Nature Reviews. Microbiology* 3, 119-128.
- [82] Kaneko, Y., Nimmerjahn, F., and Ravetch, J. V. (2006) Anti-inflammatory activity of immunoglobulin G resulting from Fc sialylation, *Science* 313, 670-673.
- [83] Lund, J., Takahashi, N., Pound, J. D., Goodall, M., and Jefferis, R. (1996) Multiple interactions of IgG with its core oligosaccharide can modulate recognition by complement and human Fc gamma receptor I and influence the synthesis of its oligosaccharide chains, *Journal of Immunology* 157, 4963-4969.
- [84] Chung, C. Y., Wang, Q., Yang, S., Ponce, S. A., Kirsch, B. J., Zhang, H., and Betenbaugh, M. J. (2017) Combinatorial genome and protein engineering yields monoclonal antibodies with hypergalactosylation from CHO cells, *Biotechnology and Bioengineering* 114, 2848-2856.
- [85] Giddens, J. P., Lomino, J. V., Amin, M. N., and Wang, L. X. (2016) Endo-F3 Glycosynthase Mutants Enable Chemoenzymatic Synthesis of Core-fucosylated Triantennary Complex Type Glycopeptides and Glycoproteins, *The Journal of biological chemistry* 291, 9356-9370.
- [86] Beck, A., Wagner-Rousset, E., Bussat, M. C., Lokteff, M., Klinguer-Hamour, C., Haeuw, J. F., Goetsch, L., Wurch, T., Van Dorselaer, A., and Corvaia, N. (2008) Trends in glycosylation, glycoanalysis and glycoengineering of

- therapeutic antibodies and Fc-fusion proteins, *Current Pharmaceutical Biotechnology* 9, 482-501.
- [87] Hodoniczky, J., Zheng, Y. Z., and James, D. C. (2005) Control of recombinant monoclonal antibody effector functions by Fc N-glycan remodeling *in vitro*, *Biotechnology Progress* 21, 1644-1652.
- [88] Washburn, N., Schwab, I., Ortiz, D., Bhatnagar, N., Lansing, J. C., Medeiros, A., Tyler, S., Mekala, D., Cochran, E., Sarvaiya, H., Garofalo, K., Meccariello, R., Meador, J. W., 3rd, Rutitzky, L., Schultes, B. C., Ling, L., Avery, W., Nimmerjahn, F., Manning, A. M., Kaundinya, G. V., and Bosques, C. J. (2015) Controlled tetra-Fc sialylation of IVIg results in a drug candidate with consistent enhanced anti-inflammatory activity, *Proceedings of the National Academy of Sciences of the United States of America* 112, E1297-1306.
- [89] Fairbanks, A. J. (2017) The ENGases: versatile biocatalysts for the production of homogeneous N-linked glycopeptides and glycoproteins, *Chemical Society Reviews* 46, 5128-5146.
- [90] Lombard, V., Golaconda Ramulu, H., Drula, E., Coutinho, P. M., and Henrissat, B. (2014) The carbohydrate-active enzymes database (CAZy) in 2013, *Nucleic Acids Research* 42, D490-495.
- [91] Henrissat, B., and Davies, G. (1997) Structural and sequence-based classification of glycoside hydrolases, *Current Opinion in Structural Biology* 7, 637-644.
- [92] Yin, J., Li, L., Shaw, N., Li, Y., Song, J. K., Zhang, W., Xia, C., Zhang, R., Joachimiak, A., Zhang, H. C., Wang, L. X., Liu, Z. J., and Wang, P. (2009) Structural basis and catalytic mechanism for the dual functional endo-beta-N-acetylglucosaminidase A, *Plos One* 4, e4658.
- [93] Wang, L. X. (2008) Chemoenzymatic synthesis of glycopeptides and glycoproteins through endoglycosidase-catalyzed transglycosylation, *Carbohydrate Research* 343, 1509-1522.
- [94] Li, C., and Wang, L. X. (2018) Chemoenzymatic Methods for the Synthesis of Glycoproteins, *Chem Rev* 118, 8359-8413.
- [95] Tews, I., vanScheltinga, A. C. T., Perrakis, A., Wilson, K. S., and Dijkstra, B. W. (1997) Substrate-assisted catalysis unifies two families of chitinolytic enzymes, *Journal of the American Chemical Society* 119, 7954-7959.
- [96] Li, C., and Wang, L. X. (2016) Endoglycosidases for the synthesis of polysaccharides and glycoconjugates, *Advances in Carbohydrate Chemistry and Biochemistry* 73, 73-116.
- [97] Fujita, M., Shoda, S., Haneda, K., Inazu, T., Takegawa, K., and Yamamoto, K. (2001) A novel disaccharide substrate having 1,2-oxazoline moiety for detection of transglycosylating activity of endoglycosidases, *Biochimica Et Biophysica Acta-General Subjects* 1528, 9-14.
- [98] Wang, L. X. (2011) The Amazing Transglycosylation Activity of Endo-beta-N-acetylglucosaminidases, *Trends in Glycoscience and Glycotechnology : TIGG* 23, 33-52.
- [99] Umekawa, M., Huang, W., Li, B., Fujita, K., Ashida, H., Wang, L. X., and Yamamoto, K. (2008) Mutants of *Mucor hiemalis* endo-beta-N-acetylglucosaminidase show enhanced transglycosylation and glycosynthase-like activities, *Journal of Biological Chemistry* 283, 4469-4479.

- [100] Umekawa, M., Li, C., Higashiyama, T., Huang, W., Ashida, H., Yamamoto, K., and Wang, L. X. (2010) Efficient glycosynthase mutant derived from *Mucor hiemalis* endo-beta-N-acetylglucosaminidase capable of transferring oligosaccharide from both sugar oxazoline and natural N-glycan, *Journal of Biological Chemistry* 285, 511-521.
- [101] Abbott, D. W., Macauley, M. S., Vocadlo, D. J., and Boraston, A. B. (2009) Streptococcus pneumoniae endohexosaminidase D, structural and mechanistic insight into substrate-assisted catalysis in family 85 glycoside hydrolases, *Journal of Biological Chemistry* 284, 11676-11689.
- [102] Huang, W., Yang, Q., Umekawa, M., Yamamoto, K., and Wang, L. X. (2010) *Arthrobacter* endo-beta-N-acetylglucosaminidase shows transglycosylation activity on complex-type N-glycan oxazolines: one-pot conversion of ribonuclease B to sialylated ribonuclease C, *Chembiochem : a European Journal of Chemical Biology* 11, 1350-1355.
- [103] Huang, W., Giddens, J., Fan, S. Q., Toonstra, C., and Wang, L. X. (2012) Chemoenzymatic glycoengineering of intact IgG antibodies for gain of functions, *Journal of the American Chemical Society* 134, 12308-12318.
- [104] Wang, L. X., and Amin, M. N. (2014) Chemical and chemoenzymatic synthesis of glycoproteins for deciphering functions, *Chemistry & Biology* 21, 51-66.
- [105] Eshima, Y., Higuchi, Y., Kinoshita, T., Nakakita, S., and Takegawa, K. (2015) Transglycosylation activity of glycosynthase mutants of endo-beta-N-acetylglucosaminidase from *Coprinopsis cinerea*, *Plos One* 10, e0132859.
- [106] Wei, Y., Li, C., Huang, W., Li, B., Strome, S., and Wang, L. X. (2008) Glycoengineering of human IgG1-Fc through combined yeast expression and in vitro chemoenzymatic glycosylation, *Biochemistry* 47, 10294-10304.
- [107] Higuchi, Y., Eshima, Y., Huang, Y., Kinoshita, T., Sumiyoshi, W., Nakakita, S., and Takegawa, K. (2017) Highly efficient transglycosylation of sialo-complex-type oligosaccharide using *Coprinopsis cinerea* endoglycosidase and sugar oxazoline, *Biotechnology Letters* 39, 157-162.
- [108] Goodfellow, J. J., Baruah, K., Yamamoto, K., Bonomelli, C., Krishna, B., Harvey, D. J., Crispin, M., Scanlan, C. N., and Davis, B. G. (2012) An endoglycosidase with alternative glycan specificity allows broadened glycoprotein remodelling, *Journal of the American Chemical Society* 134, 8030-8033.
- [109] Lin, C. W., Tsai, M. H., Li, S. T., Tsai, T. I., Chu, K. C., Liu, Y. C., Lai, M. Y., Wu, C. Y., Tseng, Y. C., Shivatare, S. S., Wang, C. H., Chao, P., Wang, S. Y., Shih, H. W., Zeng, Y. F., You, T. H., Liao, J. Y., Tu, Y. C., Lin, Y. S., Chuang, H. Y., Chen, C. L., Tsai, C. S., Huang, C. C., Lin, N. H., Ma, C., Wu, C. Y., and Wong, C. H. (2015) A common glycan structure on immunoglobulin G for enhancement of effector functions, *Proceedings of the National Academy of Sciences of the United States of America* 112, 10611-10616.
- [110] Higuchi, Y., Eshima, Y., Huang, Y., Kinoshita, T., Sumiyoshi, W., Nakakita, S. I., and Takegawa, K. (2017) Highly efficient transglycosylation of sialo-complex-type oligosaccharide using *Coprinopsis cinerea* endoglycosidase and sugar oxazoline, *Biotechnology Letters* 39, 157-162.

- [111] Iwamoto, M., Sekiguchi, Y., Nakamura, K., Kawaguchi, Y., Honda, T., and Hasegawa, J. (2018) Generation of efficient mutants of endoglycosidase from *Streptococcus pyogenes* and their application in a novel one-pot transglycosylation reaction for antibody modification, *Plos One* *13*, e0193534.
- [112] Manabe, S., Yamaguchi, Y., Abe, J., Matsumoto, K., and Ito, Y. (2018) Acceptor range of endo-beta-N-acetylglucosaminidase mutant endo-CC N180H: from monosaccharide to antibody, *Royal Society open science* *5*, 171521.
- [113] Shade, K. T., Platzer, B., Washburn, N., Mani, V., Bartsch, Y. C., Conroy, M., Pagan, J. D., Bosques, C., Mempel, T. R., Fiebiger, E., and Anthony, R. M. (2015) A single glycan on IgE is indispensable for initiation of anaphylaxis, *The Journal of Experimental Medicine* *212*, 457-467.
- [114] Collin, M., and Olsen, A. (2001) EndoS, a novel secreted protein from *Streptococcus pyogenes* with endoglycosidase activity on human IgG, *The EMBO Journal* *20*, 3046-3055.
- [115] Allhorn, M., Briceno, J. G., Baudino, L., Lood, C., Olsson, M. L., Izui, S., and Collin, M. (2010) The IgG-specific endoglycosidase EndoS inhibits both cellular and complement-mediated autoimmune hemolysis, *Blood* *115*, 5080-5088.
- [116] Trastoy, B., Lomino, J. V., Pierce, B. G., Carter, L. G., Gunther, S., Giddens, J. P., Snyder, G. A., Weiss, T. M., Weng, Z., Wang, L. X., and Sundberg, E. J. (2014) Crystal structure of *Streptococcus pyogenes* EndoS, an immunomodulatory endoglycosidase specific for human IgG antibodies, *Proceedings of the National Academy of Sciences of the United States of America* *111*, 6714-6719.
- [117] Wadood, A., Ghufuran, M., Khan, A., Azam, S. S., Jelani, M., and Uddin, R. (2018) Selective glycosidase inhibitors: A patent review (2012-present), *International Journal of Biological Macromolecules* *111*, 82-91.
- [118] Knapp, S., Vocadlo, D., Gao, Z. N., Kirk, B., Lou, J. P., and Withers, S. G. (1996) NAG-thiazoline, an N-acetyl-beta-hexosaminidase inhibitor that implicates acetamido participation, *Journal of the American Chemical Society* *118*, 6804-6805.
- [119] Macdonald, J. M., Tarling, C. A., Taylor, E. J., Dennis, R. J., Myers, D. S., Knapp, S., Davies, G. J., and Withers, S. G. (2010) Chitinase Inhibition by Chitobiose and Chitotriose Thiazolines, *Angewandte Chemie-International Edition* *49*, 2599-2602.
- [120] Reid, C. W., Blackburn, N. T., Legaree, B. A., Auzanneau, F. I., and Clarke, A. J. (2004) Inhibition of membrane-bound lytic transglycosylase B by NAG-thiazoline, *FEBS Letters* *574*, 73-79.
- [121] Li, B., Takegawa, K., Suzuki, T., Yamamoto, K., and Wang, L. X. (2008) Synthesis and inhibitory activity of oligosaccharide thiazolines as a class of mechanism-based inhibitors for endo-beta-N-acetylglucosaminidases, *Bioorganic & Medicinal Chemistry* *16*, 4670-4675.
- [122] Parsons, T. B., Struwe, W. B., Gault, J., Yamamoto, K., Taylor, T. A., Raj, R., Wals, K., Mohammed, S., Robinson, C. V., Benesch, J. L., and Davis, B. G.

- (2016) Optimal synthetic glycosylation of a therapeutic antibody, *Angewandte Chemie-International Edition* 55, 2361-2367.
- [123] Tong, X., Li, T., Li, C., and Wang, L. X. (2018) Generation and comparative kinetic analysis of new glycosynthase mutants from *Streptococcus pyogenes* endoglycosidases for antibody glycoengineering, *Biochemistry* 57, 5239-5246.
- [124] Li, C., Zhu, S. L., Tong, X., Ou, C., and Wang, L. X. (2017) A facile synthesis of a complex type N-glycan thiazoline as an effective inhibitor against the antibody-deactivating endo-N-acetylglucosaminidases, *Journal of Carbohydrate Chemistry* 36, 336-346.
- [125] Zhao, X. Y., Li, G. S., and Liang, S. F. (2013) Several affinity tags commonly used in the chromatographic purification, *Journal of Analytical Methods in Chemistry* 440, 83-98.
- [126] Yan, B. X., and Sun, Y. Q. (1997) Glycine residues provide flexibility for enzyme active sites, *The Journal of Biological Chemistry* 272, 3190-3194.
- [127] Seko, A., Koketsu, M., Nishizono, M., Enoki, Y., Ibrahim, H. R., Juneja, L. R., Kim, M., and Yamamoto, T. (1997) Occurrence of a sialylglycopeptide and free sialylglycans in hen's egg yolk, *Biochimica et Biophysica Acta* 1335, 23-32.
- [128] Li, B., Takegawa, K., Suzuki, T., Yamamoto, K., and Wang, L. X. (2008) Synthesis and inhibitory activity of oligosaccharide thiazolines as a class of mechanism-based inhibitors for endo-beta-N-acetylglucosaminidases, *Bioorganic & Medicinal Chemistry* 16, 4670-4675.
- [129] Huang, Y., and Orlando, R. (2017) Kinetics of N-Glycan release from human immunoglobulin G (IgG) by PNGase F: all glycans are not created equal, *Journal of Biomolecular Techniques : JBT* 28, 150-157.
- [130] Trastoy, B., Klontz, E., Orwenyo, J., Marina, A., Wang, L. X., Sundberg, E. J., and Guerin, M. E. (2018) Structural basis for the recognition of complex-type N-glycans by Endoglycosidase S, *Nature Communications* 9, 1874.
- [131] Liu, L., Prudden, A. R., Capicciotti, C. J., Bosman, G. P., Yang, J. Y., Chapla, D. G., Moremen, K. W., and Boons, G. J. (2019) Streamlining the chemoenzymatic synthesis of complex N-glycans by a stop and go strategy, *Nature Chemistry* 11, 161-169.
- [132] Liu, C. P., Tsai, T. I., Cheng, T., Shivatare, V. S., Wu, C. Y., Wu, C. Y., and Wong, C. H. (2018) Glycoengineering of antibody (Herceptin) through yeast expression and in vitro enzymatic glycosylation, *Proceedings of the National Academy of Sciences of the United States of America* 115, 720-725.
- [133] Wang, N., Seko, A., Daikoku, S., Kanie, O., Takeda, Y., and Ito, Y. (2016) Non-enzymatic reaction of glycosyl oxazoline with peptides, *Carbohydrate Research* 436, 31-35.
- [134] Ge, X., Sirich, T. L., Beyer, M. K., Desaire, H., and Leary, J. A. (2001) A strategy for the determination of enzyme kinetics using electrospray ionization with an ion trap mass spectrometer, *Analytical Chemistry* 73, 5078-5082.
- [135] Danan, L. M., Yu, Z., Hoffhines, A. J., Moore, K. L., and Leary, J. A. (2008) Mass spectrometric kinetic analysis of human tyrosylprotein sulfotransferase-1 and -2, *Journal of the American Society for Mass Spectrometry* 19, 1459-1466.

- [136] Pi, N., Armstrong, J. I., Bertozzi, C. R., and Leary, J. A. (2002) Kinetic analysis of NodST sulfotransferase using an electrospray ionization mass spectrometry assay, *Biochemistry* 41, 13283-13288.
- [137] Guo, W. L., Tang, F., Qin, K., Zhou, M., Le, Z. P., and Huang, W. (2017) Glycoengineering and glycosite-specific labeling of serum IgGs from various species, *Carbohydrate Research* 446, 32-39.
- [138] Sjogren, J., Cosgrave, E. F., Allhorn, M., Nordgren, M., Bjork, S., Olsson, F., Fredriksson, S., and Collin, M. (2015) EndoS and EndoS2 hydrolyze Fc-glycans on therapeutic antibodies with different glycoform selectivity and can be used for rapid quantification of high-mannose glycans, *Glycobiology* 25, 1053-1063.
- [139] Li, T., Tong, X., Yang, Q., Giddens, J. P., and Wang, L. X. (2016) Glycosynthase mutants of endoglycosidase S2 show potent transglycosylation activity and remarkably relaxed substrate specificity for antibody glycosylation remodeling, *The Journal of Biological Chemistry* 291, 16508-16518.
- [140] Tong, X., Li, T., Orwenyo, J., Toonstra, C., and Wang, L. X. (2018) One-pot enzymatic glycan remodeling of a therapeutic monoclonal antibody by endoglycosidase S (Endo-S) from *Streptococcus pyogenes*, *Bioorganic & Medicinal Chemistry* 26, 1347-1355.
- [141] Shen, A., Lupardus, P. J., Morell, M., Ponder, E. L., Sadaghiani, A. M., Garcia, K. C., and Bogyo, M. (2009) Simplified, enhanced protein purification using an inducible, autoprocessing enzyme tag, *Plos One* 4, e8119.
- [142] Eshima, Y., Higuchi, Y., Kinoshita, T., Nakakita, S. I., and Takegawa, K. (2015) Transglycosylation activity of glycosynthase mutants of endo-beta-N-acetylglucosaminidase from *Coprinopsis cinerea*, *Plos One* 10, e0132859.
- [143] Biancucci, M., Dolores, J. S., Wong, J., Grimshaw, S., Anderson, W. F., Satchell, K. J., and Kwon, K. (2017) New ligation independent cloning vectors for expression of recombinant proteins with a self-cleaving CPD/6xHis-tag, *BMC Biotechnology* 17, 1.
- [144] Li, T., Tong, X., Yang, Q., Giddens, J. P., and Wang, L. X. (2016) Glycosynthase mutants of endoglycosidase S2 show potent transglycosylation activity and remarkably relaxed substrate specificity for antibody glycosylation remodeling, *The Journal of Biological Chemistry* 291, 16508-16518.
- [145] Williams, R. L., Greene, S. M., and Mcpherson, A. (1987) The Crystal-Structure of Ribonuclease-B at 2.5-Å Resolution, *Journal of Biological Chemistry* 262, 16020-16031.
- [146] Yang, Q., An, Y. M., Zhu, S. L., Zhang, R. S., Loke, C. M., Cipollo, J. F., and Wang, L. X. (2017) Glycan Remodeling of Human Erythropoietin (EPO) Through Combined Mammalian cell engineering and chemoenzymatic transglycosylation, *ACS Chemical Biology* 12, 1665-1673.
- [147] Li, C., Zhu, S., Ma, C., and Wang, L. X. (2017) Designer alpha1,6-fucosidase mutants enable direct core fucosylation of intact N-glycopeptides and N-glycoproteins, *Journal of the American Chemical Society* 139, 15074-15087.

- [148] Platts-Mills, T. A., Heymann, P. W., Commins, S. P., and Woodfolk, J. A. (2016) The discovery of IgE 50 years later, *Annals of Allergy, Asthma & Immunology : Official Publication of the American College of Allergy, Asthma, & Immunology* 116, 179-182.
- [149] Mukai, K., Tsai, M., Starkl, P., Marichal, T., and Galli, S. J. (2016) IgE and mast cells in host defense against parasites and venoms, *Seminars in Immunopathology* 38, 581-603.
- [150] Gould, H. J., Sutton, B. J., Bevil, A. J., Bevil, R. L., McCloskey, N., Coker, H. A., Fear, D., and Smurthwaite, L. (2003) The biology of IgE and the basis of allergic disease, *Annual Review of Immunology* 21, 579-628.
- [151] Cockcroft, D. W. (2018) Epidemic thunderstorm asthma, *The Lancet. Planetary Health* 2, e236-e237.
- [152] Karagiannis, S. N., Josephs, D. H., Bax, H. J., and Spicer, J. F. (2017) Therapeutic IgE Antibodies: Harnessing a macrophage-mediated immune surveillance mechanism against cancer, *Cancer Research* 77, 2779-2783.
- [153] Gould, H. J., and Sutton, B. J. (2008) IgE in allergy and asthma today, *Nature Reviews. Immunology* 8, 205-217.
- [154] Dhaliwal, B., Pang, M. O., Keeble, A. H., James, L. K., Gould, H. J., McDonnell, J. M., Sutton, B. J., and Bevil, A. J. (2017) IgE binds asymmetrically to its B cell receptor CD23, *Scientific Reports* 7, 45533.
- [155] Chen, J. B., Ramadani, F., Pang, M. O. Y., Bevil, R. L., Holdom, M. D., Mitropoulou, A. N., Bevil, A. J., Gould, H. J., Chang, T. W., Sutton, B. J., McDonnell, J. M., and Davies, A. M. (2018) Structural basis for selective inhibition of immunoglobulin E-receptor interactions by an anti-IgE antibody, *Scientific Reports* 8, 11548.
- [156] Tu, Y., Salim, S., Bourgeois, J., Di Leo, V., Irvine, E. J., Marshall, J. K., and Perdue, M. H. (2005) CD23-mediated IgE transport across human intestinal epithelium: inhibition by blocking sites of translation or binding, *Gastroenterology* 129, 928-940.
- [157] Arnold, J. N., Radcliffe, C. M., Wormald, M. R., Royle, L., Harvey, D. J., Crispin, M., Dwek, R. A., Sim, R. B., and Rudd, P. M. (2004) The glycosylation of human serum IgD and IgE and the accessibility of identified oligomannose structures for interaction with mannan-binding lectin, *J Immunol* 173, 6831-6840.
- [158] Fridriksson, E. K., Bevil, A., Holowka, D., Gould, H. J., Baird, B., and McLafferty, F. W. (2000) Heterogeneous glycosylation of immunoglobulin E constructs characterized by top-down high-resolution 2-D mass spectrometry, *Biochemistry* 39, 3369-3376.
- [159] Dore, K. A., Davies, A. M., Drinkwater, N., Bevil, A. J., McDonnell, J. M., and Sutton, B. J. (2017) Thermal sensitivity and flexibility of the Cepsilon-3 domains in immunoglobulin E, *Biochimica et biophysica acta. Proteins and proteomics* 1865, 1336-1347.
- [160] Wan, T., Bevil, R. L., Fabiane, S. M., Bevil, A. J., Sohi, M. K., Keown, M., Young, R. J., Henry, A. J., Owens, R. J., Gould, H. J., and Sutton, B. J. (2002) The crystal structure of IgE Fc reveals an asymmetrically bent conformation, *Nature Immunology* 3, 681-686.

- [161] Holdom, M. D., Davies, A. M., Nettleship, J. E., Bagby, S. C., Dhaliwal, B., Girardi, E., Hunt, J., Gould, H. J., Beavil, A. J., McDonnell, J. M., Owens, R. J., and Sutton, B. J. (2011) Conformational changes in IgE contribute to its uniquely slow dissociation rate from receptor FcepsilonRI, *Nature Structural & Molecular Biology* 18, 571-576.
- [162] Basu, M., Hakimi, J., Dharm, E., Kondas, J. A., Tsien, W. H., Pilson, R. S., Lin, P., Gilfillan, A., Haring, P., Braswell, E. H., Nettleton, M. Y., and Kochan, J. P. (1993) Purification and characterization of human recombinant IgE-Fc fragments that bind to the human high-affinity IgE receptor, *Journal of Biological Chemistry* 268, 13118-13127.
- [163] Hunt, J., Beavil, R. L., Calvert, R. A., Gould, H. J., Sutton, B. J., and Beavil, A. J. (2005) Disulfide linkage controls the affinity and stoichiometry of IgE Fc-epsilon3-4 binding to FcepsilonRI, *The Journal of Biological Chemistry* 280, 16808-16814.
- [164] Zosky, G. R., and Sly, P. D. (2007) Animal models of asthma, *Clinical and Experimental Allergy : Journal of the British Society for Allergy and Clinical Immunology* 37, 973-988.
- [165] Taner, S. B., Pando, M. J., Roberts, A., Schellekens, J., Marsh, S. G. E., Malmberg, K. J., Parham, P., and Brodsky, F. M. (2011) Interactions of NK cell receptor KIR3DL1\*004 with chaperones and conformation-specific antibody reveal a functional folded state as well as predominant intracellular retention, *Journal of Immunology* 186, 62-72.
- [166] Sutton, B. J., Davies, A. M., Bax, H. J., and Karagiannis, S. N. (2019) IgE antibodies: from structure to function and clinical translation, *Antibodies* 8, 19.
- [167] Taylor, A. I., Fabiane, S. M., Sutton, B. J., and Calvert, R. A. (2009) The crystal structure of an avian IgY-Fc fragment reveals conservation with both mammalian IgG and IgE, *Biochemistry* 48, 558-562.
- [168] Aikawa, J., Takeda, Y., Matsuo, I., and Ito, Y. (2014) Trimming of glucosylated N-glycans by human ER alpha1,2-mannosidase I, *Journal of Biochemistry* 155, 375-384.
- [169] Feige, M. J., Nath, S., Catharino, S. R., Weinfurtner, D., Steinbacher, S., and Buchner, J. (2009) Structure of the murine unglycosylated IgG1 Fc fragment, *Journal of Molecular Biology* 391, 599-608.
- [170] Rosenwasser, L. J., and Meng, J. F. (2005) Anti-CD23, *Clinical Reviews in Allergy & Immunology* 29, 61-72.
- [171] Vercelli, D., Helm, B., Marsh, P., Padlan, E., Geha, R. S., and Gould, H. (1989) The B-Cell binding-site on human immunoglobulin-E, *Nature* 338, 649-651.
- [172] Hibbert, R. G., Teriete, P., Grundy, G. J., Beavil, R. L., Reljic, R., Holers, V. M., Hannan, J. P., Sutton, B. J., Gould, H. J., and McDonnell, J. M. (2005) The structure of human CD23 and its interactions with IgE and CD21, *The Journal of Experimental Medicine* 202, 751-760.
- [173] Dhaliwal, B., Yuan, D. P., Pang, M. O. Y., Henry, A. J., Cain, K., Oxbrow, A., Fabiane, S. M., Beavil, A. J., McDonnell, J. M., Gould, H. J., and Sutton, B. J. (2012) Crystal structure of IgE bound to its B-cell receptor CD23 reveals a mechanism of reciprocal allosteric inhibition with high affinity receptor Fc

- epsilon RI, *Proceedings of the National Academy of Sciences of the United States of America* 109, 12686-12691.
- [174] Epp, A., Sullivan, K. C., Herr, A. B., and Strait, R. T. (2016) Immunoglobulin glycosylation effects in allergy and immunity, *Current Allergy and Asthma Reports* 16, 79.
- [175] Davies, A. M., Allan, E. G., Keeble, A. H., Delgado, J., Cossins, B. P., Mitropoulou, A. N., Pang, M. O. Y., Ceska, T., Beavil, A. J., Craggs, G., Westwood, M., Henry, A. J., McDonnell, J. M., and Sutton, B. J. (2017) Allosteric mechanism of action of the therapeutic anti-IgE antibody omalizumab, *The Journal of Biological Chemistry* 292, 9975-9987.
- [176] Yang, Q., and Wang, L. X. (2016) Mammalian-1,6-Fucosyltransferase (FUT8) Is the Sole Enzyme Responsible for the N-Acetylglucosaminyltransferase I-independent Core Fucosylation of High-mannose N-Glycans, *The Journal of Biological Chemistry* 291, 11064-11071.
- [177] Li, T., DiLillo, D. J., Bournazos, S., Giddens, J. P., Ravetch, J. V., and Wang, L. X. (2017) Modulating IgG effector function by Fc glycan engineering, *Proceedings of the National Academy of Sciences of the United States of America* 114, 3485-3490.
- [178] Tong, X., Li, T., Orwenyo, J., Toonstra, C., and Wang, L. X. (2017) One-pot enzymatic glycan remodeling of a therapeutic monoclonal antibody by endoglycosidase S (Endo-S) from *Streptococcus pyogenes*, *Bioorganic & Medicinal Chemistry* 26, 1347-1355.
- [179] Klontz, E. H., Trastoy, B., Deredge, D., Fields, J. K., Li, C., Orwenyo, J., Marina, A., Beadenkopf, R., Gunther, S., Flores, J., Wintrode, P. L., Wang, L. X., Guerin, M. E., and Sundberg, E. J. (2019) Molecular basis of broad spectrum N-Glycan specificity and processing of therapeutic IgG monoclonal antibodies by endoglycosidase S2, *ACS Central Science* 5, 524-538.
- [180] Kizuka, Y., and Taniguchi, N. (2018) Neural functions of bisecting GlcNAc, *Glycoconjugate Journal* 35, 345-351.
- [181] Reusch, D., and Tejada, M. L. (2015) Fc glycans of therapeutic antibodies as critical quality attributes, *Glycobiology* 25, 1325-1334.
- [182] Ruhaak, L. R., Uh, H. W., Beekman, M., Koeleman, C. A. M., Hokke, C. H., Westendorp, R. G. J., Wuhler, M., Houwing-Duistermaat, J. J., Slagboom, P. E., and Deelder, A. M. (2010) Decreased levels of bisecting GlcNAc glycoforms of IgG are associated with human longevity, *Plos One* 5(9), e12566.
- [183] Sjogren, J., Struwe, W. B., Cosgrave, E. F. J., Rudd, P. M., Stervander, M., Allhorn, M., Hollands, A., Nizet, V., and Collin, M. (2013) EndoS(2) is a unique and conserved enzyme of serotype M49 group A *Streptococcus* that hydrolyses N-linked glycans on IgG and alpha(1)-acid glycoprotein, *Biochemical Journal* 455, 107-118.
- [184] Giddens, J. P., Lomino, J. V., DiLillo, D. J., Ravetch, J. V., and Wang, L. X. (2018) Site-selective chemoenzymatic glycoengineering of Fab and Fc glycans of a therapeutic antibody, *Proceedings of the National Academy of Sciences of the United States of America* 115, 12023-12027.

- [185] Sheldon, E., Schwickart, M., Li, J., Kim, K., Crouch, S., Parveen, S., Kell, C., and Birrell, C. (2016) Pharmacokinetics, pharmacodynamics, and safety of MEDI4212, an anti-IgE monoclonal antibody, in subjects with atopy: a Phase I study, *Advances in Therapy* 33, 225-251.
- [186] Pennington, L. F., Tarchevskaya, S., Brigger, D., Sathiyamoorthy, K., Graham, M. T., Nadeau, K. C., Eggel, A., and Jardetzky, T. S. (2016) Structural basis of omalizumab therapy and omalizumab-mediated IgE exchange, *Nature Communications* 7, 11610.